TECHNISCHE UNIVERSITÄT MÜNCHEN
Lehrstuhl für Botanik

Regulatory components of the abscisic acid receptors in
Arabidopsis thaliana

Izabela Szostkiewicz

Vollständiger Abdruck der von der Fakultät Wissenschaftszentrum Weihenstephan für Ernährung, Landnutzung und Umwelt der Technischen Universität München zur Erlangung des akademischen Grades eines

Doktors der Naturwissenschaften

genehmigten Dissertation.

Vorsitzender: Univ.-Prof. Dr. J. Schnyder

Prüfer der Dissertation: 1.   Univ.-Prof. Dr. E. Grill
                                 2.   Univ.-Prof. Dr. A. Gierl

Die Dissertation wurde am 10.06.2010 bei der Technischen Universität München eingereicht und durch die Fakultät Wissenschaftszentrum Weihenstephan für Ernährung, Landnutzung und Umwelt am 06.08.2010 angenommen.

Content

List of Figures

Abbreviations

ABA	Abscisic acid
ABI/abi	Abscisic acid-insensitive
ABF	ABRE binding factor
ABRC	ABA-responsive complex
ABRE	ABA responsive element
AHG	ABA-hypersensitive germination
Amp	Ampicillin
APS	Ammonium persulfate
ATHB	*Arabidopsis thaliana* homeobox protein
BAP	Benzyl adenine
BiFC	Bimolecular fluorescence complementation
bp	Base pair
BRs	Brassinosteroids
BSA	Bovine serum albumin
Cam	Chloramphenicol
CaMV	Cauliflower mosaic virus
CBL	Calcineurin B-like protein
CD	Circular dichroism
cDNA	Complementary deoxyribonucleic acid
CDPK	Calcium-dependent protein kinase
CE	Coupling element
CIPK	CBL interacting protein kinase
Col	*Columbia*
CTAB	Cetyl-trimethyl-ammonium bromide
2,4-D	2,4-Dichlorophenoxyacetic acid
ddH$_2$O	Double-distilled water
DMSO	Dimethyl sulfoxide
DNA	Deoxyribonucleic acid
DTT	Dithiothreitol
E. coli	*Escherichia coli*
EDTA	Ethylenediamine tetraacetic acid
era	Enhanced response to ABA
EtBr	Ethidium bromide
EtOH	Ethanol
FTICR	Fourier Transform Ion Cyclotron Resonance
GAs	Gibberellins
gca	Growth control exerted by ABA
Gen	Gentamicin
GFP	Green fluorescent protein
GSH	Glutathione
GUS	β-D-glucuronidase

7

HAB/hab	Hypersensitive to ABA
IAA	Indole-3-acetic acid
InsP$_3$	Inositol 1,4,5 trisphosphate
InsP$_6$	Inositol hexakisphosphate
IPTG	Isopropyl β-D-thiogalactoside
ITC	Isothermal titration calorimetry
JAs	Jasmonates
Kan	Kanamycin
kb	Kilobase
kDa	Kilo Dalton
LB	Luria-Bertani medium
La-*er*	Landsberg *erecta*
LS	Linsmaier and Skoog medium
LUC	Luciferase
M	mol/l
MES	2-morpholinoethansulfone acid
MeOH	Methanol
mRNA	messenger RNA
miRNA	micro RNA
MS	Murashige and Skoog medium
MUG	4-methyl-umbelliferone-β-D-glucuronide
MUP	4-methyl-umbelliferylphosphate
NAA	α-naphthalene acetic acid
NCED	9-*cis*-epoxycarotenoid dioxygenase
NOS	Napaline synthase
NSY	Neoxanthin synthase
OD	Optical density
OST	Open stomata
PAGE	Polyacrylamide gel electrophoresis
PCR	Polymerase chain reaction
PE	Plant extract
PEG	Polyethylene glycol
PPase	Phosphatase
PP2C	Protein serine/threonine phosphatases type 2C
PYL	PYR-like
PYR	Pyrobactin resistant
RAB	Regulated by abscisic acid
RCAR	Regulatory component of ABA receptor
RD	Responsive to desiccation
RFU	Relative fluorescence units
Rif	Rifampicin
RLU	Relative light units

RNA	Ribonucleic acid
rpm	Rotations per minute
RT-PCR	Reverse transcription PCR
SA	Salicylic acid
SDS	Sodium dodecylsulfate
SnRK	Sucrose non-fermenting - related protein kinase
TEMED	N,N,N,N'-tetramethylethylene diamine
Tris	Tris (hydroxymethyl) aminomethane
U	Units
UV	Ultraviolet
WT	Wild type
Y2H	Yeast two hybrid
YFP	Yellow fluorescent protein
ZEP	Zeaxanthin epoxidase

Summary

Abscisic acid (ABA) plays a central role in coordinating plant adaptive responses to abiotic stress and also regulates plant growth and development. Key players in ABA signal transduction include the type 2C protein phosphatases (PP2Cs) ABI1 and ABI2, which act by negatively regulating ABA responses.

Although numerous proteins have been identified, there has until very recently not been any strong candidate widely accepted to act as an ABA receptor. In this study, interactors of PP2Cs ABI1 and ABI2 were identified and named Regulatory Components of the ABA Receptors (RCARs). In *Arabidopsis thaliana,* RCARs belong to a family with 14 members that share structural similarity with class 10 pathogen-related proteins (PR-10). Functional analysis showed that RCAR proteins were able to bind ABA, to mediate ABA-dependent inactivation of ABI1 or ABI2 *in vitro*, and to stimulate ABA signaling in protoplast cells. As such, they act as ABA receptors.

Further analysis revealed that RCARs and PP2Cs are forming heterodimeric receptor complexes, and they function as co-receptors. The receptor complexes between RCAR1, 3, 9, 10, 13 or 14 and the PP2Cs ABI1 or ABI2 differ considerably with respect to their sensitivity to ABA. Selectivity for (*S*)-ABA compared with (*R*)-ABA and *trans*-ABA was less stringent for RCAR3, 9, 10, 13 and 14 as compared with RCAR1.

Based on the differences, which were observed in transcriptional regulation of RCARs and PP2Cs and biochemical properties of different receptor complexes, a model was proposed whereby differential expression of the co-receptors and combinatorial assembly of the receptor complexes act in concert to modulate and fine-tune ABA responses.
The structural similarity of RCAR proteins with PR-10 family of proteins raises the possibility that other small molecules can bind to RCAR proteins and modulate ABA responses. Protein activity analysis showed that among known plant hormones only abscisic acid has the ability to regulate the catalytic activity of PP2Cs in the presence of RCAR proteins. Additionally, further experiments revealed that cell-free extracts from *Arabidopsis thaliana* cell suspension cultures contain small, unknown molecules that are able to inhibit phosphatase activity in the absence and more efficiently, in the presence of RCAR proteins, in an ABA-independent manner. By using comparative Fourier Transform Ion Cyclotron Resonance Mass Spectrometry analysis (FT-ICR-MS), molecular masses of several interesting candidates that appear to bind specifically to functional but not to truncated RCAR proteins were identified.

Zusammenfassung

Das Hormon Abscisinsäure (ABA) spielt bei der Auslösung von Schutzmechanismen in der Pflanze als Reaktion auf abiotischen Stress eine zentrale Rolle und reguliert darüber hinaus Wachstums- und Entwicklungsvorgänge. Schlüsselkomponenten der ABA-Signaltransduktion sind Proteinphosphatasen des Typs 2C (PP2Cs) wie ABI1 und ABI2, die hierbei als negative Regulatoren wirken.

Unter mehreren Proteinen, die als mögliche Kandidaten für einen ABA-Rezeptor isoliert worden waren, befand sich bis in jüngster Zeit kein allgemein als vielversprechend anerkannter Kandidat. In Rahmen dieser Arbeit wurden Proteine identifiziert, die mit den PP2Cs ABI1 und ABI2 interagieren und die die Bezeichnung *Regulatory Components of the ABA Receptors* (RCARs) erhielten. In der Ackerschmalwand *Arabidopsis thaliana* sind die RCARs Teil einer Proteinfamilie die aus 14 Proteinen besteht und deren Mitglieder strukturelle Ähnlichkeit mit *class 10 pathogen-related proteins* (PR-10) aufweisen. Bei den PR-10 Proteinen handelt es sich um eine Gruppe von Proteinen, die an der Reaktion von Pflanzen auf den Befall mit Pathogenen beteiligt sind. Eine Funktionsanalyse der RCAR-Proteine ergab, dass diese ABA zu binden vermögen, *in vitro* die ABA-abhängige Inaktivierung von ABI1 und ABI2 vermitteln und in Mesophyllzell-Protoplasten die ABA-Signaltransduktion stimulieren. Somit üben die RCAR-Proteine die Funktion eines ABA-Rezeptors aus.

In weiteren Analysen zeigte sich, daß RCARs und PP2Cs heterodimere Rezeptorkomplexe bilden, RCARs und PP2Cs also Co-Rezeptoren darstellen. Die Rezeptorkomplexe zwischen RCAR1, 3, 9, 10, 13 oder 14 und den PP2Cs ABI1 oder ABI2 unterschieden sich hinsichtlich ihrer Empfindlichkeit gegenüber ABA stark voneinander. Auch die Stereoselektivität der Rezeptorkomplexe, d.h. die gegenüber dem synthetischen Enantiomeren (*R*)-ABA und dem inaktiven Stereoisomeren *trans*-ABA bevorzugte Bindung der natürlich vorkommenden (*S*)-ABA war unterschiedlich. Rezeptorkomplexe, an denen RCAR1 beteiligt war, wiesen dabei eine hohe Selektivität auf, während sie für Rezeptorkomplexe mit RCAR3, 9, 10, 13 und 14 deutlich geringer ausfiel.

Auf der Grundlage nachgewiesener Unterschiede in der transkriptionellen Regulation von RCARs und PP2Cs sowie der charakteristischen biochemischen Eigenschaften der verschiedenen Rezeptorkomplexe wurde ein Modell entwickelt, nach dem die Intensität der ABA-Antwort durch ein Zusammenwirken von differentieller Expression der Co-Rezeptoren und einer angepassten Kombination verschiedener Rezeptorkomplexen feinjustiert wird.
Die strukturelle Ähnlichkeit von RCAR- und PR-10-Proteinen lässt vermuten, dass weitere kleine Moleküle an die RCAR-Proteine binden und dadurch die ABA-Antwort modulieren.

Eine Analyse der PP2C-Aktivität in Gegenwart von RCAR-Proteinen und Vertretern der verschiedenen bekannten Pflanzenhormongruppen ergab zunächst, dass unter diesen Bedingungen ausschließlich das Phytohormon ABA in der Lage ist, die Phosphataseaktivität zu regulieren. In zellfreien Extrakten aus *Arabidopsis thaliana* Zellsuspensionskulturen fanden sich noch weitere bislang nicht identifizierte, niedermolekulare Substanzen, die die Aktivität von PP2Cs in Abwesenheit oder noch effektiver in Gegenwart von RCAR-Proteinen zu hemmen vermögen. Darüber hinaus gelang es mit Hilfe vergleichender Massenspektometrie, *Fourier Transform Ion Cyclotron Resonance Mass Spectrometry* (FT-ICR-MS), mehrere interessante Verbindungen in der Molekularmasse zu identifizieren, die offenbar spezifisch an funktionelle RCAR-Proteine, nicht aber an verkürzte Formen binden.

1 Introduction

1.1 Abscisic acid (ABA)

Higher plants are sessile organisms that have evolved a high plasticity for adaptation to environmental challenges. Pathogens and abiotic stress such as drought and salt stress severely impact plant performance and productivity. The phytohormone abscisic acid (ABA) serves as an endogenous messenger in biotic and abiotic stress responses (Christmann et al., 2006; Melotto et al., 2006; Adie et al., 2007; Hirayama and Shinozaki, 2007).

ABA was first discovered in the 1960s, initially under the names of either dormin or abscisin in young cotton fruits and sycamore leaves (Ohkuma et al., 1963).

A few years later the compound was renamed as abscisic acid (ABA) (Addicott et al., 1968).
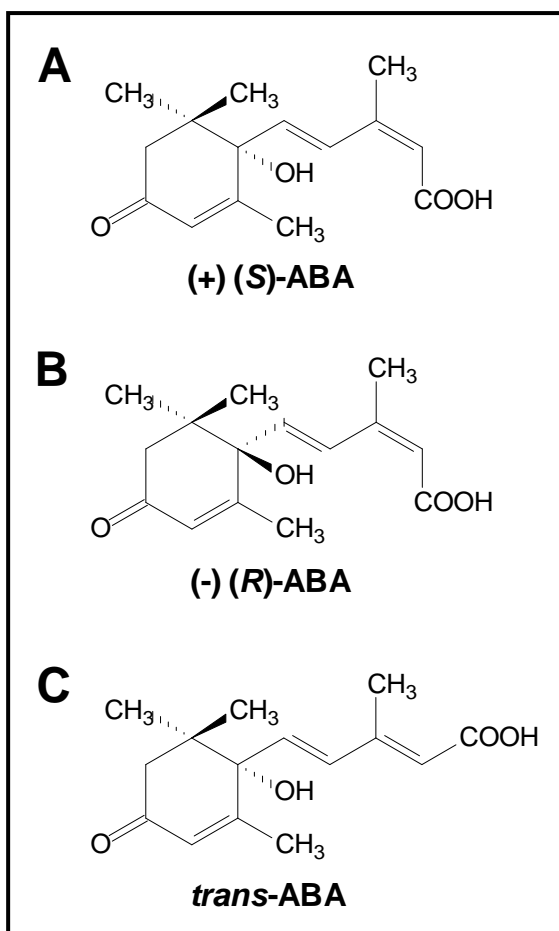
Figure 1-1   **Isomere and enantiomere of abscisic acid (ABA)**

(A) (+) (S)-ABA,
(B) (-) (R)-ABA
(C) trans-ABA

ABA is a monocyclic sesquiterpene with 15 carbon atoms, which configure an aliphatic ring with one double bond, two methyl groups, and an unsaturated chain with a terminal

carboxyl group (Figure 1-1). The naturally occurring form of abscisic acid is (+) (*S*)-ABA and the unnatural isomere of natural ABA is (-) (*R*)-ABA. Both molecules are very similar in shape, differing only in the position of the methyl groups on the ring (Nambara et al., 2002). Furthermore, abscisic acid exists as a *cis*- and *trans*-isomer depending on the orientation of carboxyl group at C-2.

ABA has been found in a great number of plants species, where it has been detected in every organ or living tissue. Interestingly, ABA is not restricted to the plant kingdom. Evidence indicates that ABA also exists in humans, where it acts as a pro-inflammatory cytokine in granulocytes (Bruzzone et al., 2007) and as a stimulator of insulin release from human pancreatic islets (Bruzzone et al., 2008). Moreover, ABA is involved in the development of atherosclerosis (Magnone et al., 2009) and stimulates the proliferation of human hemopoietic progenitors (Scarfi et al., 2009). These cross-kingdom comparisons suggest that the mechanisms of ABA signaling may have an ancient origin.

1.2 Biosynthesis of Abscisic acid

The biosynthesis of ABA is initiated by a five-carbon (C5) precursor, isopentyl diphosphate (IPP). Two distinct biosynthetic routes for ABA biosynthesis are known. In fungi such as *Cercospora rosicola* or *Botrytis cinerea*, the ABA is formed via the mevalonate pathway (MVA) (Hirai et al., 2000; Yamamoto et al., 2000), while in *Arabidopsis thaliana*, ABA is derived from 2-C-methyl-D-erythritol-4-phosphate (MEP) pathway (Lichtenthaler et al., 1997; Kuzuyama, 2002; Eisenreich et al., 2004).

Initial steps of ABA biosynthesis are confined to the chloroplasts, where glyceraldehyde 3-phosphate and pyruvate are combined and rearranged, to give isopentenyl diphosphate (IPP). This leads to the production of phytoene and lycopene as the intermediates, the latter of which is cyclized and hydoxylated to form zeaxanthin, the first oxygenated carotenoid (C40) (Figure 1-2).

Four distinct enzymes are possible candidates for catalyzing in plastids the conversion of zeaxanthin to xanthoxin, which is the C15 intermediate: zeaxanthin epoxidase (ZEP) (Marin et al., 1996; Agrawal et al., 2001; Xiong et al., 2002), neoxanthin synthase (NSY) (North et al., 2007), an unidentified epoxycarotenoid isomerase, and 9-*cis*-epoxycarotenoid dioxygenase (NCED) (Iuchi et al., 2001; Schwartz et al., 2001).
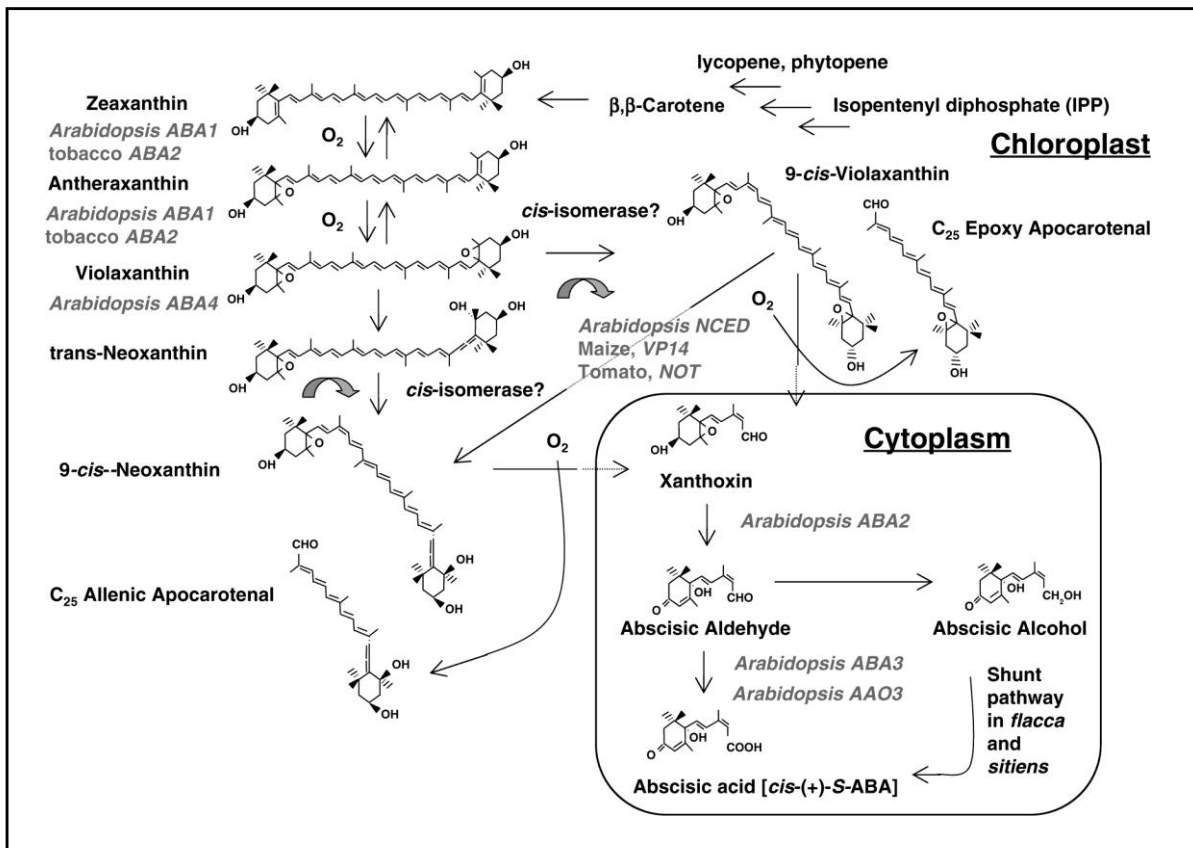
Figure 1-2   **ABA biosynthetic pathway in plants**
(Wasilewska et al., 2008)

Xanthoxin is then converted to ABA via abscisic aldehyde in the cytosol. The oxidation of xanthoxin to produce abscisic aldehyde is catalyzed by ABA2, a short-chain dehydrogenase/reductase in *Arabidopsis* (Cheng et al., 2002; Gonzalez-Guzman et al., 2002). In turn, the conversion of abscisic aldehyde to ABA is catalyzed by *Arabidopsis* aldehyde oxidase 3 (AAO3), which requires molybdenum cofactor for its activity (Seo et al., 2000). A variety of studies have indicated that the 9-*cis*-epoxycarotenoid cleavage reaction catalyzed by NCEDs is a key regulatory step in ABA biosynthesis (Qin and Zeevaart, 1999; Thompson et al., 2000; Iuchi et al., 2001).

The mutants *aba1, aba2, aba3*, and *aao3* block ABA biosynthesis at different steps. These mutants exhibit a wilty phenotype and decreased expression of genes that can be induced by stress. Their phenotypes can be reversed to the wild type by exogenous application of ABA (Marin et al., 1996; Schwartz et al., 1997; Seo et al., 2000).
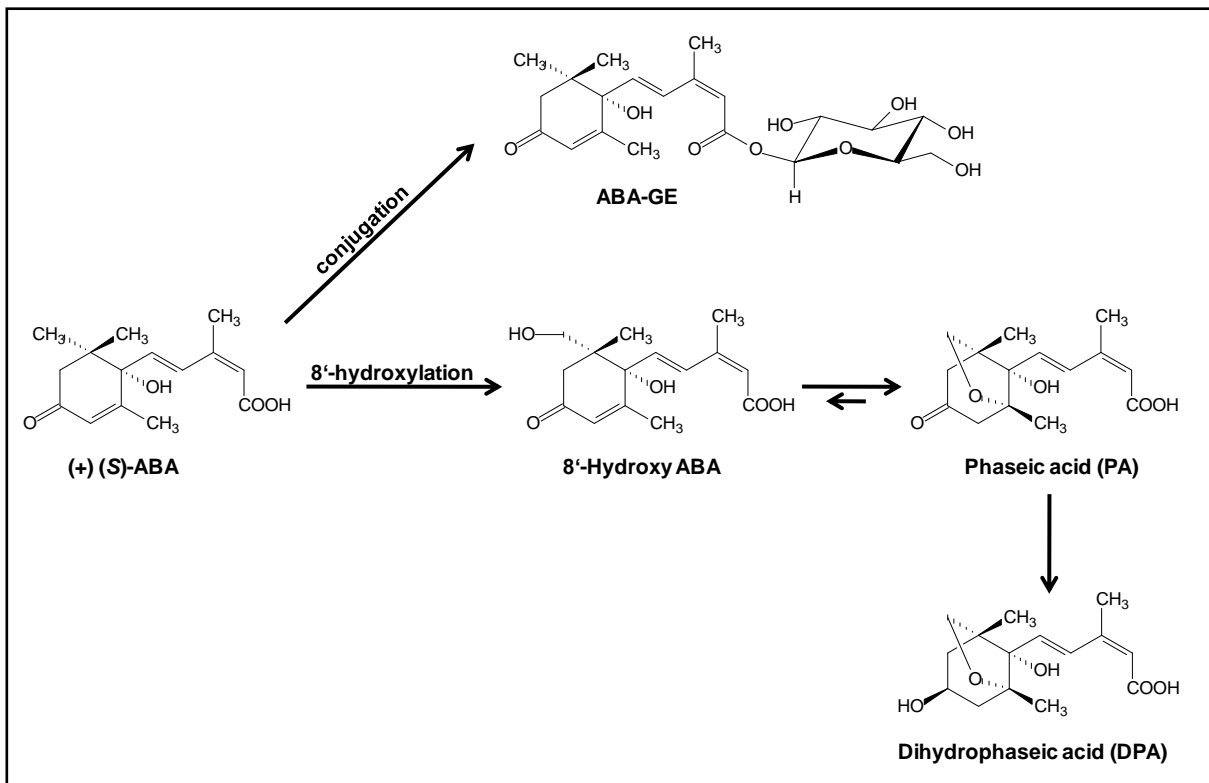
Figure 1-3   ABA catabolic pathways
Inactivation of ABA by conjugation and 8'-hydroxylation is shown. The 8'-hydroxylation is commonly thought to be the predominant ABA catabolic pathway (Jadhav et al., 2008).

The inactivation of ABA is caused by the reactions of hydroxylation and conjugation (Figure 1-3). In the ABA-hydroxylation pathways, one of the methyl groups of the ring structure (C-7', C-8', and C-9') is oxidized (Nambara and Marion-Poll, 2005). The hydroxylation at C-8' position is a major regulatory step in the oxidative pathway of ABA catabolism and is mediated by the CYP707 class of cytochrome P450 monooxygenases, which are strongly induced by exogenous ABA treatment, dehydration and rehydration (Kushiro et al., 2004; Saito et al., 2004). The reaction of 8'-hydroxylation leads to formation of phaseic acid (PA) and dihydrophaseic acid (DPA), which are the most widespread and abundant ABA catabolites (Cutler and Krochko, 1999). In addition to hydroxylation pathways, ABA and its hydroxylated catabolites are conjugated with glucose. ABA-β-D-glucopyranosyl ester (ABA-GE) is the most widespread conjugate (Schroeder and Nambara, 2006; Kato-Noguchi and Tanaka, 2008).

1.3 Perception

The phytohormone abscisic acid (ABA) serves as the prime signal in the responses of plants to environmental stress imposed by cold, drought, or high salinity (Christmann et al., 2006). The hunt for an ABA receptor, a plant protein that recognizes the hormone and conveys its gene regulating orders to the nucleus, has been full of frustration and controversy.

The first report in 2006 showed that FCA (Flowering time control protein A) is an ABA receptor. Regrettably, the paper was retracted due to lack of evidence that FCA binds ABA (Risk et al., 2008). Other candidates for ABA receptor are: the Mg-chelatase H subunit (ABAR/CHLH) (Shen et al., 2006), a G protein-coupled receptor GCR2 (Liu et al., 2007) and two membrane proteins GTG1 (GPCR-type G protein 1) and GTG2 (Pandey et al., 2009). The validity of the hypothesis that ABAR/CHLH and GCR2 act as true ABA receptors has been questioned. Müller and Hansson argue that if the magnesium chelatase is an ABA receptor, then the mutants should show little to no response to ABA treatment. The mutants, however behave like a wild-type plants (Müller and Hansson, 2009). There are also doubts concerning the role of GCR2, which is neither a G protein-coupled receptor nor a transmembrane protein (Gao et al., 2007; Johnston et al., 2007; Illingworth et al., 2008). In addition, new data indicate that GCR2 does not bind ABA (Risk et al., 2009).

Studies on GTG1 and GTG2, membrane localized ABA receptors showed that these proteins interact with GPA1 and they have an intrinsic GTP-binding and GTPase activities. In addition, the mutant plants lacking both GTGs have impaired ABA responses. However, in binding assays only 1% of the GTG1/2 was functional in binding of the ABA (Pandey et al., 2009). This raises the question as to how effectively the GTG proteins might function as ABA receptors.

In summary, although numerous proteins have been put forth, there has until very recently not been any strong candidate widely accepted to act as an ABA receptor.

1.4 Signal transduction

ABA is an important phytohormone and plays a critical role in plant adaptative responses to various stress signals. It has been reported that ABA concentrations can increase up to 30-fold during drought stress (Outlaw, 2003). Other stresses, such as salinity and cold, also cause ABA biosynthesis and accumulation. ABA also plays important roles in many other physiological processes such as seed dormancy and germination, development of seeds, embryo morphogenesis, synthesis of storage proteins and lipids, leaf senescence

and also defense against pathogens (Wasilewska et al., 2008; Bari and Jones, 2009). Moreover, ABA curtails transpirational water loss by promoting stomatal closure and inhibiting stomatal opening.

To mediate all these developmental and physiological processes, ABA signaling appears to depend on coordinated interactions between receptor proteins, protein phosphatases and kinases, and secondary messengers such as calcium, inositol 1,4,5 trisphosphate (InsP$_3$), inositol hexakisphosphate (InsP$_6$), and diacylglycerol pyrophosphate (DGPP). The intracellular signals, including redox signals and pH interfere as well with ABA responses (Finkelstein et al., 2002; Lemtiri-Chlieh et al., 2003; Zalejski et al., 2005; Bright et al., 2006; Christmann et al., 2006; Perera et al., 2008; Siegel et al., 2009).

1.4.1   ABA signaling elements

At the membrane level, ABA signaling events have been extensively studied in guard cells. This is because of the role of ABA in regulating stomatal closure to limit water loss through transpiration (Sirichandra et al., 2009). The response of guard cells to ABA is a very rapid process in which intracellular secondary messengers are involved (Figure 1-4). The cytosolic free Ca^{2+} concentration (Ca$^{2+}_{cyt}$) during the ABA response of guard cells have been found to show a distinct pattern of reiterated phases of increase and decrease. These Ca^{2+} oscillations result from two opposing reactions, Ca^{2+} influx through ABA-activated channels or Ca^{2+} efflux through pumps (Christmann et al., 2006; Tuteja and Mahajan, 2007).

Ca^{2+} has been shown to mediate ABA induced stomatal closure, during which the membrane depolarization occurs, due to the inhibition of an H$^+$-ATPase activity and activation of anion channels. The anion channels mediate passive efflux of Cl$^-$, malate^{2-}, and NO$_3^-$.

SLAC1 (SLOW ANION CHANNEL-ASSOCIATED 1) is the first cloned plasma-membrane anion channel (Vahisalu et al., 2008). Membrane depolarization creates a driving force for K$^+$ efflux via outwardly-rectifying K$^+$ channels (Pandey et al., 2007; Siegel et al., 2009). The loss of osmotically relevant ions leads to water and turgor loss causing stomatal closing.

At least six Shakertype (voltage-dependent) K$^+$ channels are known to be expressed in the guard cells of *Arabidopsis thaliana*: KAT1, KAT2, AKT1, AtKC1, AKT2, and GORK (Gambale and Uozumi, 2006; Lebaudy et al., 2007). Among them, the inward-rectifying K$^+$ channel KAT1 has been suggested to have a key role in stomatal opening (Sato et al., 2009).

The ABA insensitive mutants *abi1* and *abi2* have been shown to cause a reduction in the ABA-induced increases in cytoplasmic calcium in guard cells but do not interfere with Ca^{2+}-induced stomatal closure (Allen et al., 1999). Cytosolic calcium increases were also analyzed in guard cells of the *Arabidopsis* farnesyltransferase deletion mutant *era1-2* (enhanced response to ABA). The *era1-2* mutation causes ABA-hypersensitive S-type anion current activation and stomatal closure, which leads to reduced rates of water loss from *era1-2* plants compared with wild-type plants under drought stress (Pei et al., 1998). Another type of ABA insensitive mutant is *gca2* (growth control by ABA *2*), which exhibits a strong CO_2 insensitivity in cytosolic Ca^{2+} pattern regulation in guard cells (Israelsson et al., 2006; Young et al., 2006).

Phospholipases are involved in ABA signal transduction in guard cells (Figure 1-4). Early experiments have shown that the action of phospholipase C (PLC) can generate the secondary messengers such as $InsP_3$ and diacylglycerol (DAG) (Berridge, 1993). Both $InsP_3$ and PLC have been shown to be important for ABA-mediated stomatal regulation (Staxen et al., 1999). In early work in *Commelina communis* epidermal peels, the release of caged $InsP_3$ caused an elevation of cytosolic Ca^{2+} leading to stomatal closure (Gilroy et al., 1990). $InsP_3$ has been also shown to trigger Ca^{2+} release from intracellular stores such as the vacuole and to regulate the diurnal Ca^{2+} fluctuations (Sanders et al., 2002; Tang et al., 2007). In addition, $InsP_6$ another important component of ABA signaling has been shown to act as a calcium-mobilizing agent (Lemtiri-Chlieh et al., 2003).

The hydrolysis of phospholipids by phospholipase Dα1 (PLDα1) produces phosphatidic acid (PA). This reaction has been an important step in ABA signaling in the barley aleurone cells (Ritchie and Gilroy, 1998), guard cells (Jacob et al., 1999) and in suspension cells (Hallouin et al., 2002). PA has shown to bind to ABI1 and to inhibit its phosphatase activity, thus promoting ABA signaling (Zhang et al., 2004).

The pH and the redox status of the cell are also critical factors that mediate or regulate ABA signal transduction. Nitric oxide (NO) and H_2O_2 have shown to be required for stomatal closure in response to ABA (Garcia-Mata and Lamattina, 2002; Neill et al., 2002).

Major enzymatic sources of NO in guard cells involved in ABA signaling: nitric oxide synthase (NOS) and nitrate reductase (NR) (Desikan et al., 2002; Guo et al., 2003).

Experiments with the epidermal peels of the *nia1, nia2* NR-deficient mutant revealed strong impairment of both NO synthesis and stomatal closure in the presence of ABA (Desikan et al., 2002). The cellular redox balance regulates the protein phosphatases

ABI1 and ABI2, which are rapidly inactivated by H_2O_2, probably via oxidation of crucial cysteine residues (Meinhard and Grill, 2001; Meinhard et al., 2002).
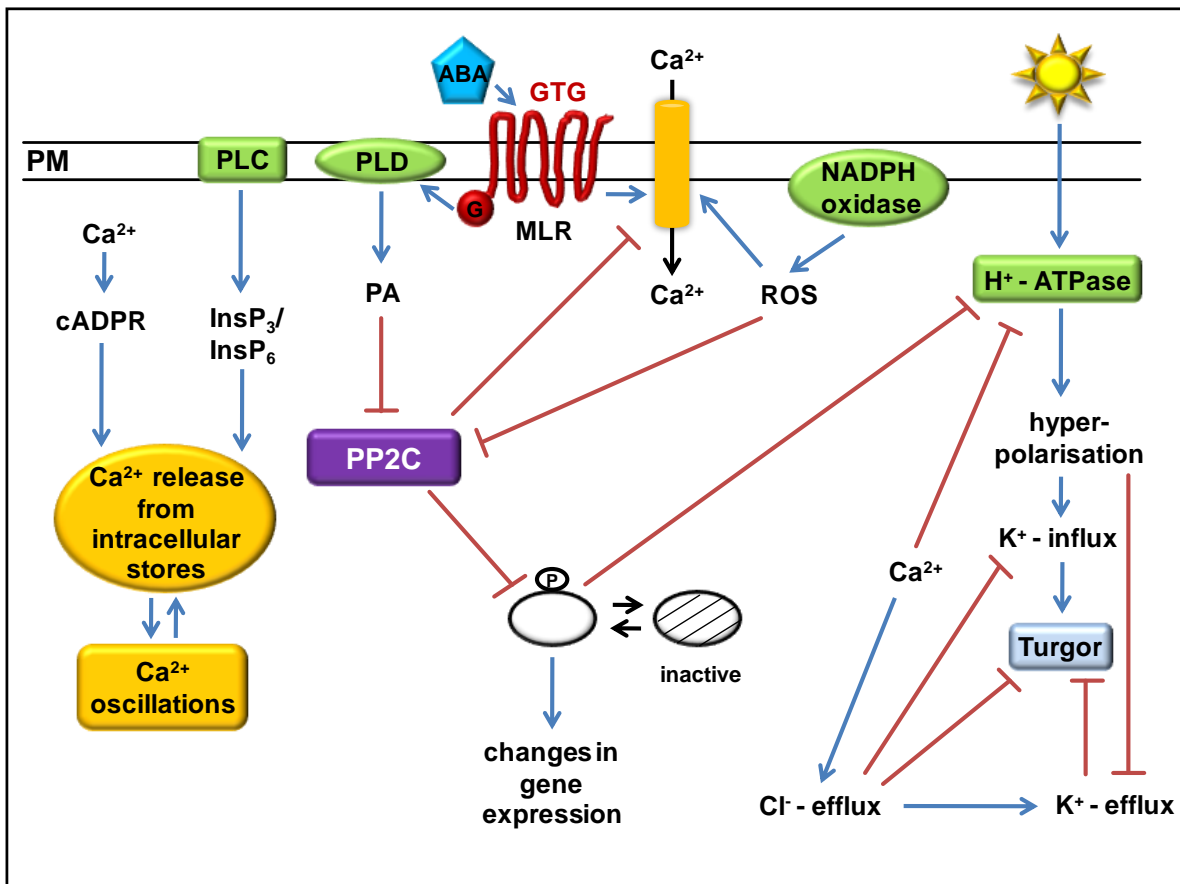
Figure 1-4 **Action of ABA signaling elements during stomatal closure**
Abbreviations: PM: *plasma membrane;* **PLC:** *Phospholipase C;* **PLD:** *Phospholipase D;* **cADPR:** *cyclic ADP-ribose;* **PA:** *phosphatidic acid;* **InsP$_3$/ InsP$_6$:** *inositol 1,4,5 trisphosphate/ inositol hexakisphosphate;* **MLR:** *membrane localized receptor such as GTG1/2;* **ROS:** *reactive oxygen species;* **PP2Cs:** *protein phosphatase 2C.*

1.4.2 Phosphorylation and dephosphorylation events in ABA signaling

A major mechanism of signal transduction is reversible protein phosphorylation mediated by protein kinases and protein phosphatases, thereby regulating many biological processes (Hirayama and Shinozaki, 2007).

Protein kinases

The first kinase involved in the ABA signaling in guard cells was purified from *Vicia faba* and was named AAPK (ABA-activated protein kinase). The transient transformation of guard cells with a dominant mutant form AAPK impairs ABA activiation of S-type anion

channels and disrupts ABA-induced stomatal closure, which indicates that AAPK is important for ABA-induced stomatal closure (Li et al., 2000). The orthologous kinase from *Arabidopsis* is OPEN STOMATA 1 OST1/SRK2E/SnRK2.6, which functions as a positive regulator of ABA-induced stomatal closure (Mustilli et al., 2002; Yoshida et al., 2002). OST1 belongs to SNF1 (sucrose non-fermenting 1) - related protein kinase 2 (SnRK2) proteins. The *Arabidopsis* genome encodes 38 SnRKs, 10 of which are SnRK2s (Hrabak et al., 2003). Besides OST1, two other members in the same clade - SnRK2.2 (SRK2D) and SnRK2.3 (SRK2l) are also highly inducible by exogenous ABA and regulate ABA responses in seed germination, root growth and gene expression (Boudsocq et al., 2004; Boudsocq et al., 2007; Fujii et al., 2007). A similar situation exists in rice, where three (SAPK8, SAPK9 and SAPK10) kinases (stress-activated protein kinases – SAPK) are also activated by ABA stimulus (Kobayashi et al., 2004).

snrk2.2/snrk2.3 double mutants behave insensitive to the ABA in seed germination and seedling growth (Fujii et al., 2007), which demonstrate that SnRK2.2 and SnRK2.3 are positive regulators in ABA signal transduction. *snrk2.2/snrk2.3/snrk2.6* triple mutants show very strong ABA insensitive phenotype with respect to seed germination, root growth and gene expression, suggesting that SnRK2.2, SnRK2.3 and OST1/SnRK2.6 have overlapping functions in ABA signaling (Fujii and Zhu, 2009; Nakashima et al., 2009).

Calcium serves as a ubiquitous second messenger in diverse adaptation and developmental processes in plants. Specific calcium signatures are recognized by different calcium sensor proteins including calmodulin (CaM) and CaM-like proteins (CMLs), Ca^{2+} dependent protein kinases (CDPKs), calcineurin B-like proteins (CBLs) and CBL-interacting protein kinases (CIPKs) (Luan et al., 2002; Pandey et al., 2004; Zhu et al., 2007; Weinl and Kudla, 2009).

CDPKs are Ser/Thr protein kinases that are mostly found in plants and in certain groups of protists, including *Plasmodium* (Harmon et al., 2000; Billker et al., 2004).

In *Arabidopsis*, the CDPKs form a gene family with 34 members, consisting of four distinct domains. These proteins possess a variable N-terminal domain, followed by highly conserved protein kinase domain, an autoinhibitory domain, and a calmodulin-like domain. This unique molecular structure allows the direct activation of CDPKs by calcium (Cheng et al., 2002). Studies on CDPK function in ABA responses have shown that CPK3 and CPK6 play a role in guard cell ion channel regulation (Mori et al., 2006). Loss-of-function mutations of CPK4 and CPK11 show pleiotropic ABA-insensitive phenotypes in seed germination, seedling growth, and stomatal movement and lead to salt insensitivity in seed germination and decreased tolerance of seedlings to salt stress. Two ABA-responsive transcription factors, ABF1 and ABF4 have been shown to be phosphorylated

in vitro by CPK4 and CPK11 kinases. This suggests that, these two kinases may regulate ABA signaling through the ABF transcription factors. All these data indicate that CPK4 and CPK11 are two important positive regulators in CDPK/calcium-mediated ABA signaling pathways (Zhu et al., 2007).

SnRK3-type kinases (SnRK3/CBL-interacting protein kinases (CIPKs)/PKS) are also implicated in the ABA response and interact with PP2Cs (Ohta et al., 2003). Analysis of a CIPK3 loss-of-function allele established a function of this kinase as a negative regulator of ABA responses during seed germination and in stress-induced gene expression (Kim et al., 2003).

Protein phosphatases

Major players in ABA responses are a subclass of Mg^{2+} - and Mn^{2+} -dependent serine/threonine phosphatases type 2C (PP2Cs). There are approximately 80 PP2Cs (Figure 1-5) in *Arabidopsis* (Schweighofer et al., 2004; Xue et al., 2008; Shi, 2009) and six (ABI1, ABI2, HAB1, HAB2, PP2CA/AHG3 and AHG1) of the nine PP2Cs in clade A have been identified as negative regulators of ABA responses (Merlot et al., 2001; Kuhn et al., 2006; Robert et al., 2006; Saez et al., 2006; Yoshida et al., 2006; Nishimura et al., 2007; Rubio et al., 2009). FsPP2C1 is a functional protein phosphatase type C from beechnut (*Fagus sylvatica*) and also plays a role of negative regulator in ABA signaling (Lorenzo et al., 2001; Saavedra et al., 2010).

The enzymatic activity of PP2Cs is commonly measured by dephosphorylation of 4-methyl-umbelliferylphosphate (4-MUP) or phosphopeptide RRA(pT)VA, artificial substrates used for *in vitro* reactions. PP2Cs require Mg^{2+} or Mn^{2+} for their activity and have been shown to be insensitive to naturally occurring inhibitors and toxins, including okadaic acid and other phosphatase inhibitors (Cohen, 1989).

Prototypes of PP2Cs are ABI1 and its close homologue ABI2, and their involvement in ABA signaling was revealed by the characterization of the ABA-insensitive *Arabidopsis* mutants *abi1-1* and *abi2-1*. ABI1 and ABI2 proteins display a similar architecture and their catalytic domains share 86% identity in the amino acid sequence, while the N-terminal extensions are less conserved (42% identity) (Meyer et al., 1994; Leung et al., 1997). The *Arabidopsis* mutant proteins *abi1* and *abi2* are characterized by a single amino acid exchange in the catalytic domain, ABI1^{G180D} and ABI2^{G168D}, conferring a dominant ABA-insensitive phenotype in seed germination and root growth responses, as well as attenuation of seed dormancy and stomatal closure (Koornneef et al., 1984). The mutation impairs magnesium binding and results in a strong reduction of the protein phosphatase activity (Leube et al., 1998).
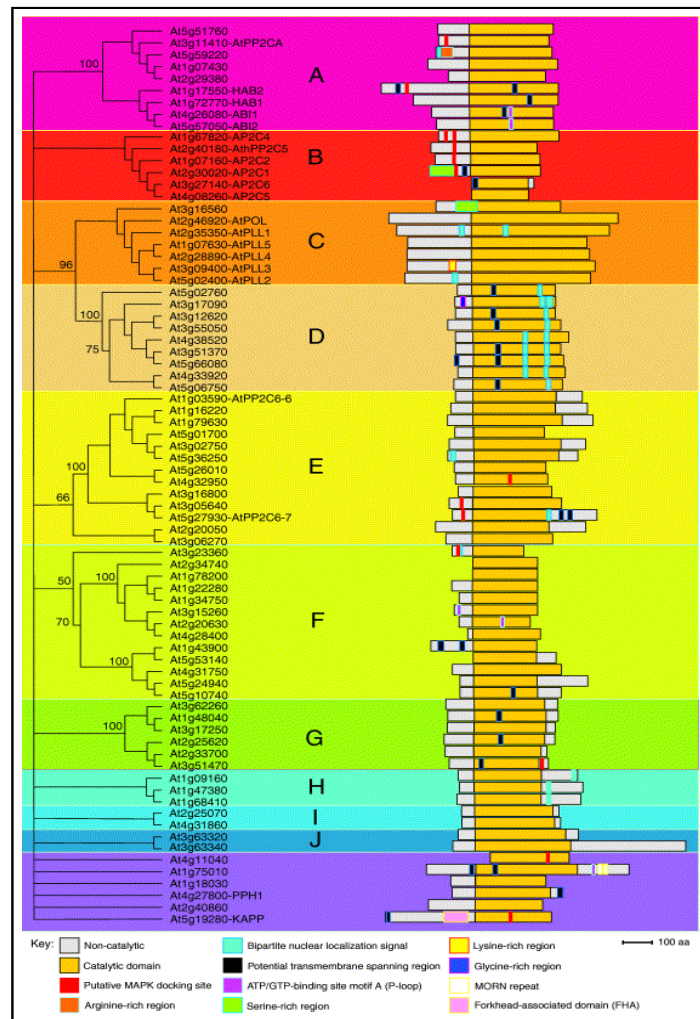
Figure 1-5   Topographic cladogram and domain structure of Arabidopsis type-2C protein phosphatases
Seventy-six Arabidopsis genes were clustered into ten groups (A–J), with the exception of six ungrouped genes (Schweighofer et al., 2004).

In addition, it has been shown for *abi1-1* that the hypermorphic mutant requires a nuclear localization for conveying insensitivity towards ABA responses (Moes et al., 2008).

Moreover, isolated intragenic loss-of-function revertants of the *abi1-1* and *abi2-1* mutants show a recessive ABA-hypersensitive phenotypes and an apparent reduction of PP2C activity in the *in vitro* enzymatic assay. These results indicate that ABI1 and ABI2 are negative regulators in the ABA response (Gosti et al., 1999; Merlot et al., 2001).

Signal transduction in guard cells also showed that *abi1* and *abi2* mutations impair ABA signaling mechanisms including ABA activation of slow anion channels (Pei et al., 1997) and ABA-induced Ca^{2+}_{cyt} elevations but not the Ca^{2+}-induced stomatal closure (Allen et al., 1999). ABI1 phosphatase have been shown to interact with a number of substrates including the homeodomain transcriptional factor ATHB6 (Himmelbach et al., 2002), gluthathione peroxidase 3 (AtGPX3) (Miao et al., 2006), protein kinases OST1, SnRK2.2 and SnRK2.3 (Yoshida et al., 2006; Fujii et al., 2009; Nishimura et al., 2010) and recently

identified family of ABA receptors – RCAR proteins (Ma et al., 2009; Park et al., 2009; Szostkiewicz et al., 2010).

HYPERSENSITIVE TO ABA1 (HAB1), previously named AtPP2C-HA, is one of the closest relatives of ABI1 and ABI2. Constitutive overexpression of HAB1 (*35S:HAB1*) leads to ABA insensitivity of seeds and vegetative tissues, which is consistent with a role as a negative regulator of ABA signaling. The recessive *hab1-1* mutant showed ABA-hypersensitive inhibition of seed germination and growth, enhanced ABA-mediated stomatal closure, and enhanced expression of ABA-responsive genes (Leonhardt et al., 2004; Saez et al., 2004; Saez et al., 2006). Generation of double *hab1-1/abi1-2* and *hab1-1/abi1-3* mutants strongly enhanced plant responsiveness to ABA and drought avoidance, while triple *hab1-1/abi1-2/abi2-2* mutant revealed an extreme response to exogenous ABA, impaired growth and partial constitutive response to endogenous ABA (Saez et al., 2006; Rubio et al., 2009).

In addition, HAB1 was shown to interact with the Arabidopsis SWI3B subunit of SWI/SNF chromatin-remodeling complex and with OST1 kinase (Saez et al., 2008; Vlad et al., 2009).

ABA-HYPERSENSITIVE GERMINATION 1 (AHG1) and 3 (AHG3/PP2CA) appear to play an essential role for ABA signaling in germination and post-germination growth, and both *ahg1-1* and *ahg3-1* mutants do not show any clear ABA-related phenotype in adult plants (Nishimura et al., 2004; Kuhn et al., 2006; Yoshida et al., 2006; Nishimura et al., 2007). Analysis of double *ahg1-1/ahg3-1* mutant revealed stronger hypersensitivity compared to both monogenic mutants, which suggests that AHG1 has specific functions in seed development and germination, shared partially with PP2CA/AHG3 (Nishimura et al., 2007). Additionally, PP2CA appears to interact with inward-rectifying potassium channels AKT2 and AKT3. This interaction is aborted when part of the catalytic domain of PP2CA is deleted. These observations suggest that plant K^+ channels may be directly dephosphorylated by PP2Cs (Vranova et al., 2001; Cherel et al., 2002).

1.4.3   Expression of ABA-regulated genes

Water deficit stresses such as drought and high salinity have an adverse effect on the growth of plants and seriously affect crop productivity. Under such conditions, various biochemical and physiological responses, including the expression of many stress-inducible genes that function in stress tolerance and ABA accumulation, are triggered. Several reports have described drought stress-responsive genes that are induced by ABA (Busk and Pages, 1998; Yamaguchi-Shinozaki and Shinozaki, 2006) and genome

analysis and transcriptional profiling indicate that more than 2.900 genes are responsive to ABA in *Arabidopsis* (Nemhauser et al., 2006).

The molecular analysis of promoters of ABA-responsive genes has led to the identification of several motifs capable of conferring ABA responsiveness to a minimal promoter. One such motif is the ABA-responsive *cis*-acting element ABRE, which leads to ABA-dependent activation of transcription. The ABRE motif contains an ACGT core, 8-10 base pairs sequence known to be recognized by plant bZIP proteins (Hobo et al., 1999; Uno et al., 2000). This sequence was first identified in the *Em* gene from wheat, and in the rice *RAB16* gene (Marcotte Jr et al., 1989; Mundy et al., 1990).

It has been established that a single copy of ABRE is not sufficient for ABA-mediated induction of transcription, but multiple ABREs or the combination of an ABRE with a so-called coupling element (CE) can establish an ABA-responsive complex (ABRC), and thereby confer ABA responsiveness to a minimal promoter. Two coupling elements such as CE1 and CE3 in the barley *HVA1* and *HVA22* genes are necessary for activation by ABA (Shen et al., 1996; Gomez-Porras et al., 2007).

The dehydration-responsive element (DRE) containing the TACCGACAT sequence is another *cis*-acting element which may function as a coupling element for ABRE in the ABA-dependent expression of *Arabidopsis RD29A* gene in response to dehydration and high-salinity stresses (Yamaguchi-Shinozaki and Shinozaki, 1994; Narusaka et al., 2003).

In addition to ABRE motifs, MYC and MYB recognition sites also play an important role in ABA signaling for some stress-inducible genes such as dehydration-responsive gene *RD22* (Abe et al., 2003).

By using ABRE sequences as baits in the yeast one-hybrid screening, ABRE-binding (AREB) proteins or ABRE-binding factors (ABFs) were isolated. The AREB/ABFs encode basic-domain leucine zipper (bZIP) transcription factors (Choi et al., 2000; Uno et al., 2000). Among them, AREB1/ABF2, AREB2/ABF4, and ABF3, are upregulated by dehydration, high-salinity stress and require ABA for full activation (Fujita et al., 2005; Yoshida et al., 2009). The triple *areb1/areb2/abf3* mutant displays enhanced ABA insensitivity and reduced drought stress tolerance in comparison to the single and double knockout mutants of AREB/ABFs transcription factors (Yoshida et al., 2009). The *Arabidopsis* ABA-insensitive 5 (ABI5) gene also encodes basic leucine zipper transcription factor. The *abi5* mutant reveals pleiotropic defects in ABA response, including decreased sensitivity to ABA inhibition of germination and altered expression of some ABA-regulated genes (Finkelstein and Lynch, 2000).

Arabidopsis ABI4 encodes an AP2/ERF transcription factor and acts as an essential activator of its own expression during development, in ABA signaling and in sugar responses (Finkelstein et al., 1998; Bossi et al., 2009). Another ABI gene, ABI3 encodes a

transcription factor that contains a B3 domain, and has been demonstrated to be an important regulator of LEA (late embryogenesis abundant) genes (Parcy et al., 1994). ABI3 was also shown to interact with ABI5 in a yeast two-hybrid assay suggesting that ABI3 might modulate transcriptional activity mediated by ABI5 (Nakamura et al., 2001).

ABA or abiotic stress also induces the expression of some members of the homeodomain-leucine zipper (HD-Zip) family of transcription factors. HD-Zip proteins are characterized by the presence of a homeodomain (HD) and a leucine zipper motif (Zip). The HD domain is involved in DNA binding whereas the Zip domain is involved in protein homo- and heterodimerization (Lee and Chun, 1998). Based on sequence analyses these proteins have been classified into four distinct groups (I-IV). Proteins involved in responses related to abiotic stress and ABA belong to group I and have the ability to recognize and bind the pseudopalindromic sequence CAATTAATTA (Elhiti and Stasolla, 2009). A member of this class, ATHB6, is a crucial regulator in the ABA signal pathway. It has been demonstrated that ATHB6 interacts with ABI1 but not with the point-mutated, catalytically inactive *abi1*. *Arabidopsis* plants with constitutive expression of ATHB6 displays a reduced sensitivity towards ABA during seed germination and stomatal closure. Thus, the homeodomain protein ATHB6 acts as a negative regulator of ABA signaling (Himmelbach et al., 2002).

In addition, the characterization of the mutants *abh1, sad1* and *hyl1* revealed that they are hypersensitive to ABA in seed germination and stomatal regulation, and their corresponding genes encode proteins involved in RNA metabolism. ABH1 encodes the large subunit (CBP80) of the mRNA 5' cap-binding complex, while SAD1 gene encodes a Sm-like small nuclear ribonuleoproteins (snRNAs) that participate in mRNA splicing, export or degradation (Hugouvieux et al., 2001; Xiong et al., 2001; Hugouvieux et al., 2002).

HYL1 encodes a double stranded RNA-binding protein important for miRNA biogenesis (Han et al., 2004). The *hyl1* mutant is hypersensitive to ABA in seed germination and root growth, and shows reduced sensitivity to auxin and cytokinin (Lu and Fedoroff, 2000). These findings indicate that there is a link between mRNA processing and modulation of ABA signal transduction.

1.5 The aim of this work

The plant hormone abscisic acid (ABA) acts as a developmental signal and as an integrator of environmental cues such as drought and cold. The ABA response triggered by plants due to abiotic stress depends on the coordinated interactions between positive and negative regulators. Although many important ABA signaling components have been identified, insufficient evidence exists on the interactions of some candidate proteins with known ABA signaling components. Over the past few years, several distinct proteins have been reported to encode ABA receptors, but their role in ABA perception is contested.

Key regulators of diverse ABA-mediated responses are two proteins ABI1 and ABI2. Both are homologous protein phosphatases 2C (PP2Cs) that act to a large extent in a redundant manner as negative regulators of ABA signaling. Regulatory component of ABA receptor 1 (RCAR1) and RCAR3 are interacting partners of these PP2Cs and they were recently characterized (Ma, 2010).

In this work, the major interest was to better understand the role of RCAR protein family in ABA responses. The yeast two-hybrid system and bimolecular fluorescence complementation analysis were recruited to confirm the physical interaction between RCARs and PP2Cs.
To elucidate the function of the protein interactions, the ectopic expression of RCARs and ABI1/2 genes was studied in a protoplast transient expression system. In addition, RCAR1 cellular localization was established via histochemical GUS staining.
Moreover, the PP2C enzymatic assays were used to examine a possible regulatory role of PP2Cs and RCARs in a complex with ABA and other biologically relevant ligands.

.

2 Materials and Methods

2.1 Materials

2.1.1 Chemicals

General chemicals

All chemicals used in this work were of analytic grade or highest purity and purchased from Sigma-Aldrich (Munich, Germany), Merck KGaA (Darmstadt, Germany), Roth (Carl Roth GmbH & Co. KG, Karlsruhe, Germany), J.T.Baker (Deventer, Holland), Serva (Serva Electrophoresis GmbH, Heidelberg, Germany), Qiagen (Hilden, Germany) and Macherey-Nagel (Düren, Germany).

Molecular weight standards and primers

DNA ladders and prestained protein markers were provided by MBI Fermentas GmbH (St. Leon-Rot, Germany). λ-Hind III was produced by Hind III digestion of λ-DNA.

All primers were synthesized by MWG-Biotech GmbH (Ebersberg, Germany).

Abscisic acid (ABA)

Abscisic acid was purchased from Lomon Bio Technology ((S)-ABA; Sichuan Province, China,), Sigma-Aldrich, ((R)-ABA; Munich, Germany) and A.G. Scientific (*trans* (R,S)-ABA; San Diego, USA). The ABA enantiomers and *trans* (R,S)-ABA were analyzed for purity by HPLC on a Cyclobond I column (Sigma-Aldrich), with stereoselective separation and isocratic elution (volume ratios of water:methanol:acetic acid = 65:35:0.25). Detection was at 265 nm. *Trans* (R,S)-ABA was purified from contaminating (R,S)-ABA by preparative HPLC on a Kromasil C8 column from Knauer (Berlin, Germany). Separation was achieved by a methanol gradient from 10 to 80% (initial volume ratios of water:methanol:acetic acid = 90:10:0.25 and final ratios 20:80:0.25) in 20 minutes.

2.1.2   Equipment

Equipment	Model	Company
CCD Camera	ORCAII ERG	Hamamatsu Photonics
Centrifuge	Avanti J-25	Beckman Coulter
Electrophoresis Power Supply	EPS 200/EPS 3500 XL	Pharmacia Biotech
Electrotransfer System	Trans-Blot Semi-Dry Transfer Cell	BioRad
Fluorescence Micropscope	Fluoview FV1000	Olympus
Fluorescence Micropscope	BX61	Olympus
FTICR Mass Spectrometer	12 Tesla FTICR-MS ApexQ System	Bruker Daltonics
Gel electrophoresis unit	E844 (400 V-400 mA)	Consort
Lab Balance	Handy	Sartorius analytic
Laboratory Incubator	ED 53	WTC Binder
Luminometer	Flash n glow	Berthold
Magnetic Stirrer	Stuart	Bibby
Micro-Calorimeter	VP-ITC	MicroCal
Microcentrifuge	5415D	Eppendorf
PCR Cycler	T-Gradient	Biometra
pH meter	pH 526	WTW
Photometer	Ultrospec 2000 UV/Visible Spectrometer	Pharmacia Biotech
Photometer	Reprostar 3	Camag
Pipetman		Gilson
Plate Reader	HTS 7000 Plus	Perkin Elmar
Plate Reader	Synergy 2	BioTek
SDS-PAGE unit	Mini-PROTEAN Tetra Cell	BioRad
SDS-PAGE unit	PerfectBlue Dual Gel System Twin ExW S	Peqlab
Spectropolarimeter	J-715 (PTC343 peltier unit)	Jasco
SpeedVac	Bachofer Vacuum Concentrator	Bachofer, Reutlingen
Sterile Bench	Laminar Flow Workstation	Microflow
Thermomixer	Comfort	Eppendorf
ThermoShaker	Laboshake	Gerhardt
Ultrasonic Homogenizer	Sonoplus	Bandelin electronic
UV	P91D	Mitsubishi
Vortex	MS1	IKA

2.1.3   Bacterial strains

Escherichia coli strains

Strain	Genotype	Resistance	Company
DH5α	F– Φ80lacZΔM15 Δ(lacZYA-argF) U169 recA1 endA1 hsdR17 (rK–, mK+) phoA supE44 λ– thi-1 gyrA96 relA1	no	Invitrogen
XL1-Blue	recA1 endA1 gyrA96 thi-1 hsdR17 supE44 relA1 lac [F´ proAB lacIqZΔM15 Tn10 (Tetr)]	Tetracycline	Invitrogen
M15[pREP4]	K12, NalS strS rifS thi-lac- ara- gal+ mtl-, F- recA+ uvr+ lon+ [pREP4 KanR]	Kanamycin	Qiagen
Rosetta(DE3)pLysS	F- ompT hsdSB(RB-mB-) gal dcm λ(DE3 [lacI lacUV5-T7 gene 1 ind1 sam7 nin5]) pLysSRARE (CamR)	Chloramphenicol	Novagen

E. coli strains were cultured at 37°C either on agar plates or in liquid LB medium with shaking at 200 rpm.

LB (Luria-Bertani) medium:

NaCl	10 g/l
Peptone	10 g/l
Yeast extract	5 g/l
Agar (for plates)	18 g/l
Autoclaved, pH 7.0	

After the medium was cooled down to 60°C, antibiotics were applied.

Ampicillin: 100 mg/l (stock solution 100 mg/ml in ddH_2O)

Kanamycin: 50 mg/l (stock solution 50 mg/ml in ddH_2O)

Chloramphenicol: 34 mg/l (stock solution 80 mg/ml in 100% EtOH).

Agrobacterium tumefaciens strains

Strain	Genotype	Resistance	Company
C58pGV3101	Ti-Plasmid: pPMP90 (Koncz and Schell, 1986)	Rifampicin and Gentamycin	Csaba Koncz (MPI Cologne)

A. tumefaciens strain was cultured at 28-30°C either on agar plates or in liquid LB medium with shaking at 200 rpm. The medium was supplemented with antibiotics such as rifampicin at final concentration of 12.5 mg/l.

For a long-term storage of bacterial strains sterile glycerol stocks (0.5 ml 87% glycerol (v/v) mixed with 1 ml of bacterial culture) were used. The LB culture was then frozen in liquid nitrogen and stored at – 80°C.

2.1.4 Plant materials

Arabidopis thaliana

All the *Arabidopsis* lines used in this study were in the ecotype Columbia (Col), Landsberg *erecta* (La-*er*) and Reschiev (RLD). These plants were used for stable transformation, protoplast preparation and as a source of wild-type DNA and RNA. All accessions were received from the Arabidopsis Biological Resource Center (ABRC), Ohio, USA.

2.1.5 Vector and primers

Vectors and primers used for transient expression in protoplasts

The *pRAB18::LUC* and *pRDB29::LUC* reporter plasmid have been described previously by (Moes et al., 2008). The effector plasmids used for transient expression in protoplasts are all derivatives of pBI221. The plasmids pBI221-*p35S::ABI1,*and *-p35S::abi1* were created by Dr. Danièle Moes by replacing the glucuronidase gene of pBI221 by a BamHI-Eco147I fragment of ABI1 and abi1, respectively. The corresponding ABI2/abi2 constructs (pBI221-*p35S::ABI2, -p35S::abi2)* were generated accordingly by cloning BamHI und Ecl136II cDNA fragments into pBI221. The cDNA was obtained by using the primer pair 5´-CCTAGATCTATGGACGAAGTTTCTCCT-3’, 5´-CCTTCTTTTTCAATTCAAGG-3’.
The plasmids pBI221-*p35S::RCAR1* and pBI221-*p35S::RCAR3* were generated by Ma Yue by replacing the GUS-NOS terminator cassette in pBI221 with the RCAR1/3-NOS terminator cassette from pBI121-RCAR1/3 via BamHI and EcoRI.

Vectors and primers used for generation RCAR1-GUS fusion construct

To obtain the endogenous promoter RCAR1-GUS fusion construct, a 3.4 kb DNA fragment encompassing 2.6 kb of endogenous promoter and 5’UTR, plus the entire RCAR1 coding region was amplified from *Arabidopsis* with the primer pair
5’-CCCAACCGCGGTAAGAGTTGTGTGTGTGTTAATG-3’ and
5’-TATCCGGATCCCTGAGTAATGTCCTGAGAAGC-3’.
The DNA fragment was cloned into pSKAsclGUSTer via SacII and BamHI, and the endogenous promoter::RCAR1:GUS::NOS terminator cassette was subsequently cloned into the binary vector pBIAsclBar via AscI. RCAR1-GUS fusion was generated by Ma Yue.

Vectors and primers used for generation RCAR1/3-RNAi construct

The RCAR1/3-RNAi constructs were generated by amplifying a fragment of RCAR1/3 cDNA with the primer pairs

5'-CCGGAATTCTGTACCTCTGCTCTTGTC-3',

5'-GCCGGTACCGACGAGTAATTCTTAAGTCTG-3' (sense construct) and

5'-GAAGGATCCTGTACCTCTGCTCTTGTC-3',

5'-CCATCGATGACGAGTAATTCTTAAGTCTGTG-3' (antisense construct),

which was cloned into pHannibal. The control RNAi-vector (cRNAi) was similarly designed using a partial sequence of ACO2 (At1g62380) and the primer pair

5'-TCCCTCGAGGGATCCGACGGCCATGAAAGACTTTGG-3',

5-GTTGGTACCATCGATCCAAGATTGATGACAATAGAG-3'.

The amplified fragment was inserted into pHannibal via XhoI and KpnI sites (sense orientation) or BamHI and ClaI sites (antisense orientation). RCAR1/3-RNAi constructs were generated by Ma Yue.

Vectors and primers used for generation split-YFP constructs

To generate the split-YFP constructs, RCAR1 and RCAR3 cDNA with no stop codon were linked to the N-terminally truncated YFP genes via BamHI and SmaI sites in pSPYNE-35S (YFP^{N1-155}, aa 1-155) and pSPYCE-35S (YFP$^{C156-239}$) vectors (Walter et al., 2004). The cDNA of RCAR1 with no stop codon was amplified with the primer pair

5'-TAAGGATCCATGATGGACGGCGTTG-3' and

5'-TAACCCGGGCTGAGTAATGTCCTGAG-3' to generate *p35S::SPYNE:RCAR1* and *p35S::SPYCE:RCAR1.* The cDNA of RCAR3 was amplified with the primer pair

5'-ATCTTGGATCCATGGAAGCTAACGGG-3' and

5'-AATACCCGGGGACTCTCGATTCTGTCG-3'. to generate *p35S::SPYNE:RCAR3* and *p35S::SPYCE:RCAR3.* Split-YFP constructs were generated by Ma Yue.

Vectors and primers used for the heterologous expression of RCARs and PP2Cs RCAR1 and RCAR3

For heterologous expression, the cDNAs of RCAR1 (At1g01360) and RCAR3 (At5g53160) were amplified with the primer pairs

5'-TAATCTAGCTAGCGTCGACATATGATGGACGGCGTTGAAGGCGGC-3',

5'-TGGGAGCTCGTCGACTGATTATGTAGTTCACTG-3' and

5'-ATTCTGGATCCGCATGCATGGAAGCTAACGGG-3',

5'-TGGGAGCTCCTTTAGACTCTCGATTCTGTC -3', respectively. The PCR fragments were subsequently cloned into the pQE30 vector (Qiagen, Germany), yielding pQE30-

RCAR1 (cloning via a SalI site) and pQE30-RCAR3 (cloning via BamHI and SacI sites). RCAR1/3 constructs were generated by Ma Yue.

RCAR9 and RCAR10

For heterologous expression, the cDNAs of RCAR9 (At2g40330) and RCAR10 (At2g38310) were amplified with the primer pairs

5'-GATCGCATGCCAACGTCGATACAGTTTCAGAG-3',

5'-GATCAGATCTCGAGAATTTAGAAGTGTTCTCGGCG-3' and

 5'-GATCGCATGCTTGCCGTTCACCGTCCTTCTTCC-3',

5'-GATCGGATCCCAGAGACATCTTCTTCTTGCTCTC-3', respectively. The PCR fragments were subsequently cloned into pQE70 vector (Qiagen), yielding pQE70-RCAR9 (cloning via SphI and BglII sites) and pQE70-RCAR10 (cloning via SphI and BamHI sites). A cDNA clones for RCAR9 and RCAR10 were provided by Arabidopsis Biological Resource Center (ABRC), USA. RCAR9 and RCAR10 constructs were generated by bachelor students Markus Kornprobst and Simone Vuong, respectively.

RCAR13 and RCAR14

For heterologous expression, the cDNAs of RCAR13 (At1g73000) and RCAR14 (At2g26040) were amplified with the primer pairs

5'-TATAGCTAGCAATCTTGCTCCAATCCATG-3',

5'-TATACTCGAGGGTCGGAGAAGCCGTGGAAATG-3' and

5'-TATACATATGAGCTCATCCCCGGCCGTG-3',

5'-TATACTCGAGTTCATCATCATGCATAGGTGC-3', respectively. The PCR fragments were subsequently cloned into pET-24a(+) (Novagen), yielding pET-24a(+)-RCAR13 (cloning via NheI and XhoI sites) and pET-24a(+)-RCAR14 (cloning via NdeI and XhoI sites). A cDNA clones for RCAR13 and RCAR14 were provided by Arabidopsis Biological Resource Center (ABRC), USA. RCAR13 and RCAR14 constructs were generated by Dr. Jana Wünschmann.

PP2Cs

For heterologous expression of PP2Cs, the corresponding cDNAs were amplified with the primer pairs 5'-GAGCTGCATGCATGGAGGAGATGACTCCCGCAGTTG-3',

5'-CTCGAGGATCCGGTTCTGGTCTTGAACTTTC-3' (HAB1, At1g72770),

5'-GAGTCGGATCCATGGGTACATACCTAAGTTCTCC-3',

5'-CTCGAAGATCTGCTTGATGAGCTCGGCTCATCT-3' (At2g25070),

5'-GAGCTGCATGCATGCCCAAGATCTGCTGCTCTCGTTCC-3',

5'-CTCGAGGATCCTCTAAACCGGACAACAATGC-3' (At1g78200) and

5'-GATCGCTAGCATGGCTGGGATTTGTTGCGG-3',

5'-GATCGCGGCCGCAGACGACGCTTGATTATTCC-3' (PP2CA, At3g11410). The PCR fragments were subsequently cloned into pQE70 vector (Qiagen) and pET-21a(+) (Novagen), yielding pQE70-HAB1 (cloning via SphI and BamHI sites), pQE70-At2g25070 (cloning via BamHI and BglII sites), pQE70-At1g78200 (cloning via SphI and BamHI sites) and pET-21a(+)-PP2CA (cloning via NheI and NotI sites). The cDNA clones for HAB1, At2g25070 and At1g78200 were provided by ABRC (USA), whereas for PP2CA by RIKEN (Japan). The PP2CA construct was generated by bachelor student Sebastian Pfeilmeier, whereas the HAB1, At2g25070 and At1g78200 by Christian Kornbauer.

2.2 Methods

2.2.1 Methods for DNA analysis

2.2.1.1 Genomic DNA isolation from plants

Method of genomic DNA isolation from plants was modified after (Murray and Thompson, 1980). A single rosette leaf was grinded in a 1.5 ml reaction tube and then incubated with 300 µl of 2 x CTAB buffer at 65°C for at least 10 minutes (up to several hours). After cooling down the sample, 300 µl of chloroform was added and then spinned briefly (14.000 rpm) to separate the phases. Then the upper, aqueous phase was transferred into a fresh reaction tube. 300 µl of 2-propanol was added, mixed well and centrifuged (14.000 rpm) to pellet the DNA. After centrifugation, supernatant was removed and the pellet was washed with 500 µl of 70% (v/v) ethanol. After this step sample was spinned down again and air dried at 37°C for 10 minutes. In the last step the DNA pellet was dissolved in 50 µl of 0.1 x TE buffer.

2x CTAB buffer: 2% Cetyl-Trimethyl-Ammonium Bromide (CTAB)
1.4 M NaCl
100 mM Tris HCl (pH 8.0)
20 mM EDTA
Not auctoclaved !

1 x TE buffer: 10 mM Tris HCl (pH 8.0)
1 mM EDTA

Chloroform

2-Propanol

70% Ethanol

2.2.1.2   Plasmid DNA isolation

Mini-preparation of plasmid DNA

2 ml of overnight culture was spinned down at 4000 rpm for 5 minutes to pellet the cells. The cells were re-suspended in 200 µl of Solution 1 and then mixed gently with 200 µl of Solution 2, kept on ice for 5 minutes. After this 200 µl of Solution 3 was added and mixed by inverting the tube 5 times. After 3 minutes of incubation at room temperature the cell debris was pelleted (14.000 rpm) for 5 minutes and the supernatant was transferred to a new tube with 1 ml of (-20°C) 96% ethanol. The mixture was then centrifuged for 5 minutes at 14.000 rpm, at 4°C. The pellet was washed with 500 µl of 70% (v/v) ethanol, then centrifuged for 5 minutes (14.000 rpm) and air-dried for 30 minutes. The dried DNA was re-suspended in 50 µl MQ water or 0.1x TE buffer with 25 µg RNase/ml.

<u>**Solution 1:**</u>	50 mM Glucose 25 mM Tris HCl (pH 8.0) 10 mM EDTA
<u>**Solution 2 (Lysis Buffer):**</u>	0.2 M NaOH 1 % SDS
<u>**Solution 3:**</u>	3 M NaAc (pH 4.8-5.2)
<u>**0.1 x TE buffer:**</u>	1 mM Tris HCl (pH 8.0) 0.1 mM EDTA

Ethanol (-20°C) 96% and 70%

Midi-preparation of plasmid DNA

Isolation of higher amount of plasmid DNA was performed according to JetStar-MIDI Kit (GENOMED, Löhne).

2.2.1.3   Quantification of the DNA concentration

To determine the DNA concentration, spectrophotometric (OD_{260nm}) DNA quantification was performed. According to the Beer-Lambert Law there is a linear ralationship between the amount of the light absorbed and concentration of the absorbing molecule ($c = A \times d^{-1} \times \varepsilon^{-1}$). At a wavelength of 260 nm, the average extinction coefficient for double-stranded DNA is $\varepsilon = 20$ µl $\times$ µg^{-1} $\times$ cm^{-1}. The optical density (OD_{260nm}) of 1 corresponds to a concentration of 50 µg/ml for double-stranded DNA.

2.2.1.4   Heat-shock transformation of E. coli with plasmid DNA

Competent cells from *E. coli* were thawn on ice, then gently mixed with 2-10 µl of plasmid DNA and incubated on ice for 30 minutes. Heat-Shock treatment of the cells was applied in the water bath at 42°C for exactly 30 seconds. Then the heat-shocked cells were immediately transferred into ice, and kept for 5 minutes. The cells were mixed with 400 µl of LB medium without antibiotics, and incubated at 37°C for 1 hour in thermo-mixer. Afterwards 10-100 µl of transformation were spread onto LB agar plates with appropriate antibiotics.

2.2.1.5   Polymerase chain reaction (PCR)

PCR products were amplified from the DNA template using GoTaq Polymerase (Promega).

Standard components of PCR reaction tube:

Components	Final concentration	Volume [µl] for 20 µl of total reaction mixture
DNA template	1-50 ng	1
10x Buffer*	1x	2
MgCl2 (25 mM)	2.5 mM	2
dNTP-Mix (10 mM)	0.5 mM	1
Forward-Primer (20 µM)	1 µM	1
Reverse-Primer (20 µM)	1 µM	1
DNA polymerase (5U/µl)	0.5 U	0.1
MQ H_2O		filled up to 20 µl

* For GoTaq Polymerase 4 µl of 5x Buffer were used.

Standard PCR Program:

Time	Temperature	Function	No. of cycles
3 min	95°C	Denaturation	1
30 sec	95°C	Denaturation	30[†]
30 sec	50-60°C	Primer annealing	30[†]
1 min*	72°C	Elongation	30[†]
5 min	72°C	Final elongation	1

[†] The number of the cycles differ between 28-35 depending on the primers
 * Elongation time depends on the length of the fragment, which need to be amplified (1 min/kb)

2.2.1.6   Electrophoresis of DNA in agarose gels

To separate DNA fragments which have been generated by digestion of plasmid DNA and to determine their size and concentration, agarose gel electrophoresis is necessary. The agarose powder was mixed with 1xTAE buffer to the desired concentration (0.8-2.0%),

then heated in a microwave until completely melted. After cooling the solution to 60°C, ethidium bromide was added (final concentration 1 µg/ml). DNA samples were mixed with 6x loading buffer (final concentration 1x) and loaded into wells. The gel was run at 200 V and 400 mA.

Et-Br stock solution: 10 mg EtBr in 1 ml ddH$_2$O

50 x TAE Buffer: 242 g/l Tris-Base
57.1 ml/l Acetic Acid
100 ml/l 0.5 M EDTA (pH 8.0)

6x Loading Dye: 50% (v/v) Glycerol
0.25% (w/v) Orange G
1 mM EDTA (pH 8.0)

2.2.1.7 DNA markers

λ-Hind III-Marker is suitable for sizing and quantifying linear double-stranded DNA molecules of between 125 bp and 23.1 kb. The marker was prepared by complete digestion of λ-DNA (MBI Fermentas, St. Leon-Rot, Germany) with Hind III restriction enzyme. The 1 kb DNA-ladder, 100 bp ladder and 100 bp ladder Plus were provided by MBI Fermentas (Figure 2-1).
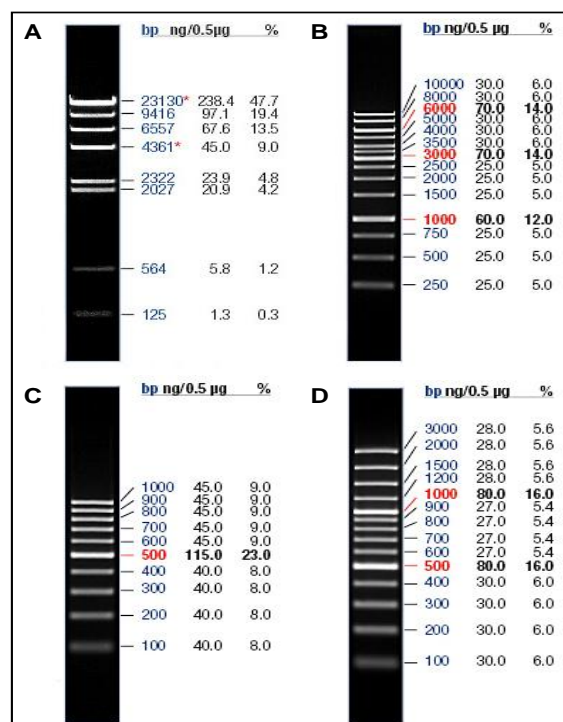
Figure 2-1   DNA markers
(A) *λ-Hind III-Marker,* **(B)** *1 kb DNA-ladder,* **(C)** *100 bp ladder and* **(D)** *100 bp ladder Plus.*

2.2.1.8   Extraction of DNA fragment from agarose gel

The band of interest was excised from the agarose gel with a razor blade and further purified by QIAquick Gel Extraction Kit (Qiagen).

2.2.1.9   Digestion of DNA with restriction enzymes

The restriction enzymes were provided by New England BioLabs (NEB) and MBI Fermentas. For restriction digestion of the plasmid or any DNA fragment, 0.5-1 µg of DNA was used. Every 1 µg of plasmid DNA was diluted in the appropriate restriction buffer (10x) and digested with 1-2 U of restriction enzyme. Incubation time differed from 2 hours to overnight at 37°C. Digestion was checked on a gel if necessary.

2.2.2   Methods for RNA analysis

2.2.2.1   RNA isolation

Total RNA was isolated from 5-day old *Arabidopsis* seedlings which were growing on MS agarose medium. If necessary seedlings were treated with ABA in the appropriate concentration before RNA isolation. After grinding ~100 mg of the frozen (liquid nitrogen) seedlings, the RNA was isolated by using Rneasy Plant Mini Kit (Qiagen). The total RNA was stored at -80°C.

2.2.2.2   Quantification of the RNA concentration

To determine the RNA concentration and purity, UV spectroscopy was used. The absorbance of a diluted RNA (1:100) sample was measured at 260 and 280 nm. The nucleic acid concentration was calculated using the Beer Lambert Law. At a wavelength of 260 nm, the average extinction coefficient for RNA is $\varepsilon = 25$ µl x µg^{-1} x cm^{-1}. The optical density (OD_{260nm}) of 1 corresponds to a concentration of 40 µg/ml for single-stranded RNA. The A_{260}/A_{280} ratio was used to assess RNA purity. An A_{260}/A_{280} ratio of 1.8-2 was an indication of highly purified RNA.

2.2.2.3   RT-PCR

Synthesis of the first strand cDNA from mRNA template was performed by using the cDNA Synthesis Kit from Promega. 1-5 µg of total RNA isolated from *Arabidopsis* seedlings was used as a template. 1 µl of oligo(dT)$_{18}$ primer (0.5 µg/µl) and DEPC water (up to 11 µl) were added and incubated at 70°C for 5 minutes. After cooling down, the sample was centrifuged for a short time. Then the mixture was supplemented with 4 µl of 5x reaction buffer, 1µl of ribonuclease inhibitor (20 U) and 2 µl of 10 mM dNTPs mixture.

After incubation at 37°C for 5 minutes, 2 µl of M-MuLV reverse transcriptase (20 U) were added. The reaction was incubated at 37°C for 1 hour and stopped by heating at 70°C for 10 minutes. In the next step 0.5-1 µl of synthesized cDNA was used as a template in the PCR reaction consisting of 28 cycles. In order to quantify mRNA, actin primers were used. After RT-PCR samples were analysed on agarose gels with EtBr staining.

2.2.3 Methods for protein analysis

2.2.3.1 Protein extraction from Arabidopsis thaliana

In order to extract protein from *Arabidopsis*, the plant leaves (20-30 mg) were frozen in liquid nitrogen, and then grinded to fine powder. The material was incubated with 250-300 µl of 2D-buffer at 95°C for 15 minutes. Afterwards the sample was centrifuged at 16.000 rpm for 15 minutes and the supernatant was transferred to a fresh Eppendorf tube. The sample was checked by SDS-PAGE electrophoresis.

2D-Buffer:
50 mM Tris HCl (pH 6.8)
2% SDS
36% Urea (8 M)
30% Glycerol
5% β-mercaptoethanol
0.5% Bromophenol Blue
1.25 mM NaOH

2.2.3.2 Expression of RCARs and PP2Cs in E. coli

All His-tagged proteins were expressed in *Escherichia coli* by using pQE30, pQE70, pET21a(+) and pET24a(+) clones. For protein expression, cells were grown overnight in 20 ml LB broth and used for inoculation of 1 litre of culture. The cells were grown at 37°C with vigorous shaking until an OD_{600} of 0.5-0.6 was reached. Protein expression was subsequently induced by administration of IPTG (0.5 mM final concentration) and cells were harvested by centrifugation at 4000 x g for 20 min, 2 hours (PP2Cs) or 1-4 hours (RCARs) after induction. The cell pellet was used directly or stored overnight at - 20°C prior to purification.

2.2.3.3 Protein purification under denaturing conditions

For purification of highly expressed His-tagged proteins forming insoluble aggregates known as inclusion bodies, purification under denaturing conditions with subsequent refolding step was used. The cell pellet (3-4 g) was thawn on ice and resuspended in 10 ml of Binding Buffer. The cells were stirred for 15-60 minutes at room temperature, and

then the lysate was centrifuged at 10.000 x g for 20 minutes to pellet the cellular debris. A cleared protein lysate was loaded onto a Ni-TED 2000 column (Macherey-Nagel, Germany) equilibrated with Binding Buffer. The column with bound protein was washed with 4 ml of Binding Buffer and then step gradient was applied in order to completely remove urea from the protein solution (initial concentration of urea was 8 M and final 0 M). In order to remove unspecifically bound proteins, 8 ml of Washing Buffer were applied to the column. The recombinant protein was then eluted with 3 ml of Elution Buffer. In order to remove imidazole, the recombinant protein was dialysed three times against Dialysis Buffer and stored at - 80°C.

Binding Buffer: 100 mM NaH_2PO_4
10 mM Tris HCl
8 M Urea
pH 8.0

Refolding Buffer A: 20 mM Tris HCl
500 mM NaCl
20% Glycerol
6 M Urea
pH 7.4

Refolding Buffer B: 20 mM Tris HCl
500 mM NaCl
20% Glycerol
pH 7.4

Washing Buffer: 20 mM Tris HCl
150 mM NaCl
20% Glycerol
5 mM Imidazole
pH 7.4

Elution Buffer: 20 mM Tris HCl
150 mM NaCl
20% Glycerol
250 mM Imidazole
pH 7.4

Dialysis Buffer: 100 mM Tris HCl
100 mM NaCl
2 mM dithiothreitol
20% Glycerol (only for storage at - 80°C)
pH 7.9

2.2.3.4 *Protein purification under native conditions*

The most common method of protein purification used in this study was purification under native conditions. The method was used when the recombinant proteins were well expressed in *E. coli* and remained in the cytoplasm in their native configuration.

The cell pellet (3-4 g) was thawn on ice, lysed in 10 ml of Lysis Buffer and treated with lysozyme (1 mg/ml) for 30 min. Cells were disrupted by sonication on ice (Bandelin Sonoplus; six times for 10 sec with 10 sec cooling intervals; 5 cycles and 80% of maximal sonicator power). A cleared protein lysate was obtained after centrifugation at 30.000 x g for 30 minutes and loaded onto a Ni-TED 2000 column (Macherey-Nagel, Germany). In order to remove unspecifically bound proteins, 8 ml of Washing Buffer were applied to the column. Proteins of interest were eluted with 3 ml of Elution Buffer and dialysed three times against Dialysis Buffer.

Lysis Buffer: 50 mM NaH_2PO_4
                      300 mM NaCl
                       5 mM Imidazole
                       pH 8.0

Washing Buffer: 50 mM NaH_2PO_4
                      300 mM NaCl
                      20 mM Imidazole
                      pH 8.0

Elution Buffer: 50 mM NaH_2PO_4
                      300 mM NaCl
                      250 mM Imidazole
                      pH 8.0

Dialysis Buffer: 100 mM Tris HCl
                      100 mM NaCl
                      2 mM dithiothreitol
                      pH 7.9

2.2.3.5 *Determination of protein concentration*

Protein concentration was determined on SDS-PAGE gels stained with Coomassie Blue or Silver, respectively. The bovine serum albumin (BSA) at defined concentration was used as a protein standard (Ramagli, 1985).

2.2.3.6   SDS polyacrylamide gel electrophoresis (SDS-PAGE)

SDS-PAGE was performed as described by (Laemmli, 1970) with minor modifications. In this work, 15% separating gel and 4% stacking gel were used. Protein samples before loading on a gel were mixed with 2 x Loading Buffer and heated at 95°C for 5 minutes. The gel was run at first with low voltage (80 V) and then increased to a higher voltage (120-200 V) when the protein samples entered the separating part of the gel (Bio-Rad and Peqlab with the gel size (W x L) of 8.6 x 6.8 cm and 20 x 10 cm, respectively). The electrophoresis continued until the blue dye has reached the bottom of the gel.

	15% Separating Gel	4% Stacking Gel
Acrylamid solution	5.0 ml	390 µl
ddH2O	2.3 ml	2.3 ml
Buffer for Separating Gel	2.5 ml	-
Buffer for Stacking Gel	-	255 µl
10% SDS	100 µl	30 µl
TEMED	5 µl	3 µl
10% APS	50 µl	15 µl
Total volume	10 ml	3 ml

Acrylamid Solution: 30% (w/v) Acrylamid / 0.8% Bisacrylamid

Buffer for Separating Gel: 1.5 M Tris HCl, pH 8.8

Buffer for Stacking Gel: 0.5 M Tris HCl, pH 6.8

SDS Solution: 10% (w/v) SDS

TEMED: not diluted

APS Solution: 10% (w/v) Ammonium persulfate

SDS Running Buffer (1x):   25 mM Tris base
                                 192 mM Glycine
                                 0.1% SDS

2 x Loading Buffer: 90 mM Tris HCl, pH 6.8
                                 20% Glycerol
                                 2% SDS
                                 0.02% Bromophenol blue
                                 100 mM DTT

2.2.3.7   Protein markers

PageRuler™ Prestained Protein Ladder and PageRuler™ Prestained Protein Ladder Plus (MBI Fermentas) were used in this study (Figure 2-2).
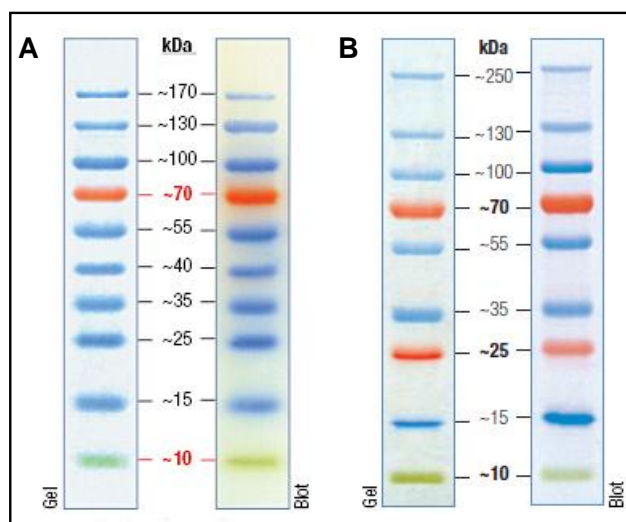
Figure 2-2   Protein markers
(A) PageRuler™ Prestained Protein Ladder and (B) PageRuler™ Prestained Protein Ladder Plus.

2.2.3.8   Coomassie Blue staining

In this study rapid Coomassie Blue Staining was used as described by (Wong et al., 2000). The SDS-PAGE gels immersed in the Staining Solution were heated in 1000 W output microwave oven on full power for 2 minutes. Afterwards the gels were cooled at room temperature for approximately 5 minutes with gentle shaking. After this step the gels were placed in Destaining Solution and microwaved for 1 minute 30 seconds. The gels were then allowed to cool at room temperature for 5 minutes with gentle shaking. At this point, protein bands containing 5 ng or more could be observed.

Staining Solution: 0.05% Coomassie R-250
                                             25% Isopropanol
                                             10% Acetic Acid

Destaining Solution: 10% Acetic Acid

2.2.3.9   Silver staining

Silver staining of SDS-PAGE gels was as described by (Blum et al., 1986). The SDS-PAGE gels were incubated in Fixation Solution for at least 1 hour to prevent the diffusion of separated proteins. The gel was washed 3 times for 20 minutes in 50% ethanol and soaked for exactly 1 minute in Sensitizing Solution, then rinsed 3 x 20 seconds with ddH$_2$O to remove the excess thiosulfate from the gel surface. Following, the gel was incubated in Staining Solution for 20 minutes, then rinsed 3 x 20 seconds with ddH$_2$O. In order to visualize the protein bands, the gel was incubated in Developing Solution until the bands reached the desired intensity. The staining reaction was stopped by applying Terminating Solution.

Fixation Solution: 50% Methanol
                                             12% Acetic Acid
                                             0.05% Formaldehyde (37%)

Sensitizing Solution: 0.02% Na$_2$S$_2$O$_3$·5H$_2$O

Staining Solution: 0.2% AgNO$_3$

Developing Solution: 6% Na$_2$CO$_3$
                                             0.0004% Na$_2$S$_2$O$_3$·5H$_2$O
                                             0.05% Formaldehyde (37%)

Terminating Solution: 50% Methanol
                                             12% Acetic Acid

2.2.3.10   Western Blot

Proteins separated by SDS-PAGE were transferred onto a Protran® nitrocellulose membrane (Whatman, Schleicher & Schuell, Germany) by using a Semi-Dry Transfer Cell (BioRad). The gel, membrane and filter paper (Whatman) were soaked in the Transfer Buffer. Then a blot sandwich consisting of 3 layers of filter paper, pre-wetted membrane, gel and again 3 x filter paper was prepared. All formed air bubbles were rolled out of the blot sandwich. The electrotransfer was run at 25 V, 200 mA for 1 hour.

Transfer Buffer: 25 mM Tris HCl
                                             192 mM Glycine
                                             20% Methanol
                                             pH 8.3

Afterwards, in order to block the unspecific binding sites of antibody, the membrane was soaked in Blocking Buffer at room temperature for 1 hour with shaking or overnight at 4°C. After blocking, the membrane was incubated in 1x TBST buffer with the primary antibody at room temperature for 1 hour with shaking or overnight at 4°C. After the membrane was washed (3 x 5 minutes) with 1x TBST buffer, the secondary antibody conjugated with alkaline phosphatase or peroxidase was added and incubated for 1 hour with shaking. After the secondary incubation, the membrane was washed (3 x 5 minutes) with 1x TBST buffer. For detection, the membrane was incubated with peroxidase substrate (SuperSignal West Femto Maximum Sensitivity Substrate, Pierce, USA) and monitored with a CCD camera (ORCAII ERG, Hamamatsu Photonics, www.jp.hamamatsu.com) with SimplePCI Imaging Software (Version 5.0.0.1503, Compix Inc., Imaging Systems, USA).

TBS (10x):   1.5 M NaCl
                                        0.2 M Tris HCl, pH 7.5

TBST: 1x TBS
                                        0.05% Tween 20

Blocking Buffer: 5% (w/v) nonfat dried milk in 1x TBST

2.2.3.11 Antibodies

Primary Antibody	Company	Dilution
Rabbit-anti-α-RCAR1	Eurogentec (Germany)	1:5.000
Rabbit-anti-α-RCAR3	Eurogentec (Germany)	1:5.000

Secondary Antibody	Company	Dilution
Goat-anti rabbit	Pierce (USA)	1:100.000

2.2.3.12 Phosphatase assays

The protein phosphatase activity was measured using 4-methyl-umbelliferylphosphate (4-MUP) as a substrate (Meinhard and Grill, 2001). Briefly, the PP2Cs were preincubated in the presence or absence of RCAR proteins in Buffer A for 15-20 minutes at 35°C. In case of low protein levels (below 1 μg/ml), bovine serum albumin was added (30 μg/ml). The reaction (total volume of 100 μl) was initiated by administration of an equal volume of Substrate Solution at 30°C. The PP2C inhibition studies were performed with approximately 0.1 μg enzyme and excess of binding protein (>15 fold) to shift the equilibrium to protein complex formation. Product release was recorded by the increase of

fluorescence using a microplate reader (Synergy 2, BioTek, Germany) with excitation and emission wavelengths at 360 nm and 460 nm, respectively.

Alternatively, the assay was performed with the phosphopeptide RRA(pT)VA as substrate according to the supplier (Protein Phosphatase Assay Kit, Promega, USA).

The analysis was carried out in the presence of 0.1 mM substrate and buffer A with 5 mM Mg^{2+} substituting the Mn^{2+} ions.

Buffer A:	100 mM Tris HCl, pH 7.9
	100 mM NaCl
	0.3 mM Mn^{2+}
	4 mM Dithiothreitol
Substrate Solution:	100 mM Tris HCl, pH 7.9
	100 mM NaCl
	0.3 mM Mn^{2+}
	5 mM 4-methyl-umbelliferylphosphate (MUP)

2.2.3.13   Circular dichroism spectroscopy

Circular dichroism (CD) spectra were performed in a J-715 with PTC343 peltier unit (Jasco, http://www.jascoinc.com). Far-UV spectra of RCAR1, RCAR3 (0.5 mg/ml) and ABI1 (0.25 mg/ml) in the absence or presence of (*S*)-ABA (100 µM) were registered in the range 195–260 nm using an optical path cell of 0.1 cm. Samples were analysed in 15 mM sodium phosphate, pH 7.5, at a constant temperature of 20°C. Spectra were recorded with a 0.1 nm resolution at a scan speed of 20 nm/min and results were expressed as an average of 15 scans. Final spectra were baseline-corrected and ellipticities were calculated for a mean residue weight. Estimations of secondary structure were performed with the SOMCD method (http://geneura.ugr.es/cgi-bin/somcd/index.cgi) (Unneberg et al., 2001). To determine the thermal stability of the RCAR1 and RCAR3 in the presence and absence of (*S*)-ABA (100 µM), the CD signal was monitored at 222 nm from 10°C to 90°C at a protein concentration of 0.5 mg/ml and a heating rate of 20°C/hour (Barral et al., 2005).

2.2.3.14   Isothermal titration calorimetry

Isothermal titration calorimetry (ITC) measurements were performed on a MicroCal VP-ITC (MicroCal, www.microcal.com). The ORIGIN software package (Origin Lab, http://www.originlab.com) was used for data analysis. Purified protein samples were dialysed overnight in buffer containing 100 mM Tris-Cl, pH 7.9, 100 mM NaCl and 2 mM dithiothreitol, and were degassed briefly before loading into the ITC cell. The syringe was

filled with (*S*)-ABA in dialysis buffer. A typical experiment consisted of 5 µl injections (with 1 µl pre-injection) of (*S*)-ABA (in 5 minutes intervals) at 30°C under continuous stirring. The final concentration of RCAR1 or RCAR3 in the cell was adjusted to 8 µM or to 1 µM, respectively, whereas the injection syringe was filled with (*S*)-ABA solution ranging from 100-400 µM.

2.2.3.15 *Screening for a ligand by using FT-ICR-MS analysis*

FT-ICR-MS analysis was used in order to screen for a specific low molecular weight ligand(s) that by binding to the receptor complexes inactivates the PP2Cs, thereby activating the large variety of physiological processes regulated by ABA.

Purification of *Arabidopsis thaliana* cell extracts

7-day old *Arabidopsis* cell suspension cultures (source of ligands) growing on LS medium were harvested and filtrated in order to separate the cell pellet from the supernatant. The cell pellet was frozen in liquid nitrogen and stored overnight at - 80°C prior to purification. After thawing, the 200 g of cell pellet was resuspended in 100 ml of ddH$_2$O adjusted to pH 3.0 with 0.25% formic acid. The cells were stirred for 2 hours at 4°C, filtrated and then centrifuged at 8.000 x g for 15 minutes to pellet the cellular debris. Volume of 100 ml of cleared cell-free extract (pH 3.0) was loaded onto a Bakerbond SPE C$_{18}$ column (J.T. Baker) equilibrated with 6 ml of 100% methanol, and washed with 6 ml of 0.25% formic acid in ddH$_2$O. The column, after applying 100 ml of cell-free extract, was washed with 6 ml of 0.25% formic acid in ddH$_2$O. Pure plant extract was eluted with 6 ml of 100% methanol. After evaporation (speed-vac) of methanol, the pellet was resuspended in 6 ml of ddH$_2$O. The pH of the plant extract was adjusted to 7.5 by using 1 mM (NH$_4$)$_2$CO$_3$.

In order to exclude the possibility of the interference from the solvents used in the study, the control samples were prepared. The C$_{18}$ buffer control was obtained by elution with 6 ml of 100% methanol from C$_{18}$ column equilibrated with 6 ml of 100% methanol and washed with 12 ml of 0.25% formic acid in ddH$_2$O. The 0.25% formic acid (≥ 98%, p.a; Roth, Karlsruhe, Germany) used in all C$_{18}$ washing steps due to unexpected effect on the activity of PP2Cs in the phosphatase assay was further purified on C$_{18}$ column. Pure 0.25% formic acid was collected by passing through the new C$_{18}$ column equilibrated with 6 ml of 100% methanol. All the formic acid impurities, which had an impact on the regulation of protein activity were adsorbed on C$_{18}$ column.

Immobilization of RCARs on affinity columns

Different RCAR proteins (0.5 mg) and ABI2, freshly purified and dialysed, were immobilized on Ni-TED 2000 columns (Macherey-Nagel) equilibrated with Dialysis Buffer. Columns with bound RCARs were rinsed with 6 ml of plant extract (pH 7.5). The 6 ml of flow through was collected, evaporated (speed vac) and resuspended in 200 µl of ddH$_2$O (FT-ICR). In the next step column was washed with 3 ml of 150 mM (NH$_4$)$_2$CO$_3$ (pH 7.5) and 3 ml of ddH$_2$O. After the washing step the RCARs-ligand or RCARs-ABI2-ligand complexes were eluted from the columns with 3 ml of 10 mM trifluoroacetic acid (pH 2.5). The elution fraction was collected and mixed with 2 mM dimethylglyoxime (in the presence of 10 mM ammonia solution), in order to precipitate the Ni^{2+} ions released from the Ni-TED 2000 column after low pH buffer treatment (Haim and Tarrant, 1946; Dulski, 1997). Afterwards the elution fraction was evaporated (speed vac) and resuspended in 200 µl of ddH$_2$O (FT-ICR).

Concentrated plant extract, flow through and elution fractions were analysed by FT-ICR-MS analysis in positive mode by mixing 20 µl of each fraction with 80 µl of H$_2$O:methanol:formic acid (30:70:0.1) mixture.

Fourier Ion Cyclotron Resonance Mass Spectrometry (FT-ICR-MS)

High-resolution mass spectra (resolution Δ(m/z)/(m/z) of 220.000 at m/z 200 in full scan mode) were acquired on a Fourier Transform Ion Cyclotron Resonance Mass Spectrometer (Bruker, Bremen, Germany), equipped with a 12 Tesla superconducting magnet and an Apollo II ESI source. Samples were infused with the micro-electrospray source at a flow rate of 120 µl/h at 200°C. Positive electrospray ionisation was used. Spectra were externally calibrated on clusters of arginine (m/z of 173.10440, 347.21607, 521.32775 and 695,43943) dissolved in methanol at a concentration of 10 mg/l; calibration errors in the relevant mass range were always below 0.1 ppm. One MW (MegaWord; data file size) time domains were applied in the mass range of 147–2000 m/z. The ion accumulation time in the hexapol in the front of the ICR cell was set to 0.1 s and 256 scans were accumulated per sample. Before Fourier transformation of the time-domain transient (convertion of the time domain signal (image current) to a frequency domain spectrum (mass spectrum)), a sine apodization (windowing; method of enhancing resolution of the spectra by improving (maximizing) the signal/noise ratio) was performed. The raw data were processed with DataAnalysis 3.4 (Bruker Daltonics, Bremen) software, hard-coded in the instrument.

2.2.4 Methods for plant analysis

2.2.4.1 Cultivation of Arabidopsis thaliana plants

All the *Arabidopsis* lines used in this study were in the ecotype Columbia (Col), Landsberg *erecta* (La-*er*) and Reschiev (RLD). These plants were grown in a perlite–soil mixture in a controlled growth chamber (Conviron, Canada) at 23°C under long-day conditions with 16 hours of light (250 µE m^{-2} s^{-1}).

2.2.4.2 Sterilization of Arabidopsis seeds

For the seed surface sterilization, *Arabidopsis* seeds were immersed in 80% (v/v) ethanol and 0.1% (v/v) Triton X-100 solution for 20 minutes, followed by a 3 minute soak in 4% sodium hypochloride (NaOCl). Afterwards seeds were rinsed five times with sterile mQ H$_2$O and sown under sterile conditions on MS agar plates (Murashige and Skoog, 1962), followed by stratification for 1-2 days at 4°C. Seedling were grown at 23°C in cell culture room under constant light (50 µE m^{-2} s^{-1}). If necessary, 4 days old seedlings were transferred onto MS plates supplemented with ABA (0.1-25 µM) or other phytohormones. *Arabidopsis* seedlings were grown on agar (10 g/l in 1x MS medium) plates for physiological assays or on agarose (10 g/l in 1x MS medium) plates for RNA extraction.

10x MS-Macrosalts:	16.5 g/l NH$_4$NO$_3$
	19 g/l KNO$_3$
	3.32 g/l CaCl$_2$
	1.7 g/l KH$_2$PO$_4$
	3.7 g/l MgSO$_4$ x 7 H$_2$O
400x B5-Microsalts:	0.01 g/l CoCl$_2$ x 6 H$_2$O
	0.01 g/l CuSO$_4$ x 5 H$_2$O
	14.6 g/l Na$_2$EDTA
	1.2 g/l H$_3$BO$_3$
	0.3 g/l KI
	4 g/l MnSO$_4$ x 4 H$_2$O
	0.1 g/L Na$_2$MoO$_4$ x 2 H$_2$O
	0.8 g/l ZnSO$_4$ x 4 H$_2$O
	11.2 g/l FeSO$_4$ x 7 H$_2$O
1x MS-Medium:	100 ml/l 10x MS-Macrosalts
	2.5 ml/l 400x B5-Microsalts
	10 g/l Sucrose
	1 g/l MES
	10 g/l Agar/Agarose
	Autoclaved, pH 5.8 (KOH)

ABA stock solution: 10 mM ABA in 1% MES ($\equiv$ 47 mM), pH 7.5

2.2.4.3   Cultivation of Arabidopsis cell suspension cultures

Arabidopsis thaliana cell suspension cultures (ecotype Landsberg *erecta*) were grown in LS medium (Linsmaier and Skoog, 1965) supplemented with 3% (w/v) sucrose, 0.5 mg/l NAA (Sigma), 0.1 mg/l kinetin (Sigma), with pH adjusted to 6.0 using 1 N NaOH. Cell cultures were maintained by weekly subculturing of 75 ml saturated culture into 675 ml of fresh LS in 1.8 l Fernbach type flasks (Schott Duran). Cell cultures were grown in the cell culture room under continuous light (50 µE m^{-2} s^{-1}), and rotated at 100 rpm, at a temperature of 23°C.

20x LS-Medium: 1.65 g/l NH_4NO_3
                               1.9 g/l KNO_3
                               0.37 g/l $MgSO_4$ x 7 H_2O
                               0.17 g/l KH_2PO_4
                               0.332 g/l $CaCl_2$
                               0.0373 g/l Na_2EDTA
                               0.0278 g/l $FeSO_4$ x 7H_2O
                               0.0062 g/l H_3BO_3
                               0.0223 g/l $MnSO_4$ x 4 H_2O
                               0.0086 g/l $ZnSO_4$ x 4 H_2O
                               0.00083 g/l KI
                               0.00025 g/l Na_2MoO_4 x 2H_2O
                               0.000025 g/l $CuSO_4$ x 5 H_2O
                               0.000025 g/l $CoCl_2$ x 6 H_2O
                               0.0004 g/l Thiaminiumdichlorid
                               0.1 g/l Myo-Inositol

1x LS-Medium: 50 ml/l 20x LS-Medium
                              30 g/l Sucrose
                              Autoclaved, pH 6.0 (1 N NaOH)

Phytohormones: NAA: 0.5 mg/l (stock solution 0.5 mg/ml in KOH)
                              Kinetin: 0.1 mg/l (stock solution 0.1 mg/ml in KOH)

2.2.4.4   Pollen studies

Freshly dehisced anthers from *Arabidopsis* plants expressing the RCAR1-β-glucuronidase fusion were collected with forceps and hand-pollinated on stigmas of wild-type *Arabidopsis* flowers. Emasculated stigmas were analyzed by GUS staining, 6 hours after pollination.

For pollen tube growth studies, the pollen grains from plants expressing the RCAR1-β-glucuronidase fusion were collected by gently shaking the pollen from flowers into 1.5 ml

50

tube. Pollen was incubated in 1 ml of liquid GM media (Brewbaker and Kwack, 1963) at room temperature for 1-3 hours. Pollen germination and growth were assessed by light microscopy.

Pollen Germination Medium (GM):   1.27 mM $Ca(NO_3)_2$ x 4 H_2O
0.87 mM $MgSO_4$ x 7 H_2O
0.99 mM KNO_3
1.62 mM H_3BO_3
10% (w/v) Sucrose
Autoclaved, pH 7.0

2.2.4.5 *Histochemical staining for GUS activity*

Localization of GUS activity with ELF-97 as a substrate

For histochemical assay with ELF-97 as a substrate, transgenic *Arabidopsis* seedlings or plant tissues expressing RCAR1-GUS fusion were fixed on ice with Fixing Solution for 60 minutes. After that, plant samples were washed with Washing Solution 1, followed by incubation for 2-4 hours at 37°C in Staining Solution. Afterwards, Washing Solution 2 was applied, and the samples were stored at 4°C in Storage Buffer.

Fixing Solution: 0.15 M Sodium Phosphate Buffer (pH 7.0)
0.2% Triton X-100
1% Formaldehyde

Washing Solution 1:   0.15 M Sodium Phosphate Buffer (pH 7.0)
0.02% Triton X-100

Washing Solution 2:   0.15 M Sodium Phosphate Buffer (pH 7.0)

Staining Solution: 25 µM ELF-97 β-D-glucuronide
0.15 M Sodium Phosphate Buffer (pH 7.0)
0.02% Triton X-100

Storage Buffer: 0.15 M Sodium Phosphate Buffer (pH 7.0)
0.02% NaN_3

Localization of GUS activity with X-gluc as a substrate

For GUS staining with X-Gluc (5-bromo-4-chloro-3-indolyl-β-D-glucuronide) as a substrate, transgenic *Arabidopsis* seedlings or plant tissues expressing RCAR1-GUS fusion were fixed on ice in 90% acetone for 30 minutes. After the acetone was removed, plant samples were washed with Washing Solution for 1 minute and then stained overnight at 37°C in Staining Solution. After staining, samples were washed with series of

25%, 50%, 75% and 95% of ethanol, for 20 minutes each in order to remove chlorophyll. In case of *Arabidopsis* seeds, the samples were washed for several hours with the mixture of ethanol:acetic acid (1:1). At the end all tested tissues were cleared by incubation at 4°C with the Clearing Solution.

Washing Solution:	50 mM Sodium Phosphate Buffer (pH 7.2)
	0.5 mM $K_3Fe(CN)_6$
	0.5 mM $K_4Fe(CN)_6$
Staining Solution:	50 mM Sodium Phosphate Buffer (pH 7.2)
	0.5 mM $K_3Fe(CN)_6$
	0.5 mM $K_4Fe(CN)_6$
	2 mM X-Gluc
Clearing Solution:	2.67 g/ml Chloral Hydrate

2.2.4.6   *Transient expression in protoplasts*

Isolation of *Arabidopsis* protoplasts

The method of protoplast preparation was a modified version of the protocol published by (Abel and Theologis, 1998). In this work 3 to 4 weeks old *Arabidopsis* plants (La-*er* and *aba2* mutant) were used. In order to isolate protoplasts, 30-50 rosette leaves (2-3 g of fresh weight) were incubated for 3-5 hours in a Petri dish with 15 ml of Enzyme Solution, on a vertical shaker (40-50 rpm) at room temperature. Afterwards, the protoplast solution was filtered through 150 μm mesh nylon net into a new Petri dish, and then transferred into a fresh Falcon tube. After the transfer of the protoplast solution, 8 ml of WIMK Solution was added, followed by centrifugation for 3 minutes at 60 x g at room temperature. The supernatant was discarded and another 4 ml of WIMK solution were added into the pellet. Centrifugation was repeated and the pellet was resuspended in an appropriate volume of MaMg Solution (final protoplast concentration was adjusted to 0.5-1 x 10^6 protoplasts/ml). The protoplasts were kept at 4°C for at least 30 minutes prior to transfection.

Enzyme Solution:	1% Cellulase
	0.25% Macerozyme
	400 mM Mannitol
	8 mM $CaCl_2$
	0.1% BSA
	5 mM MES-KOH (pH 5.6)
WIMK Solution:	500 mM Mannitol
	5 mM MES-Tris (pH 5.8-6.0)
	Autoclaved

MaMg Solution:	400 mM Mannitol
	15 mM MgCl$_2$
	5 mM MES-KOH (pH 5.6-5.8)

Protoplast transfection

For transfection experiments, approximately 5×10^4 *Arabidopsis* protoplasts (0.1 ml) were transfected with 10 µg DNA of the reporter plasmid (*pRAB18::LUC* or *pRD29B::LUC*) and 0.1-10 µg DNA of effector plasmid. In addition, 2 µg of *p35S::GUS* plasmid was included in each transfection as a control for internal normalization of expression. Then, 130 µl of warm (37°C) PEG Solution was applied into the tube and mixed gently by inverting the tube two times. After incubation for 3-5 minutes, 750 µl of WIMK Solution was added. The suspension was mixed again and centrifuged for 3 minutes at 800 x g at room temperature. The supernatant was removed and another 350 µl of WIMK was used to resuspend the pellet. After the next centrifugation the supernatant was removed and 100 µl of WIMK was mixed with the protoplast pellet. If necessary, the appropriate amount of ABA was applied. Protoplasts were incubated overnight at 23°C on a vertical shaker at 30-50 rpm.

PEG Solution:	40 % PEG-4000
	300 mM CaCl$_2$
	0.5% MES-KOH (pH 5.8)

| **ABA Stock:** | 10 mM ABA in 1% MES, pH 7.4 |

Measurements of β-D-glucuronidase activity in *Arabidopsis* protoplasts

To measure the β-D-glucuronidase activity, 50 µl of the protoplast suspension was mixed with 100 µl of 2x MUG in the CCLR Buffer, in the black microtiter plate. Product release was recorded by the increase of fluorescence (proportional to the enzyme activity) using a microplate reader (HTS 7000 Plus, Perkin Elmar) with excitation and emission wavelengths at 360 nm and 460 nm, respectively. The assay was performed at 30°C for 8 minutes (25 cycles).

CCLR Buffer:	25 mM Tris-Phosphate (pH 7.8)
	2 mM Dithiothreitol
	2 mM DCTA
	10% (v/v) Glycerol
	1% (v/v) Triton X-100

| **20x MUG Substrate:** | 4 mM Methylumbelliferyl β-D-glucuronide |
| | (MUG) in CCLR Buffer |

Detection of *Photinus pyralis* luciferase activity

Determination of luciferase activity was according to the method of (Luehrsen et al., 1992). The sample (150 µl) used for the GUS activity measurement was transferred into the plastic tube (Sarstedt) and analyzed in the flash`n glow luminometer (Berthold). The luminometer determinated first a 10 second background-value (bkg) in the absence of the substrate. Then, after applying 100 µl of the substrate (LAR) the activity of the luciferase (RLU) was determinated (read-out time was 20 seconds).

For calculation of the specific luciferase activity (dRLU) the formula dRLU = (RLU-2 x bkg)/20 was applied.

<u>**LAR Buffer**</u>**:**	20 mM Tricine/NaOH (pH=7.8)
	1.07 mM $(MgCO_3)_4Mg(OH)_2$ x 5 H_2O
	2.7 mM $MgSO_4$
	0.1 mM Na_2EDTA
	33.3 mM Dithiothreitol
	0.27 mM Coenzyme A
	0.47 mM D-Luciferin
	0.53 mM ATP

2.2.5   *In silico* analysis

Phylogenetic analyses were conducted in *MEGA* version 4. The evolutionary history was inferred using the Minimum Evolution method. The sum of branch lengths of the RCAR tree is 2.89. Transcriptional profiling was carried out with the Genevestigator database (www.genevestigator.com/gv/doc/citing.jsp) (Zimmermann et al., 2005).

3 Results

3.1 RCAR protein family

Plant PP2Cs such as ABI1 and ABI2 have been found to play a role as negative regulators in abscisic acid signal transduction. Hence, both PP2Cs are of central importance for elucidating the integrative network of ABA signaling. A yeast two-hybrid system was used to screen for interaction partners of ABI2. Screening of *Arabidopsis* cDNA libraries for interactors of ABI2 in yeast resulted in the identification of six clones that showed *lacZ* activation and histidine autotrophy in dependence on the expression of the cDNA fusion protein (Yang et al., 2006). Two of the positive clones expressed cDNAs fusions encoded highly similar proteins of unknown function. They were named Regulatory Component of ABA Receptor 1 (RCAR1) and 3 (RCAR3) (Yang, 2003). RCAR1 and RCAR3 belong to a protein family in *Arabidopsis thaliana* with 14 members and three subfamilies (I, II, III) (Figure 3-1).

RCAR proteins also known as PYR1/PYLs (Pyrabactin Resistance1/PYR1-Like) (Park et al., 2009) share structural similarity with Bet v 1 from the plant pathogenesis-related class 10 proteins (van Loon et al., 2006) and sequence homology with the star-related lipid-transfer (START) domain (Iyer et al., 2001).

In this study six proteins, two from each clade were characterized and described.
In order to characterize clade I, RCAR1 (187 aa; At1g01360) and RCAR3 (188 aa; At5g53160), which share 82% similarities and 70% identities in the amino acid sequence were used. RCAR9 (207 aa; At2g38310) and RCAR10 (215 aa; At2g40330) are representatives of clade II. They share 81% similarities and 69% identities in the amino acid sequence. Clade III is described by presenting RCAR13 and RCAR14 proteins, which share 75% similarities and 60% identities in their primary structure. The cDNAs of RCAR13 and RCAR14 encoded a full length protein of 209 amino acid residues (At1g73000) and 190 amino acid residues (At2g26040), respectively.
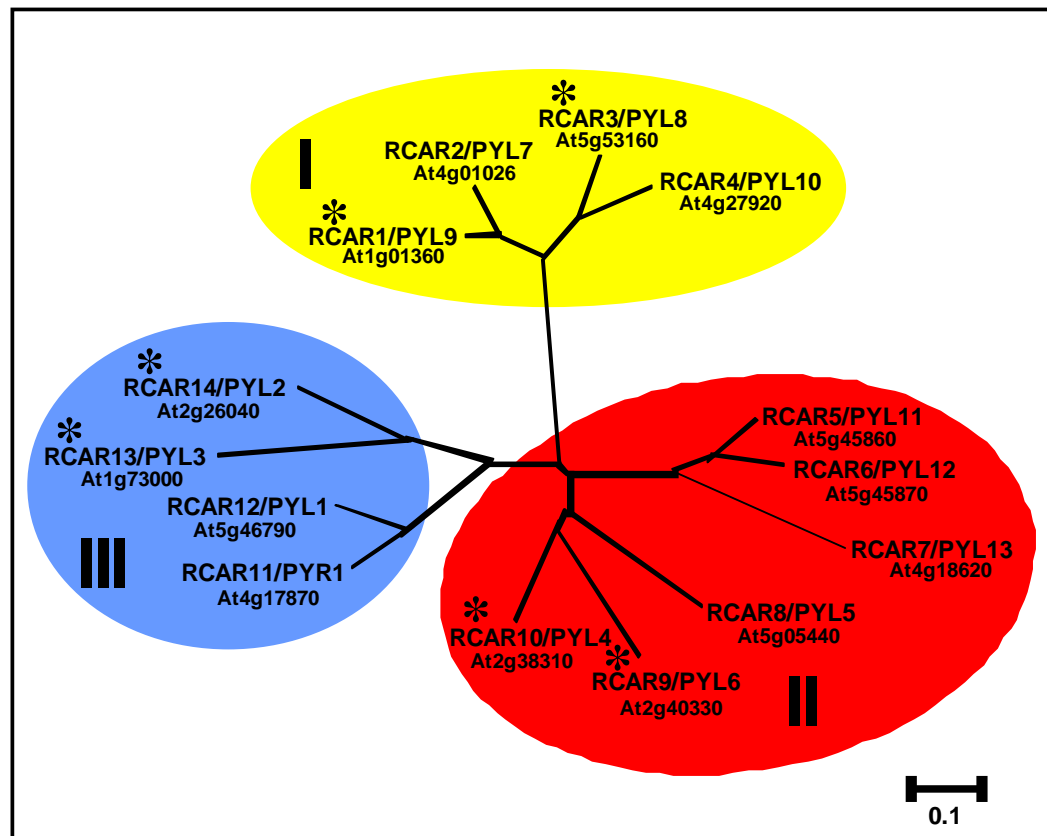
Figure 3-1   Phylogenetic tree of the RCAR (PYR/PYLs) proteins of Arabidopsis thaliana with AGI nomenclature
RCAR proteins of Arabidopsis belong to a protein family with 14 members, which are grouped into three subfamilies (I, II, III). RCAR proteins marked with asterisks indicate the members of the family analyzed in this study. The evolutionary history was inferred using the Minimum Evolution method of the MEGA version 4 Software (Tamura et al., 2007).

3.2 Physical interaction between RCAR proteins and PP2Cs

In order to study physical interactions between RCAR proteins and ABI1 and ABI2, two different methods were applied. RCAR1 and RCAR3 proteins were used as binding partners of ABI1 and ABI2 in the interaction studies.

3.2.1   Yeast two hybrid analysis

The yeast two-hybrid system was used in this work to further characterize the interactions between the various bait variants of ABI1 and ABI2 (wild-type versus mutant) and preys, such as RCAR1 and RCAR3. Enzymatic assays for expressed β-galactosidase activity in the yeast extracts were used to quantify the strength of protein-protein interactions.

As shown on Figure 3-2A, there is a strong interaction between RCAR1 and ABI2 (more than 4.0 β-gal units). RCAR3 protein (Figure 3-2B) revealed more than 1.5 fold lower interaction with ABI2, compared to RCAR1 protein.
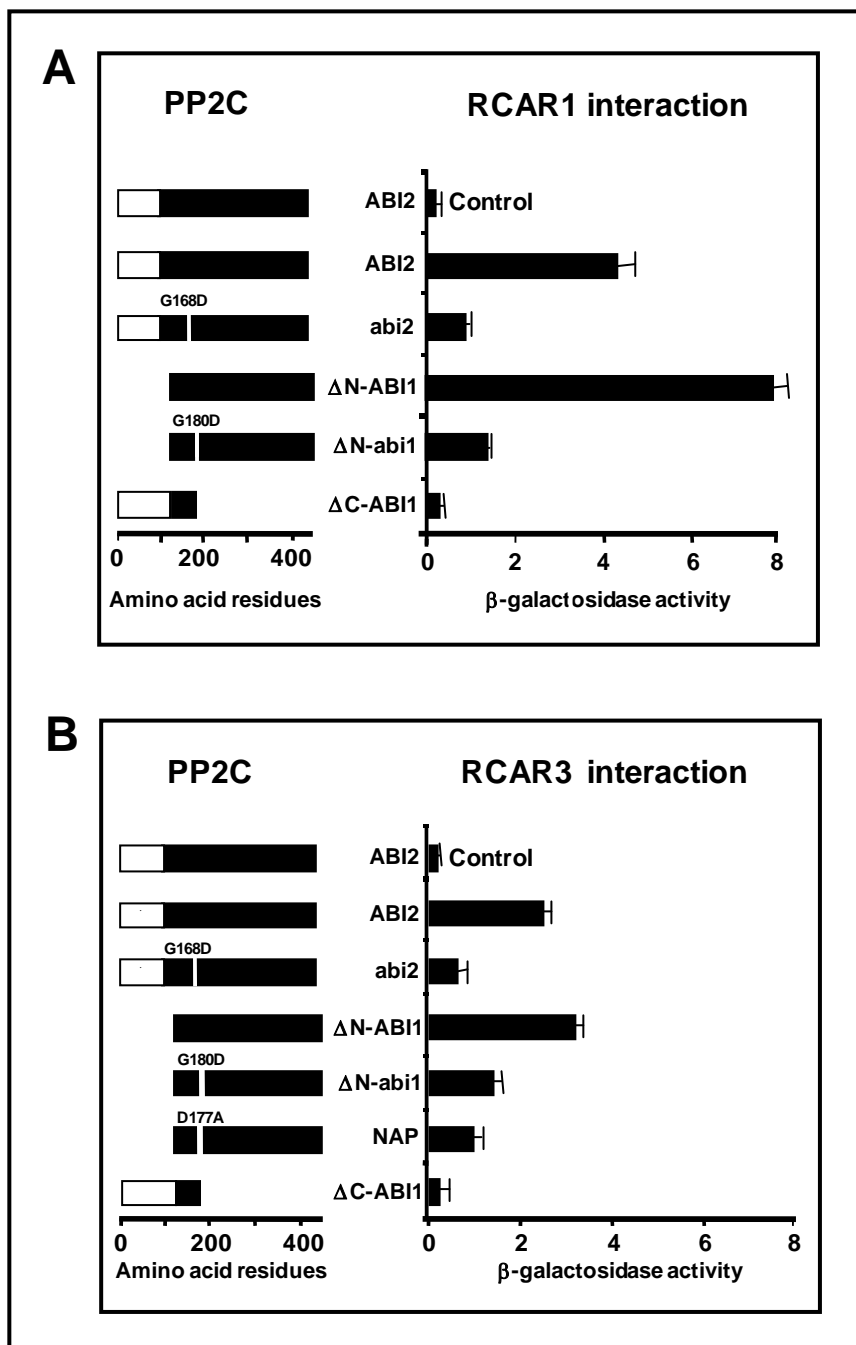
Figure 3-2   Physical interaction between RCAR proteins and ABI1 and ABI2
*The specificity of ABI1 and ABI2 interaction with RCAR1 **(A)** and RCAR3 **(B)** was examined in the yeast two-hybrid system. (Left) The analysis included different ABI1 and ABI2 variants (wild-type versus mutant) fused to the GAL4 DNA binding domain (BD fusions). (Right) Binding of RCAR1 or RCAR3 to the PP2Cs is indicated by transactivation of the β-gal reporter activity above basal levels. Reporter activity is given in Miller units and was calculated as the mean value of three independent experiments (±SD).*

The interaction with RCAR1 and RCAR3 was almost completely abolished by the single amino acid exchange present in *abi2* (ABI2^{G168D}). The mutations in *abi1* (ABI1^{G180D}) and *abi2* impair Mg^{2+}-binding, which is required for the phosphatase activity of PP2Cs, and negatively affect protein interactions. The *abi1-1* and *abi2-1* mutants are ABA-insensitive and both alleles are dominant. The full length ABI1 protein was not examined in yeast because of the autoactivation of the reporter system (Himmelbach et al., 2002). Instead, N-terminally truncated versions of the wild type and mutant proteins, ABI1$^{121-434}$ and *abi1*$^{121-434}$ were analyzed. RCAR1 and RCAR3 have been shown to interact with N-terminal deleted ABI1 even more strongly than with full length ABI2, and they reached 8.0 and 3.2 β-gal units, respectively. The single point mutation present in *abi1* and the catalytically non-active ABI1 (NAP^{D177A}) also impaired RCAR1 and RCAR3 binding. The partial inhibition of the protein interaction suggests that the structure of the phosphatase domain may affect RCAR1/3-PP2C complex formation. Indeed, a truncated ABI1$^{1-180}$ devoid of the phosphatase domain was incapable of binding to RCAR1 and RCAR3 (Figure 3-2).

3.2.2   Bimolecular fluorescence complementation analysis

In order to confirm the protein interactions between RCAR1 and RCAR3 and PP2Cs inside living plant cells, bimolecular fluorescence complementation (BiFC) analysis was recruited. BiFC is based on the formation of a fluorescent complex by two non-fluorescent fragments of the yellow fluorescent protein (YFP) brought together by association of interacting proteins fused to these fragments (Walter et al., 2004).

Figure 3-3 shows that co-expression of RCAR1/3-YFP^N and PP2C-YFP^C in *Arabidopsis* protoplasts resulted in YFP signals located both in the cytosol and in the nucleus. The presence of ABA (10 µM) did not detectably affect the interaction. The data support the yeast-two-hybrid analyses and provide evidence for a physical interaction between RCAR and PP2C proteins.
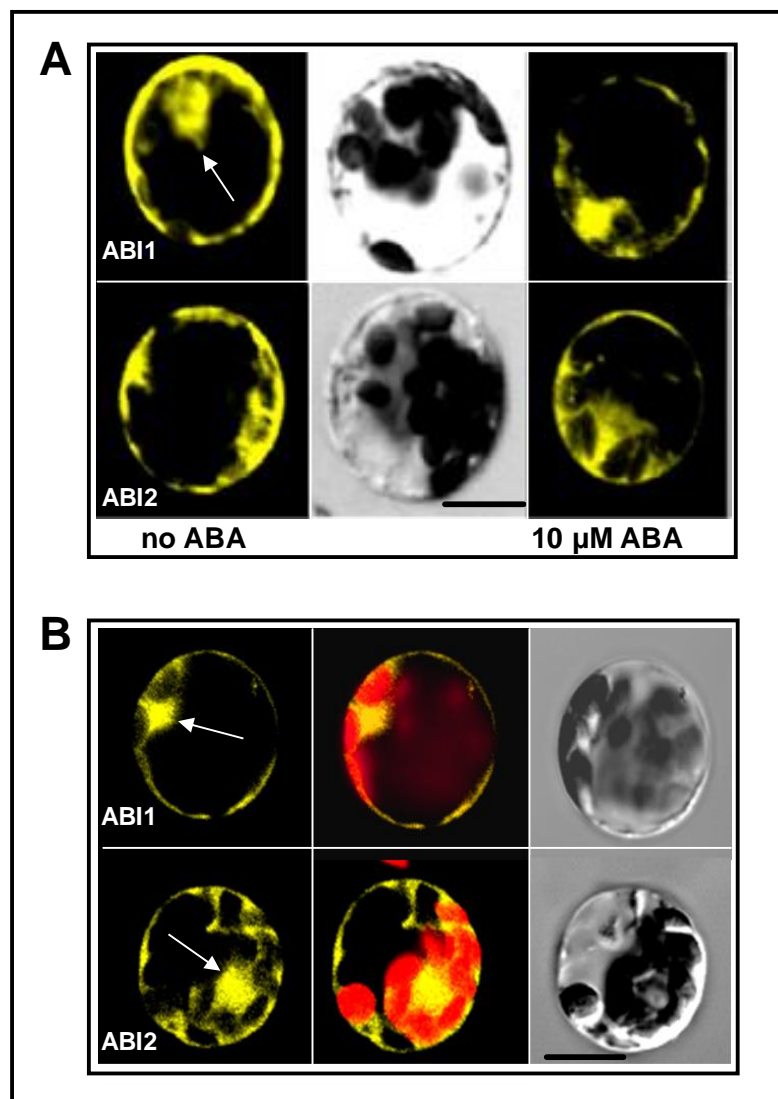
Figure 3-3 **Interaction analysis in Arabidopsis protoplasts by bimolecular fluorescence complementation**
(**A**) RCAR1-YFP^N was analyzed for YFP complementation with ABI1-YFP^C and ABI2-YFP^C (top and bottom, respectively). YFP complementation in the absence (left) and presence (right) of exogenous ABA. Bright-field images (middle) correspond to the left images.
(**B**) Interaction of RCAR3-YFP^N with ABI1-YFP^C and ABI2-YFP^C (top and bottom, respectively). YFP signal (left part), YFP and chloroplast autofluorescence (middle part) and bright-field images of the analyzed protoplast (right part).
The arrows depict fluorescence of the nucleus. Scale bar: 10 µm. The data were generated by Dr. Arthur Korte.

3.3 Histochemical GUS localization of RCAR1 protein

In order to monitor the presence of RCAR1 in various organs of *Arabidopsis,* stable transgenic plants expressing β-glucuronidase RCAR1 fusion protein under the control of the endogenous RCAR1 promoter were used. To detect the expression of RCAR1-GUS fusion protein in transfected cells, two different substrates were used, X-Gluc and ELF-97.
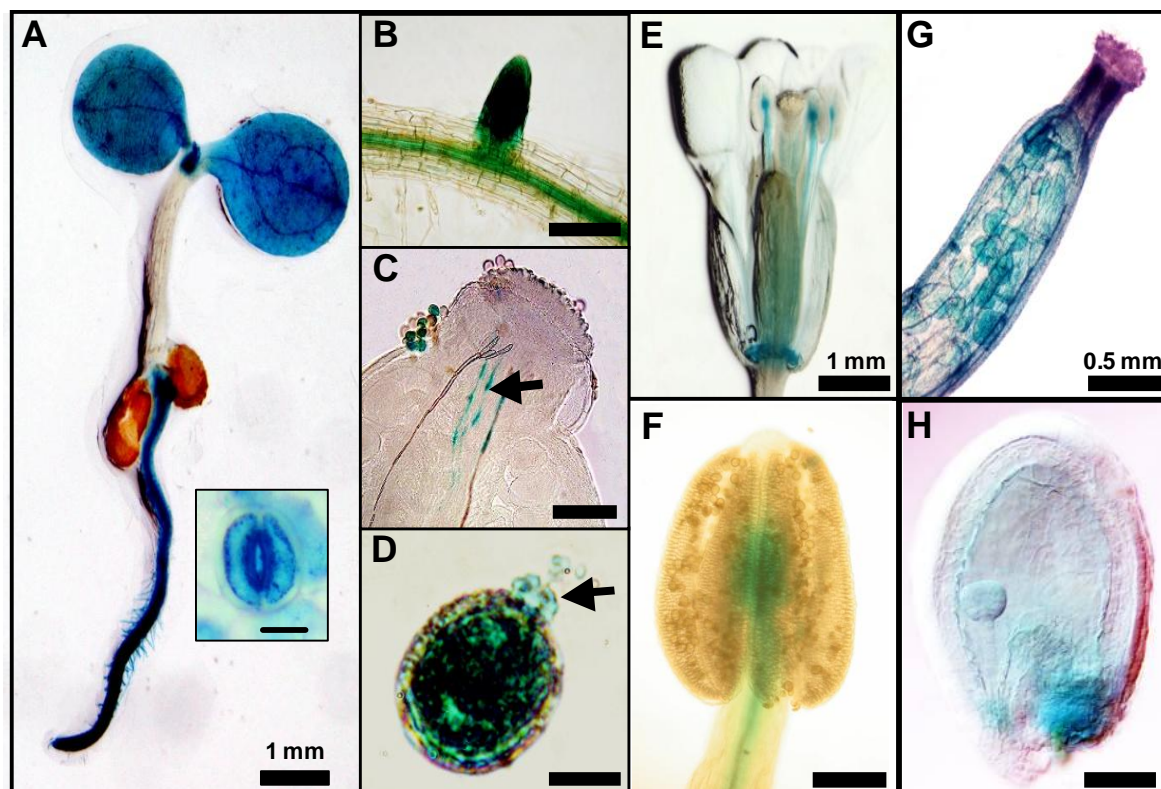
Figure 3-4   *RCAR1 in Arabidopsis, as monitored by a reporter fusion of RCAR1 and β-glucuronidase expressed under the control of the RCAR1 promoter*
(A) five day-old seedling with the seed coat remains, inset: stained guard cells. The receptor fusion is expressed in (B) vascular tissue and (secondary) root tips (C) pollen and pollen tubes (marked by an arrow) growing from the stigma of a pistil to the ovaries. (D) Germination of RCAR1:GUS-expressing pollen grain by protrusion of the pollen tube (marked by an arrow) (E) Flower (F) Anther (G) Silique and (H) seed with embryo at the globular stage. Bars correspond to 0.01 mm for inset in (A) and in (D), 0.2 mm for (B) and (C), 0.07 mm for (F) and (H). (A-H) were treated with X-Gluc as a substrate.

As shown in seedlings, reporter activity of the fusion protein was detected in the root, cotyledons including stomata, as well as in parenchyma cells along the vasculature and prominently in root tips (Figure 3-4, 3-5). The RCAR1 promoter was also strongly expressed in the 5-day old shoot apex in the stipules, after using the ELF-97 as a staining substrate (Figure 3-5B). Histochemical GUS staining also showed that the RCAR1 promoter was active in the pollen grains and pollen tubes, flowers, anthers, early stage siliques and in the seeds (Figure 3-4).
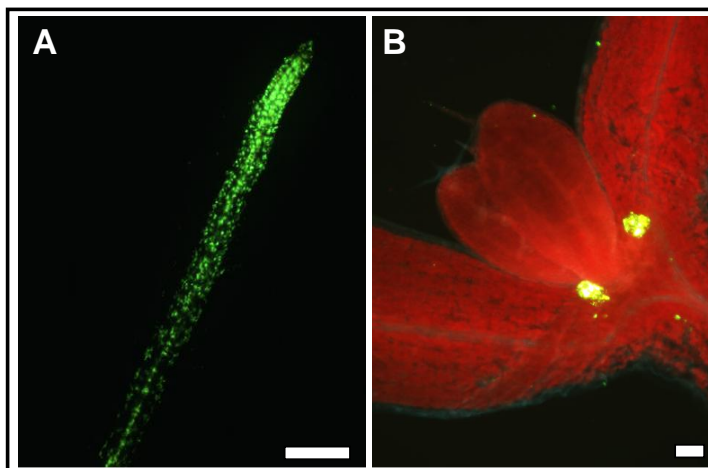
Figure 3-5   Histochemical localization of RCAR1 promoter activity in Arabidopsis
*The reporter activity was detected in **(A)** root and **(B)** stipules of the 5-day old seedlings after treatment with ELF-97 as a substrate. Bars correspond to 1.2 mm for (A) and 0.025 mm for (B).*

In order to investigate the influence of ABA on the activity of the RCAR1 promoter, the seedlings at different stage were exposed to 30 µM ABA for 24 hours. The results showed that seedlings at early stages were strongly blue stained in the cotyledons and roots. In the 10- and 15-day old plants, strong GUS expression was detected only in young leaves and root tips, whereas in the 30-day old plants weak staining was only detected in the root tips (Figure 3-6). The data indicate that treatment with ABA failed to reveal any ABA-induced change in abundance of the fusion protein.
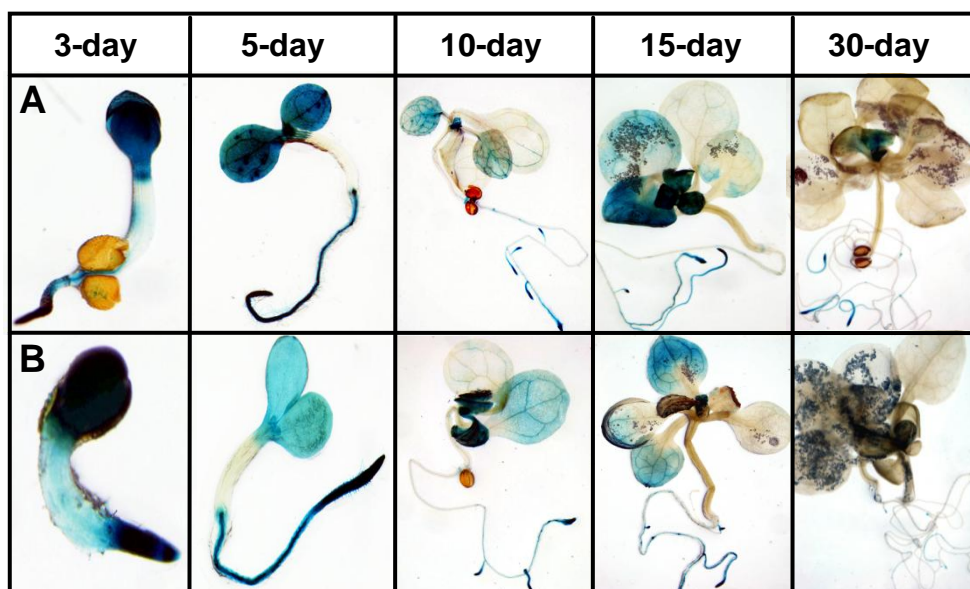
Figure 3-6   The effect of ABA on RCAR1 promoter activity in transgenic Arabidopsis plants
*Transgenic seedlings at different age **(A)** not exposed and **(B)** exposed to 30 µM ABA for 24 hours.*

3.4 Transient expression of RCAR proteins in protoplasts

The protoplast expression system is a sensitive and rapid method for the analysis of the ABA signal transduction mechanism through ABA-regulated reporter gene constructs. Co-transfection of ABA-regulated reporter gene constructs together with the effector proteins that are expressed under the control of 35S promoter is an efficient tool to analyze the ABA signal transduction. In this work, the transient expression system in *Arabidopsis* protoplasts was used to characterize the role of RCAR1 and RCAR3 effector proteins in ABA signaling.

The ABA-response was quantitatively assayed in protoplasts by using reporter constructs consisting of the ABA-upregulated promoters *pRD29B* (Figure 3-7A-D) and *pRab18* (Figure 3-7E, F) driving luciferase expression (Moes et al., 2008). Transient expression of RCAR1 and RCAR3 in the *Arabidopsis* cells resulted in an enhanced ABA-response.

The upregulation of gene expression was also observed in the absence of exogenous ABA. To examine whether the RCAR1/3 mediated activation is due to endogenous ABA levels, protoplasts derived from the ABA-deficient *Arabidopsis* mutant *aba2-1* were analyzed (Figure 3-7A, C, E). The mutant cells had a more than 2-fold lower level of reporter expression compared to the wild-type in the absence of exogenous ABA. Ectopic expression of RCAR1 stimulated luciferase activity of wild type cells by a factor of 20.5 ± 2.3 and of 9.7 ± 2.6 in *aba2-1* protoplasts (Figure 3-7A). Administration of 3 µM (*S*)-ABA to the RCAR1-transfected protoplasts resulted in a comparable increase of reporter expression in the wild type and mutant (39-, and 53-fold, respectively). As shown in Figure 3-7, ectopic expression of RCAR3 stimulated luciferase activity of wild-type cells by a factor of 18.0 ± 1.9 (Figure 3-7C) and 8.0 ± 2.2 (Figure 3-7E) with the ABA-responsive reporter constructs pRD29B::LUC and pRAB18::LUC, respectively.

The RCAR3-mediated activation in *aba2-1* protoplasts was limited to an increase of 3.9 ± 0.9 (pRAB18::LUC) and 8.3 ± 4.3 (pRD29B::LUC), respectively. After application of 3 µM (*S*)-ABA to the transfected protoplasts, a 14- and 38-fold increase of reporter expression in wild- type and a 68- and 140-fold enhancement in *aba2-1* was observed in the presence of AtRab18 and AtRD29B promoters, respectively, compared to cells not expressing the effector protein and not exposed to ABA. In this respect, *aba2-1* mutant protoplasts display a hypersensitivity to ABA. The findings of reduced reporter expression in the ABA-deficient protoplasts at endogenous ABA levels, irrespective of RCAR1 and RCAR3 expression, and the observed recovery of the ABA response in the presence of exogenous ABA, are supportive of an RCAR1 and RCAR3 controlled stimulation of ABA signaling.
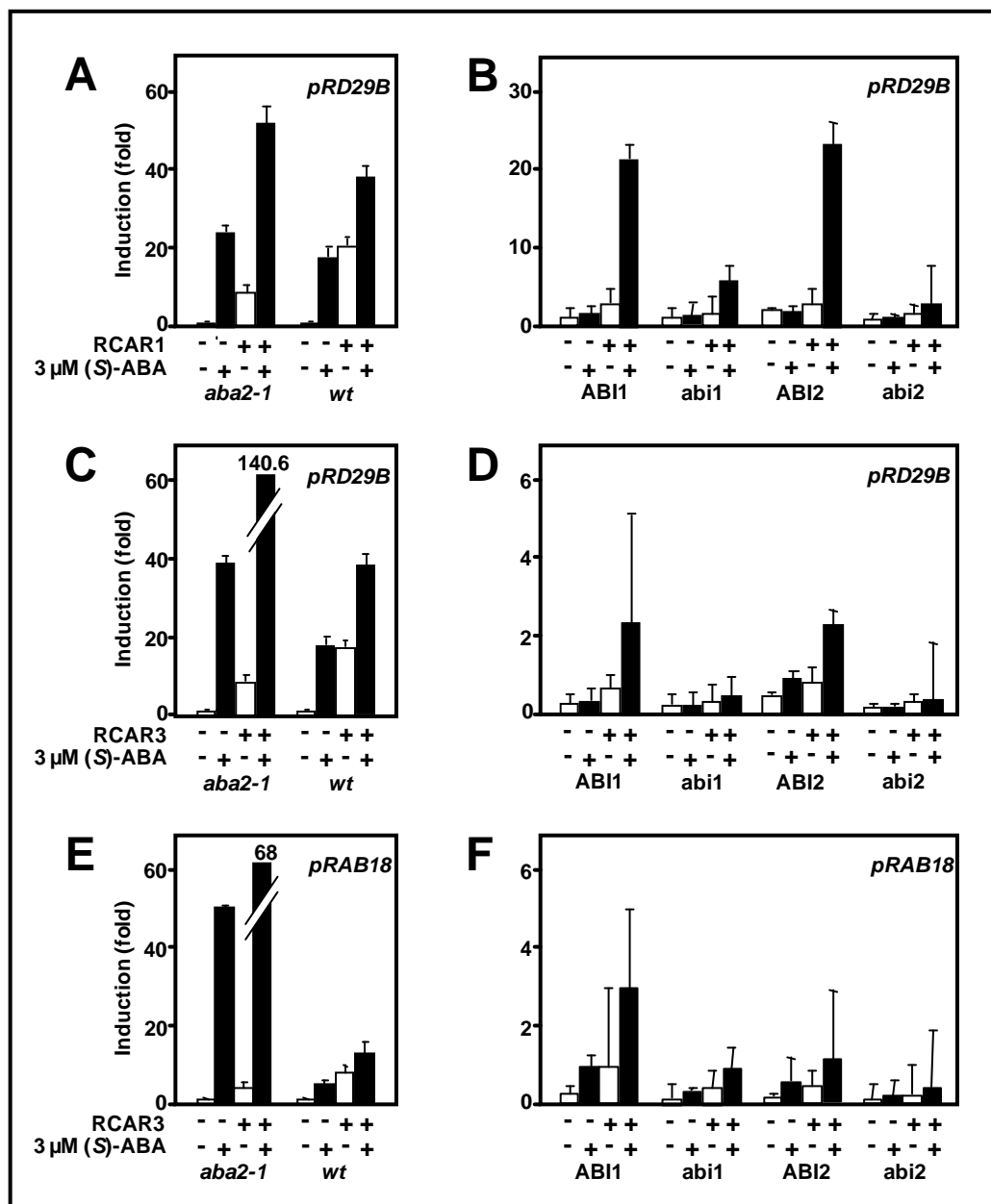
Figure 3-7 RCAR1 and RCAR3 activated and PP2C-antagonised ABA responses in Arabidopsis protoplasts

The ABA-induced upregulation of gene expression was monitored with the ABA-responsive reporter constructs pRD29B::LUC (A-D) and pRAB18::LUC (E, F) in Arabidopsis protoplasts and was measured as relative light units (RLU/RFU). Each data point represents the mean value of three independent transfections. (A, C and E) Regulation of gene expression by the 3 µg of effectors such as RCAR1 (A) and RCAR3 (C and E) in the absence (white bars) and presence of 3 µM (S)-ABA (black bars). The analysis was performed with ABA-deficient aba2-1 protoplasts (left panel) and wild-type protoplasts (right panel). (B, D and F) The RCAR1 (B) or RCAR3 (D and F) and ABA-stimulated reporter expression is inhibited by concomitant expression of various PP2Cs (1 µg) in the absence (white bars) and presence of 3 µM (S)-ABA (black bars).

The next step was to analyze the role of ABI1 and ABI2 in the RCAR1 and RCAR3 mediated responses (Figure 3-7). Expression of ABI1 and ABI2 reduced both RCAR1- and ABA-stimulated reporter expression by a factor of 1.8 and 1.6, respectively (Figure 3-7B). RCAR3- and ABA-stimulated reporter expression was reduced as well in the

presence of ABI1, by a factor of 16 and 4.6 with the ABA-responsive reporter constructs pRD29B::LUC and pRAB18::LUC, respectively (Figure 3-7D, F). The ABI2 expression diminished the RCAR3- and ABA-stimulated reporter expression by a factor of 10 (pRAB18::LUC) and 17 (pRD29B::LUC). The ABA response was almost fully blocked by PP2C expression in cells not expressing RCAR1 and RCAR3. In these analyses, the *abi1* and *abi2* mutant proteins were much more effective in blocking the RCAR1 and RCAR3-mediated stimulation of ABA signaling. Titration of the RCAR1 (Figure 3-8A) and RCAR3 (Figure 3-8B) stimulatory effect by increasing amounts of co-transfected ABI2 effector resulted in complete abrogation of ABA-signaling. Co-expression of a construct targeting RCAR1 (Figure 3-8C) and RCAR3 (Figure 3-8D) and related transcripts by RNA interference (RNAi) partially but significantly antagonised the RCAR-mediated activation of the ABA response.
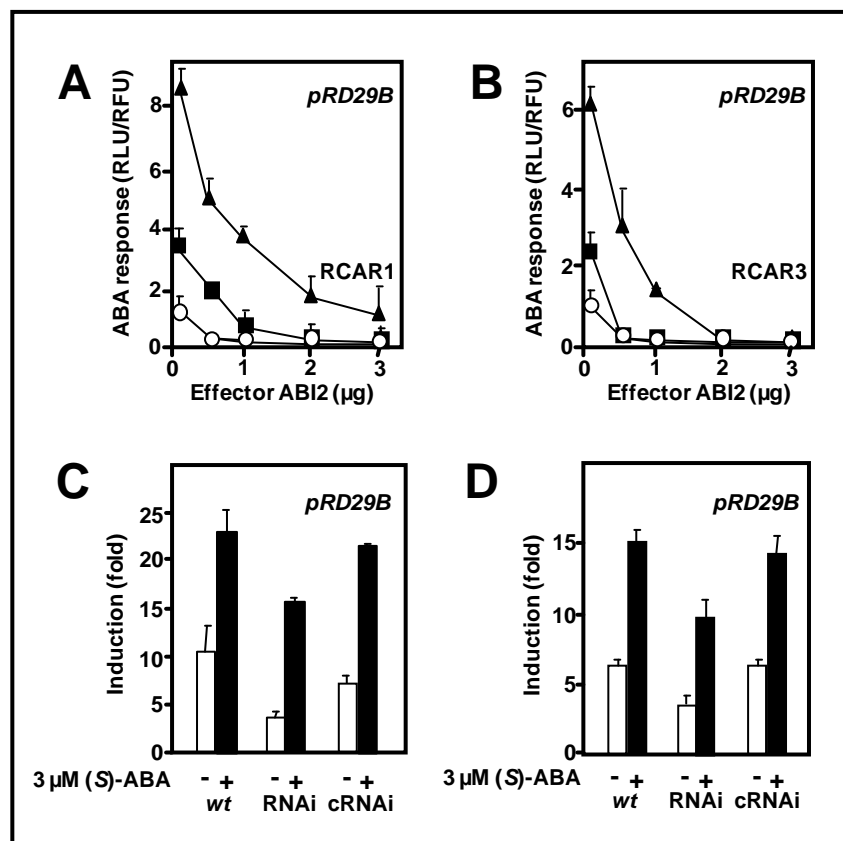
Figure 3-8 **Regulation of ABA responses by RCAR1 and RCAR3 in Arabidopsis protoplasts**
(A and B) The RCAR1 (A) and RCAR3 (B) mediated stimulation of the ABA response is antagonized by co-expression of ABI2. The levels of RCAR1 and RCAR3 effector constructs were 0, 0.3, and 3 µg plasmid (open circles, filled squares, and filled triangles, respectively) (C and D) The activation of the ABA response by RCAR1 (C) and RCAR3 (D) is partially antagonized by co-expression of an RNAi construct (1 µg) targeting RCAR1 or RCAR3 in the absence (white bars) and presence of 3 µM (S)-ABA (black bars). cRNAi: control RNAi. The fold of induction was compared to the wild-type sample not exposed to (S)-ABA and not targeting the RCAR1/3 effector constructs.

3.5 Expression, purification and detection of 6xHis-tagged RCAR proteins

His-tagged RCAR proteins from clade I (RCAR1 and RCAR3), II (RCAR9 and RCAR10) and III (RCAR13 and RCAR14) were heterologously expressed in *Escherichia coli*. Prior to purification, RCAR proteins were first tested for optimization of the expression, by applying various IPTG concentrations (data not shown) and testing different induction time points.

The results were visualized by Western Blot analysis (Figure 3-9), which was performed with rabbit-anti-α-RCAR1/3 antibodies and goat-anti rabbit HRP conjugated antibodies. Analysis showed that 6xHis-RCAR1 (Figure 3-9A) and RCAR3 (Figure 3-9B) fusion proteins reached the highest expression yield at 0.5 mM IPTG (final concentration) after 2-3 hours and 3-5 hours of induction at 37°C, respectively. The calculated molecular weight of 6xHis-RCAR1 fusion protein was near 23.3 kDa, whereas for RCAR3 near 23.5 kDa. The calculated molecular weights of RCAR1 and RCAR3 were in agreement with the size of the protein determined from SDS-PAGE and Western Blot data.

Two members of clade II, RCAR9 and RCAR10, with molecular weights of 24.9 and 23.6 kDa, respectively appeared to be induced at 37°C, with 0.5 mM IPTG. As shown in Figure 3-9C, a period of 1-2 hours after IPTG induction produced a substantial amount of 6xHis-RCAR9 fusion protein. The 6xHis-RCAR10 fusion protein started to appear after one hour post induction, and continued to increase until a maximum level was reached after three hours. In order to characterize clade III of RCAR protein family, RCAR13 (24.1 kDa) and RCAR14 (22.1 kDa) were used as a representatives. Figure 3-9 reveals that over a period of three hours, the amount of RCAR13 (Figure 3-9E) and RCAR14 (Figure 3-9F) recombinant proteins increase from background levels to an apparent maximum.
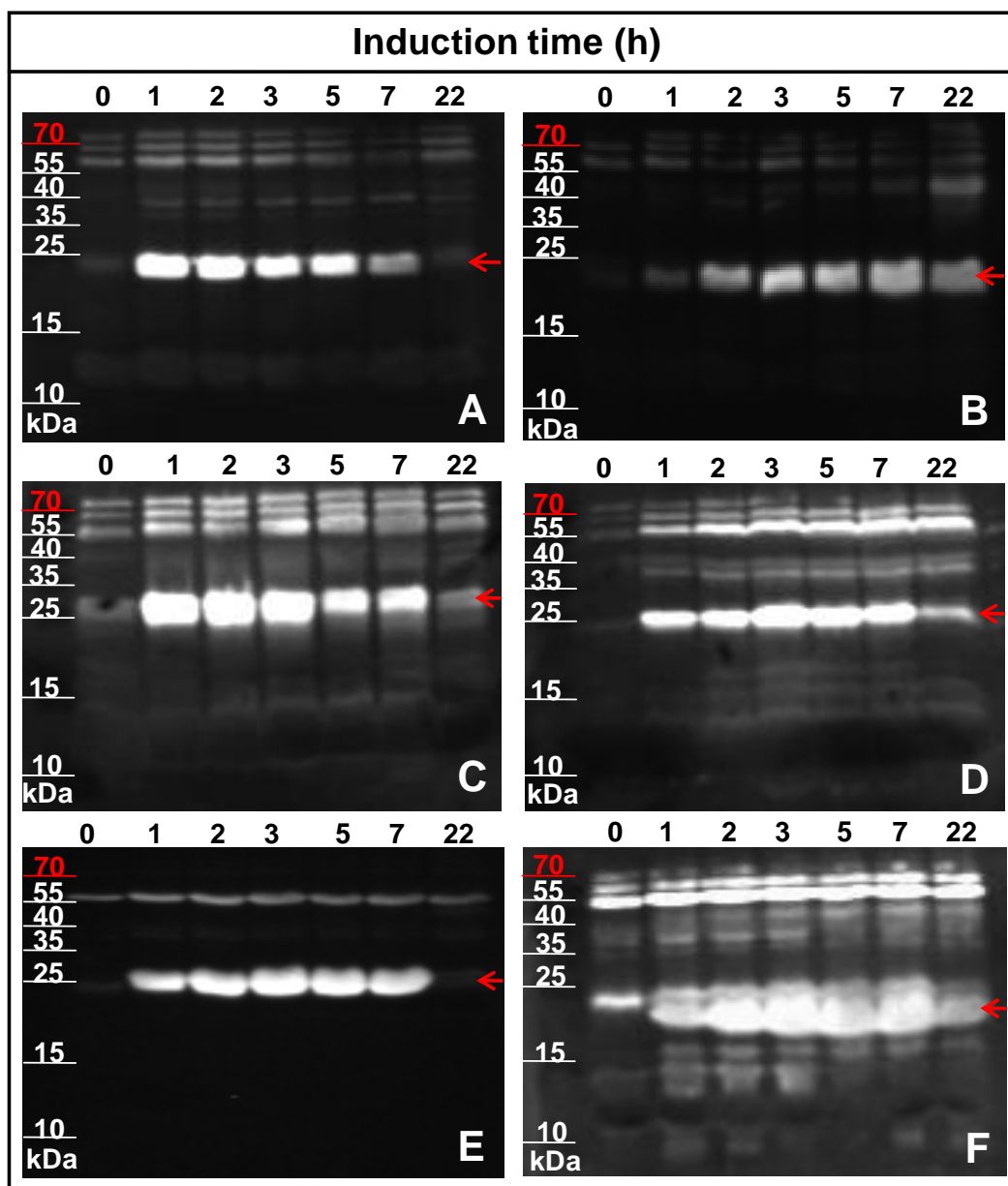
Figure 3-9 ***Time course study for the expression of His-tagged RCAR proteins in E. coli***
*Optimization of expression of **(A)** RCAR1, **(B)** RCAR3, **(C)** RCAR9, **(D)** RCAR10, **(E)** RCAR13 and*
(F) RCAR14 proteins visualized by Western Blot. Protein expression was induced with 0.5 mM
IPTG for 1, 2, 3, 5, 7 and 22 hours, at 37°C. Red arrows depict the 6xHis-RCAR fusion proteins; 20
µl of crude extract from each sample was loaded per slot. Immuno-detection of western blots was
performed using rabbit-anti-α-RCAR1/3 antibody and subsequently the secondary antibody goat-
anti-rabbit conjugated with alkaline peroxidase.

The fusion RCAR proteins were purified from bacterial extracts under native conditions by
immobilized metal ion affinity chromatography (IMAC). All tested proteins were eluted
from Ni-TED (tris-carboxymethyl ethylene diamine) columns with elution buffer containing
250 mM imidazole. Figure 3-10 shows the purification steps of His-tagged RCAR proteins,
two members from each clade. These data clearly indicate that all analyzed RCARs were

not fully bound to the Ni-TED columns, which was apparent by the presence of RCAR in the flow through fraction.
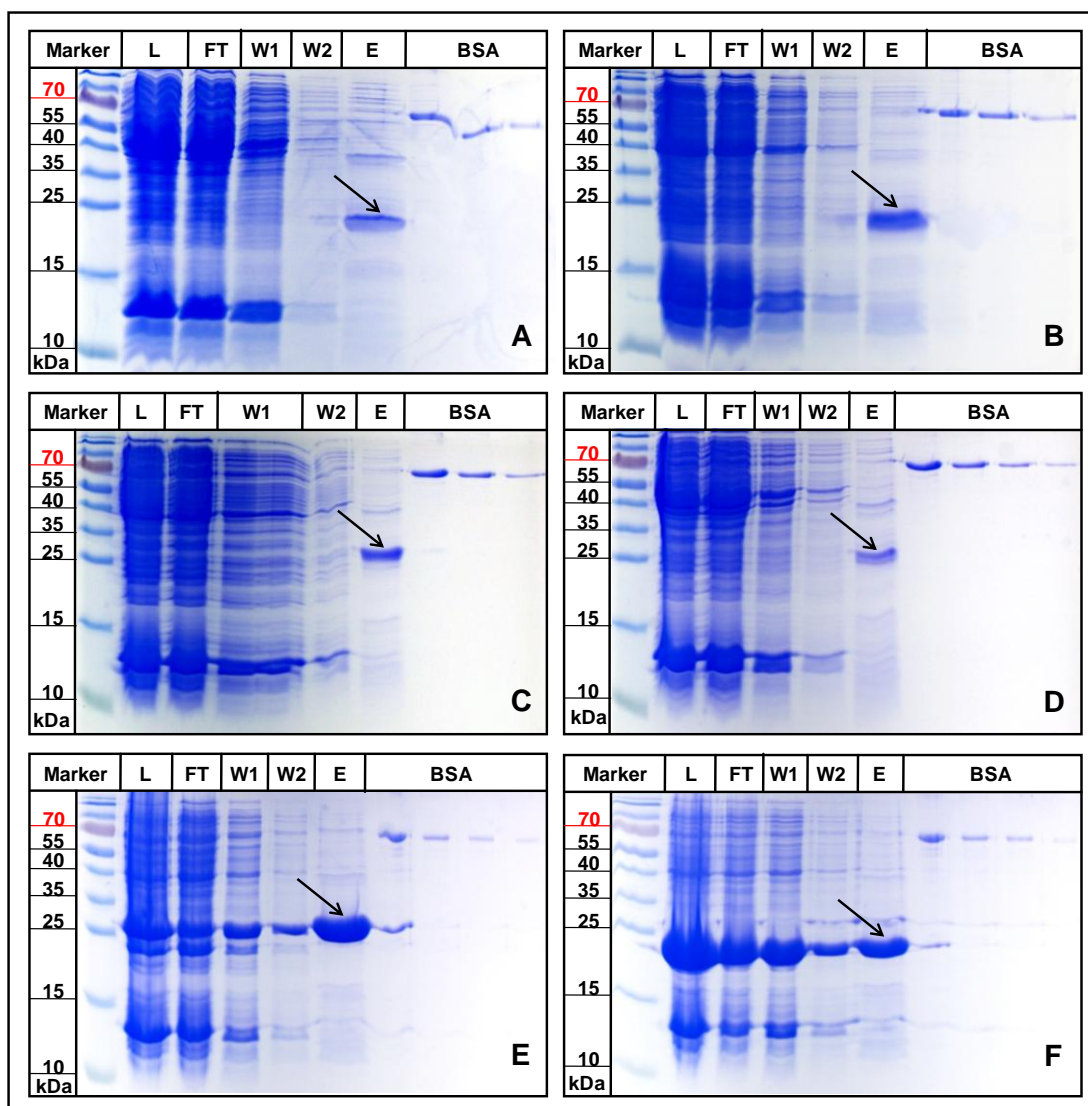
Figure 3-10   Purification of His-tagged RCAR fusion proteins
*Purified His-tagged RCAR1 **(A)**, RCAR3 **(B)**, RCAR9 **(C)**, RCAR10 **(D)**, RCAR13 **(E)** and RCAR14 **(F)** were detected by Coomassie Blue Staining. Abbreviations: L: Lysate; FT: Flow through; W1/W2: Wash 1/2; E: Elution. Serial dilution series of BSA (500 ng, 250 ng and 125 ng) were used for determination of protein concentration. Arrows depict purified 6xHis-RCAR fusion proteins. 5 µl of each eluate (A-F) was loaded per slot.*

In order to determine the concentration of the RCAR proteins, Coomassie Blue stained serial dilutions of BSA were used as a standard. Figure 3-10 shows that purified 6xHis-RCAR1 and RCAR3 fusion proteins were recovered at a concentration of about 200 ng/µl (total of 600 µg from 1 l of bacterial culture) and 250 ng/µl (total 750 µg from 1 l of bacterial culture), respectively. RCAR9 and RCAR10 (Figure 3-10C, D) from clade II and RCAR13 and RCAR14 (Figure 3-10E, F) from clade III were recovered at a concentration of 150 ng/µl, 100 ng/µl, 1000 ng/µl and 500 ng/µl, respectively. Total protein from 1 l of

bacterial culture reached 450 µg, 300 µg, 3000 µg and 1500 µg for RCAR9, RCAR10, RCAR13 and RCAR14, respectively.

3.6 Regulation of PP2C phosphatase activity by RCARs and ABA

Bet v 1 and structurally related proteins from bean species and moss have a potential phytohormone-binding capacity (Markovic-Housley et al., 2003; Pasternak et al., 2006). The three-dimensional structural analysis of Bet v 1 pollen allergen revealed a large hydrophobic cavity that spans the protein and is partly occupied by a broad spectrum of physiological ligands, including brassinosteroids, cytokinins and sterols (Mogensen et al., 2002). Yue Ma presented preliminary data, in which ABI1 and ABI2 are regulated by RCAR1 in the presence of ABA. Consequently, RCAR1, 3, 9, 10, 13 and 14 proteins were tested for binding of ABA in the phosphatase assay, in the presence of PP2Cs from clade A.

3.6.1   Control of PP2C phosphatase activity by RCARs and ABA

Previous analyses, consistently showed an up to 20% reduction of ABI1/2 phosphatase activity in the presence of micromolar levels of ABA though no PP2C-bound ABA was detected (Leube et al., 1998). The inhibition of ABI1 and ABI2 is not stereo-selective, indicating that both PP2Cs are to some extent capable of sensing ABA but that an essential component that provides high affinity and stereo-selectivity for the ligand is missing. The missing constituents are RCAR proteins. In the presence of RCAR1, purified ABI2 was instantaneously and almost fully blocked in its phosphatase activity by 1 µM (*S*)-ABA with half-maximal inhibition 10 seconds after ABA administration (Figure 3-11A). Parallel analysis of RCAR3 showed the half-maximal inhibition time of 30 seconds, indicating a slower responsiveness of RCAR3 (Figure 3-11B).
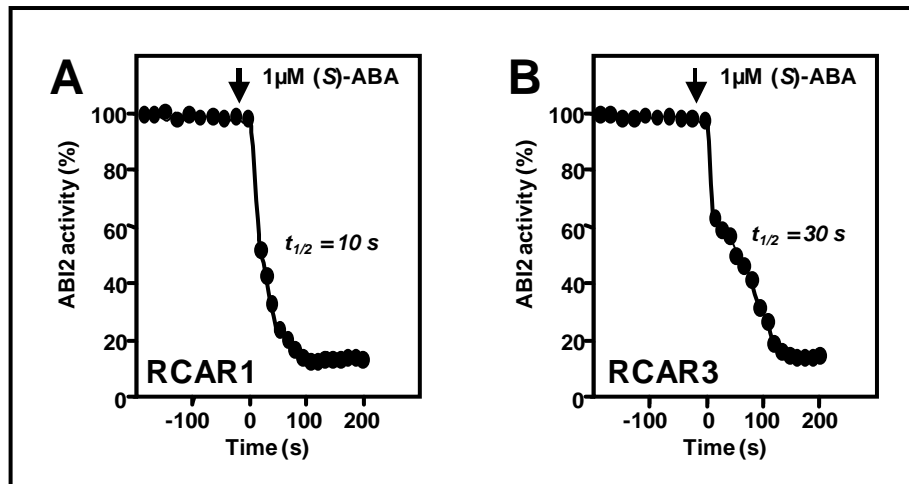
Figure 3-11   Time course of ABI2 inhibition by 1 µM (S)-ABA
Half-maximal inhibition was reached after 10 seconds and 30 seconds with RCAR1 (A) and RCAR3 (B), respectively.

Interestingly, in another phosphatase experiment it was demonstrated that enzymatic activity of ABI2 was regulated differently in the presence of various RCAR proteins and 1 µM (S)-ABA (Figure 3-12). The analysis performed at a constant molar ratio of ABI2:RCAR of approximately 1:4 indicated, that a residual PP2C inhibition of approximately 30% was recorded in the presence of RCAR3 and RCAR9 proteins, in the absence of ABA (Figure 3-12C, E). RCAR1, 10, 13 and 14 seems to show slight stimulation or no regulation of the ABI2 activity in the absence of ABA (Figure 3-12A, F, G, H). Despite this fact, all tested RCAR proteins were able to inhibit the PP2C activity in the ABA-dependent manner. Activity of the PP2C in the presence of 1 µM (S)-ABA and RCAR1, 3, 13 and 14 was reduced to 5-10% (Figure 3-12A, C, G, H).

Proteins from clade II were able to inhibit the ABI2 activity by 20% after the administration of 1 µM (S)-ABA (Figure 3-12E, F). In contrast to other RCARs, RCAR1 complexes with ABI2 were only inhibited to 30% at 10 µM (R)-ABA (Figure 3-12A). *Trans*-ABA (10 µM) was less effective than (R)-ABA in reduction of the phosphatase activity of ABI2 in the presence of RCAR1 and 14.
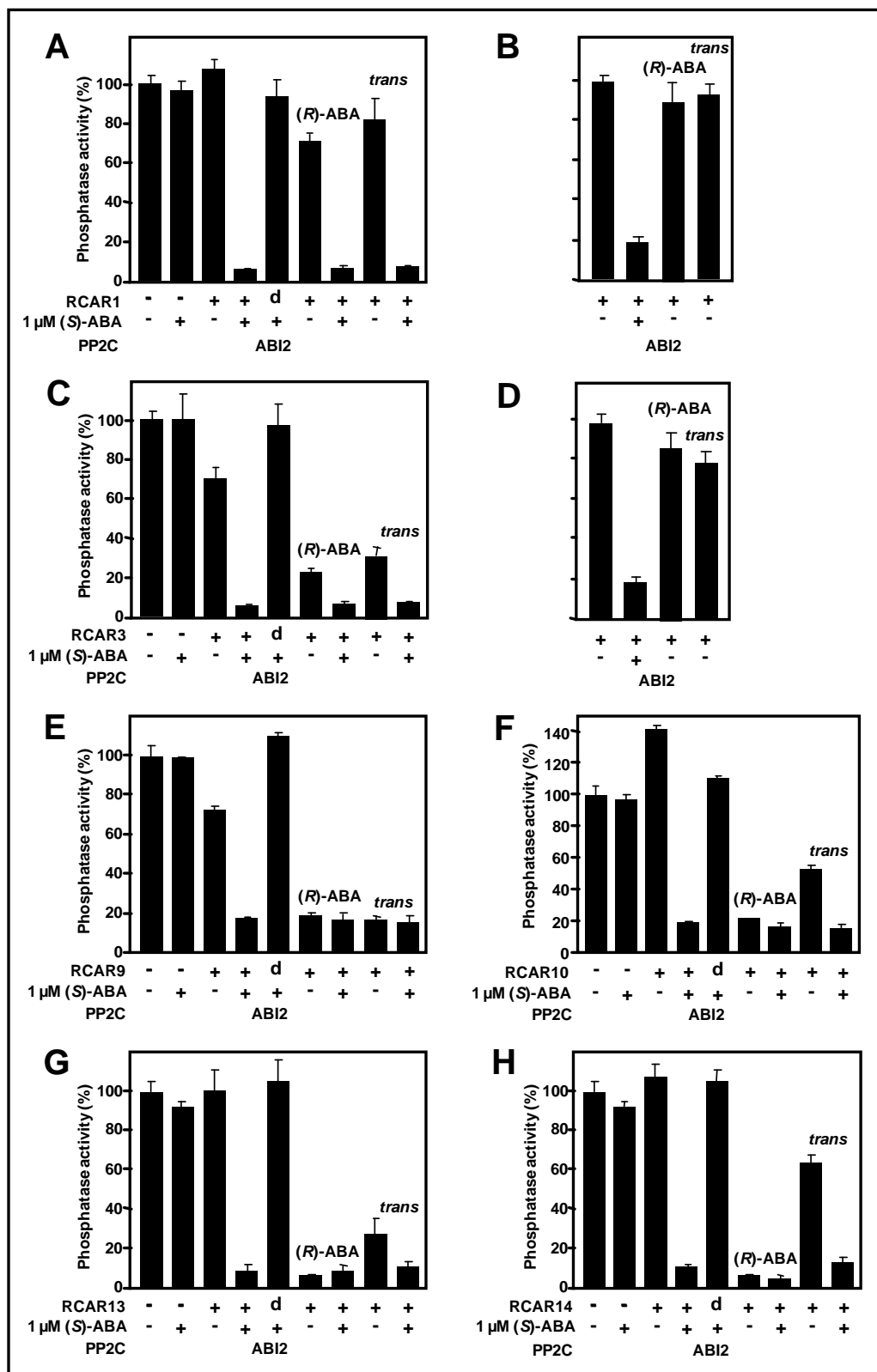
Figure 3-12   Regulation of ABI2 catalytic activities by RCAR proteins and ABA

In vitro analysis conducted with ABI2, RCAR1 (A, B), RCAR3 (C, D), RCAR9 (E), RCAR10 (F), RCAR13 (G) and RCAR14 (H) in the presence or absence of (S)-ABA (1 µM) and/or (R)-ABA and trans (R,S)-ABA (10 µM). The assays were performed with umbelliferylphosphate (A, C, E, F, G, H) or the phosphopeptide RRA(pT)VA (B, D) as a substrate. Activity of ABI2 without RCARs and phytohormone was set to 100%. Heat-denatured RCARs (d, 95°C, 10 min). The maximal ABI2 activity equaled 2 nkat/mg protein in the phosphopeptide assays.

The full extent of ABI2 inhibition was recovered by supplementation of the ABA analogues with 1 µM (*S*)-ABA, while heat-inactivation of RCARs abrogated ABA-regulation of ABI2 (Figure 3-12). To ensure that the ABA-mediated inhibition of PP2C by RCAR1 and RCAR3 is not limited by the artificial substrate methylumbelliferyl phosphate (MUP), a phosphopeptide substrate was tested and yielded comparable results (Figure 3-12B, D). Regulation of the PP2Cs by 1 µM (*S*)-ABA and RCAR1 and RCAR3 was clearly impaired by the amino acid exchange present in *abi1* and *abi2*, which were inhibited less (45 and 43%) in the presence of RCAR1 and 40 and 50% with RCAR3, respectively (Figure 3-13B, D).
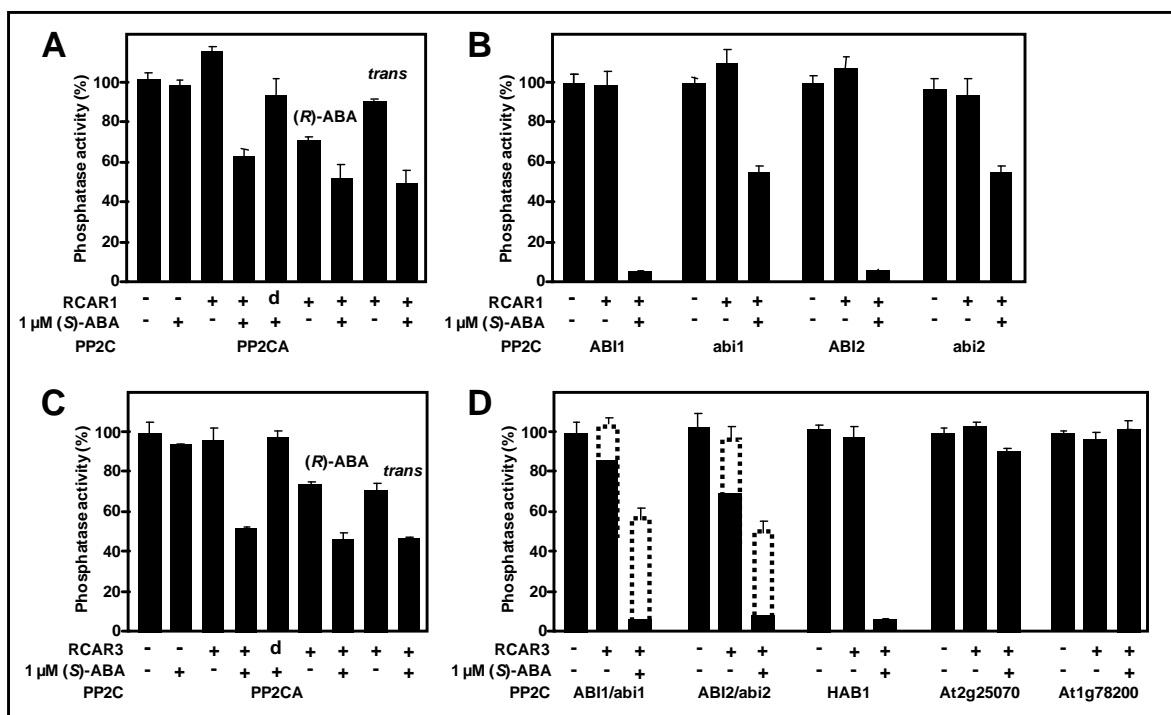
Figure 3-13   PP2C regulation by ABA and RCAR1 and RCAR3
(A, C) *Regulation of PP2CA catalytic activities by RCAR1 (A) and RCAR3 (C) in the presence or absence of (S)-ABA (1 µM) and/or (R)-ABA and trans (R,S)-ABA (10 µM). Activity of PP2CA without RCARs and phytohormone was set to 100%. Heat-denatured RCAR1/3 (d, 95°C, 10 min).*
(B) *Comparison of PP2C inhibition by 1 µM (S)-ABA and RCAR1 between mutant forms and wild-type proteins. Activity of PP2Cs without RCAR1 and phytohormone was set to 100%.*
(D) *Regulation of phosphatase activity by RCAR3 and 1 µM (S)-ABA in the point-mutated abi1 and abi2 (open,dotted line bars), wild type proteins – ABI1 and ABI2 (filled bars) and other PP2Cs from clade A (HAB1), F (At1g78200) and I (At2g25070). Activity of phosphatases without RCAR3 and ABA was set to 100%.*
The assays (B, D) were performed under comparable conditions and revealed a clear insensitivity of the point-mutated PP2Cs (abi1, abi2) compared to ABI1 and ABI2.

The inhibition level under these conditions for the corresponding wild-type proteins was close to saturation (approximately 95%). The less efficient ABA-mediated inhibition of mutant as opposed to wild-type PP2Cs can be explained by their less efficient interaction with RCAR1 and RCAR3 (Figure 3-2).

In contrast to ABI1 and ABI2, another phosphatase called PP2CA was tested. Complexes of RCAR1 with PP2CA were only inhibited to 40%, 32% and 10% at 1 µM (*S*)-ABA, 10 µM (*R*)-ABA and *trans*-ABA, respectively (Figure 3-13A). PP2CA activity in the presence of 1 µM (*S*)-ABA and RCAR3 was reduced to 50%, while the complexes of RCAR3 with PP2CA in the presence of (*R*)-ABA and *trans*-ABA (10 µM) were both inhibited up to 25%, respectively (Figure 3-13C). Supplementation of (*R*)-ABA and *trans*-ABA with (*S*)-ABA yielded the (*S*)-ABA-dependent inhibition and ABI2 inactivation was found to be heat labile (Figure 3-13A, C).

To ascertain that RCAR3 has the ability to regulate the activity of other phosphatases, HAB1 (clade A), PP2Cs from clade F (At1g78200) and I (At2g25070) were tested. HAB1 is known to act as a negative regulator of ABA responses (Saez et al., 2006), and shows an ABA-depedent inhibition in the presence of RCAR3. Two other unknown phosphatases did not reveal any ABA dependent regulation (Figure 3-13D).

A key factor affecting the rate of a reaction catalyzed by an enzyme is the substrate concentration. To clarify the effect of substrate concentration on the ABI2 inactivation, different MUP concentrations were used to study the inhibition by RCARs and ABA in more detail. Phosphatase assays with MUP revealed that the PP2C inhibition imposed by ABA and RCAR1 and RCAR3 is independent of substrate concentration and relies on a non-competitive inactivation of the enzyme (Figure 3-14). The Michaelis-Menton constant of the ABI2 catalyzed reaction was not affected by increasing RCAR1 or RCAR3/enzyme ratios while v_{max} was reduced (Figure 3-14B, D). Thus, the mode of inhibition relies on a non-competitive inactivation of the enzyme in the presence of high ligand concentration.
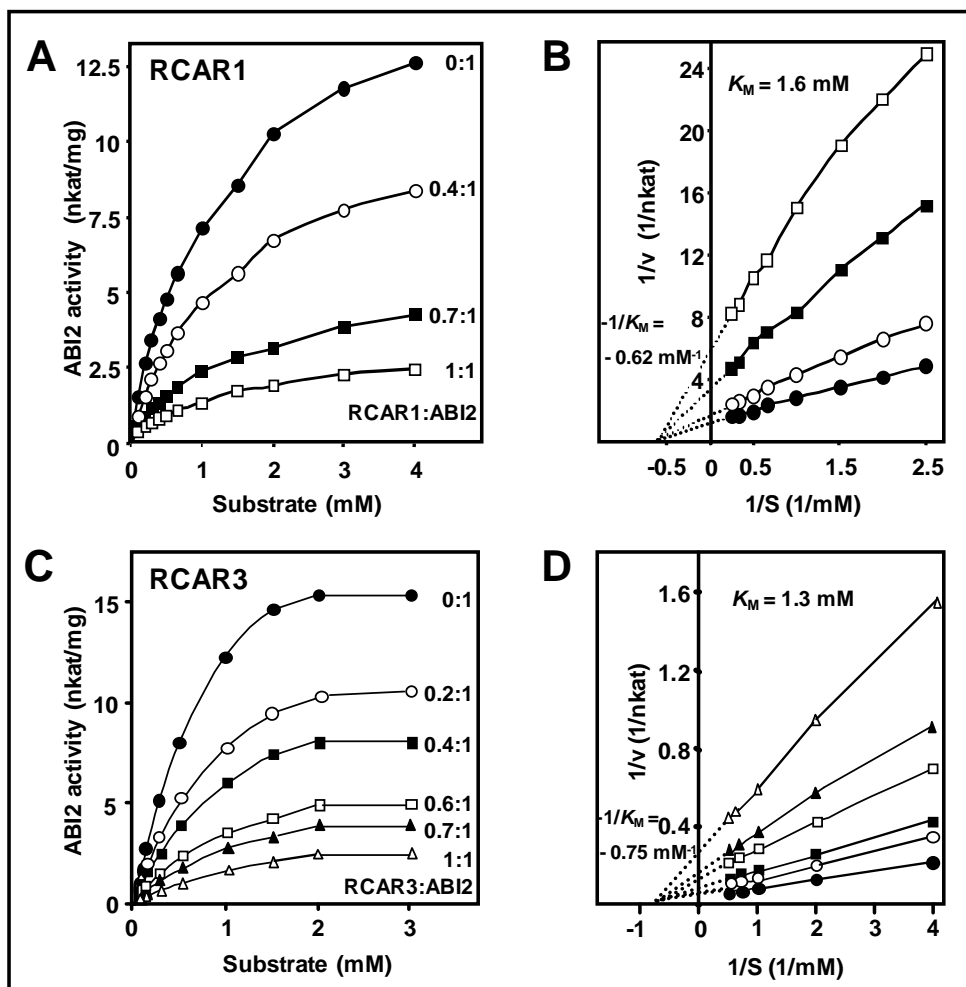
Figure 3-14   Regulation of ABI2 catalytic activities by RCAR proteins
(A) Substrate dependence of ABI2 in the absence (filled circles) or presence of RCAR1 at a molar ratio of 0.4, 0.7, and 1 (open circles, filled and open squares, respectively). The analysis was performed in the presence of 1 mM R,S-ABA (SD< 6%).
(B) Lineweaver-Burk plot of data from (A).
(C) Substrate dependence of ABI2 activity in the absence (filled circles) or presence of RCAR3 at a molar ratio 0.2, 0.4, 0.6, 0.7 and 1 (open circles, filled and open squares and filled and open triangles, respectively). The analysis was performed in the presence of 1 mM (S)-ABA (SD < 4%).
(D) Lineweaver–Burk plot of data from (C).

In the presence of saturating ABA levels, serial dilutions of an RCAR1/3-containing ABI2 solution maintained a constant inhibition level up to 5 nM ABI2 (Figure 3-15A, B). The stability of the inhibition level was only observed at saturating ABA levels, consistent with an ABA-mediated stabilization of the RCAR1/3-ABI2 complex in the low nanomolar range.
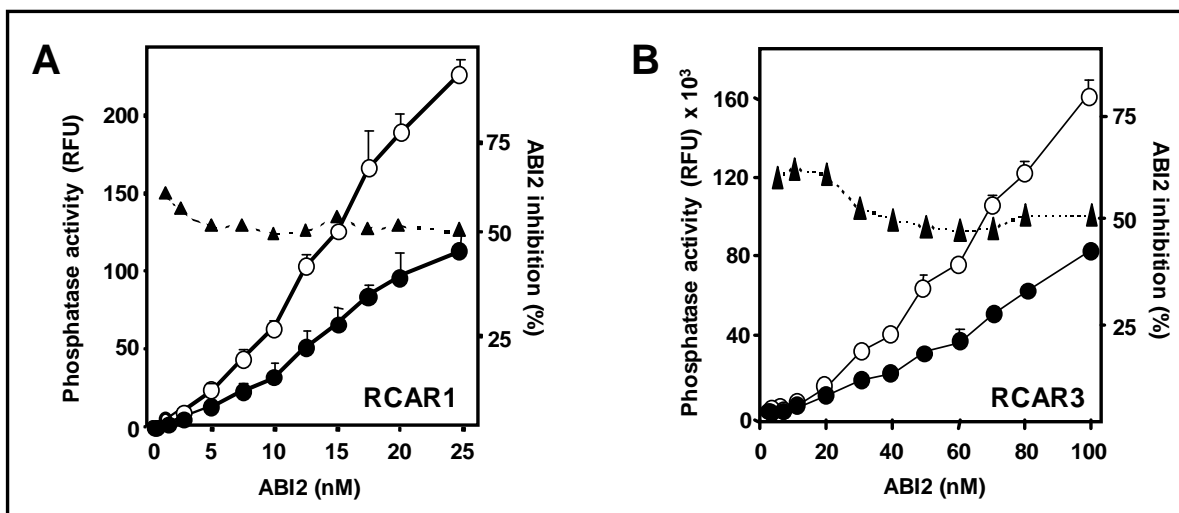
Figure 3-15   Regulation of ABI2 catalytic activities by RCAR protein
(A, B) *Regulation of ABI2 activity at a fixed molar ratio of RCAR1 (A) or RCAR3 (B) and ABI2 (approximately 1 to 1.8). The protein phosphatase activity was analyzed at different levels of ABI2 in the presence (filled circles) or absence (open circles) of 1 mM (S)-ABA. Activity is given in relative fluorescence units (RFU) and the ABI2 inhibition level is given as a percentage (filled triangles, dotted line).*

3.6.2   RCARs concentration dependence of PP2C activity

In order to investigate the effect of RCAR proteins on the regulation of ABI2 activity, several experiments were performed. First, the stoichiometry of the RCAR1/ABI2 and RCAR3/ABI2 intercations was defined. A fixed concentration of ABI2 was titrated with increasing levels of the RCAR1 or RCAR3 in the presence of saturating ABA concentrations (1 mM (S)-ABA). As shown in Figure 3-16 half-maximal inhibition occurred at an RCAR1 to ABI2 ratio of approximately 0.5 (Figure 3-16A). The same results were obtained for RCAR3 (Figure 3-16B). The values for both RCAR1 and RCAR3 ranged between 0.3 and 0.8 depending on the different protein preparations. Combined, the data for RCAR1 and RCAR3 support a one-to-one ratio of the heteromeric protein complex.
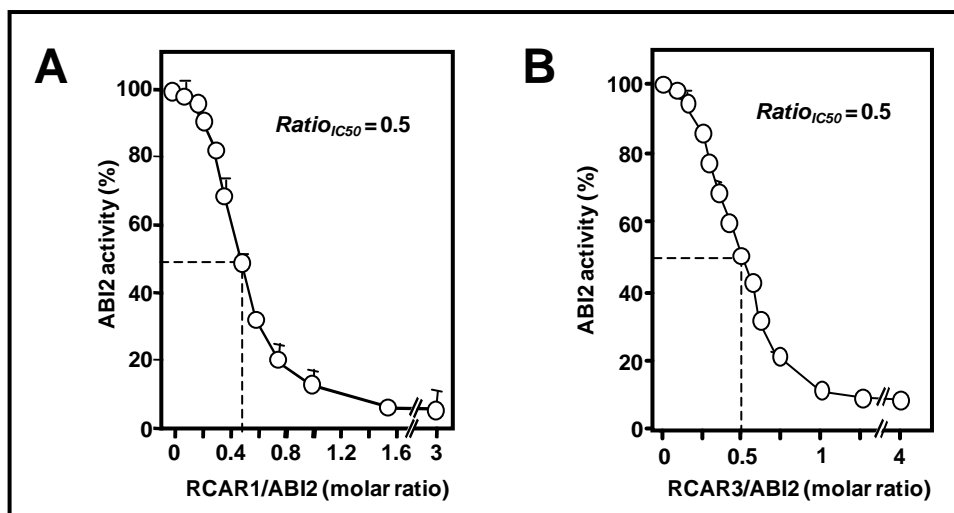
Figure 3-16 **Stoichiometric analysis of RCAR1/3-ABI2 complex**
Analysis was performed in the presence of saturating concentration of (S)-ABA (1 mM)
Half-maximal inhibition occurred at RCAR1 (A) or RCAR3 (B) to ABI2 ratio of ~0.5 (SD < 5%)
consistent with a 1:1 RCAR1/3:ABI2 complex.

The next question was whether RCAR proteins were able to regulate the PP2C activity of ABI2 in the absence of (S)-ABA. In the phosphatase assays with MUP as a substrate a fixed concentration of ABI2 was titrated with increasing levels of the RCAR1, 3, 9, 10, 13 and 14, without ABA treatment. Surprisingly, two RCAR proteins revealed an inhibitory effect on PP2C activity, and other four were able to stimulate ABI2 activity (Figure 3-17). At a value of 16 for RCAR:ABI2 molar ratio, RCAR3 and RCAR9 were effective in inhibiting ABI2 activity to approximately 60% and 50%, respectively (Figure 3-17B, C). The results recorded with RCAR1, 10, 13 and 14 at the same RCAR/ABI2 molar ratio showed, that ABI2 phosphatase activity was stimulated to 150%, 300%, 140% and 175%, respectively (Figure 3-17A, D, E, F). Heat inactivation of RCAR proteins abrogated the interaction with ABI2.
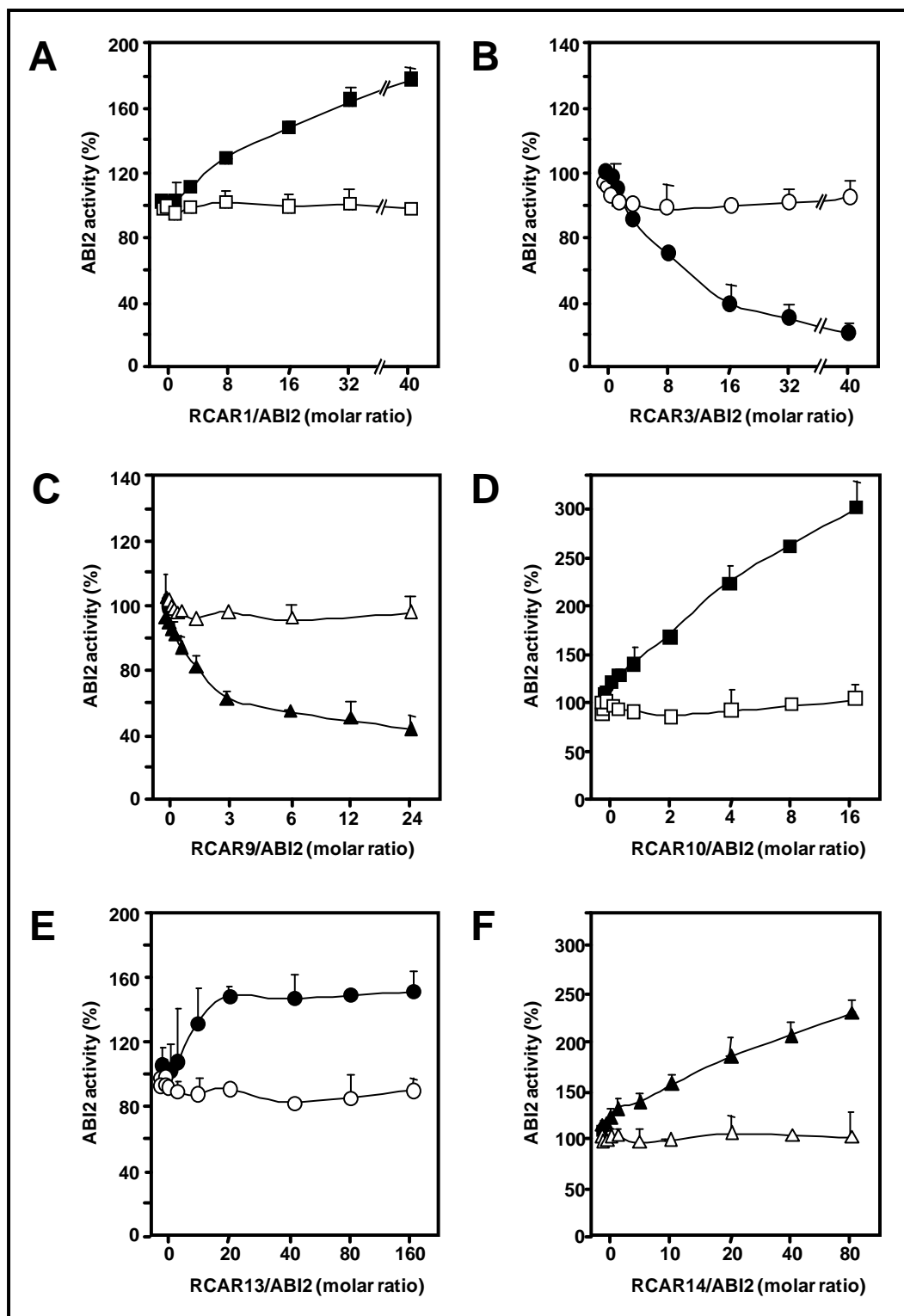
Figure 3-17   Regulation of ABI2 activity in the presence of RCAR proteins and absence of ABA

(A) Stimulation of ABI2 activity by increasing concentrations of RCAR1 (filled squares). Heat-denatured RCAR1 (95°C, 10 min, open squares)

(B, C) Inhibition of ABI2 activity by increasing concentrations of RCAR3 (filled circles) and RCAR9 (filled triangles). Heat-denatured RCAR3/9 (95°C, 10 min, open circles and open triangles, respectively)

(D, E, F) Stimulation of ABI2 activity by increasing concentrations of RCAR10, 13 and 14 (filled squares, circles and triangles). Heat-denatured RCAR10/13/14 (95°C, 10 min, open squares, circles and triangles).

3.6.3   ABA concentration dependence of PP2C activity

Analysis of RCAR proteins revealed an ABA-dependent inactivation of PP2Cs. In order to establish whether differences between RCARs exist in terms of ABA sensitivity and ligand selectivity fourteen different receptor complexes generated by different combinations of RCAR1/3/9/10/13/14 and ABI1/ABI2/PP2CA were compared.

Phosphatase assays, in which physiologically active (*S*)-ABA was titrated to ABI1 and RCAR1 revealed an IC_{50} value for phosphatase inhibition of approximately 35 nM (Figure 3-18A). Under comparable experimental conditions, ABI2 and RCAR1 yielded an IC_{50} of 60 nM (*S*)-ABA (Figure 3-18C). (*R*)-ABA and *trans*-ABA enantiomers were equally effective at promoting RCAR1-mediated inhibition of ABI1 and ABI2 activity (Figure 3-18B, D). Data showed that (*R*)-ABA and *trans*-ABA were less effective in inhibiting PP2C activity. At a concentration of 30 µM (*R*)-ABA and *trans*-ABA were not able to inhibit phosphatase activity of ABI1 and ABI2 to a level evoked by 30 nM (*S*)-ABA.

RCAR3 protein also revealed an ABA-dependent inhibitory effect on ABI1 and ABI2 activity. The ABA-IC_{50} values for ABI1 and ABI2 were 18 and 30 nM, respectively (Figure 3-19A, C). (*R*)-ABA and *trans*-ABA were effective in inhibiting ABI1 and ABI2 to approximately 80%, albeit at much higher ligand levels (Figure 3-19B, D). Indeed, compared with the 18 nM IC_{50} value for (*S*)-ABA, more than 1 µM (*R*)-ABA or 3 µM *trans*-ABA were required to accomplish half-maximal inhibition.

Interestingly, a closely related PP2C from clade A, PP2CA, also appeared to be regulated in ABA-dependent manner. Figures 3-18 and 3-19 showed that titration of physiologically active (*S*)-ABA to PP2CA, in the presence of RCAR1 and RCAR3 revealed an IC_{50} value for PP2CA inhibition of approximately 10 µM. At a concentration of 10 µM (*R*)-ABA and *trans*-ABA were able to inhibit phosphatase activity of ABI1 and ABI2 in the presence of RCAR1 to a level evoked by 1 µM and 100 nM (*S*)-ABA, respectively (Figure 3-13A). Complexes of RCAR3 with PP2CA in the presence of (*R*)-ABA and *trans*-ABA (10 µM) were both inhibited up to 25%, which correspond to the inhibition evoked by 300 nM (*S*)-ABA (Figure 3-13C).
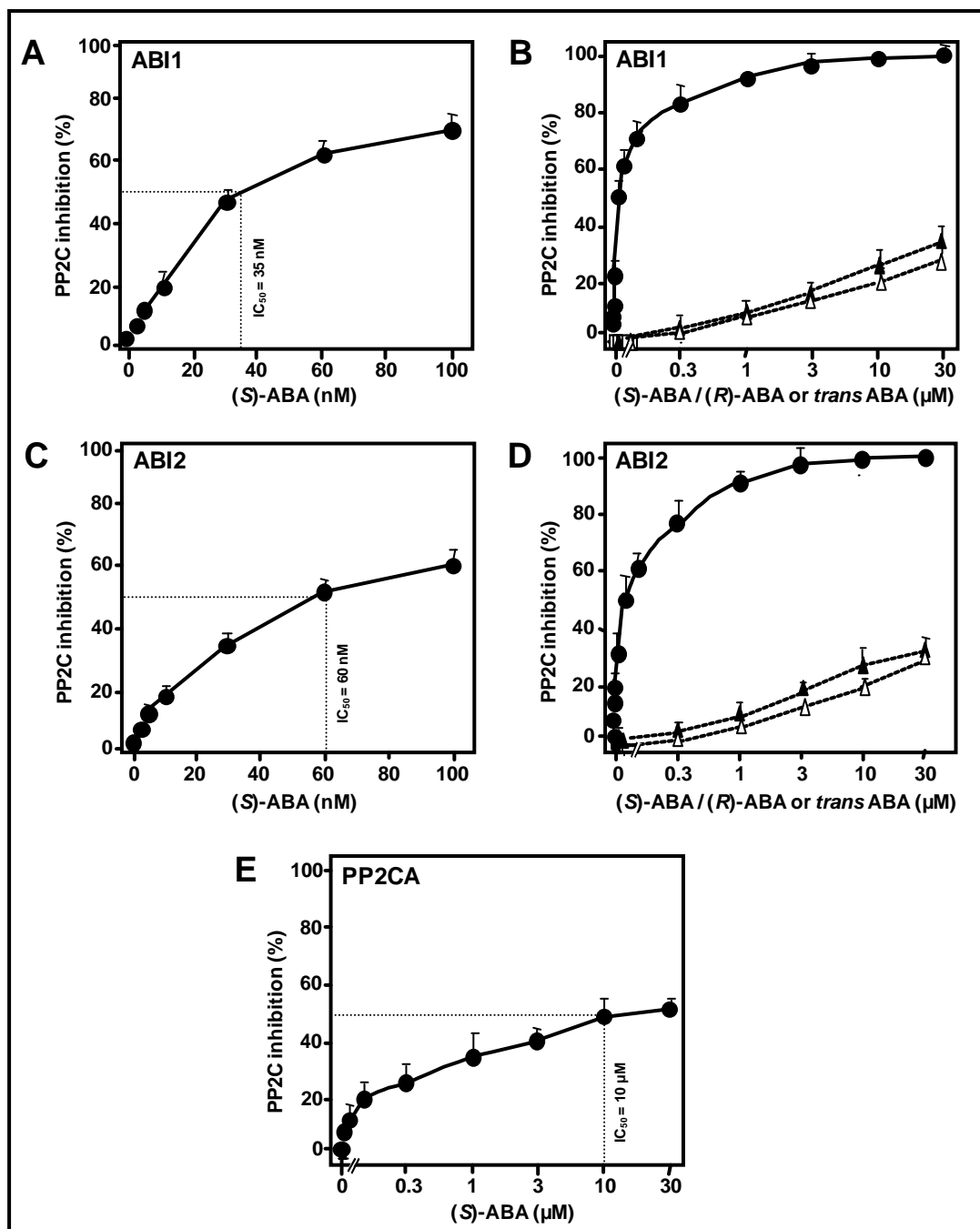
Figure 3-18   Binding of ABA to RCAR1 and PP2Cs and the regulation of PP2C phosphatase activity
*Inhibition of ABI1 **(A)** by increasing concentrations of (S)-ABA. Half-maximal inhibition of ABI1 occurred at ~35 nM of physiologically active (S)-ABA in the presence of RCAR1. **(B)** Inhibition of ABI1 by (S)-ABA (filled circles, solid line), (R)-ABA (filled triangles, dotted line), and trans (R,S)-ABA (open triangles, dotted line). **(C, D)** Corresponding analysis of ABI2 as shown in (A, B). Half-maximal inhibition of ABI2 occurred at ~60 nM of (S)-ABA with RCAR1. **(E)** Inhibition of PP2CA by (S)-ABA in the presence of RCAR1. Half-maximal inhibition of PP2CA was reached at ~10 µM of (S)-ABA in the presence of RCAR1. The analyses (A-E) were performed at a constant molar ratio of PP2C:RCAR1 of approximately 1:4 and with the PP2C level at 0.05 µM.*
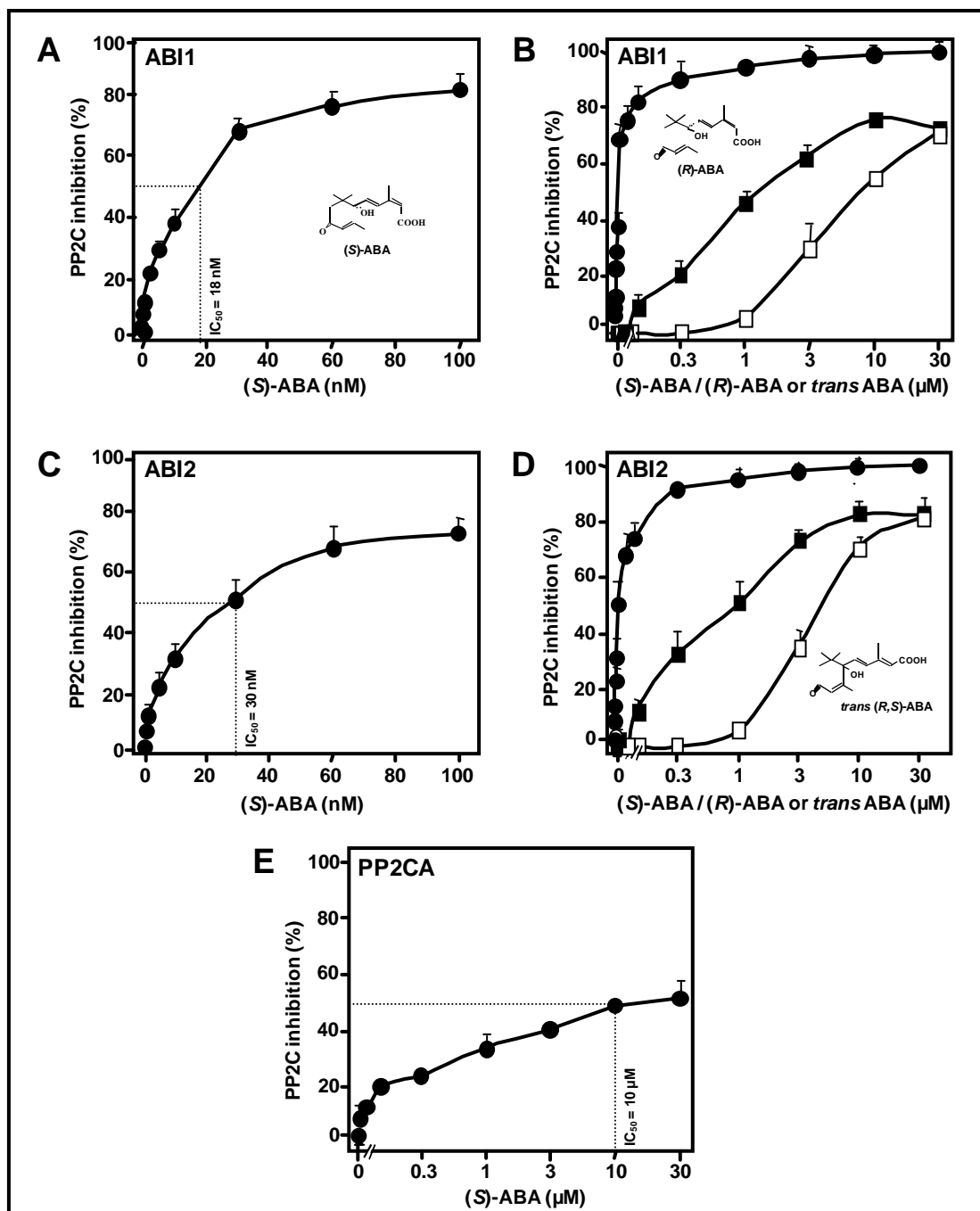
Figure 3-19   ABA-dependent inhibitory effect of RCAR3 protein on ABI1, ABI2 and PP2CA activity

*Inhibition of ABI1 **(A)** by increasing concentrations of (S)-ABA. Half-maximal inhibition of ABI1 occurred at ~18 nM of (S)-ABA in the presence of RCAR3. **(B)** Inhibition of ABI1 by (S)-ABA (filled circles, solid line), (R)-ABA (filled squares), and trans (R,S)-ABA (open squares). **(C, D)** Corresponding analysis of ABI2 as shown in (A, B). Half-maximal inhibition of ABI2 occurred at ~30 nM of (S)-ABA with RCAR3. **(E)** Inhibition of PP2CA by (S)-ABA in the presence of RCAR3. ABA-IC$_{50}$ value was reached at ~10 µM of (S)-ABA in the presence of RCAR3. The analyses (A-E) were performed at a constant molar ratio of PP2C:RCAR3 of approximately 1:4 and with the PP2C level at 0.05 µM.*

79

In order to establish whether the ABA inhibitory concentration required to achieve 50% inhibition (ABA-IC_{50}) of PP2C activity was dependent on the RCAR protein assayed, we also tested RCAR9 and 10 from clade II, and RCAR13 and 14 from clade III.

Thus, in the presence of RCAR9, the half-maximal inhibition of ABI1 and ABI2 occurred at approximately 9 nM and 3 nM of physiological active (*S*)-ABA, respectively (Figure 3-20A, C). The residual inhibition of ABI1 and ABI2 was also recorded in the presence of either (*R*)-ABA or *trans*-ABA. In the presence of RCAR9, 30 µM (*R*)-ABA was more effective in inhibiting ABI1 and ABI2 activity compared to *trans*-ABA. Half-maximal inhibition of ABI1 and ABI2 occurred at approximately 20 nM of (*R*)-ABA and more than 1 µM of *trans*-ABA (Figure 3-20B, D).
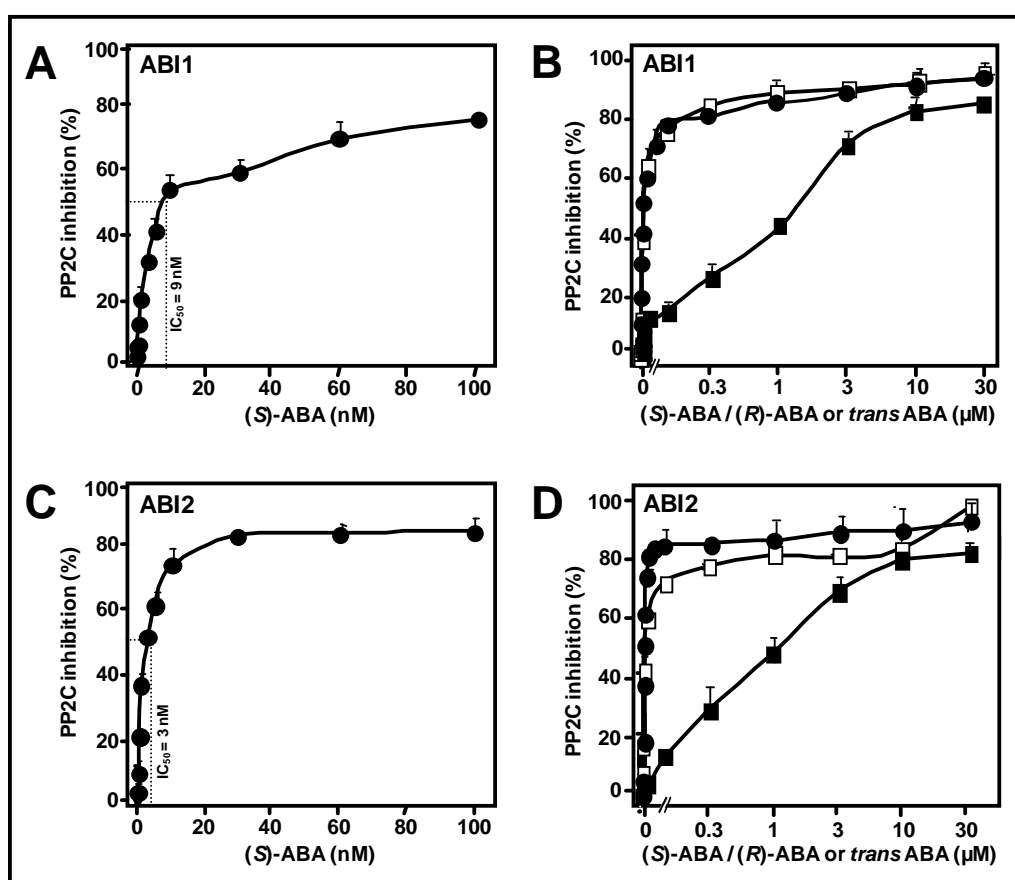
Figure 3-20   Binding of ABA to RCAR9 and PP2Cs and the regulation of PP2C phosphatase activity
*Inhibition of ABI1 **(A, B)** and ABI2 **(C, D)** by (S)-ABA (filled circles), (R)-ABA (open squares), and trans-(R,S)-ABA (filled squares) in the presence of RCAR9.*
IC_{50} value of ABI1 and ABI2 occurred at ~9 nM and 3 nM of physiologically active (S)-ABA, respectively. The analyses (A-D) were performed at a constant molar ratio of PP2C:RCAR9 of approximately 1:4 and with the PP2C level at 0.05 µM.

As another representative of clade II of the RCAR protein family, we used RCAR10. Titration of physiologically active (*S*)-ABA to ABI1 and RCAR10 revealed an IC_{50} value of 10 nM, which was comparable with IC_{50} value obtained for RCAR9, another member of clade II (Figure 3-21A). The ABA- IC_{50} for ABI2 in the presence of RCAR10 was 30 nM, which indicates that (*S*)-ABA is ten times less effective with RCAR10 than with RCAR9 at promoting inhibition of ABI2 (Figure 3-21C).

Under comparable experimental conditions, (*R*)-ABA and *trans*-ABA were able to inhibit phosphatase activity of ABI1 and ABI2. Half-maximal inhibition was recorded for ABI1 and ABI2 at 10 µM of *trans*-ABA. (*R*)-ABA was able to achieve 50% inhibition of ABI1 and ABI2 in the presence of RCAR 10 at 300 nM and 400 nM, respectively (Figure 3-21B, D).
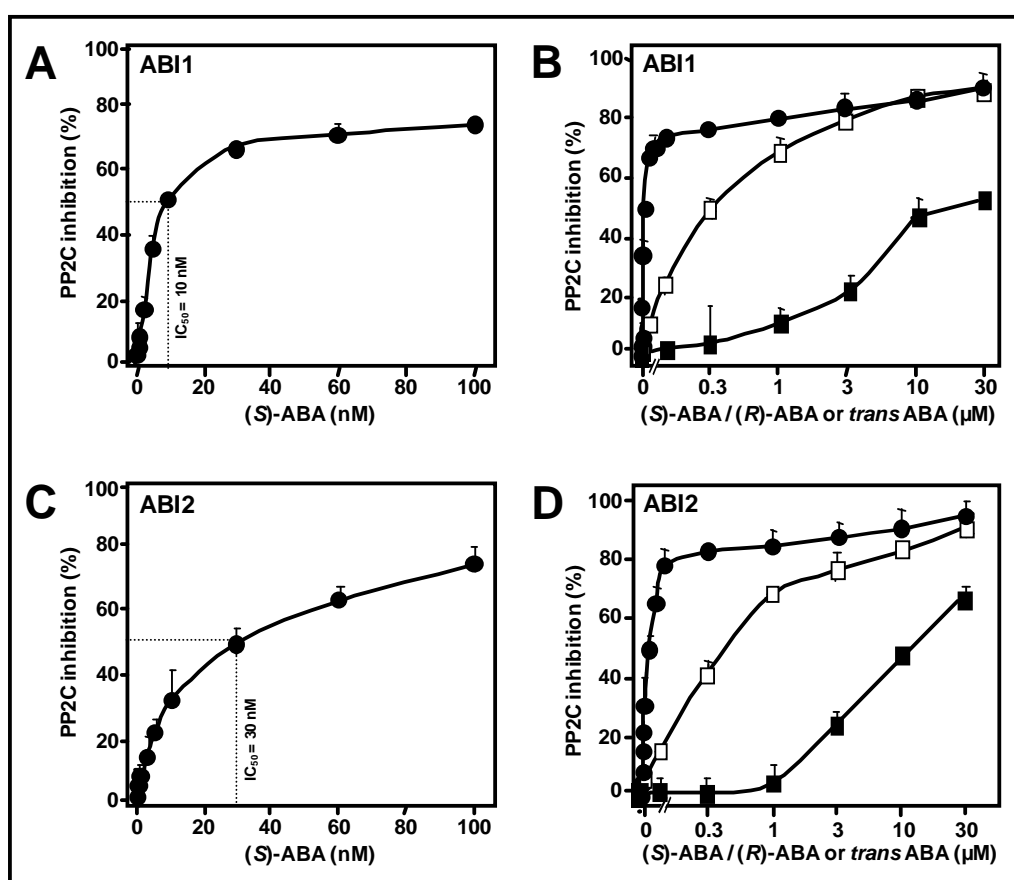
Figure 3-21   Binding of ABA to RCAR10 and PP2Cs and the regulation of PP2C phosphatase activity
*Inhibition of ABI1 **(A)** by increasing concentrations of (S)-ABA. IC_{50} value for ABI1 occurred at ~10 nM of (S)-ABA in the presence of RCAR10. **(B)** Inhibition of ABI1 by (S)-ABA (filled circles), (R)-ABA (open squares), and trans (R,S)-ABA (filled squares). **(C, D)** Corresponding analysis of ABI2 as shown in (A, B). IC_{50} value for ABI2 occurred at ~30 nM of (S)-ABA with RCAR10. The analyses (A-D) were performed at a constant molar ratio of PP2C:RCAR10 of approximately 1:4 and with the PP2C level at 0.05 µM.*

ABA-dependent inactivation of PP2Cs was also detected in the presence of RCAR13 and RCAR14, members of clade III of RCAR protein family. As shown in Figure 3-22, half-maximal inhibition values of ABI1 and ABI2 in the presence of RCAR13 were 10 nM and 5 nM for (S)-ABA, which indicates that physiologically active (S)-ABA is two times more effective with ABI2 than with ABI1, in reduction of the catalytic activity of PP2C (Figure 3-22A, C). We also tested whether (R)-ABA and *trans*-ABA enantiomers were equally effective at promoting RCAR13-mediated inhibition of ABI1 and ABI2 activity (Figure 3-22B, D). The ABA- IC_{50} for ABI1 in the presence of RCAR13 was approximately 50 nM for (R)-ABA and 3 µM for *trans*-ABA, which indicates that (R)-ABA is sixty times more effective than *trans*-ABA at promoting inhibition of ABI1 mediated by RCAR13 (Figure 3-22B). The IC_{50} value for ABI2 was 100 nM and less than 3 µM for (R)- and *trans*-ABA, respectively (Figure 3-22D).
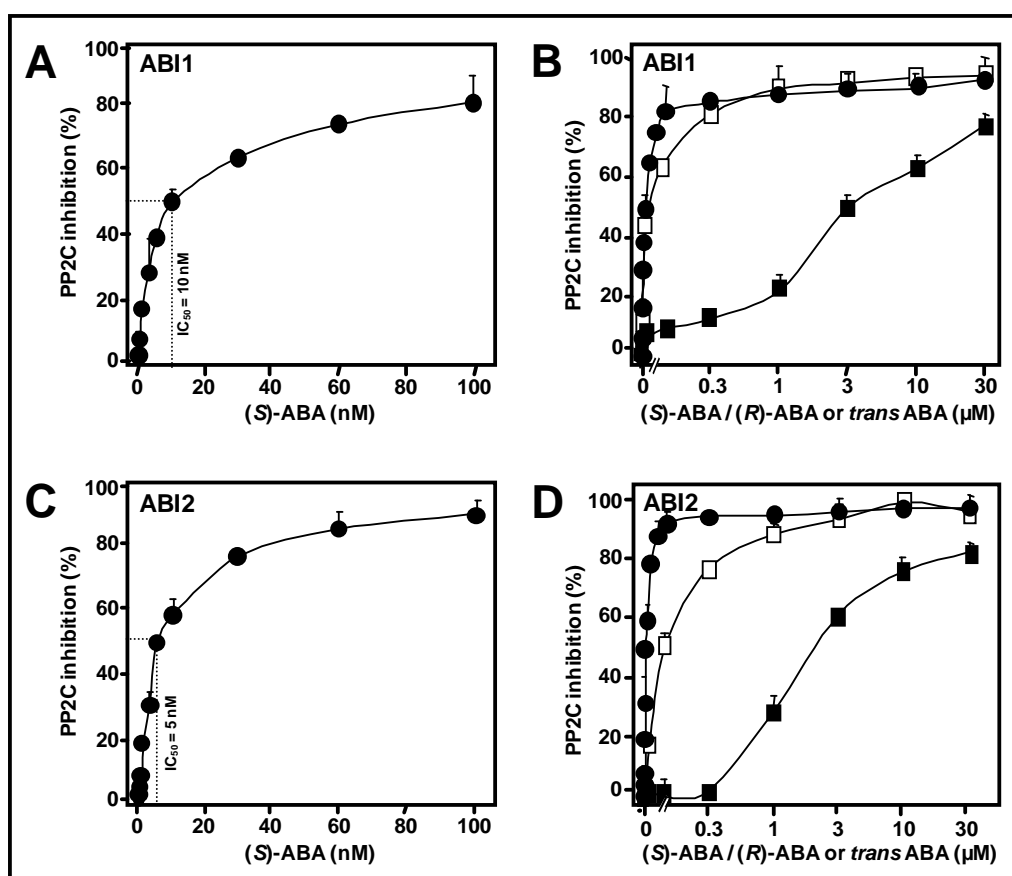
Figure 3-22   ABA-dependent inhibitory effect of RCAR13 protein on ABI1 and ABI2 activity

Inhibition of ABI1 (A) by increasing concentrations of (S)-ABA. Half-maximal inhibition of ABI1 occurred at ~10 nM of (S)-ABA in the presence of RCAR13. (B) Inhibition of ABI1 by (S)-ABA (filled circles), (R)-ABA (open squares), and trans (R,S)-ABA (filled squares). (C, D) Corresponding analysis of ABI2 as shown in (A, B). Half-maximal inhibition of ABI2 occurred at ~5 nM of (S)-ABA with RCAR13. The analyses (A-D) were performed at a constant molar ratio of PP2C:RCAR13 of approximately 1:4 and with the PP2C level at 0.05 µM.

For RCAR14, residual inhibition of ABI1 and ABI2 after administration of physiologically active (S)-ABA occurred at 60 and 83 nM, respectively (Figure 3-23A, C). These IC_{50} values were 6- and more than 16-fold higher than values obtained with ABI1 and ABI2, in the presence of RCAR13, which is also a member of clade III of RCAR family. This might indicate that there are some differences between RCARs in terms of ABA sensitivity. (R)-ABA was able to inhibit ABI1 and ABI2 activity to approximately 80-90%. Compared with the 60 nM and 83 nM IC_{50} values for (S)-ABA, more than 300 nM (R)-ABA for ABI1 and ABI2 was required to accomplish half-maximal inhibition (Figure 3-23B, D). At a concentration of 30 µM trans-ABA was able to inhibit phosphatase activity of ABI1 and ABI2 in the presence of RCAR14 to a level evoked by 40 nM and 60 nM (S)-ABA, respectively (Figure 3-23B, D).
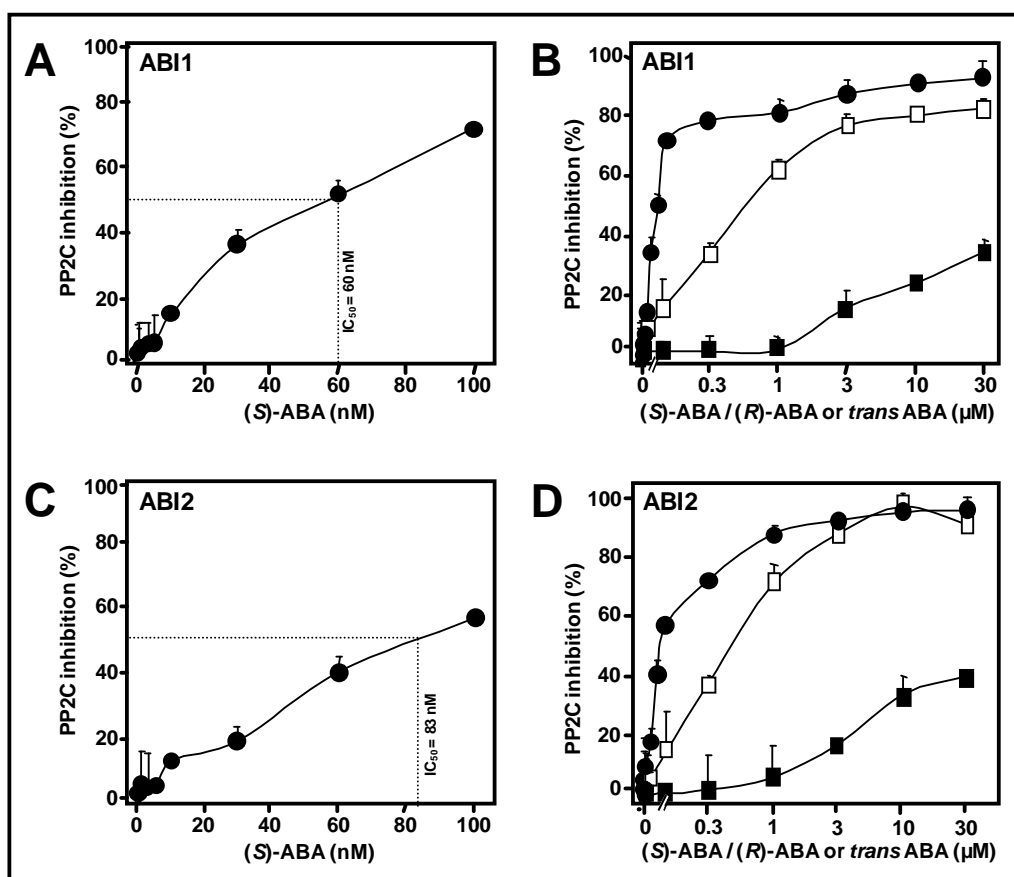
Figure 3-23 **Binding of ABA to RCAR14 and PP2Cs and the regulation of PP2C phosphatase activity**
Inhibition of ABI1 **(A, B)** and ABI2 **(C, D)** by (S)-ABA (filled circles), (R)-ABA (open squares), and trans-(R,S)-ABA (filled squares) in the presence of RCAR14.
IC_{50} value of ABI1 and ABI2 occurred at ~60 nM and 83 nM of physiologically active (S)-ABA, respectively. The analyses (A-D) were performed at a constant molar ratio of PP2C:RCAR14 of approximately 1:4 and with the PP2C level at 0.05 µM.

I tested whether the sensitivity of PP2C regulation was affected by modulations in the PP2C:RCAR ratio. The PP2C levels of ABI1 and ABI2 were kept constant while altering those of RCAR1 or RCAR3 in *in vitro* experiments. IC_{50} values correspond to the ABA concentration required to achieve a 50% inhibition of the phosphatase activity and, as such, these are a good measure of the sensitivity of the PP2C regulation by ABA. Figure 3-24 shows that the PP2C:RCAR ratio has a large impact on IC_{50} values. As RCAR levels increase, IC_{50} values decrease, indicating a more ABA-sensitive regulation of phosphatase activity. Conversely, the PP2C regulation with RCAR1 and RCAR3 becomes less sensitive to ABA, when PP2C:RCAR ratio increases. As shown in Figure 3-24, the efficiency of ABA-mediated phosphatase inhibition was higher with ABI1 than with ABI2 and higher with RCAR3 than with RCAR1. The IC_{50} values of PP2C inhibition were approximately twofold lower with RCAR3 versus RCAR1 at a 2:1 RCAR:PP2C ratio. Under these experimental conditions, ABI1 was approximately twofold more sensitive to ABA regulation than ABI2. Half-maximal inhibition of RCAR3/ABI1 was observed at 23 nM ABA, whereas RCAR1/ABI2 revealed a more than fourfold higher IC_{50} value of 95 nM ABA (Figure 3-24A, B). The finding reflects major differences in the heteromeric receptor complexes with respect to ABA-mediated inhibition. PP2C inhibition requires RCAR binding to the PP2C, and increasing the RCAR:PP2Cs ratio shifts the equilibrium towards complex formation. The differences between IC_{50} values of ABI1/RCAR3 and ABI2/RCAR1 were reduced with increasing RCAR levels, and were almost abolished at high excess levels of RCAR (PP2C:RCAR value of 0.1). Interestingly, the IC_{50} values were more responsive to changes in RCAR1 than RCAR3 levels by a factor of 2.5 and 5.4 for ABI1 and ABI2, respectively. The data imply a higher affinity of RCAR3 for PP2C interaction compared with RCAR1. Thus, both the PP2C and RCAR components modulate the sensitivity of ABA-mediated PP2C inactivation. Inactivation of the PP2Cs is required to overcome their negative regulation of the ABA signal pathway and to allow the activation of the ABA response via SnRKs (Fujii and Zhu, 2009; Nakashima et al., 2009), with RCAR3 and ABI1 providing greater ABA-sensitive regulation.
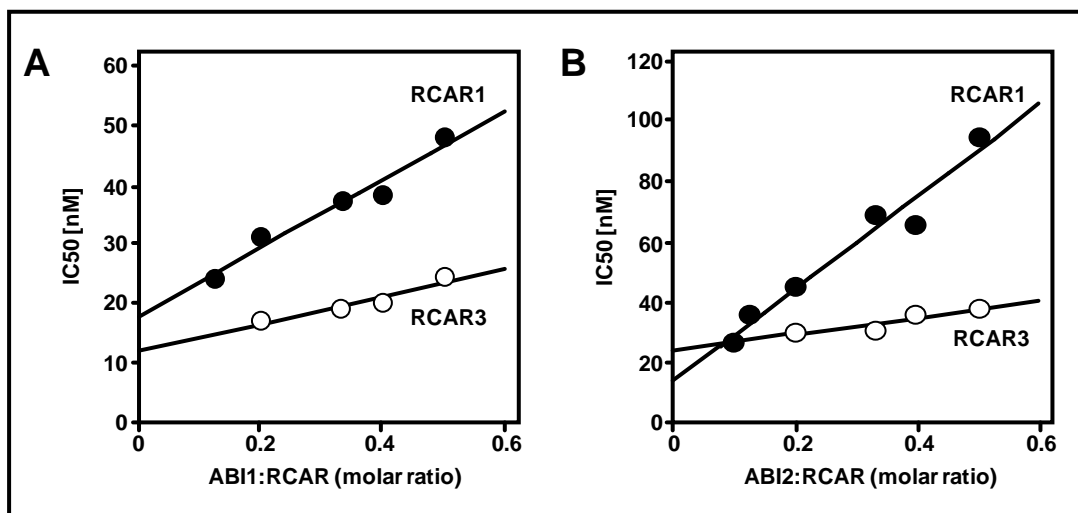
Figure 3-24 **Dependence of ABA-mediated inhibition on receptor complex composition and co-receptor ratios.**
ABI1 (A) and ABI2 (B) were titrated with increasing levels of RCAR1 (filled circles) and RCAR3 (open circles). The half-maximal inhibitory ABA concentration was determined at different molar ratios of PP2C:RCAR, and a constant PP2C level at 0.05 µM.

3.7 Isothermal titration calorimetry of RCAR proteins

Phosphatase assays revealed that RCAR proteins are able to bind small hydrophobic ligands, as has been reported for Bet v 1 (Radauer et al., 2008). Therefore, with the help of isothermal titration calorimetry (ITC), it was possible to determine whether RCAR1 and RCAR3 are able to bind ABA. ITC is a method for measuring biomolecular interactions (protein-protein or protein-ligand). This thermodynamic technique directly measures the heat released or absorbed during a biomolecular binding event. Measurement of this heat allows accurate determination of binding affinity (K_d), number of binding sites or enthalpy (ΔH) and entropy (ΔS) of binding (Pierce et al., 1999).

(*S*)-ABA is the physiologically active form of the phytohormone, used for all binding studies. Titration of the ligand ((*S*)-ABA) into the RCAR1/3 protein solution in the ITC cell resulted in heat release, which indicates that the reaction was exothermic (Figure 3-25; Inset). When the system reached saturation, the heat signal diminished (only the background heat of dilution is observed). Binding curves of RCAR1/3 were obtained from a plot of the heats from each injection against the ratio of ligand and binding partner in the ITC cell. These binding curves show that RCAR1 was binding (*S*)-ABA with apparent K_d of approximately 660 ± 80 nM ABA (Figure 3-25B). Upon addition of ABI2 to RCAR1, the analysis yielded higher energy changes and lower apparent K_d of 64 ± 8 nM ABA (Figure 3-25A). Binding between RCAR1 and ABI2 was tested as well, but did not reveal any

interaction (data not shown). This result might indicate that RCAR1 concentration was too low to achieve the saturation of ABI2.

Interaction of RCAR3 to (*S*)-ABA, examined by isothermal titration calorimetry revealed binding of (*S*)-ABA to RCAR3, with a relatively low affinity, with K_d of approximately 970 ± 150 nM ABA (Figure 3-25C). Titration of the buffer, instead of ligand into the RCAR3 protein (Figure 3-25D) did not show that the heat was absorbed or released, which indicates that measured temperature changes in Figure 3-25C were due to the action of (*S*)-ABA.

Taking together, all these binding ITC data demonstrate that phytohormone was binding to the RCAR-ABI2 protein complex with higher affinity, compared to the RCAR protein alone (Figure 3-25).
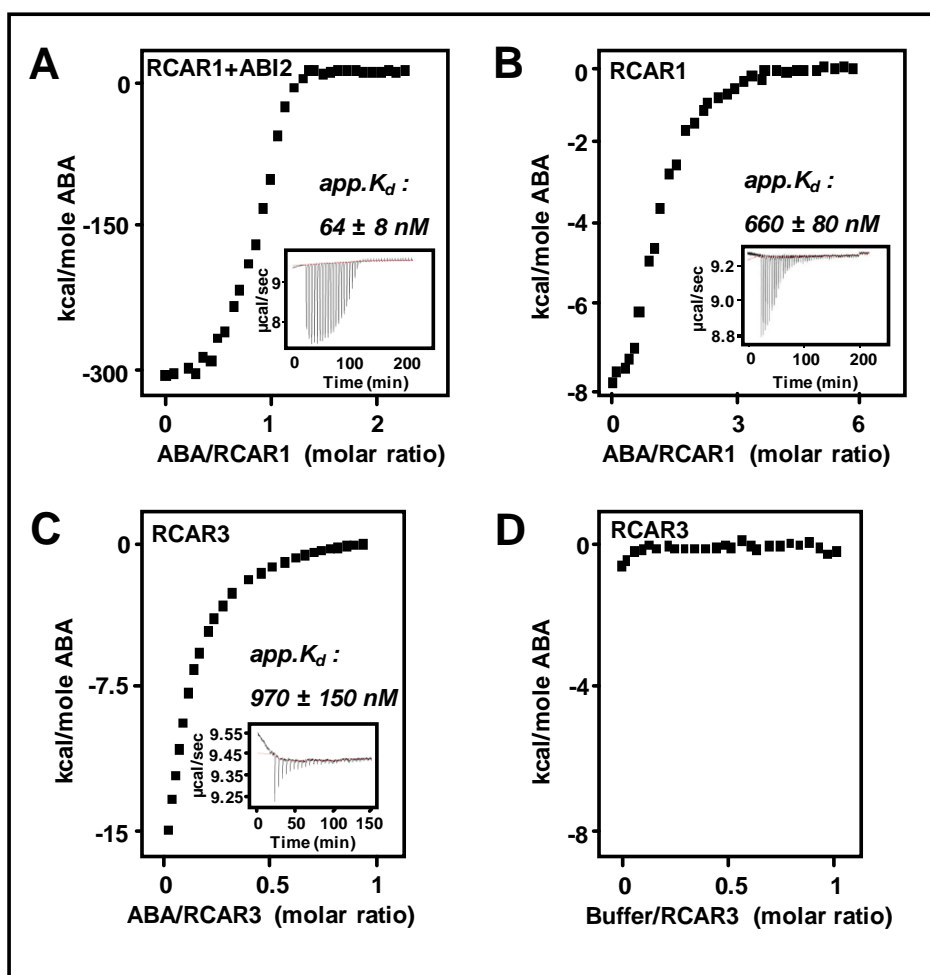
Figure 3-25 ***Analysis of ABA binding to RCAR proteins by isothermal titration calorimetry***
*A (S)-ABA solution of 100 µM (A), 300 µM (B) and 400 µM (C) was titrated to a solution of **(A)** RCAR1 + ABI2 (4 µM), **(B)** RCAR1 (8 µM) and **(C)** RCAR3 (1 µM) and the associated thermal change was monitored at 30°C (inset). After integration of the injection peaks, the resulting binding curves were fitted with the Origin software using a 1:1 stoichiometry of ligand/protein binding. **(D)** Interaction analysis between RCAR3 (1 µM) and buffer. (A) and (B) were generated by Dr. A. Korte.*

3.8 Circular dichroism analysis of RCAR proteins

In order to determine whether the presence of the phytohormone can alter the conformation of RCAR proteins, circular dichroism analysis was used. Circular dichroism (CD) spectroscopy measures differences in the absorption of left-handed polarized light versus right-handed polarized light which arise due to structural asymmetry (Greenfield, 2006, 2006). This method was used to study the secondary structure, conformational stability of RCAR proteins under stress (temperature, pH) and to determine whether there are changes in the conformation of RCAR proteins upon binding to the ligand.

Secondary structure was determined by CD spectroscopy in the "far-UV" spectral region (195-260 nm). At these wavelengths the chromophore is the peptide bond, and the signal arises when it is located in a regular, folded environment. The CD analysis of RCAR1 and RCAR3 was indicative of α-helical and β-sheet structures (Figure 3-26 and 3-27).
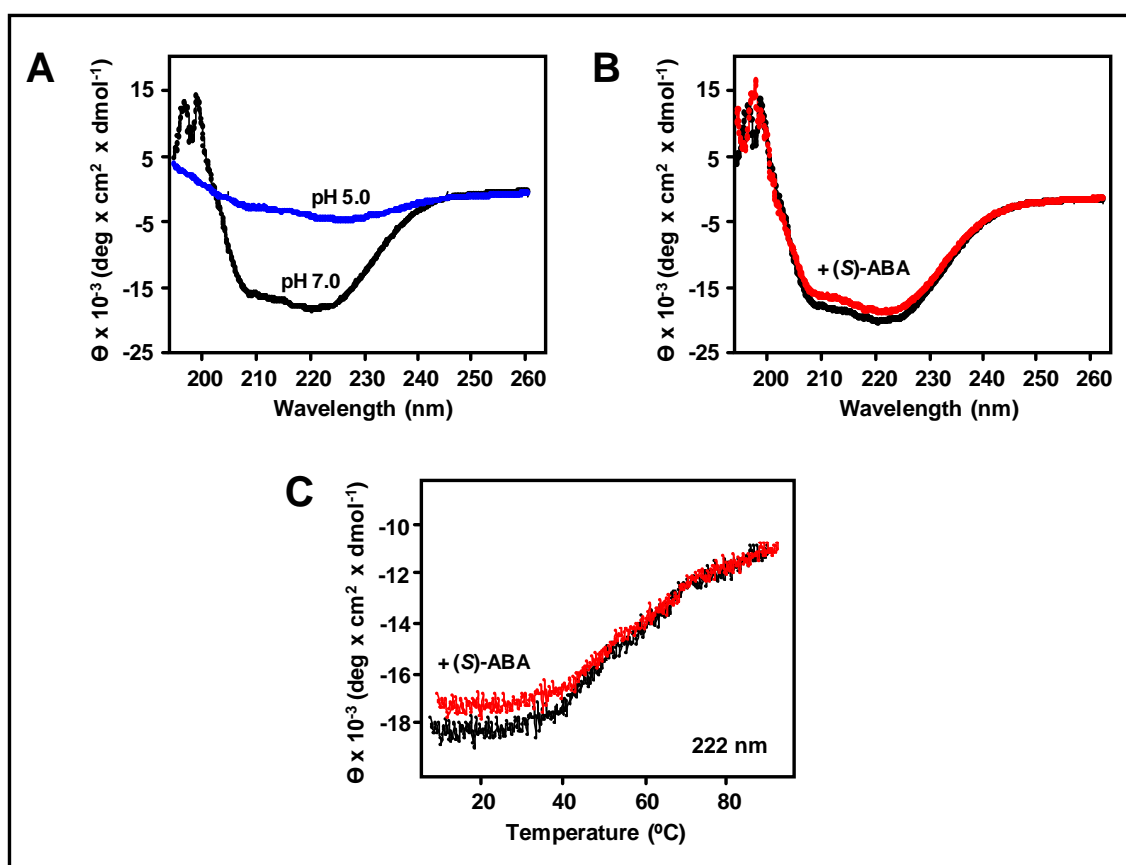
Figure 3-26   Circular dichroism analysis of RCAR1
(A) CD spectrum of RCAR1 at pH 7.0 (black line) and at pH 5.0 (blue line). (B) CD spectrum of RCAR1 in the absence (black line) and presence (red line) of 100 µM (S)-ABA in the UV range from 195 to 260 nm. Spectra were plotted to the scale given in mean molar ellipticity (θ) units (deg x cm^2 x dmol^{-1}). (C) Temperature-induced changes of RCAR1 secondary structure in the absence (black line) and presence (red line) of 100 µM (S)-ABA were monitored by CD measurements at 222 nm indicative of α-helical signatures. Data were plotted as θ222 (deg x cm^2 x dmol^{-1}) versus temperature (°C).

Additionally, CD experiments showed that RCAR1 at pH 5.0 (Figure 3-26A) appeared to be not as stable as at pH 7.0. Interestingly, administration of ABA (100 µM) did not detectably modify the shape of the spectra of RCAR1 and RCAR3, and the molar ellipticity values indicated that the secondary structure of the protein was intact (Figure 3-26B, 3-27A). I also examined whether, the secondary structure of RCAR3 would be affected by presence of ABI1 with and without (*S*)-ABA (100 µM). The data showed that the presence of ABI1 slightly changed the conformation of RCAR3 protein, and administration of ABA to RCAR3-ABI1 complex also slightly affected the secondary structure of RCAR3 (Figure 3-27B).

Thermal denaturation profile of RCAR1 and RCAR3 revealed thermal stability of up to 40°C, consistent with high thermal sensitivity of RCAR1 and RCAR3. The presence of ABA did not significantly affect the thermal stability of the protein (Figure 3-26C and 3-27C).
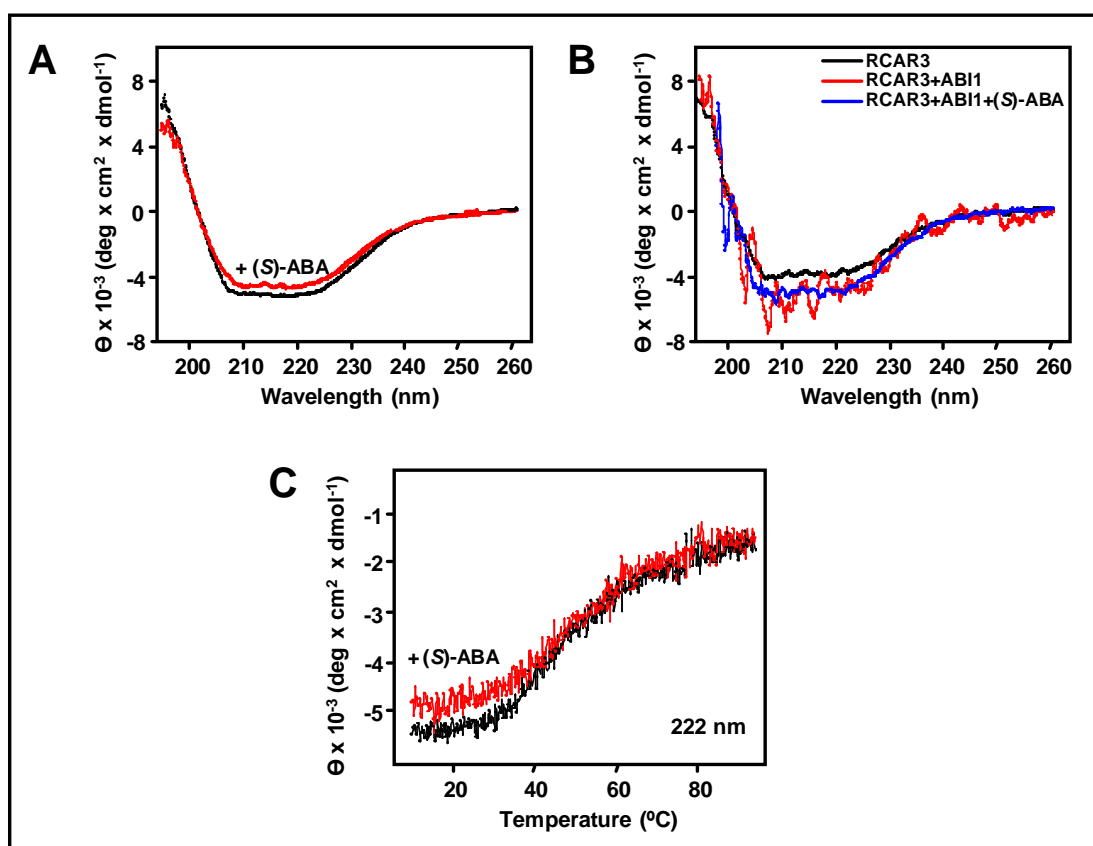
Figure 3-27   Circular dichroism analysis of RCAR3
(A) CD spectrum of RCAR3 in the absence (black line) and presence (red line) of 100 µM (S)-ABA in the UV range from 195 to 260 nm. Spectra were plotted to the scale given in mean molar ellipticity (θ) units (deg x cm^2 x dmol^{-1}). (B) CD spectrum of RCAR3 alone (0.5 mg/ml; black line), in the presence of ABI1 (0.25 mg/ml; red line) and in the presence of ABI1 and 100 µM ABA (blue line). (C) Temperature-induced changes of RCAR3 secondary structure in the absence (black line) and presence (red line) of 100 µM (S)-ABA were monitored by CD measurements at 222 nm indicative of α-helical signatures. Data were plotted as θ222 (deg x cm^2 x dmol^{-1}) versus temperature (°C).

3.9 Differential regulation of RCAR and PP2C expression throughout development and in response to abiotic stress

The Genevestigator database (Zimmermann et al., 2005) was mined to assess whether transcript levels of the diverse members of the cytosolic ABA receptor complexes may vary *in vivo* at different developmental stages, in different tissues or under different stress conditions. An interesting differential regulation of the expression of RCAR1, RCAR3, RCAR9, RCAR10, RCAR13, RCAR14, ABI1 and ABI2 under the conditions examined was found.

Treatment	RCAR									
	1	2	3	8	9	10	11	12	13	14
ABA [a]	1.66	1.29	0.48	0.18	0.14	0.04	0.37	0.41	1.57	1.03
osmoticum [b]	0.87	0.99	0.47	0.51	0.33	0.09	0.45	0.40	1.57	0.32
salt [c]	1.06	1.30	0.43	0.38	0.17	0.13	0.59	0.65	1.43	0.53
drought [d]	0.87	0.94	0.29	7.72	1.64	0.19	1.30	0.91	1.60	0.44
ethylene [e]	1.06	1.00	2.53	2.73	2.96	1.28	0.49	0.61	0.96	0.91

Treatment	PP2C					
	ABI1	ABI2	HAB1	HAB2	PP2CA	AHG1
ABA [a]	12.82	59.67	7.72	3.34	9.65	1.26
osmoticum [b]	9.99	14.18	7.52	2.58	8.44	15.52
salt [c]	5.57	6.19	3.16	1.69	5.56	5.27
drought [d]	1.83	12.56	16.00	4.24	8.74	74.91
ethylene [e]	2.85	0.89	0.80	0.77	0.67	0.77

Table 1 Transcriptional profiling upon hormone treatment and stress conditions
*ABI1: At4g26080, ABI2: At5g57050, HAB1: At1g72770, HAB2: At1g17550, PP2CA: At3g11410 and AHG1: At5g51760. The numbers given are the ratio of expression levels between experimental and control slides (linear scale). Red and orange shading indicate upregulation and green downregulation **(a)** Seedlings were exposed to 10 µM ABA for several hours (4 replicates and 4 mock treatment controls) **(b)** 300 mM Mannitol was applied to 16 day old plants, rosettes harvested 6 to 24 hours after onset of treatment (6 replicates and 6 controls) **(c)** 150 mM NaCl was applied to 16 day old plants, rosettes harvested 6 to 24 hours after onset of treatment (6 replicates and 6 controls) **(d)** Mature leaf samples from wild-type plants were not watered for 7 days (3 replicates and 1 well watered control) **(e)** 5 ppm ethylene was applied to the petioles of developed flowers for three hours (3 replicates and 3 controls). Datasets were generated by Knut Thiele and Dr. Farhah Assaad.*

Whereas RCAR1 is upregulated in the seed coat, RCAR3 exhibits peak transcript levels in the xylem (Figure 3-28A). ABI1 is upregulated in radicles, in senescent leaves, in leaf primordia and in the root hair zone (Figure 3-28A). ABI2 shows a considerably lower level of expression than ABI1 and is upregulated predominantly in senescent leaves (Figure 3-28A) and in the endodermis. RCAR1 and RCAR3 are expressed throughout development, with RCAR1 showing maximal expression levels in flowers and siliques (Figure 3-28B). By contrast, ABI1 and to a lesser extent ABI2 are upregulated late in development, in mature siliques (Figure 3-28B). Transcriptional profiling (Zimmermann et al., 2005) showed that the RCAR1/3/9/10/13/14 and ABI1/2/PP2CA genes are differentially regulated by light quality, duration and intensity, by a broad range of chemical and hormone treatments, and by stress conditions such as heat and cold. The subset of conditions that impact gene expression of the RCAR genes were listed in Table 1. The ABA treatment strongly upregulates ABI1 and ABI2 but downregulates RCAR3/9/10, whereas RCAR1, RCAR13 and RCAR14 levels are either upregulated or constant. In contrast to ABA treatment, ethylene treatment upregulates RCAR3, RCAR9 and ABI1 without affecting RCAR1/10/13/14 or ABI2 levels (Table 1). Osmotic stress and salt stress strongly upregulate ABI1 and ABI2 but downregulate RCAR3, RCAR9, RCAR10 and RCAR14. Under these conditions, RCAR1 and RCAR13 levels are either constant or upregulated. The drought stress upregulated PP2Cs and RCAR9 and RCAR13. Other RCAR members such as RCAR3, RCAR10 and RCAR14 are downregulated, whereas RCAR1 appears to stay at constant level (Table 1).

This analysis was extended to 10 RCAR and six PP2C family members linked to ABA responses, and found that whereas the PP2Cs are uniformly upregulated by ABA treatment, salt or osmotic stress and drought, different RCAR genes vary in their responses, being either unaffected, up- or downregulated under these stress conditions (Table 1). Indeed, RCAR3 and RCAR10 were consistently downregulated under examined conditions, whereas RCAR13 was slightly upregulated (Table 1). With few exceptions, it can be stated that exogenous ABA as well as conditions that increase endogenous ABA upregulate PP2C levels by up to 75-fold, leave RCAR1 levels either constant or slightly increased but downregulate RCAR3 and RCAR10 by a factor of up to 25 (Table 1).
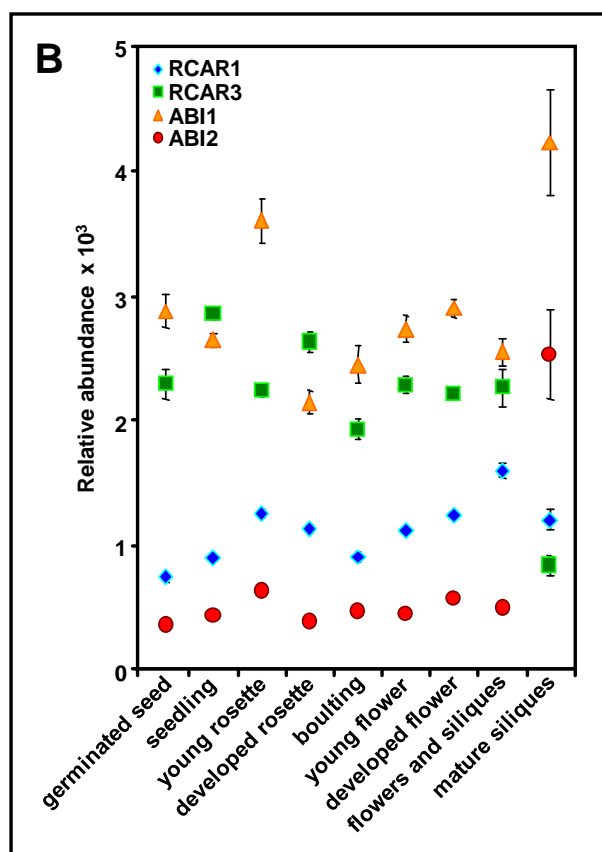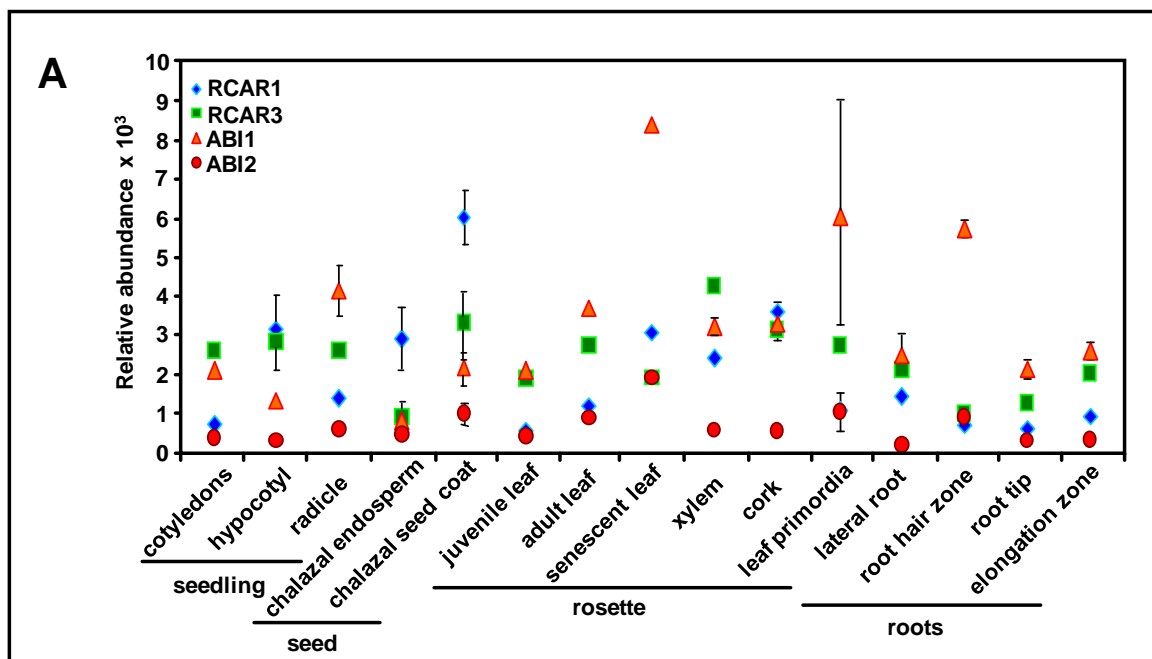
Figure 3-28   Transcriptional profiling in different tissues and at different developmental stages
(A) a selected number of tissues are shown **(B)** stages of Arabidopsis development.
The analysis is based on mining the Genevestigator database. Datasets were generated by Knut Thiele and Dr. Farhah Assaad.

3.10 Screening for a ligand(s) by using FT-ICR-MS analysis

3.10.1 PP2C phosphatase regulation by RCAR proteins and small molecules

Previous studies with Bet v 1 and structurally related proteins revealed a potential phytohormone-binding capacity (Markovic-Housley et al., 2003; Pasternak et al., 2006; Fernandes et al., 2008). Binding of a spectrum of physiologically relevant ligands, including fatty acids, flavonoids, brassinosteroids and cytokinins have been proposed for Bet v 1 (Mogensen et al., 2002).

In light of the structural similarity between RCAR and Bet v 1 proteins, it was postulated that RCAR proteins might be capable of binding other low molecular weight ligands within the cavity. In order to study the effect of ligands, PP2C enzymatic assays were carried out to examine a possible regulatory role of ABI1/2 and RCARs interaction. All enzymatic assays were performed at a constant molar ratio of PP2C:RCAR of approximately 1:4, with the PP2C level at 0.05 µM.

Interaction between RCAR proteins and other phytohormones

Plant hormones are small chemical molecules that are able to regulate plant growth. ABA has been shown to influence the enzymatic activity of PP2Cs in the presence of RCAR proteins. Due to this observation I tested different molecules and their behaviour in the presence of the ABI1-RCAR13 complex (Figure 3-29A). In the *in vitro* assay I checked for interaction by administration of three different auxins such as indole-3-acetic acid (IAA), α-naphthalene acetic acid (NAA) and 2,4-dichlorophenoxyacetic acid (2,4-D), two cytokinins (benzyl adenine-BAP and kinetin), tripeptide glutathione (GSH) and salicylic acid (SA). The analysis revealed that, at a concentration of 10 µM, none of these substances was able to reduce the phosphate activity to the same extent as observed with ABA. These results indicate that among known plant hormones only abscisic acid has the ability to inhibit the catalytic activity of PP2Cs in the presence of RCAR proteins.
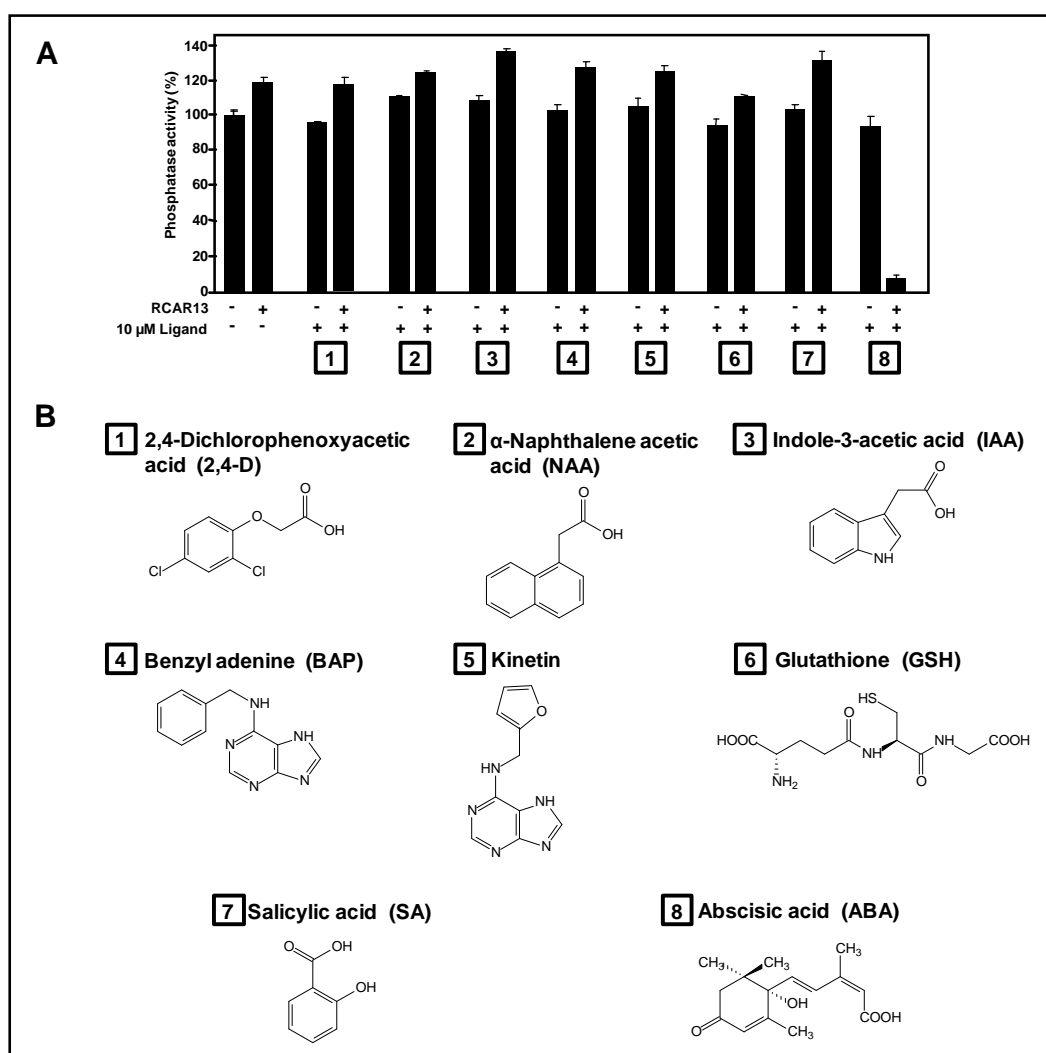
Figure 3-29   Regulation of ABI1 activity by RCAR13 and plant hormones
(A) Regulation of phosphatase acivity by RCAR13, in the absence or presence of 10 µM of various plant hormones. Activity of ABI1 without RCAR13 and phytohormones was set to 100%. (B) Structures of phytohormones or peptides (2,4-D, NAA, IAA, BAP, Kinetin, GSH, SA and ABA) used in the assay. The analysis was performed at a constant molar ratio of ABI1:RCAR13 of approximately 1:4 and with the ABI1 level at 0.05 µM.

Interaction between RCAR proteins and brassinosteroids

Brassinosteroids (BRs) are growth-promoting polyhydroxylated plant steroids that positively influence seed germination, stem elongation, vascular differentiation and fruit ripening, pollen tube growth, and leaf epinasty (Acharya and Assmann, 2009). BRs signaling outputs have been shown to be regulated by abscisic acid early signaling components, ABI1 and ABI2 (Zhang et al., 2009). It was also shown that BRs are present at moderate levels in the seed, fruit, shoots and leaves and at significantly higher levels in the pollen. The histochemical GUS staining analysis revelaed that RCAR1 is highly expressed in the pollen (Figure 3-4). This observation encouraged me to test whether RCAR1-ABI2 complex has the ability to interact with brassinosteroid molecules (Figure 3-30). Phosphatase assays demonstrated that the enzymatic activity of ABI2 was regulated

differently in the presence of RCAR1 protein and 100 µM BRs (filled columns). The analysis indicated, that a residual PP2C inhibition of approximately 50%, 40% and 30% was recorded in the absence of RCAR1 and in the presence of 100 µM epicastaterone, epibrassinolide and (22S,23S)-epicastasterone, respectively (Figure 3-30). The presence of RCAR1 had only a slight effect on the regulation of ABI2 activity in the presence of 100 µM epicastaterone, epibrassinolide and (22S,23S)-epicastasterone. Regulation of the PP2C activity in the absence of RCAR1 and presence of 100 µM BRs and 100 nM (S)-ABA did not change significantly. Only in the presence of (22S,23S)-epicastasterone the PP2C activity was reduced to 35%. Interestingly, by applying lower concentration of BRs of 10 µM (open, dotted line columns) in the presence or absence of RCAR1, the ABI2 inhibition was almost abolished (Figure 3-30). Administration of (S)-ABA to RCAR1-ABI2 complex in the presence of 10 µM or 100 µM of BRs, revealed an inhibition of ABI2 in ABA-dependent manner.
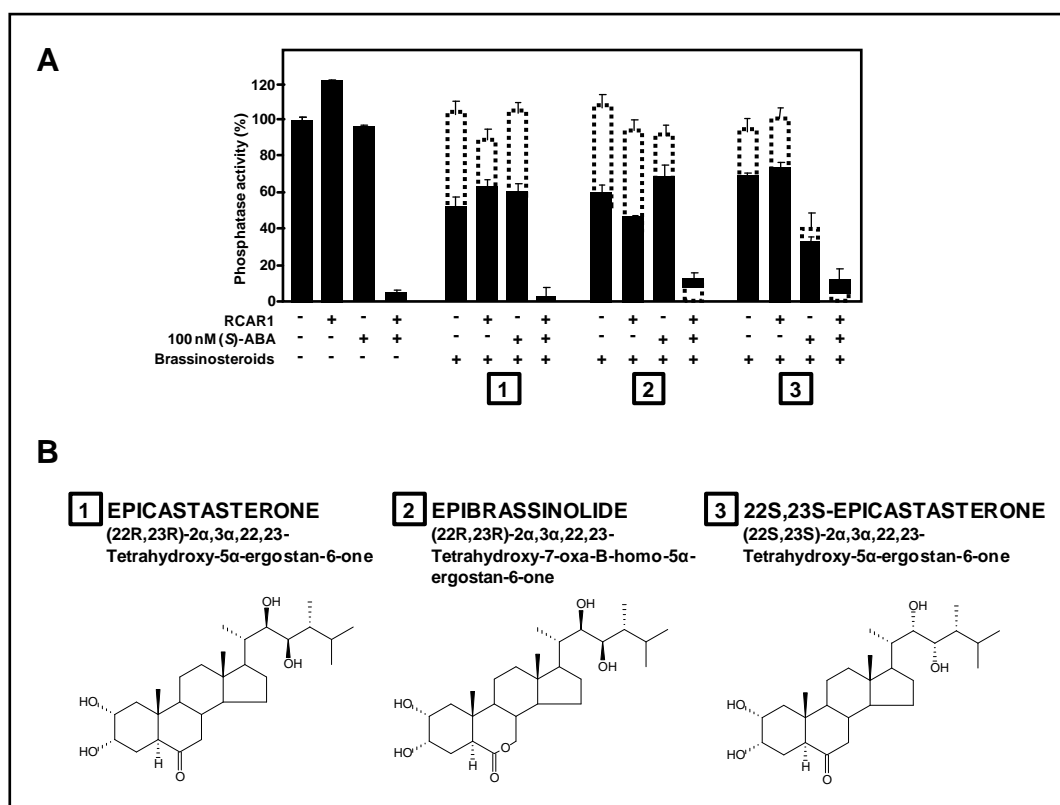
Figure 3-30   Regulation of ABI2 activity by RCAR1 and brassinosteroids
(A) Regulation of phosphatase activity by RCAR1, 10 µM (open, dotted line bars) and 100 µM (closed bars) brassinosteroids, in the presence or absence of (S)-ABA (100 nM). Activity of ABI2 without RCAR1 and phytohormones was set to 100%. (B) Structures of brassinosteroids (epicastaterone, epibrassinolide and (22S,23S)-epicastasterone) used in the assay. The analysis was performed at a constant molar ratio of ABI2:RCAR1 of approximately 1:4 and with the ABI2 level at 0.05 µM. All three brassinosteroids (8 mM stock solutions) were dissolved in 100% methanol.

Interaction between RCAR proteins and jasmonates

Jasmonates are a class of lipid-derived phytohormones involved in the regulation of vegetative and reproductive growth, and defense responses against abiotic stresses (UV light and ozone), insects and necrotrophic pathogens (Katsir et al., 2008).

Seven different jasmonate derivates and their ability to regulate ABI2 activity in the presence of RCAR1 was tested (Figure 3-31). The analysis revealed only a slight stimulation of the PP2C enzymatic activity in the presence of 10 µM of jasmonate forms. After treatment with RCAR1, the ABI2 activity did not change (Figure 3-31A). Administration of 100 nM (S)-ABA to RCAR1-ABI2 complex, treated with 10 µM jasmonates, reduced the ABI2 activity to approximately 50%, compared to the results without jasmonate treatment (Figure 3-31A). These results indicate that jasmonate intermediates have no effect on the regulation of ABI2 in the presence of the RCAR protein.
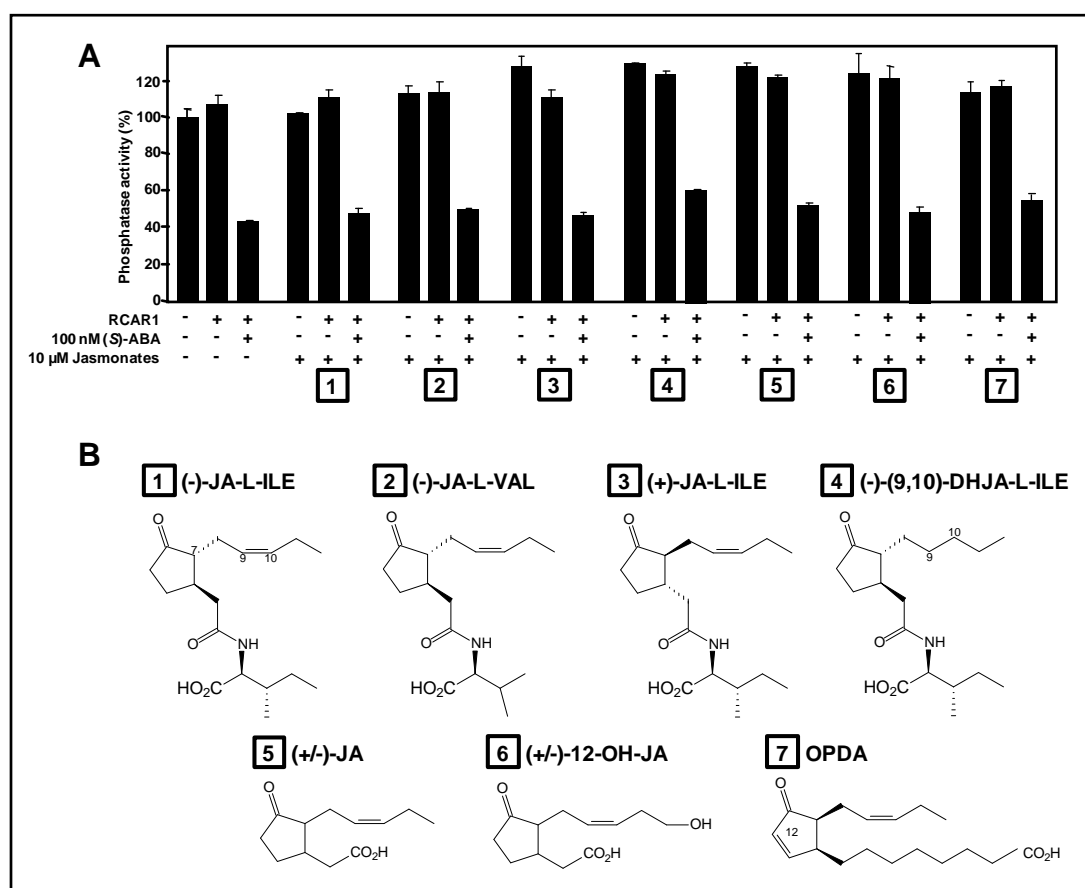
Figure 3-31   Regulation of ABI2 activity by RCAR1 and jasmonate derivatives
(A) Regulation of phosphatase activity by RCAR1 and 10 µM jasmonates, in the presence or absence of (S)-ABA (100 nM). Activity of ABI2 without RCAR1 and phytohormones was set to 100%. (B) Structures of different jasonates used in the assay. The analysis was performed at a constant molar ratio of ABI2:RCAR1 of approximately 1:4 and with the ABI2 level at 0.05 µM.

Interaction between RCAR proteins and unidentified ligands from *Arabidopsis* cell extract

Arabidopsis thaliana cell suspension cultures are a source of a broad range of physiologically relevant ligands, which might act as signaling molecules in various signaling pathways in plants. I attempted to search for specific low molecular weight compounds, which modify ABA signaling by binding to RCAR proteins, by analyzing pure cell extracts from *Arabidopsis* cell suspension cultures. 7-day old wild-type and *aba2-1* (ABA-deficient *Arabidopsis* mutant) cell suspension cultures were harvested and purified (see section 2.2.3.15 of Materials and Methods) on reversed phase octadecyl (C_{18}) Bakerbond SPE column (J.T. Baker).
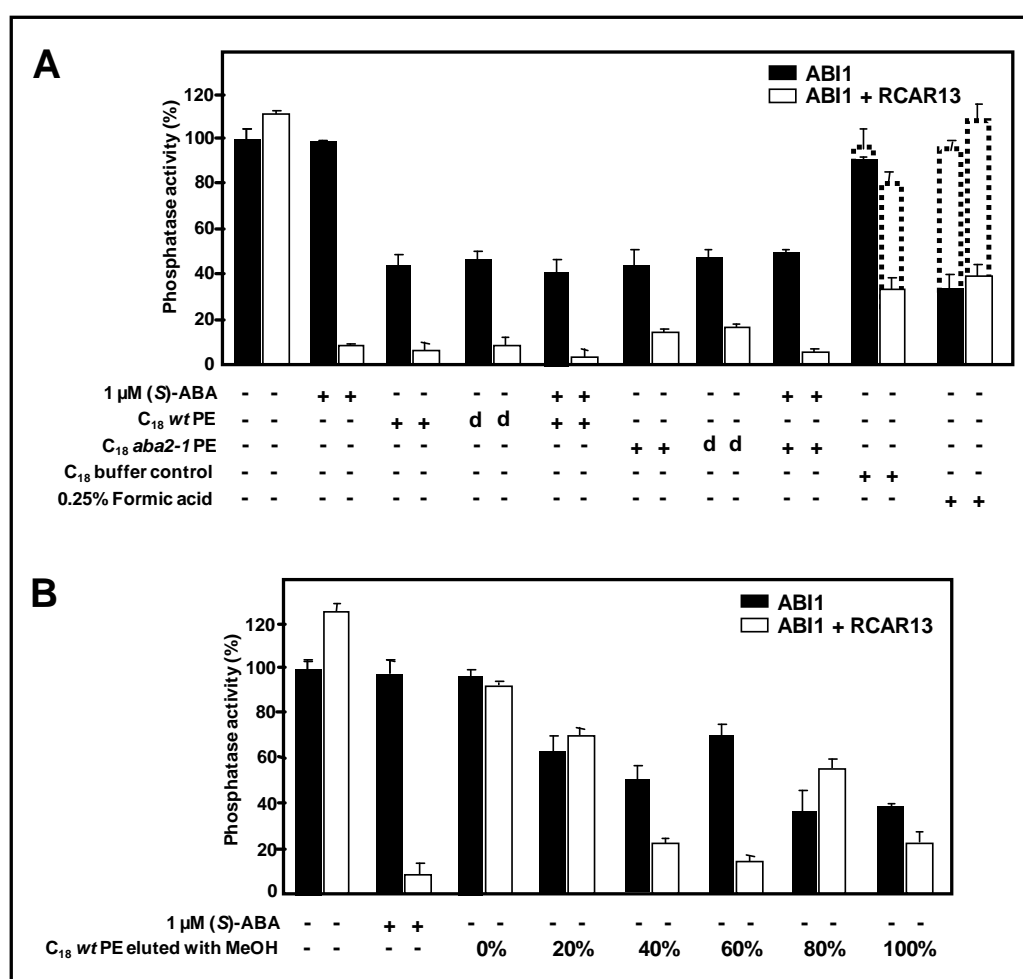
Figure 3-32   Inhibition ABI1 activity by RCAR13 and plant extract
(A) Regulation of phosphatase activity by RCAR13 and 10 µl of wild-type and aba2-1 plant extract (PE), in the presence or absence of (S)-ABA (1 µM). Activity of ABI1 without RCAR13 and PE or ABA was set to 100%. C_{18} buffer control (extract from empty column treated with 100% MeOH, 0.25% formic acid and eluted with 100% MeOH). Formic acid used in the washing step (≥ 98%, p.a. - solid line and C_{18} purified-dotted line). 0.25% formic acid (≥ 98%, p.a and C_{18} purified) was used in the assay directly as another control, in order to prove to be the source of contamination, which had an impact on regulation of ABI1 activity. (B) Regulation of ABI1 activity by wild-type PE obtained from different methanol fractions. Activity of ABI1 without RCAR13 and PE was set to 100%. Analyses (A-B) were performed at a constant molar ratio of ABI1:RCAR13 of approximately 1:4 and with the ABI1 level at 0.05 µM.

To study the effect of plant extract (PE) on the regulation of ABI1 in the presence of RCAR13, PP2C enzymatic experiments with methylumbelliferyl phosphate (MUP) as a substrate were performed (Figure 3-32). Analyses have shown that C_{18} purified plant extract from wild-type (C_{18} *wt* PE) and mutant *aba2-1*, reduced ABI1 phosphatase activity in the absence of RCAR13 to more than 40% (Figure 3-32A). Interestingly, complexes of RCAR13 with ABI1 in the presence of *wt* and *aba2-1* plant extracts and absence of ABA were inhibited up to 92% and 86%, respectively. Heat-inactivation of both cell extracts in the absence or presence of RCAR13 did not abrogated the regulation of ABI1 (Figure 3-32A). Administration of 1 µM (*S*)-ABA did not significantly influence ABI1 activity in the presence of both extracts and in the absence of RCAR13. Complexes of RCAR13 with ABI1 in the presence of wild-type and *aba2-1* plant extracts and 1 µM (*S*)-ABA were both inhibited up to 97% and 95%, respectively. Surprisingly, C_{18} buffer control showed regulation of ABI1 activity in the presence of RCAR13. Further investigation has revealed that this regulation was due to impurities present in the ≥ 98% p.a. formic acid (filled and open, solid line bars) used for washing of C_{18} column. Inhibition of ABI1 activity was abrogated after the use of a purified (open, dotted line bars) formic acid fraction (see section 2.2.3.15 of Materials and Methods titled 'Purification of *Arabidopsis thaliana* cell extracts').

In previous analyses 100% methanol was used to elute pure plant extracts from C_{18} columns. In order to get some knowledge, in which fraction the ligands regulating the phosphatase activity are eluted, we applied step gradient (Figure 3-32B). Analysis showed that 40-60% and 100% methanol fractions of wild-type PE were containing small molecules which were capable of inhibiting ABI1 activity in the absence and presence of RCAR13 protein.

In order to clarify the effect of plant extract on regulation of PP2C activity, different concentrations (volumes) of wild-type and *aba2-1* plant extract were used.

Phosphatase assays, in which both plant extracts were independently titrated to ABI1 and RCAR13 revealed regulation of ABI1 and ABI1-RCAR13 complex in a concentration (volume) dependent manner (Figure 3-33). Half-maximal inhibition of ABI1 alone was recorded at 6.7 µl and 5.5 µl of wild-type and *aba2-1* plant extract, respectively (Figure 3-33B). Under comparable experimental conditions, ABI1 and RCAR13 yielded 50% of inhibition at 1.5 µl and 3 µl of wild-type and *aba2-1* plant extract, respectively (Figure 3-33D). These volumes correspond to an IC_{50} value of ABI1 in the presence of RCAR13, evoked by 10 nM (*S*)-ABA (Figure 3-22A).
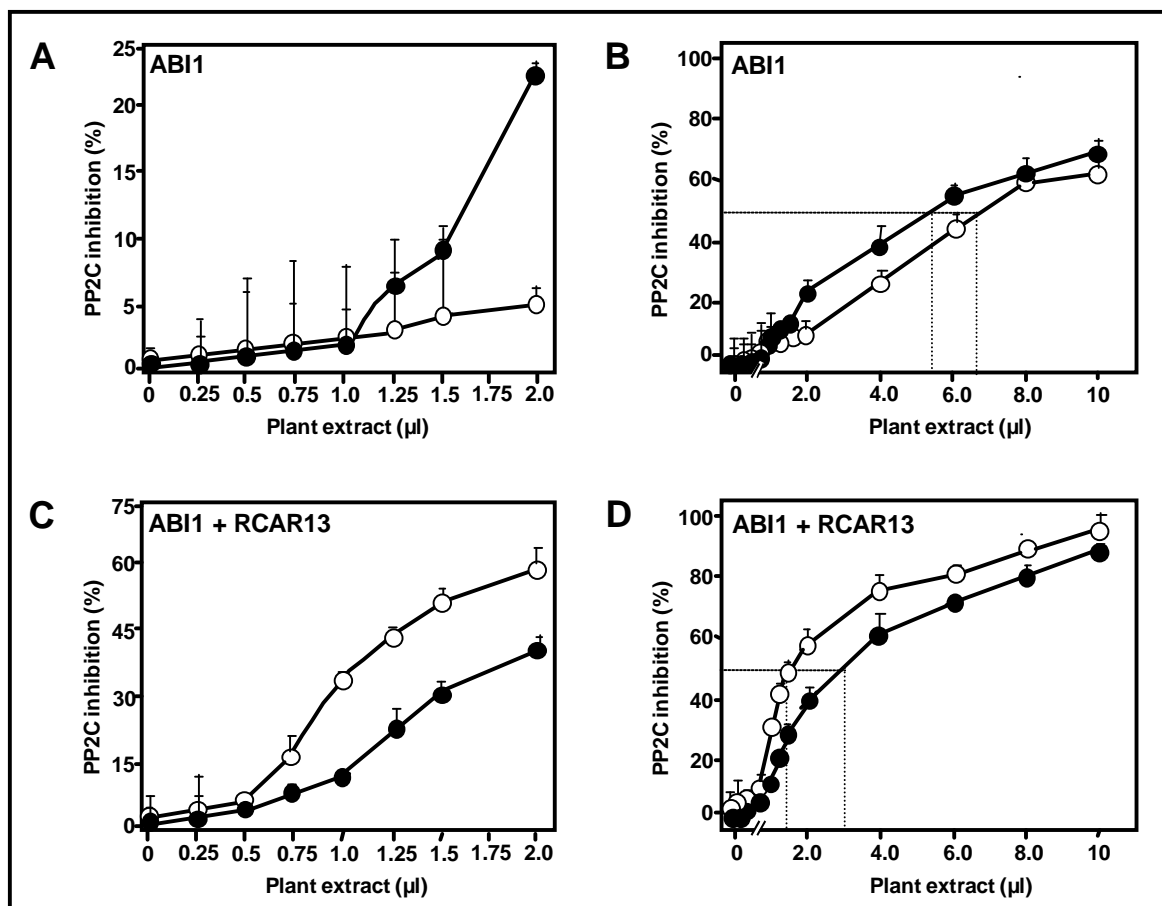
Figure 3-33   Inhibitory effect of plant extract on ABI1 activity
(A) Inhibition of ABI1 by increasing volumes of plant extract from wild-type (open circles) and aba2-1 (filled circles) cell suspension cultures. Half-maximal inhibition of ABI1 occurred at ~6.7 µl and 5.5 µl of wt and aba2-1 PE in the absence of RCAR13.
(B) Corresponding analysis of ABI1 as shown in (A), but in the presence of RCAR13. Half-maximal inhibition of ABI1 occurred at ~1.5 µl and 3 µl of wt and aba2-1 PE.
The analyses (A-B) were performed at a constant molar ratio of ABI1:RCAR13 of approximately 1:4 and with the PP2C level at 0.05 µM.

Taken together, all these data suggest that plant extracts from wild-type and *aba2-1* cell suspension cultures of *Arabidopsis* contain small molecules that are able to regulate phosphatase activity in an ABA-independent manner.

It was consistently observed before, that ABI1 phosphatase activity was reduced to approximately 10 to 20% in the presence of micromolar levels of ABA, although no PP2C-bound ABA was detected (Leube et al., 1998). In this study ABI1 activity in the presence of PE was reduced to ~ 50%, which cannot be due to presence of ABA (Figure 3-33A,B). There are probably other ligand(s) that regulate PP2C catalytic activity. The preliminary analysis revealed that these small molecules are also able to regulate PP2C activity in the presence of RCAR protein. The inhibitory effect is caused probably also by some pool of ABA present in the PE, which was reduced in the extract from the ABA-deficient *aba2-1* cells (Figure 3-33C,D). Another interesting phenomenon is that the formic acid used in this study also contains small compounds, which are capable of regulation of the complex

similar to ABA requiring the presence of RCAR and which were not present when the purified form of the acid was used. In order to understand all these results, another more sophisticated method of ligand identification is required.

3.10.2 Fourier Transform Ion Cyclotron Resonance Mass Spectrometry

Fourier Transform Ion Cyclotron Resonance Mass Spectrometry analysis (FT-ICR-MS) was used to search for ligands that modify ABA signaling by binding to and controlling RCAR protein activity.

In order to screen for binding molecules an affinity chromatography method was applied (Figure 3-34).
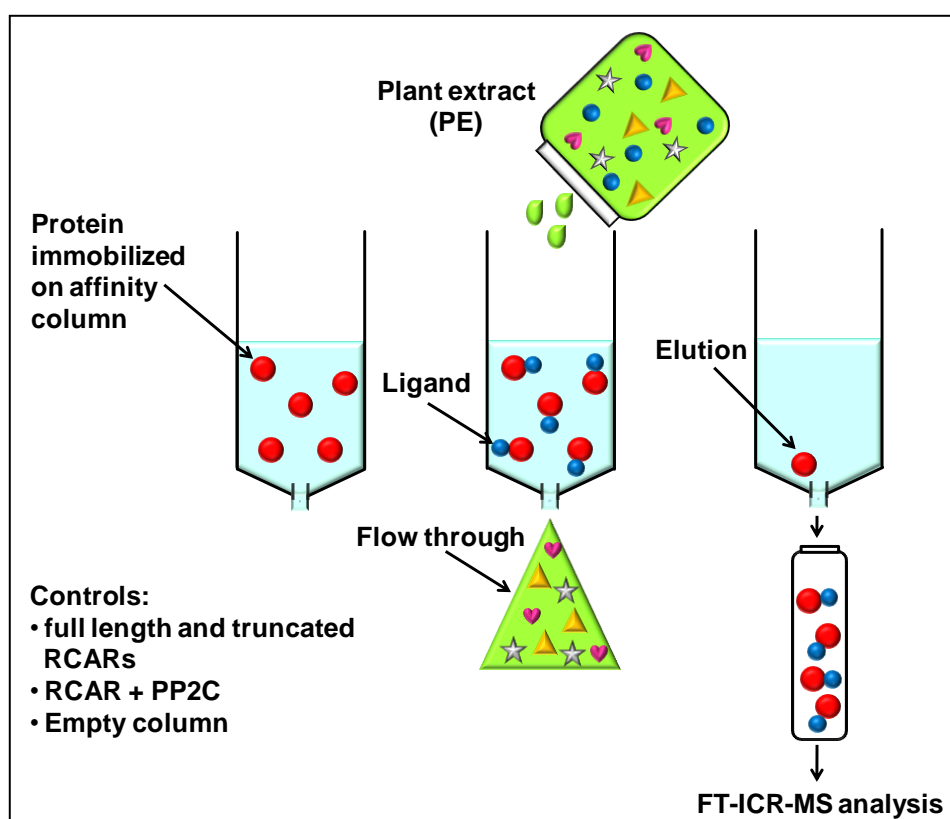
Figure 3-34   Biochemical approach of screening for a ligand(s)
Step 1: Immobilization of RCAR or RCAR-PP2C proteins on Ni-TED affinity columns. Truncated versions of RCAR1 and empty column (EC) were used as controls.
Step 2: Rinsing the column with cell-free extracts of Arabidopsis thaliana. Ligands which did not bind to the protein are passing through the column. Other unspecifically bound ligands are washed away in the washing step.
Step 3: Elution the protein-ligand(s) interaction samples by low pH buffer (TFA, pH 2.5).
Step 4: Analysis of the interaction samples by FT-ICR-MS.

His-tagged RCAR and PP2C proteins were heterologously expressed in *E.coli* and then purified under native conditions by using affinity chromatography. Purified proteins were immobilized on Ni-TED columns and subsequently chromatographed with *Arabidopsis thaliana* pure (C_{18} columns) cell extracts.

Fourier Transform Ion Cyclotron Resonance (FT-ICR) Mass Spectrometry was developed over thirty years ago by Comisarow and Marshall (Comisarow and Marshall, 1974).

The mass spectrometer is made up of two major components: the ionization source and the mass analyzer. Within the ionization source the sample of interest is ionized and then desorbed into the gas phase. The mass analyzer acts to guide the gas phase ions through the instrument to the detector. At the detector, the ions mass-to-charge (*m/z*) ratios are measured (Marshall et al., 1998).

The method of ionization used in this study is called electrospray ionization (ESI) and requires the sample of interest to be in solution so that it may flow into the ionization source region of the spectrometer (Figure 3-35B). To ionize the sample high voltage is applied to a metal capillary through which sample is flowing. The applied voltage can result in the sample becoming positively or negatively charged (Mano and Goto, 2003). The presence of a high electric field produces very small droplets, which travel toward the mass spectrometer orifice at atmospheric pressure, evaporate and eject charged analyte ions into the mass analyzer.

A FTICR-MS functions somewhat like an ion-trap analyzer, with the trap being housed within a high-strength magnetic field (12 Tesla), as shown in Figure 3-35C (Marshall et al., 1998). Ions within the trap resonate at their cyclotron frequency due to the presence of the magnetic field. By applying the appropriate electric field energy, the ions are excited into a larger orbit, and this can be measured as they pass by detector plates on opposite sides of the trap. The detector measures the cyclotron frequencies of all of the ions in the trap and a Fourier transform is used to convert these frequencies into *m/z* values.

FT-ICR mass analyzers have been proved experimentally to provide the highest resolution, mass accuracy, and sensitivity for peptide and protein measurements so far achieved (Page et al., 2004). The mass accuracy of FTICR is unequaled by other types of analyzers and is sufficiently high to enable multiple ions to be accumulated and fragmented simultaneously (Li et al., 2001).
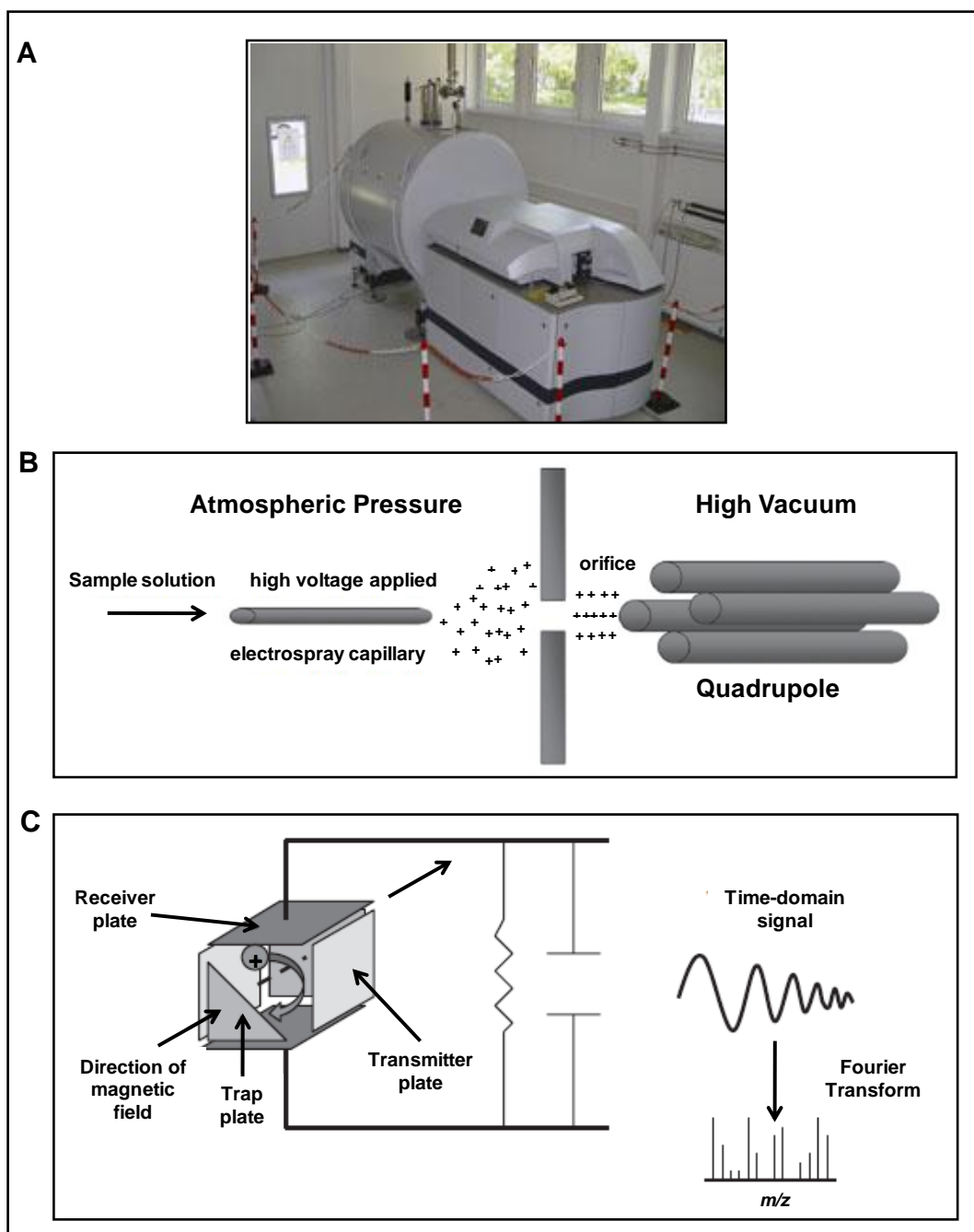
Figure 3-35 **Principles of Fourier transform ion cyclotron resonance (FT-ICR) mass spectrometry**

(A) 12 Tesla FT-ICR mass spectrometer located at GSF - National Research Center for Environment and Health, Munich, Germany. (B) Electrospray ionization (ESI). Sample in a solution is passed through a conductively coated needle. A high positive potential is applied to the capillary, causing positive ions to drift toward the tip with high voltage. The presence of a high electric field produces droplets, which travel toward the mass spectrometer orifice at atmospheric pressure and evaporate and eject charged analyte ions. (C) In FT-ICR-MS the ion trap is placed in a strong magnetic field (12 Tesla). The magnetic field causes ions captured within the trap to resonate at their cyclotron frequency.The detector measures the cyclotron frequency of all of the ions in the trap and uses a Fourier transform to convert these frequencies into m/z values (Veenstra and Yates, 2006).

The rationale of the experiment is that full length RCAR1/11 proteins alone or in the complex with ABI2 are able to bind the ligand(s) from the plant extract. Truncated versions of RCAR1 (ΔC- and ΔN-RCAR1) and negative control (empty column) do not have this ability. By using comparative FT-ICR analysis I was able to compare the spectra from all tested samples and to identify first candidates that seem to bind specifically to a functional RCAR proteins but not to a versions with a deleted domain (Figure 3-36).

Protein-ligand(s) interaction samples were analyzed in positive ion mode during the FTICR-MS measurement. This means that only the samples with groups that readily accept H^+ (such as amide and amino groups found in peptides and proteins) can be charged and detected. Due to the fact that ligand seems to be a very small molecule the measurement was performed in the small molecular mass range (150-600 Da).

Figure 3-36 shows three candidates for a ligand, screened with the FT-ICR analysis. Two first peaks of interest with a mass of 351.25310 ($C_{21}H_{34}O_4$) and 369.26369 Dalton ($C_{21}H_{36}O_5$) seem to be abundant in RCAR11 and RCAR11-ABI2 samples. Their presence in the wild-type plant extract indicate, that they are components of the plant extract (Figure 3-36A, B). Controls such as truncated version of RCAR1 and empty column gave very low intensity signals, as predicted for a true ligand. The third component of interest appeared to be very abundant in RCAR1 protein sample, with intensity of 1.25×10^8 (Figure 3-36C). The mass spectrum revealed that the mass of the ligand was 455.21798 Dalton, and the predicted molecular formula was $C_{25}H_{30}N_2O_6$.
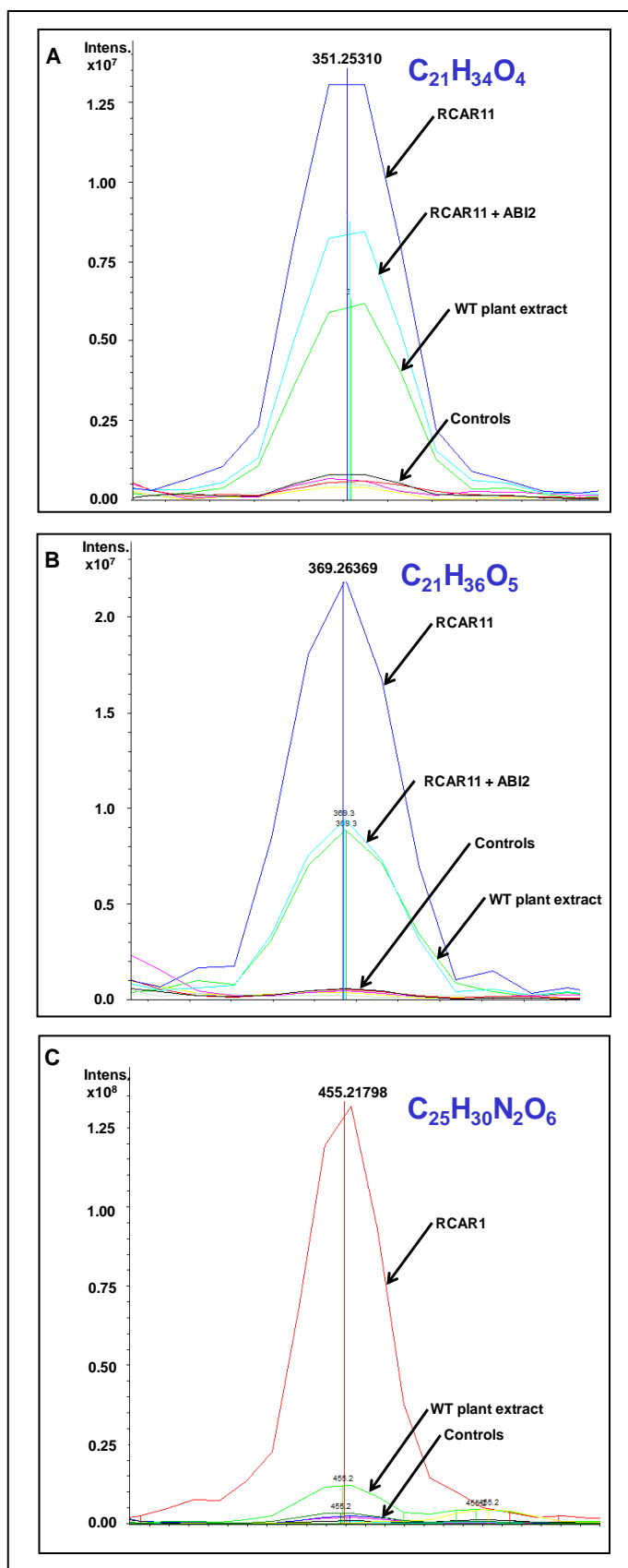
Figure 3-36   Positive mode ESI FTMS mass spectrum of putative ligands
*FT-ICR mass spectrum of a ligand with a mass of **(A)** 351.25310, **(B)** 369.26369 and **(C)** 455.21798 Dalton found in the samples of RCAR11 +/- ABI2 (A, B) and RCAR1 (C). Based on high accuracy of the predicted molecular weight, molecular formulae were proposed for the compounds.*

In order to provide structural information on candidates for a ligand, collision-induced dissociation (CID) was used (Figure 3-37). In this method, molecular ions are usually accelerated in cyclotron motion by electrical fields to high kinetic energy in a circle inside of an ion trap and then allowed to collide with neutral gas molecules (argon) by increasing the pressure. In the collision some of the kinetic energy is converted to internal energy which results in bond breakage and the fragmentation of the molecular ion into smaller fragments (Wells and McLuckey, 2005). These fragmented ions can be further analyzed by a mass spectrometer.

In my study I tried to investigate further a molecular ion with a mass of 455.21798 Dalton. This precursor ion was fragmented into one product ion at m/z 387.18010 ($C_{22}H_{26}O_6$) by applying the CID method at an energy of 6 eV. Interestingly, the formation of a product ion at m/z 68.03 ($C_3H_4N_2$) was not observed (Figure 3-37).

In light of these results, it is reasonable to suspect that I am dealing with steroid-like compounds. Moreover, due to the fact that FT-ICR-MS analysis of the eluates was variable from experiment to experiment, it is necessary to reproduce the preliminary results prior to defining the structure of the ligand.
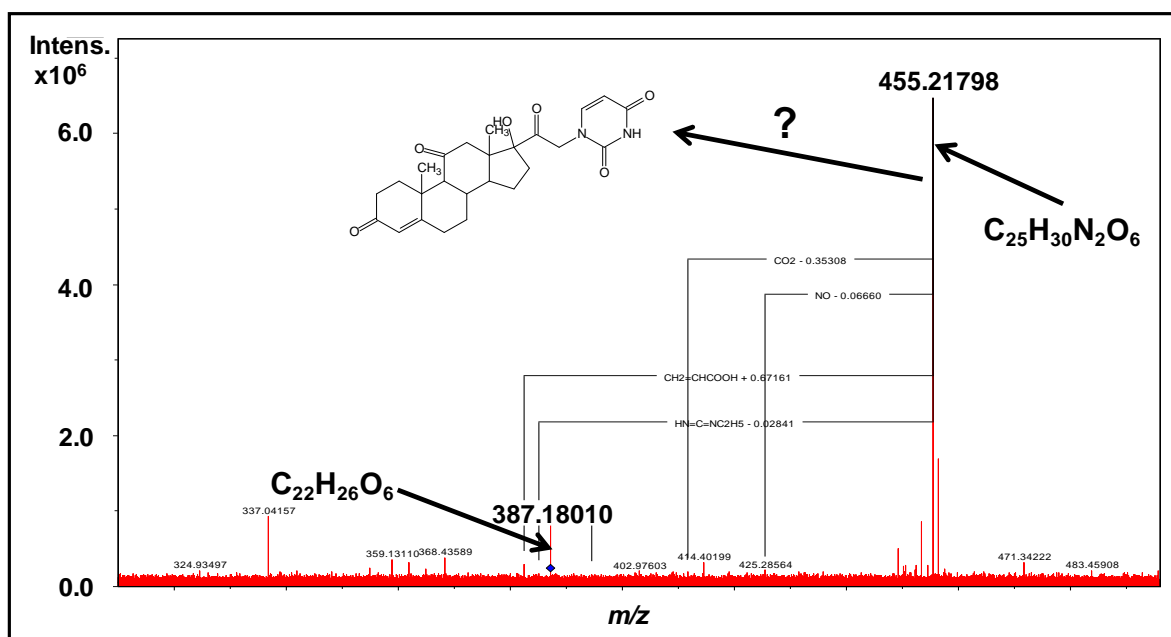
Figure 3-37 **Fragmentation of [M+H]$^+$ of putative ligand with mass of 455,21798 under conditions of collision-induced dissociation (CID)**
The main fragmentation involves the formation of an ion at m/z 387,18010 ($C_{22}H_{26}O_6$). The formation of a fragment ion at m/z 68,03 ($C_3H_4N_2$) was not observed.

4 Discussion

The phytohormone ABA plays a key regulatory role in physiological pathways for plant growth and development, and enables adaptation to abiotic stresses. ABA is also able to redirect gene expression of approximately one tenth of the *Arabidopsis* genome (Hoth et al., 2002; Nemhauser et al., 2006). A plethora of ABA signaling components have been identified (Christmann et al., 2006; Hirayama and Shinozaki, 2007). Four different types of ABA receptors have been reported (Shen et al., 2006; Liu et al., 2007; Pandey et al., 2009) but their ability to bind to ABA, to transduce the ABA signal and to thereby regulate diverse ABA responses is not unequivocally established (Gao et al., 2007; Johnston et al., 2007; Guo et al., 2008; McCourt and Creelman, 2008). Major players in ABA signaling are a subclass of Mg^{2+}- and Mn^{2+}-dependent serine/threonine phosphatases type 2C (PP2Cs), which interact with the RCAR family of proteins, discovered in this work.

4.1 Role of RCAR protein family in ABA signaling

ABI1 and ABI2 are two homologous proteins with high identity in C-terminal PPase domains (86%) and low identity in the N-terminal domains (42%) (Meyer et al., 1994; Leung et al., 1997). Both PP2Cs are the key enzymes in ABA responses, since *Arabidopsis abi1* and *abi2* mutants show a strong ABA-insensitive phenotype (Meyer et al., 1994; Leung et al., 1997). These findings indicate that ABI1 and ABI2 protein phosphatases are of central importance for elucidating the integrative network of ABA signaling.

With these premises, a search for ABI2 interaction partners in *Arabidopsis* by yeast two-hybrid system (Yang et al., 2006) resulted in the identification of two related interaction partners named regulatory component of ABA receptor 1 (RCAR1) and RCAR3. The 187 amino acid RCAR1 protein shares 82% similarities and 70% identities with 188 amino acid RCAR3. In addition, RCAR1 shares 75% and 74% amino acid identities to poplar and grape vine homologues, respectively, and 53% similarity to the major allergen of birch pollen Bet v 1.

These ABI2-interacting proteins, RCAR1 and RCAR3 belong to a 14-member family, which represents a branch of the Bet v 1-like superfamily (Radauer et al., 2008). Although the members of this superfamily share a common structural fold, evolution has diversified their function (Radauer et al., 2008). A common feature among many members of the superfamily is a hydrophobic cavity that can accommodate plant steroid hormones (Gajhede et al., 1996; Markovic-Housley et al., 2003).

Physical interaction of RCAR1 and RCAR3 with ABI1 and ABI2

The interaction between RCAR1/3 and ABI1/2 was verified by the quantative β-galactosidase assay. The analysis revealed that ABI1/2-interacting partners RCAR1 and RCAR3 did not require exogenous ABA supplementation for the Y2H interaction. The single amino acid exchange present in *abi1*, *abi2* and in the catalytically non-active ABI1 (NAP) completely abolished the interaction. Interestingly, RCAR1 together with 12 other RCARs (RCAR7 not included) have been also shown to interact in the Y2H assay with HAB1, one of the closest relatives of ABI1 and ABI2 (Park et al., 2009; Santiago et al., 2009). It was demonstrated that the interaction between RCAR3, 8, 9, 10 and 11 and the dominant ABA-insensitive ABI2^{G168D} or HAB1^{G246D} mutants disrupted the RCAR-PP2C interaction, which is in agreement with my results.

Plants harboring *abi1*, *abi2* or *hab1* show strong dominant ABA-insensitive phenotypes (Koornneef et al., 1984; Robert et al., 2006), which might partly reflect the ability of these mutant plants to escape the negative regulation by RCAR proteins.

In addition, Santiago et al. and Park et al. (2009) showed that deletions at the N- or C-terminus of RCAR8 and RCAR11^{S152L} and RCAR11^{P88S} pyrabactin-insensitive mutant forms abolished the interaction with HAB1 phosphatase.

These two research groups have also shown that the interaction between RCAR10-14 and HAB1 did not occur in the absence of exogenous ABA (Park et al., 2009; Santiago et al., 2009). Four of these RCARs belong to clade III of the RCAR protein family and the ABA-dependent interaction with PP2Cs in the Y2H might be one of the features of this clade that distinguish it from two others clades. Santiago et al. (2009) speculate that the interaction in yeast, which did not require ABA could be due to the endogenous ABA from yeast, sufficient to promote the binding between RCARs and PP2Cs. However, this argument is not in agreement with what I have observed in *in vitro* assays and what is known about ABA biosynthesis, which is restricted only to plant kingdom and to a few phytopathogenic fungi. The phosphatase activity assay with ABI2 in the absence of ABA clearly showed that by increasing the concentration of RCAR1, 10, 13 and 14, a stimulation of ABI2 activity was observed, while in the presence of RCAR3 and RCAR9 PP2C activity was reduced. These results indicate that RCAR proteins are able to interact with PP2Cs without any ABA. The isothermal titration calorimetry (ITC) experiment showed that titration of the RCAR8 protein into the ABI2 protein solution resulted in heat release, which indicated that RCAR8 bind to ABI2 (Korte, 2009).

In a recent report, Moes et al. (2008) described the nuclear localization of ABI1 wild-type and mutant proteins and the requirement of a functional nuclear localization sequence in order to regulate ABA sensitivity and ABA-dependent gene expression, and they suggest

that ABI1 reprograms sensitivity toward ABA in the nucleus (Moes et al., 2008). Similarly, it was confirmed that the interaction of HAB1 and SWI3B takes place in the nucleus, which suggests a direct involvement of HAB1 in the regulation of ABA-induced transcription (Saez et al., 2008). Bimolecular fluorescence complementation provides evidence for the interaction of PP2Cs with RCARs in plant cells. The co-expression of RCAR1/3 with ABI1/2 in *Arabidopsis* protoplasts yielded signals detected in the cytosol and in the nucleus. Similar results were demonstrated for RCAR8 and HAB1 by co-immunoprecipitation experiments in tobacco leaves (Santiago et al., 2009). Expression of a protein fusion between RCAR1 or RCAR8 and GFP was localized to the same intracellular compartments as the RCAR-PP2C complexes (Ma et al., 2009; Santiago et al., 2009). These data indicate that there is strong evidence for a cytosolic perception site of ABA as postulated from electrophysiological experiments (Levchenko et al., 2005) and a control of ABA signaling by nuclear ABI1 (Moes et al., 2008).

Ectopic expression of RCAR proteins in *Arabidopsis thaliana*

In transient studies with *Arabidopsis* protoplasts, over-expression of ABI1 and ABI2 in *Arabidopsis* inhibited the activation of ABA-dependent reporter genes by ABA (Hoffmann, 2002). In addition, over-expression of wild-type ABI1 in mesophyll protoplasts blocked ABA induction of gene expression (Sheen, 1998), suggesting that ABI1 and ABI2 act as negative regulators of ABA signaling (Merlot et al., 2001). Due to the physical interaction between RCAR proteins and PP2Cs, it is also interesting to study the role of RCAR in ABA signaling. By using the transient expression system in *Arabidopsis* protoplasts I showed that ectopic expression of RCAR1 and RCAR3 (Figure 3-7) resulted in an enhanced induction of the ABA-responsive genes *RAB18* and *RD29B*. *RAB18* is a dehydrin only found in ABA-treated plants and accumulates in *Arabidopsis* dry seeds (Nylander et al., 2001). The *abi1-1* and *abi2-1* mutants show impaired induction of this gene (Leung et al., 1997). *RD29B* is a drought- and ABA-inducible gene that contains ABA-responsive promoter elements (Yamaguchi-Shinozaki and Shinozaki, 1994).

The results from Figure 3-7 showed that the ABA response was almost fully blocked by ABI1 or ABI2 expression in protoplast cells in the absence of RCAR1 or RCAR3. The *abi1* and *abi2* mutant proteins were even more effective in blocking the RCAR1 or RCAR3 mediated stimulation of ABA signaling. I also demonstrated that reduction of RCAR1 and RCAR3 expression by RNA interference (RNAi) counteracted the ABA response. These data support a function of RCAR1 and RCAR3 as positive regulators in ABA response and are consistent with what was observed by others (Park et al., 2009; Santiago et al., 2009; Saavedra et al., 2010).

The analysis of transgenic plants over-expressing RCAR1, RCAR3 and RCAR8 showed an enhanced ABA response (Ma et al., 2009; Santiago et al., 2009; Saavedra et al., 2010). Plants over-expressing RCAR proteins were hypersensitive to ABA with respect to seed germination and root elongation. The regulation of stomatal aperture was also impaired in these plants. Moreover, double transgenic plants over-expressing both HAB1 and RCAR8 or FsPP2C1 (protein phosphatase 2C from beechnut) and RCAR3 showed a phenotype similar to that of over-expressing only RCARs, which confirmed the role of RCARs by antagonizing phosphatase function in the presence of ABA (Santiago et al., 2009; Saavedra et al., 2010).

The functional knockouts of RCAR1 and RCAR3 I analyzed (data not shown) in *Arabidopsis* did not reveal altered ABA responses consistent with functional redundancy among the RCAR proteins. However, triple (*rcar10/rcar11/rcar12*) and quadruple (*rcar10/rcar11/rcar12/rcar14*) knockout lines displayed strong ABA-insensitive phenotypes, which can be reversed by introducing RCAR10-12 and RCAR14 expressing transgenes (Park et al., 2009).

Taken together, RCAR proteins play a positive role in ABA signaling, by inhibiting the PP2C function in an ABA-dependent manner.

The analysis in this work using RCAR1 promoter-GUS constructs in transgenic plants demonstrated that the RCAR1 promoter is active in the root, cotyledons including stomata, as well as in parenchyma cells along the vasculature and prominently in root tips. In addition the RCAR1 promoter was strongly upregulated in the stipules, pollen grains and pollen tubes, flowers, anthers, early stage siliques and in the seeds. The GUS activity was easily detected even after staining for only few hours. These results, therefore suggest that RCAR1 expression in *Arabidopsis thaliana* is related to plant growth and development and ABA signaling.

Effect of RCAR proteins on the PP2C enzymatic activity

The analysis of the protein-protein interaction in yeast revealed that RCAR proteins interacted with ABI1, ABI2, HAB1 and PP2CA phosphatases type 2C. Therefore, the PP2C enzymatic analysis could be used to determine RCARs role in the interaction with PP2Cs *in vitro*.

Protein serine/threonine phosphatases are classified into PPP and PPM gene families. The PPP family includes phosphatases type 1 (PP1), type 2A (PP2A) and type 2B (PP2B), whereas the PPM family includes type 2C (PP2C) and pyruvate dehydrogenase phosphatase (Cohen, 1997). Around 80 *Arabidopsis* genes were identified as PP2C-type

phosphatase candidates, and they fall into ten groups (A–J; Figure 1-5), except for six genes that could not be clustered (Schweighofer et al., 2004). Protein phosphatases used in this study belong to clade A of the PP2C family. The PP2Cs strictly require magnesium (Mg^{2+}) or manganese (Mn^{2+}) ions for their activity and are highly sensitive to pH *in vitro* (Leube et al., 1998). Characterization of the redox sensitivity of ABI1 and ABI2 revealed that hydrogen peroxide (H_2O_2), a secondary messanger of ABA signaling, strongly inactivated the protein phosphatase activity of both PP2Cs (Meinhard and Grill, 2001; Meinhard et al., 2002).

According to this study, the enzymatic activity of clade A PP2Cs such as ABI1, ABI2, HAB1 and PP2CA was strongly reduced in the presence of RCAR1, 3, 9, 10, 13 and 14 in an ABA-dependent manner, showing that RCAR proteins act as negative regulators of PP2Cs and, hence, are positive regulators of ABA responses. Similar observations were made for RCAR8 and RCAR11 (Park et al., 2009; Santiago et al., 2009).

In the absence of RCAR proteins, only 10-20% reduction of PP2C phosphatase activity was observed in the presence of micromolar levels of ABA though no PP2C-bound ABA was detected (Leube et al., 1998).

My analysis revealed that the PP2C inhibition imposed by ABA and RCAR1 or RCAR3 is independent of substrate (MUP) concentration and relies on a non-competitive inactivation of the enzyme in the presence of high ABA level (1 mM). The stability of the inhibition level was only observed at saturating ABA levels, consistent with an ABA-mediated stabilization of the RCAR1/3-ABI2 complex in the low nanomolar range.

ITC analysis of RCAR1 has shown saturable and partially stereospecific binding to (*S*)-ABA with an apparent K_d of 0.66 µM. However, equimolar presence of ABI2 in the binding assay resulted in a K_d of 64 nM, which indicates that the affinity of the complex for ABA is approximately 10-fold higher under these conditions. Santiago et al. (2009) have shown that addition of HAB1 in a similar ITC experiment in which they measured binding of (*S*)-ABA to RCAR8 led to an apparent K_d of 38 nM, which is 25-fold lower than in the absence of RCAR8 (Santiago et al., 2009). The results revealed binding of a single ABA molecule per RCAR1 or RCAR8 and that the ternary complex ABA-RCAR-PP2C behaves as a high-affinity system for ABA in the nanomolar range. The considerably lower K_d value of the heteromeric protein-ABA complex argues for a ligand-induced complex stabilization similar to BRI1 and BAK1 receptor stabilization by brassinolides (Wang et al., 2008).

Thus, in light of these results I postulate that RCAR proteins together with PP2C protein phosphatases assemble into ABA receptor complexes that reside in the cytosol-nucleus and bind ABA. Binding of ABA to the receptor complexes inactivates the PP2Cs, thereby activating the large variety of physiological processes regulated by ABA.

In vitro reconstitution of ABA signaling pathway

Protein phosphatases and kinases are known to excert opposite regulatory effects by removing or adding phosphate groups to substrate proteins. These protein dephosphorylation and phosphorylation events are important mediators of ABA signal transduction. ABA-activated SNF1-related protein kinases 2 (SnRK2s) and Ca^{2+} dependent protein kinases (CDPKs) are positive transducers of ABA signaling (Mustilli et al., 2002; Yoshida et al., 2002; Mori et al., 2006; Fujii et al., 2007; Zhu et al., 2007), whereas PP2Cs belonging to cluster A of the PP2C family ABI1, ABI2, HAB1, HAB2, AHG1 and PP2CA/AHG3 function as negative regulators of ABA signaling and have independent and overlapping functions (Merlot et al., 2001; Kuhn et al., 2006; Robert et al., 2006; Saez et al., 2006; Yoshida et al., 2006; Nishimura et al., 2007; Rubio et al., 2009).
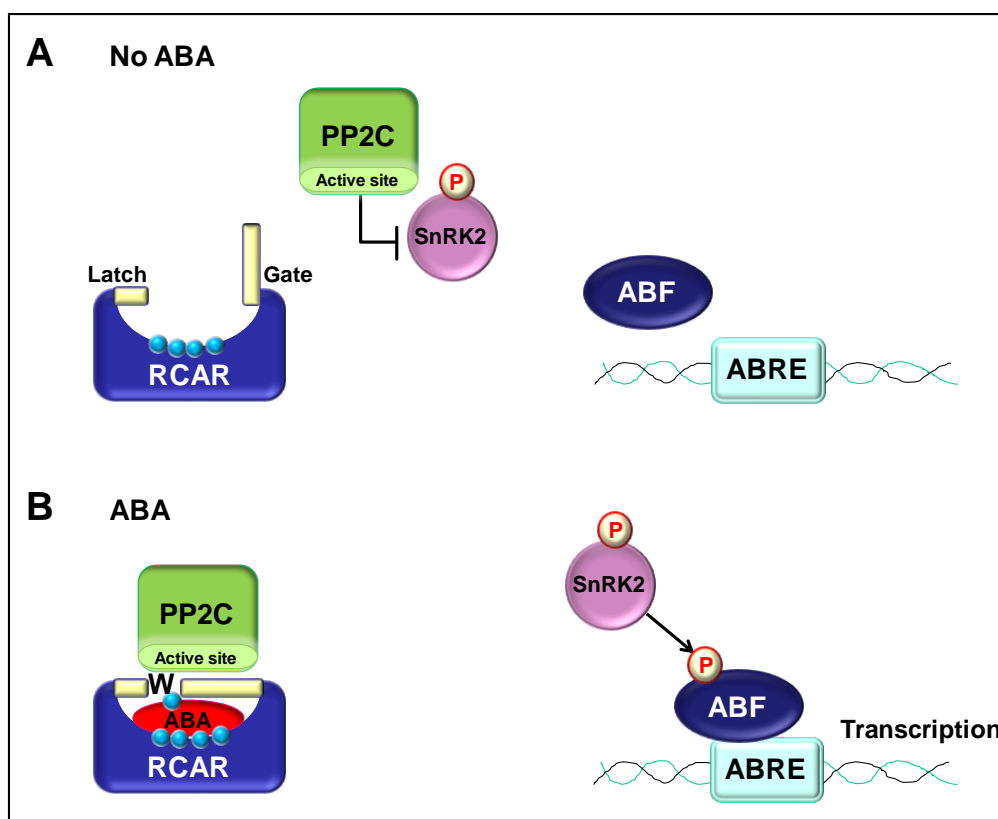
Figure 4-1   ***Minimal abscisic acid (ABA) signaling pathway***
(A) In the absence of ABA, PP2C inactivate the family of SnRK2 kinases by dephosphorylation. (B) ABA enables the RCAR/PYR/PYL family of proteins to bind to PP2Cs, and inactivate them. This relieves inhibition on the SnRK2 kinase, which becomes auto-activated and can subsequently phosphorylate and activate downstream transcription factors (ABF) to initiate transcription at ABA-responsive promoter elements – ABRE. Modified after (Sheard and Zheng, 2009).

My studies revealed that RCAR proteins negatively regulated PP2C activity after ABA treatment *in vitro*, though RCARs can constitutively interact with PP2Cs. In the absence of ABA, PP2Cs are active and through physical interaction and dephosphorylation events, keep the SnRK2 kinases inactive (Yoshida et al., 2006; Fujii et al., 2009). In the presence of ABA, the RCAR receptor proteins inhibited the negatively acting PP2Cs and disrupted their interaction with the SnRK2s, thus preventing the PP2C-mediated dephosphorylation of the SnRK2s and resulting in the activation of the SnRK2 kinases (Figure 4-1).

Activated kinases were able to phosphorylate the basic leucine zipper (bZIP) transcription factors called ABFs/AREBs, which in turn bind to ABA-responsive promoter elements (ABRE) to induce the expression of ABA-responsive genes (Johnson et al., 2002; Furihata et al., 2006; Fujii et al., 2009). These findings reveal that RCAR family members act as ABA co-receptors in a three step signal relay to induce ABA-responsive gene expression.

4.2 Receptor complexes and their differences in ABA selectivity and sensitivity

Plant adaptation requires the fine-tuning of a large number of responses to subtle or extreme changes in environmental conditions. Cytosolic levels of the phytohormone ABA can range from the nano-molar to the micro-molar range depending on environmental challenge and/or developmental stage (Priest et al., 2006; Christmann et al., 2007). The high dynamic range of ABA levels and the distinct responses evoked imply the existence of mechanisms to fine-tune distinct ABA signaling pathways in response to varying ABA concentrations. Different heteromeric receptor complexes may provide a means of adjusting the sensitivity of ABA perception and signaling. In order to test this hypothesis, I compared different receptor complexes formed by a combinatorial assembly of the co-receptors RCAR1/3 and of the PP2Cs ABI1/2.

Different receptor complexes differ in their stereo-selectivity for and responses to ABA

The sensitivity of the receptor complexes efficiency of ABA-mediated phosphatase inhibition was higher both with ABI1 than with ABI2 and higher with RCAR3 than with RCAR1. The IC_{50} values of PP2C inhibition were approximately two-fold lower with RCAR3 versus RCAR1 at a 2:1 RCAR:PP2C ratio (Figure 3-24). Under these experimental conditions, ABI1 was approximately twofold more sensitive to ABA regulation than ABI2. Half maximal inhibition of RCAR3/ABI1 was observed at 23 nM ABA, while RCAR1/ABI2 revealed a more than fourfold higher IC_{50} value of 95 nM ABA. The finding reflects differences in the heteromeric receptor complexes. PP2C inhibition

requires RCAR binding to the PP2C and increasing the RCAR:PP2Cs ratio shifts the equilibrium towards complex formation. The differences between IC_{50} values of ABI1/RCAR3 and ABI2/RCAR1 were reduced with increasing RCAR levels and almost abolished at high excess levels of RCAR. Interestingly, the IC_{50} values were more responsive to changes in RCAR1 than RCAR3 levels by a factor of 2.5 and 5.4 for ABI1 and ABI2, respectively. The data imply a higher affinity of RCAR3 for PP2C interaction compared to RCAR1. Thus, both the PP2C and RCAR components modulate the sensitivity of ABA-mediated PP2C inactivation, which is required to overcome their negative regulation of the ABA signal pathway and to allow the activation of the ABA response by via SnRKs (Fujii and Zhu, 2009; Nakashima et al., 2009). RCAR3 and ABI1 lend greater ABA-sensitivity to the receptor regulation.

The biochemical analysis was also extended to other RCAR proteins and clade A, F and I PP2Cs. As a general result, it was found that RCARs such as RCAR3 and RCAR9 have an inhibitory effect on ABI2 in an ABA-independent manner. Moreover, I showed that six members of RCAR protein family were able to regulate the activity of PP2Cs from clade A, while the members from clade F and I did not reveal any regulation in the presence of ABA. Given the multiplicity of both clade A PP2Cs (nine members) and RCAR proteins (14 members), I anticipated that certain RCAR-PP2C receptor complexes could differ in terms of interaction pattern, stereo-selectivity, and sensitivity to ABA.

In the phospatase assays, I found differences in IC_{50} values among 14 different receptor complexes. As mentioned above, RCAR3 showed higher affinity for ABI1 and ABI2 than RCAR1, with half-maximal inhibition at 18 and 30 nM (*S*)-ABA, respectively, compared to 35 and 60 nM (*S*)-ABA for RCAR1. To ascertain whether the effect of RCAR1 and RCAR3 was not specific for ABI1 and ABI2, I tested their effect on PP2CA activity. The IC_{50} values were higher (10 μM) than values obtained for other combinations, which might indicate that RCAR1 and RCAR3 interacted weakly with PP2CA and other members such as RCAR6 and RCAR10 should be tested for interaction, as they revealed very strong binding with PP2CA in the Y2H assay (Park et al., 2009). Santiago et al. (2009) showed that RCAR8 - member of clade II of RCAR family, did not inhibit PP2CA activity, and other distantly related PP2C from clade D, which is indicative of a selective effect of RCARs on the ABI1/ABI2/HAB1 PP2Cs.

I showed also that in the case of RCARs from clade II and III such as RCAR9, 10 and 13, 14 the IC_{50} values for ABI1 were approximately 9, 10, 10 and 60 nM and for ABI2 3, 30, 5 and 83 nM, respectively. Santiago et al. (2009) reported a half-maximal inhibition IC_{50} value for RCAR3 that is 4-fold higher with both ABI1 and ABI2 and for RCAR10 with ABI1 and ABI2 27- and 3.6-fold higher, respectively. These differences could be due to the

different substrate (RRA(phosphoT)VA peptide) and different protein ratios used in the phosphatase assays.

Finally, I tested whether (*S*)-ABA, (*R*)-ABA and *trans*-ABA were equally effective at promoting RCAR-mediated inhibition of ABI1 and ABI2 activity.

Data showed that only RCAR1 conferred almost absolute stereo-selectivity to the receptor complex, whereas complexes with five other RCARs responded to the (*R*)-ABA and *trans*-ABA stereoisomers. Taken together, I conclude that the different receptors differ in terms of stereo-selectivity for and sensitivity to the ABA ligand. However, it is still an open question, whether all PP2Cs involved in ABA responses are regulated by RCARs or whether all RCARs can regulate the same PP2C.

A model for fine-tuning the ABA response

Several overlapping mechanisms may act to modulate ABA responses. First, the combinatorial assembly of receptor complexes showed that different complexes had different properties with respect to the sensitivity of the response. Second, transcriptional profiling showed that the different members of the RCAR and PP2C gene families were differentially expressed in different tissues and at different developmental stages. Third, ABA-related stress conditions alter the transcript levels of distinct co-receptors differentially, which in turn may alter the sensitivity and plasticity of the response. Fourth, different PP2Cs are known to target overlapping but distinct targets (Vranova et al., 2001; Himmelbach et al., 2002; Ohta et al., 2003; Miao et al., 2006; Yang et al., 2006; Yoshida et al., 2006), which is likely to modulate the nature of ABA responses.

In combination with ABI1 and ABI2, RCAR1 and RCAR3 generate high affinity receptors for ABA, which function within the nano-molar range of the phytohormone. Stress conditions, however, may lead to very high ABA levels, within the micro-molar range, and these high levels may persist in the plant over long periods of time. Transcriptional profiling suggests that stress conditions such as salt stress and osmotic stress upregulate the levels of PP2C phosphatases such as ABI1, ABI2, HAB1, HAB2, PP2CA and AHG1 and down-regulate some RCAR family members, such as RCAR3, RCAR8, RCAR9 and RCAR10, while leaving the levels of other RCARs, such as RCAR1 and RCAR2, relatively constant. Exposure to drought stress upregulated all PP2Cs, which act as negative regulators of ABA responses and some positive regulators such as RCAR8, RCAR9 and RCAR13. Three other RCARs (3, 10 and 14) were downregulated by drought, while RCAR1, 2, 11 and 12 appeared to remain at a constant level. The data are entirely consistent with the transcriptional profiling presented by Santiago et al. (2009).

As transcriptional profiling showed, exogenous ABA or abiotic stress conditions differentially regulated expression levels of RCARs and PP2Cs. This observation leads to a conclusion that ABA-related stress conditions or treatments alter the relative levels of RCAR proteins and increase the co-receptor (PP2C:RCAR) ratio (Figure 3-24). The PP2C:RCAR ratio has a large impact on IC_{50} values. As RCAR levels increase, IC_{50} values decrease, indicating a more ABA-sensitive regulation of phosphatase activity. Conversely, the PP2C regulation with RCAR1 and RCAR3 becomes less sensitive to ABA, when PP2C:RCAR ratio increases. The in vitro measurements suggest that higher PP2C to RCAR ratios and higher levels of RCAR1 over RCAR3 would lead to a desensitisation of the ABA response. In addition, higher PP2C to RCAR ratios greatly enhance the difference between the RCAR1 and RCAR3 receptor complexes, yielding a greater plasticity of the response. Thus, although RCAR1 and RCAR3 may, under physiological conditions, function at low ABA concentrations, their differential regulation under stress conditions may provide a means for the plant to cope with sustained high levels of ABA.

It is also important to note that I have looked at only few of a potential of at least 84 different receptor complexes. While these few receptor complexes have shown considerable differences, all are highly sensitive to ABA. An analysis of different combinations of RCARs and PP2Cs may further our understanding of the entire dynamic range of ABA levels in the cell.

Phytohormone perception

The heteromeric ABA receptor complexes have a greater affinity for ABA than the ABA-binding regulatory components alone. The affinity of RCAR1, RCAR3 (clade I) and RCAR8 (clade II) (Santiago et al., 2009), for (S)-ABA did not considerably differ, with K_ds of 0.66, 0.97 and 1.1 µM, respectively. Only RCARs from clade III such as RCAR12 (Miyazono et al., 2009) and RCAR14 (Yin et al., 2009) represented very high K_ds of 52 and 59 µM, respectively. By contrast, (S)-ABA binding to heteromeric receptor complexes revealed a pronounced shift in affinity. The low K_ds of 64 nM for ABI2/RCAR1 and 38 nM for a truncated HAB1/RCAR8 combination (Santiago et al., 2009) are reflected by low IC_{50} values of the complexes with 60 and 35 nM S-ABA, respectively. Similarly, RCAR3 revealed half-maximal inhibition of ABI1 and ABI2 in the range of 15 to 40 nanomolar, consistent with the generation of a high-affinity binding site for ABA by the heteromeric receptor complex. Varying IC_{50} values were also observed for other RCAR members and truncated HAB1 with RCAR11 yielding the highest value of 390 nM ABA (Santiago et al., 2009). These observations support a co-receptor function of both RCARs and PP2Cs, due

to the fact that interaction between both proteins generates the high affinity ABA binding site relevant at physiological ABA levels.

Moreover, the ABA ligand appears to promote or stabilize receptor complex formation. This conclusion is supported by enhanced interaction of some RCARs/HAB1 combinations in yeast in the presence of ABA (Park et al., 2009) and by stabilization of PP2C inhibition even in the low nanomolar range in the presence of high ABA levels, as observed in this study for RCAR1 and RCAR3. In protoplasts, the interaction of RCAR1 and RCAR3 and ABI1/2 was not visibly enhanced by exogenous ABA, pointing to an efficient receptor complex formation *in vivo*.

Plant hormones other than ABA also act to promote or stabilize protein interactions. Auxin, for example, acts as a "glue" in the interaction between its receptor, the E3 Ubiquitin ligase TIR1, and the Aux/IAA transcriptional repressors that are targeted for degradation (Tan et al., 2007). Similarly, gibberellin binding to GID1 (GIBBERELIN-INSENSITIVE DWARF 1) stabilizes the interaction between a E3 Ubiquitin ligase SLY1 (SLEEPY1) and DELLA repressors, which are targeted for degradation (Murase et al., 2008; Shimada et al., 2008). A third example is that of brassinolides. Brassinolides are required for the assembly of a heterodimeric receptor complex that consists of two leucine-rich repeat receptor-like kinases (LRR RLKs) BRI1 (BRASSINOSTEROID INSENSITIVE 1) and BAK1 (BRI1-ASSOCIATED RECEPTOR KINASE1) (Wang et al., 2008). These three examples are reminiscent of my findings for ABA, in which the hormone may act to promote or stabilize protein interactions between the components of the heteromeric co-receptors.

Phytohormone-binding proteins and their targets or co-receptors are encoded by gene families in *Arabidopsis*, which provides a plethora of similar yet distinct possible combinations. The *Arabidopsis* genome encodes, for example, 6 TIR1 family members and 29 Aux/IAAs (Santner and Estelle, 2009), 3 GID1 genes and 5 DELLA protein (Suzuki et al., 2009), and 14 RCAR genes and 9 clade A PP2Cs. In this study, I showed that different combinations of RCARs and PP2Cs alter the sensitivity of the ABA receptor complex. The transcript levels of the different RCARs and PP2Cs varies throughout development and in response to environmental challenge *in vivo*. Furthermore, changes in the combinatorial assembly of the receptor or in the relative proportions of RCAR and PP2C proteins affect the sensitivity of the receptor complex *in vitro* lending support for changing combinatorial receptor complexes. Given the complexity of the gene families involved, a combinatorial assembly and altered relative ratios of receptors, co-receptors and their targets may act to regulate not only ABA responses, but might provide a general model for the fine-tuning of hormone responses.

4.3 Model of binding ABA to the receptor complexes

Members of RCAR protein family in *Arabidopsis thaliana* have been shown in this study to bind to and inhibit the activity of specific protein phophatases, the type 2C PP2Cs, in an ABA-dependent manner.

Sequence data disclosed that RCARs are structurally related to the Bet v 1 family, including the pathogenesis-related 10 (PR-10) protein family. The Bet v 1 family consists of particulary potent allergens from white birch (*Betula verrucosa*) pollen. The Bet v 1 fold consists of a curved seven-stranded β-sheet wrapped around a long C-terminal helix, α3, and has been classified as a type of 'helix-grip' fold (Iyer et al., 2001). The most characteristic feature in the Bet v 1 structure is the large hydrophobic cavity inside the protein, which can accommodate plant steroid hormones (Markovic-Housley et al., 2003).

On the basis of known structures of Bet v 1 family, it was predicted that RCAR proteins also contain a ligand-binding pocket that could be a binding site for ABA. It was attempted, via crystallization studies of RCAR1, to address the question as to whether ABA binds to the RCAR-PP2C co-receptor complex, or whether it first binds to RCAR proteins in a manner that is subsequently stabilized by an interaction with PP2Cs. Although crystallization trials were unsuccessful, five other groups have recently revealed the atomic structures of RCARs from clade III such as RCAR11, 12 and 14 in different functional states (Melcher et al., 2009; Miyazono et al., 2009; Nishimura et al., 2009; Santiago et al., 2009; Yin et al., 2009).

A 'gate-latch-lock' mechanism of ABA binding

Crystal structures of RCAR14 in particular, have been captured in all critically relevant forms such as apo-RCAR14 (ligand free), ABA-bound RCAR14 and the ABA-RCAR14-HAB1 complex (Figure 4-2). The highlight of these studies is the ABA binding model called a 'gate-latch-lock' mechanism (Melcher et al., 2009). The structures of apo- and ABA-bound RCAR14 exhibited nearly identical helix-grip folds, which are also found among Bet v 1 family members.

A dominant feature of the RCAR14 structure is the long C-terminal α-helix wrapped around by seven anti-parallel β-sheets and short α2 and α3 helices. The entry to the ligand binding cavity of RCAR14 is covered by two loops, the gate-like loop (β3-β4) on one side, on the other side, a latch-like loop (β5-β6).
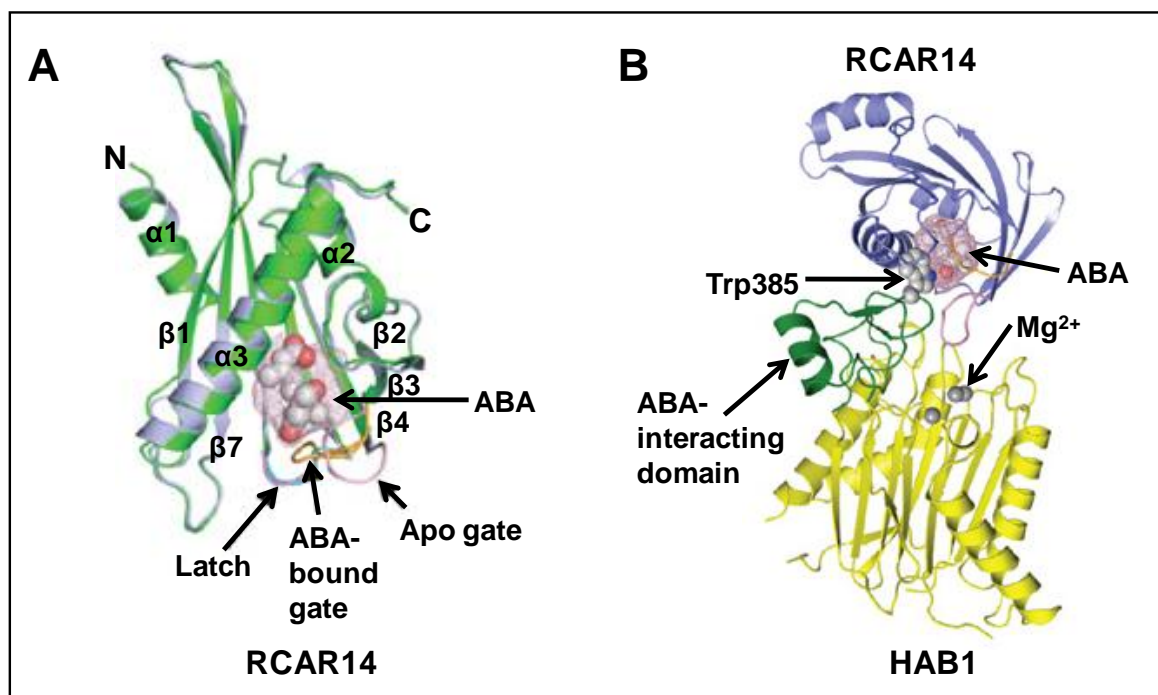
Figure 4-2   Structures of apo-RCAR14, ABA-bound RCAR14 and RCAR14-ABA-HAB1 co-receptor complex
(A) Overlay of the apo (grey) and ABA-bound (green) RCAR14 structures. The latch (magenta for apo- and cyan for ABA-bound RCAR14) and the conformational change in the gate (pink and yellow in apo- and ABA-bound structures, respectively) are indicated by arrows.
(B) RCAR14–ABA–HAB1 complex. HAB1 is shown with its catalytic domain in yellow (magnesium ions as balls), the ABA-interacting domain in green (W385 lock as a ball model) and RCAR14 is in blue. ABA (A and B) is shown as a ball model with its surrounding ligand binding pocket as mesh. Modified after Melcher et al. (2009).

In the absence of ABA (apo-form of RCAR), the gate and latch reside in an open conformation. When the water-filled pocket is occupied by phytohormone, the conformations of both loops change from the mobile, open state to the fixed, closed state. Due to the fact that the amino acid residues in contact with ABA, as well as the sequences of the two entrance loops, are evolutionary conserved among all RCAR proteins, the ABA binding and gate-latch-lock mechanism are likely to be common for all members of the RCAR family (Figure 4-3).

The analysis of the crystal structure of the RCAR14-ABA-HAB1 complex revealed a 1:1:1 stoichiometry and showed that ABA-bound RCAR14 docks with its gate-like loop into the active, catalytic site of HAB1, blocking its ability to bind and dephosphorylate its substrate. In addition, a conserved tryptophan (W385 for HAB1 or W300 for ABI1) residue of HAB1 inserts between both gate-like and latch-like loops of RCAR14 and keeps them closed. Furthermore, this residue makes a water-mediated interaction with the ketone group of ABA, thus allowing HAB1 to sense the presence of ABA in the RCAR14 ligand-binding pocket (Figure 4-3).

Mutations in both the gate-like loop caused a reduction in the capacity of RCAR to interact with and inhibit the protein phosphatase HAB1. This suggests that the β3-β4 loop is not only important for the stabilization of the ligand, as the RCAR structure suggested, but that it is also involved in interactions with the PP2Cs. Additionally, the single point mutations in the active site of PP2Cs causing the dominant ABA-insensitive phenotype (*abi1, abi2* and *hab1*) disrupted the interaction of PP2Cs with RCARs (Melcher et al., 2009).

Taken together, these structural analyses provide an explanation for the RCAR-mediated PP2C inhibition in an ABA-dependent manner and a direct proof that PP2C can serve as a co-receptor that senses the binding of ABA by the RCAR receptors (Melcher et al., 2009).
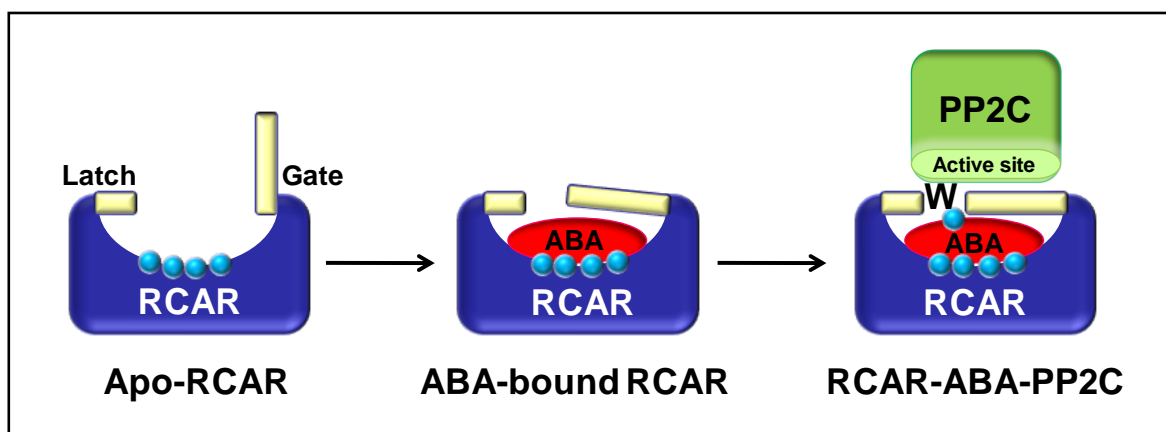
Figure 4-3   A model of ABA-induced PP2C regulation by RCAR protein
In the ligand-free form, the RCAR co-receptor presents an open and accessible pocket with two loops (gate and latch). When ABA enters the water-filled cavity, the conformation of the loops change from open-to-close state. This exposes a hydrophobic binding site on the gate-like loop, which is binding PP2C via active site of the PP2C domain. The PP2C inserts a conserved tryptophan (W) between both loops and keeps them closed. The conserved tryptophan is contacting with ABA by water-mediated interaction with the ketone group of ABA.

However, Yin et al. (2009) strongly argue against such a model, indicating that ABA is buried within the conserved cavity of RCAR14, and thereby unable to interact with ABI2 (Yin et al., 2009).

These observations are not in agreement with ITC data from this work, which showed that the binding affinity between ABA and RCAR1 increased by approximately ten-fold in the presence of phosphatase ABI2, which indicates that RCARs and PP2Cs act as co-receptors. Moreover, the *in vitro* phosphatase assays in the presence of RCAR3 and RCAR9 showed at a value of 16 for RCAR:ABI2 molar ratio (Figure 3-17B, C) the reduction of ABI2 activity to 60% and 50%, respectively. An application of ABA stabilized the receptor complex and almost completely reduced the ABI2 activity (Figure 3-19 and 3-

20). Thus, experimental evidence supports the function of RCARs and PP2Cs as ABA co-receptors rather than receptors.

In three reports of the structural studies, RCAR11 and RCAR14 dimer formation was observed, both in the presence and absence of exogenously applied ABA and in the absence of PP2C (Nishimura et al., 2009; Santiago et al., 2009; Yin et al., 2009).
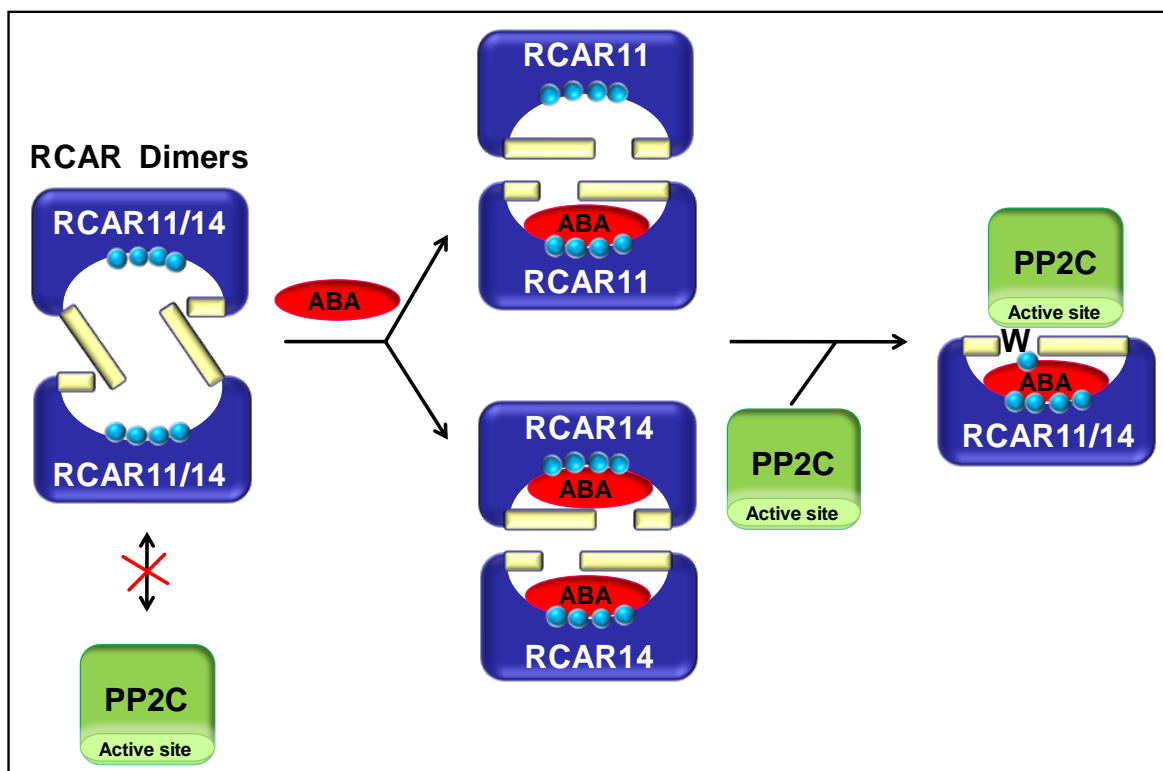
Figure 4-4   A model for ABA-dependent recognition and inhibition of PP2Cs by dimeric RCAR11 and RCAR14
RCAR11 and RCAR14 dimerization occur in the absence and presence of ABA and absence of PP2C. RCAR11 binds one ABA, while RCAR14 two ABA molecules per dimer. More details can be found in the text.

The exact purpose of this dimerization remains unclear. In the structure of homodimeric RCAR11, only one molecule of ABA can bind per dimer, whereas in the related structure of the RCAR14 dimer, both proteins are occupied by ABA molecules (Figure 4-4). In all of these models, the dimer interface involves the gate-like loop of the RCAR, which suggests that the dimer formation is functionally relevant. However, the RCAR dimerization is not required for the final action of ABA, because only monomeric RCARs are bound to form a complex with PP2Cs in the presence of phytohormone.

'Closing lid' and 'molecular glue' mechanisms of binding other phytohormones

The gate-latch-lock mechanism is reminiscent of the 'closing lid' mechanism used by the receptor GID1 to sense gibberellins (GAs), which comprise a large family of tetracyclic diterpenoid plant hormones. The phytohormone gibberellin stimulates growth by promoting the destruction of DELLAs, negative regulators of GA signaling (Peng et al., 1997). All DELLA proteins contain an N-terminal regulatory DELLA domain important for GID1 binding, and as well as a C-terminal GRAS domain (Pysh et al., 1999; Ueguchi-Tanaka et al., 2007). The nuclear gibberellin receptor, GIBBERELLIN INSENSITIVE DWARF1 (GID1), has a primary structure similar to members of the hormone-sensitive lipases (HSLs). Like HSLs, the GID1 primary structure forms a deep binding pocket whose access is controlled by an N-terminal flexible lid. GA binding to GID1 within the pocket induces the protein to adopt a compact form, with the N-terminal lid folding back to cover the GA-bound pocket (Murase et al., 2008; Shimada et al., 2008). GA binding to GID1 promotes interaction with DELLAs, which directly contact the N-terminal lid of GID1 via the DELLA domain (Figure 4-5). This GA-GID1-DELLA complex formation enhances GRAS domain binding to the F-box protein SLY1 (SLEEPY1) that targets the DELLA protein for degradation (Murase et al., 2008). Both ABA and gibberellin allosterically remodel their respective receptors, in contrast to the 'molecular glue' mechanism used by auxin (Tan et al., 2007).

At the centre of the auxin signaling cascade is the Skp1/Cullin/F-box (SCF) ubiquitin ligase complex, which promotes the ubiquitin-dependent proteolysis of a family of transcription factors known as Aux/IAAs in an auxin-dependent manner (Gray et al., 2001). Degradation of the Aux/IAAs activates the auxin response factor (ARF) family of transcription factors, which regulate auxin-responsive genes, normally inhibited by Aux/IAA proteins. The F-box protein subunit of SCF, called TRANSPORT INHIBITOR RESPONSE 1 (TIR1), functions as a true auxin receptor (Dharmasiri et al., 2005). A single hydrophobic pocket on the surface of the leucine-rich repeat domain of TIR1 binds both auxin and the Aux/IAA polypeptide substrate. Auxin binds to the base of the TIR1 pocket, while on top of auxin, the Aux/IAA substrate peptide occupies the rest of the TIR1 pocket and completely encloses the hormone binding site (Figure 4-5). Thus, auxin promotes TIR1-substrate binding by acting as a 'molecular glue' rather than an allosteric switch (Tan et al., 2007).
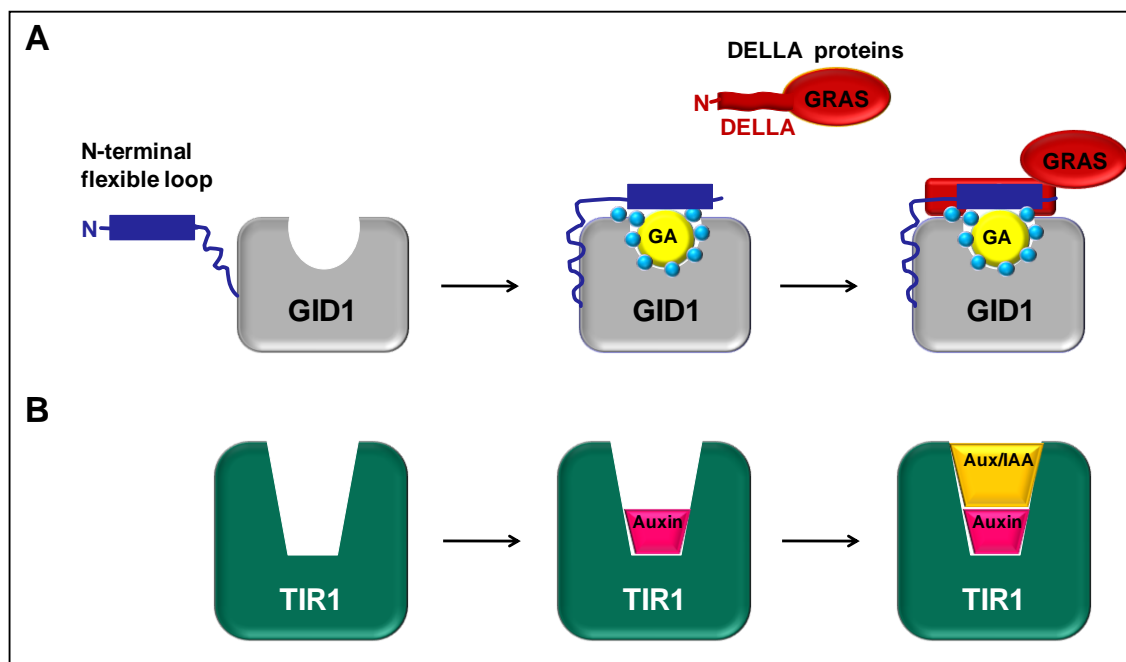
Figure 4-5   A model of gibberellin and auxin binding to the receptor
(A) 'Closing lid' mechanism of gibberellin action, where GA functions as a allosteric inducer to enhance GID1-DELLA interactions (Murase et al., 2008) (B) A 'molecular glue' mechanism of auxin action to enhance TIR1-substrate interactions (Tan et al., 2007).

Although the mechanisms of binding phytohormones differ at some points, there is a common feature in plant hormone action at soluble receptors. The hormone signal enhances protein-protein interactions in order to modulate important modifications such phosphorylation or ubiquitylation, which alter the activity of the target protein. Moreover, in all cases, the phytohormone binds to a site that is at or close to the protein-protein interface, engaging the associating protein as a co-receptor.

4.4 Searching for new ligands

The pollen of *Betula* species is a main cause of allergic reactions in the Northern hemisphere. The protein Bet v 1 and related proteins from other plant species are prominent causative agents for pollen and food allergy. The function of Bet v 1-related proteins in plants has been elusive. Some Bet v 1-structurally related proteins are assigned to class 10 pathogenesis-related proteins (PR-10) that are proved to be induced by pathogens and related abiotic stresses. The PR-10 protein family together with major latex proteins (MLPs), the (S)-norcoclaurine synthases and cytokinin-specific binding proteins (CSBPs) have been included to Bet v 1 superfamily (Radauer et al., 2008). High structural similarity between Bet v 1 and the START domain of human MLN64 protein, which is steroid binding domain related to steroidogenic acute regulary protein (StAR) involved in cholesterol translocation suggested a similar function for Bet v 1 as a steroid binding protein (Tsujishita and Hurley, 2000; Mogensen et al., 2002; Markovic-Housley et al., 2003).

Crystallization studies of Bet v 1 revealed a large Y-shaped, hydrophobic cavity, which functions as the ligand-binding site (Markovic-Housley et al., 2003). The Bet v 1 ligand binding studies showed that Bet v 1 interacts with several biologically important molecules, including cytokinin, flavonoid glycosides, sterols, brassinosteroids and emodin but does not interact with indole-3-acetic acid (IAA) and gibberellic acid (Mogensen et al., 2002; Markovic-Housley et al., 2003; Koistinen et al., 2005; Mattila and Renkonen, 2009). Moreover, another allergen from cherry Pru av 1 has been reported to bind the phytosteroids (Neudecker et al., 2001). In addition, competition experiments with kinetin and deoxycholate demonstrated that these ligands have two binding sites where they can bind without interfering with each other.

These results indicate that PR-10 family, which belongs to Bet v 1 superfamily is capable of binding several different types of ligands using different binding sites for different binding molecules. These data suggest that Bet v 1 may play a role in the storage and transport of biologically important molecules.

Cytokinins are plant-growth hormones that control the differentiation and proliferation of plant cells. Naturally occurring cytokinins are usually adenine derivatives with different substituents attached to N6 position of the purine ring. In this group, the most common substituent is an isoprenoid tail present in zeatin (Mok and Mok, 2001). Additionally, there is a class of artificial, urea-type cytokinins, which are structurally unrelated, but highly active biologically. The most potent urea cytokinins are 4-PU and 4-CPPU. The cytokinin-

specific binding proteins (CSBPs) from mung bean (*Vigna radiata*) have been found to have the capacity to bind to cytokinins such as zeatin. The crystal structure revealed that two cytokinin molecules are bound within a large cavity inside the protein. One zeatin is bound deep in the binding cavity, whereas the other is found at the entrance of the pocket (Pasternak et al., 2006).

Recent studies revealed that CSBPs from mung bean are also able to bind to gibberellins, but do not interact with other phytohormones like auxin, ABA, brassinosteroids or jasmonic acid. Gibberellin A4 showed 10-fold higher affinity (10 µM) to CSBP than the natural cytokinins (100 µM). However, synthetic cytokinin 4-CCPU, which shows even stronger cytokinin activity that natural cytokinin zeatin, revealed as strong an affinity (10 µM) to CSBP as GA4. Interestingly, the studies showed that both zeatin and GA4 compete for the same binding site (Zawadzki et al., 2010).

Studies with protein from yellow lupine (*Lupinus luteus*) called LlPR-10.2B revealed that this PR-10 class protein is also able to bind cytokinins (Pasternak et al., 2005). The crystal complex of LlPR-10.2B with *trans*-zeatin showed that three molecules of *trans*-zeatin are buried differently in the large internal cavity of the protein (Fernandes et al., 2008).

However, the LlPR-10.2B is also able to accommodate in the hydrophobic pocket four molecules of synthetic urea-type cytokinin - N,N'-diphenylurea at distinct positions that do not overlap (Fernandes et al., 2009). These results indicate that LlPR-10.2B can like CSBP act as a reservoir of cytokinin molecules in the aqueous environment of a plant cell.

Hyp-1, a St. John's wort protein is another example of protein that belongs to PR-10 family, and it is implicated in the biosynthesis of hypericin used in the pharmaceutical industry in treatment of depression. The crystal structure of Hyp-1 showed that, like other members of PR-10 family, Hyp-1 posseses a huge cavity within the protein interior, loosely occupied by a variable number of polyethylene glycol (PEG) molecules (Michalska et al., 2010).

The major latex proteins (MLPs) are a protein family first identified in the latex of opium poppy (*Papaver somniferum*), and display a Bet v 1 like helix-grip fold (Radauer et al., 2008). NMR studies with one MLP member At1g24000.1 showed binding within the cavity a progesterone molecule, which is known to share a structural similarity to the plant steroid, brassinolide. This finding may indicate the role of MLP family in biochemical processes through plant hormone-mediated cell signaling (Lytle et al., 2009).

In this work a function of Bet v 1-related proteins of *Arabidopsis* in specifically recognizing physiologically active ABA and regulating ABI1 and ABI2 in ABA responses was reported. The association between RCARs and the PP2Cs generated ABA-selective high affinity receptors, which control a broad range of ABA responses including stomatal regulation, germination and growth.

Crystallization studies showed that RCAR proteins such as Bet v 1 contain a ligand-binding cavity that acts as a binding site for ABA (Melcher et al., 2009; Miyazono et al., 2009; Nishimura et al., 2009; Santiago et al., 2009; Yin et al., 2009). Whether RCARs are also able to bind ligands other than ABA is an open question. By using phosphatase assays, my preliminary results showed that various phytohormones and related substances such as auxins (IAA, NAA, 2,4-D), cytokinins (BAP, kinetin), salicylic acid, glutathione, jasmonate derivatives and brassinosteroids did not reveal RCAR1/13-dependent regulation of PP2C activity. Santiago et al. (2009) showed that brassinosteroids and gibberellins did not promote inhibition of HAB1 activity by RCAR8 and RCAR11 proteins. Similar results were obtained with the Y2H system in which administration of epibrassinolide, gibberellin, methyl jasmonate, kinetin and 2,4-D did not show any significant change in the interaction between RCAR10-14 and HAB1 (Park et al., 2009). It might be possible that RCAR proteins have the ability to bind some of these phytohormones but their action cannot be detected in the phosphatase assay, due to the fact that their role might be not linked to the regulation of PP2Cs activity.

The general mode of ABA recognition by RCARs is reminiscent of ligand binding by other members of the PR10 family, although most details, including the size and hydrophobicity of the ligand binding pocket and the ligand stoichiometry, are different. In the case of Bet v 1, the internal cavity yielded a volume of 3500 $Å^3$ (Gajhede et al., 1996). Interestingly, an unusually large volume of 4500 $Å^3$ has been determinated for LIPR-10.2B, a classic PR-10 protein from *Lupinus luteus,* which binds three molecules of the plant hormone trans-zeatin and four molecules of synthetic urea-type cytokinin - N,N'-diphenylurea (Fernandes et al., 2008; Fernandes et al., 2009). In contrast, in the RCAR14 protein the volume of the cavity is significantly reduced to 543 $Å^3$ and 480 $Å^3$ in the apo- and ABA-bound structure, respectively (Melcher et al., 2009). This small binding pocket present in RCAR14 can hold only one ABA molecule, and did not show any binding with other phytohormones, which raises the question as to whether RCAR proteins are really able to bind other molecules than ABA. I tried to answer this question, by testing the influence of the cell-free extract from *Arabidopsis thaliana* cell suspension cultures, which are the reservoir of various plant-specific ligands. The phosphatase assay analysis showed that some as yet unidentified molecules from plant extract have the ability to inhibit the phosphatase activity

of ABI1 to 50-60% and RCAR13 supplementation resulted in almost complete inhibition of ABI1 catalytic activity (Figure 4-6).

In previous analyses, it was consistently observed an up to 20% reduction of ABI1 phosphatase activity in the presence of micromolar levels of ABA, although no PP2C-bound ABA was detected (Leube et al., 1998). These results suggest that the new ligand from plant extracts that inhibits PP2C activity is not ABA. The question was, whether the inhibition of ABI1 in the presence of RCAR13 was achieved due to some pool of ABA present in plant extract or whether this is the effect of a new, unknown ligand which has the ability to inhibit PP2Cs. To solve this problem I used plant extract from *aba2-1* (ABA-deficient *Arabidopsis* mutant) suspension cultures and I obtained comparable results, which might indicate that I am dealing with unknown binding molecules.
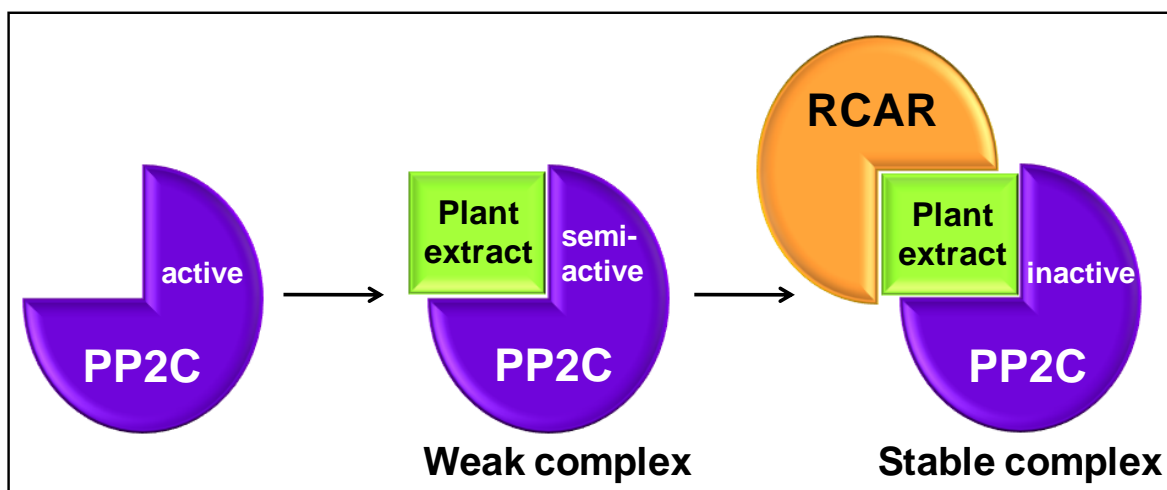
Figure 4-6   Model of PP2C inactivation in the presence of RCAR protein and unidentified molecules from Arabidopsis thaliana plant extract

In order to screen for ligands from plant extracts that bind to RCAR proteins alone and in the complex with PP2Cs I used 12 Tesla Fourier Transform Ion Cyclotron Resonance Mass Spectrometer (FT-ICR-MS), which has been proved experimentally to provide the highest resolution, mass accuracy, and sensitivity for peptide and protein measurements. The analysis identified several interesting candidates among which I have chosen three that seem to bind specifically to functional RCAR proteins but not to versions with a deleted domain. Further analysis of one of these candidates with a predicted molecular formula of $C_{25}H_{30}N_2O_6$ suggested that I might be dealing with steroid-like compounds, although further analyses are required.

Plants treated with ABA before a drought occurs become more water efficient in order to survive the water shortage so they become more tolerant to drought. Due to the fact that ABA is very difficult and expensive to produce it is very important to know what ABA

interacts with and how. This can help to find other molecules that could be useful to cope with water stress in crops and which can be feasibly produced and applied. In addition, finding other than ABA ligands that are binding to RCAR proteins can uncover new roles of RCARs in plant development and identify new classes of signaling molecules with hormonal function.

5 References

Abe H, Urao T, Ito T, Seki M, Shinozaki K, Yamaguchi-Shinozaki K (2003) Arabidopsis AtMYC2 (bHLH) and AtMYB2 (MYB) function as transcriptional activators in abscisic acid signaling. Plant Cell **15:** 63-78

Abel S, Theologis A (1998) Transient gene expression in protoplasts of *Arabidopsis thaliana*. Methods Mol Biol **82:** 209-217

Acharya B, Assmann S (2009) Hormone interactions in stomatal function. Plant Molecular Biology **69:** 451-462

Addicott FT, Lyon JL, Ohkuma K, Thiessen WE, Carns HR, Smith OE, Cornforth JW, Milborrow BV, Ryback G, Wareing PF (1968) Abscisic Acid: A New Name for Abscisin II (Dormin). 10.1126/science.159.3822.1493. Science **159:** 1493-

Adie BA, Perez-Perez J, Perez-Perez MM, Godoy M, Sanchez-Serrano JJ, Schmelz EA, Solano R (2007) ABA is an essential signal for plant resistance to pathogens affecting JA biosynthesis and the activation of defenses in Arabidopsis. Plant Cell **19:** 1665-1681

Agrawal GK, Yamazaki M, Kobayashi M, Hirochika R, Miyao A, Hirochika H (2001) Screening of the rice viviparous mutants generated by endogenous retrotransposon Tos17 insertion. Tagging of a zeaxanthin epoxidase gene and a novel ostatc gene. Plant Physiol **125:** 1248-1257

Allen GJ, Kuchitsu K, Chu SP, Murata Y, Schroeder JI (1999) *Arabidopsis abi1-1* and *abi2-1* Phosphatase Mutations Reduce Abscisic Acid–Induced Cytoplasmic Calcium Rises in Guard Cells. Plant Cell **11:** 1785-1798

Bari R, Jones JDG (2009) Role of plant hormones in plant defence responses. Plant Mol Biol **69:** 473-488

Barral P, Suárez C, Batanero E, Alfonso C, Alché JD, Rodríguez-García MI, Villalba M, Rivas G, Rodríguez R (2005) An olive pollen protein with allergenic activity, Ole e 10, defines a novel family of carbohydrate-binding modules and is potentially implicated in pollen germination. Biochem J. **390:** 77-84

Berridge MJ (1993) Inositol trisphosphate and calcium signalling. Nature **361:** 315-325

Billker O, Dechamps S, Tewari R, Wenig G, Franke-Fayard B, Brinkmann V (2004) Calcium and a calcium-dependent protein kinase regulate gamete formation and mosquito transmission in a malaria parasite. Cell **117:** 503-514

Blum H, Beier H, Gross HJ (1986) Improved silver staining of plant proteins, RNA and DNA in polyacrylamide gels. Electrophoresis **8:** 93-99

Bossi F, Cordoba E, Dupre P, Mendoza MS, Roman CS, Leon P (2009) The Arabidopsis ABA-INSENSITIVE (ABI) 4 factor acts as a central transcription activator of the expression of its own gene, and for the induction of ABI5 and SBE2.2 genes during sugar signaling. Plant J **59:** 359-374

Boudsocq M, Barbier-Brygoo H, Lauriere C (2004) Identification of nine sucrose nonfermenting 1-related protein kinases 2 activated by hyperosmotic and saline stresses in Arabidopsis thaliana. J Biol Chem **279:** 41758-41766

Boudsocq M, Droillard MJ, Barbier-Brygoo H, Lauriere C (2007) Different phosphorylation mechanisms are involved in the activation of sucrose non-fermenting 1 related protein kinases 2 by osmotic stresses and abscisic acid. Plant Mol Biol **63:** 491-503

Brewbaker JL, Kwack BH (1963) The essential role of calcium ion in pollen germination and pollen tube growth. Am. J. Bot. **50:** 747-858

Bright J, Desikan R, Hancock JT, Weir IS, Neill SJ (2006) ABA-induced NO generation and stomatal closure in Arabidopsis are dependent on H2O2 synthesis. Plant J **45:** 113-122

Bruzzone S, Bodrato N, Usai C, Guida L, Moreschi I, Nano R, Antonioli B, Fruscione F, Magnone M, Scarfi S, De Flora A, Zocchi E (2008) Abscisic acid is an endogenous stimulator of insulin release from human pancreatic islets with cyclic ADP ribose as second messenger. J Biol Chem **283:** 32188-32197

Bruzzone S, Moreschi I, Usai C, Guida L, Damonte G, Salis A, Scarfi S, Millo E, De Flora A, Zocchi E (2007) Abscisic acid is an endogenous cytokine in human granulocytes with cyclic ADP-ribose as second messenger. 10.1073/pnas.0609379104. Proceedings of the National Academy of Sciences **104:** 5759-5764

Busk PK, Pages M (1998) Regulation of abscisic acid-induced transcription. Plant Molecular Biology **37:** 425-435

Cheng SH, Willmann MR, Chen HC, Sheen J (2002) Calcium signaling through protein kinases. The Arabidopsis calcium-dependent protein kinase gene family. Plant Physiol **129:** 469-485

Cheng WH, Endo A, Zhou L, Penney J, Chen HC, Arroyo A, Leon P, Nambara E, Asami T, Seo M, Koshiba T, Sheen J (2002) A unique short-chain dehydrogenase/reductase in Arabidopsis glucose signaling and abscisic acid biosynthesis and functions. Plant Cell **14:** 2723-2743

Cherel I, Michard E, Platet N, Mouline K, Alcon C, Sentenac H, Thibaud JB (2002) Physical and functional interaction of the Arabidopsis K(+) channel AKT2 and phosphatase AtPP2CA. Plant Cell **14:** 1133-1146

Choi H, Hong J, Ha J, Kang J, Kim SY (2000) ABFs, a family of ABA-responsive element binding factors. J Biol Chem **275:** 1723-1730

Christmann A, Moes D, Himmelbach A, Yang Y, Tang Y, Grill E (2006) Integration of abscisic acid signalling into plant responses. Plant Biol (Stuttg) **8:** 314-325

Christmann A, Weiler EW, Steudle E, Grill E (2007) A hydraulic signal in root-to-shoot signalling of water shortage. Plant J **52:** 167-174

Cohen P (1989) The structure and regulation of protein phosphatases. Annu Rev Biochem **58:** 453-508

Cohen PT (1997) Novel protein serine/threonine phosphatases: variety is the spice of life. Trends Biochem Sci **22:** 245-251

Comisarow MB, Marshall AG (1974) Fourier transform ion cyclotron resonance spectroscopy. Chem Phys Lett **25:** 282-283

Cutler AJ, Krochko JE (1999) Formation and breakdown of ABA. Trends Plant Sci **4:** 472-478

Desikan R, Griffiths R, Hancock J, Neill S (2002) A new role for an old enzyme: nitrate reductase-mediated nitric oxide generation is required for abscisic acid-induced stomatal closure in Arabidopsis thaliana. Proc Natl Acad Sci U S A **99:** 16314-16318

Dharmasiri N, Dharmasiri S, Estelle M (2005) The F-box protein TIR1 is an auxin receptor. Nature **435:** 441-445

Dulski TR (1997) A Manual for the Chemical Analysis of Metals. American Society for Testing & Materials**:** p.106-107

Eisenreich W, Bacher A, Arigoni D, Rohdich F (2004) Biosynthesis of isoprenoids via the non-mevalonate pathway. Cellular and Molecular Life Sciences (CMLS) **61:** 1401-1426

Elhiti M, Stasolla C (2009) Structure and function of homodomain-leucine zipper (HD-Zip) proteins. Plant Signal Behav **4:** 86-88

Fernandes H, Bujacz A, Bujacz G, Jelen F, Jasinski M, Kachlicki P, Otlewski J, Sikorski MM, Jaskolski M (2009) Cytokinin-induced structural adaptability of a Lupinus luteus PR-10 protein. Febs J **276:** 1596-1609

Fernandes H, Pasternak O, Bujacz G, Bujacz A, Sikorski MM, Jaskolski M (2008) Lupinus luteus pathogenesis-related protein as a reservoir for cytokinin. J Mol Biol **378:** 1040-1051

Finkelstein RR, Gampala SS, Rock CD (2002) Abscisic acid signaling in seeds and seedlings. Plant Cell **14 Suppl:** S15-45

Finkelstein RR, Lynch TJ (2000) The *Arabidopsis* Abscisic Acid Response Gene *ABI5* Encodes a Basic Leucine Zipper Transcription Factor. Plant Cell **12:** 599-610

Finkelstein RR, Wang ML, Lynch TJ, Rao S, Goodman HM (1998) The *Arabidopsis* Abscisic Acid Response Locus *ABI4* Encodes an APETALA 2 Domain Protein. Plant Cell **10:** 1043-1054

Fujii H, Chinnusamy V, Rodrigues A, Rubio S, Antoni R, Park SY, Cutler SR, Sheen J, Rodriguez PL, Zhu JK (2009) In vitro reconstitution of an abscisic acid signalling pathway. Nature **462:** 660-664

Fujii H, Verslues PE, Zhu JK (2007) Identification of two protein kinases required for abscisic acid regulation of seed germination, root growth, and gene expression in Arabidopsis. Plant Cell **19:** 485-494

Fujii H, Zhu JK (2009) Arabidopsis mutant deficient in 3 abscisic acid-activated protein kinases reveals critical roles in growth, reproduction, and stress. Proc Natl Acad Sci U S A **106:** 8380-8385

Fujita Y, Fujita M, Satoh R, Maruyama K, Parvez MM, Seki M, Hiratsu K, Ohme-Takagi M, Shinozaki K, Yamaguchi-Shinozaki K (2005) AREB1 Is a transcription activator of novel ABRE-dependent ABA signaling that enhances drought stress tolerance in Arabidopsis. Plant Cell **17:** 3470-3488

Furihata T, Maruyama K, Fujita Y, Umezawa T, Yoshida R, Shinozaki K, Yamaguchi-Shinozaki K (2006) Abscisic acid-dependent multisite phosphorylation regulates the activity of a transcription activator AREB1. Proc Natl Acad Sci U S A **103:** 1988-1993

Gajhede M, Osmark P, Poulsen F, Ipsen H, Larsen J, Joost van Neerven R, Schou C, Lowenstein H, Spangfort M (1996) X-ray and NMR structure of Bet v 1, the origin of birch pollen allergy. Nat Struct Biol **3:** 1040 - 1045

Gambale F, Uozumi N (2006) Properties of shaker-type potassium channels in higher plants. J Membr Biol **210:** 1-19

Gao Y, Zeng Q, Guo J, Cheng J, Ellis BE, Chen J-G (2007) Genetic characterization reveals no role for the reported ABA receptor, GCR2, in ABA control of seed germination and early seedling development in Arabidopsis. Plant J **52:** 1001-1013

Garcia-Mata C, Lamattina L (2002) Nitric oxide and abscisic acid cross talk in guard cells. Plant Physiol **128:** 790-792

Gilroy S, Read ND, Trewavas AJ (1990) Elevation of cytoplasmic calcium by caged calcium or caged inositol triphosphate initiates stomatal closure. Nature **346:** 769-771

Gomez-Porras JL, Riano-Pachon DM, Dreyer I, Mayer JE, Mueller-Roeber B (2007) Genome-wide analysis of ABA-responsive elements ABRE and CE3 reveals divergent patterns in Arabidopsis and rice. BMC Genomics **8:** 260

Gonzalez-Guzman M, Apostolova N, Belles JM, Barrero JM, Piqueras P, Ponce MR, Micol JL, Serrano R, Rodriguez PL (2002) The short-chain alcohol dehydrogenase ABA2 catalyzes the conversion of xanthoxin to abscisic aldehyde. Plant Cell **14:** 1833-1846

Gosti F, Beaudoin N, Serizet C, Webb AA, Vartanian N, Giraudat J (1999) ABI1 protein phosphatase 2C is a negative regulator of abscisic acid signaling. Plant Cell **11:** 1897-1910

Gray WM, Kepinski S, Rouse D, Leyser O, Estelle M (2001) Auxin regulates SCF(TIR1)-dependent degradation of AUX/IAA proteins. Nature **414:** 271-276

Greenfield NJ (2006) Analysis of the kinetics of folding of proteins and peptides using circular dichroism. Nat Protoc **1:** 2891-2899

Greenfield NJ (2006) Determination of the folding of proteins as a function of denaturants, osmolytes or ligands using circular dichroism. Nat Protoc **1:** 2733-2741

Guo FQ, Okamoto M, Crawford NM (2003) Identification of a plant nitric oxide synthase gene involved in hormonal signaling. Science **302:** 100-103

Guo J, Zeng Q, Emami M, Ellis BE, Chen JG (2008) The GCR2 gene family is not required for ABA control of seed germination and early seedling development in Arabidopsis. PLoS ONE **3:** E2982

Haim GG, Tarrant B (1946) Colorimetric Determination of Nickel in Bronzes. Ind. Eng. Chem. Anal. Ed. **18:** 51-52

Hallouin M, Ghelis T, Brault M, Bardat F, Cornel D, Miginiac E, Rona JP, Sotta B, Jeannette E (2002) Plasmalemma abscisic acid perception leads to RAB18 expression via phospholipase D activation in Arabidopsis suspension cells. Plant Physiol **130:** 265-272

Han MH, Goud S, Song L, Fedoroff N (2004) The Arabidopsis double-stranded RNA-binding protein HYL1 plays a role in microRNA-mediated gene regulation. Proc Natl Acad Sci U S A **101:** 1093-1098

Harmon AC, Gribskov M, Harper JF (2000) CDPKs - a kinase for every Ca2+ signal? Trends Plant Sci **5:** 154-159

Himmelbach A, Hoffmann T, Leube M, Hohener B, Grill E (2002) Homeodomain protein ATHB6 is a target of the protein phosphatase ABI1 and regulates hormone responses in Arabidopsis. Embo J **21:** 3029-3038

Hirai N, Yoshida R, Todoroki Y, Ohigashi H (2000) Biosynthesis of abscisic acid by the non-mevalonate pathway in plants, and by the mevalonate pathway in fungi. Biosci Biotechnol Biochem **64:** 1448-1458

Hirayama T, Shinozaki K (2007) Perception and transduction of abscisic acid signals: keys to the function of the versatile plant hormone ABA. Trends Plant Sci **12:** 343-351

Hobo T, Asada M, Kowyama Y, Hattori T (1999) ACGT-containing abscisic acid response element (ABRE) and coupling element 3 (CE3) are functionally equivalent. Plant J **19:** 679-689

Hoffmann T (2002) Signaltransduktion von Abscisinsäure in *Arabidopsis thaliana*: Transiente Expression in Protoplasten als Modellsystem. Technische Universität, München

Hoth S, Morgante M, Sanchez JP, Hanafey MK, Tingey SV, Chua NH (2002) Genome-wide gene expression profiling in Arabidopsis thaliana reveals new targets of abscisic acid and largely impaired gene regulation in the abi1-1 mutant. J Cell Sci **115:** 4891-4900

Hrabak EM, Chan CW, Gribskov M, Harper JF, Choi JH, Halford N, Kudla J, Luan S, Nimmo HG, Sussman MR, Thomas M, Walker-Simmons K, Zhu JK, Harmon AC (2003) The Arabidopsis CDPK-SnRK superfamily of protein kinases. Plant Physiol **132:** 666-680

Hugouvieux V, Kwak JM, Schroeder JI (2001) An mRNA cap binding protein, ABH1, modulates early abscisic acid signal transduction in Arabidopsis. Cell **106:** 477-487

Hugouvieux V, Murata Y, Young JJ, Kwak JM, Mackesy DZ, Schroeder JI (2002) Localization, ion channel regulation, and genetic interactions during abscisic acid signaling of the nuclear mRNA cap-binding protein, ABH1. Plant Physiol **130:** 1276-1287

Illingworth CJR, Parkes KE, Snell CR, Mullineaux PM, Reynolds CA (2008) Criteria for confirming sequence periodicity identified by Fourier transform analysis: Application to GCR2, a candidate plant GPCR? Biophysical Chemistry **133:** 28-35

Israelsson M, Siegel RS, Young J, Hashimoto M, Iba K, Schroeder JI (2006) Guard cell ABA and CO2 signaling network updates and Ca2+ sensor priming hypothesis. Current Opinion in Plant Biology **9:** 654-663

Iuchi S, Kobayashi M, Taji T, Naramoto M, Seki M, Kato T, Tabata S, Kakubari Y, Yamaguchi-Shinozaki K, Shinozaki K (2001) Regulation of drought tolerance by gene manipulation of 9-cis-epoxycarotenoid dioxygenase, a key enzyme in abscisic acid biosynthesis in Arabidopsis. Plant J **27:** 325-333

Iyer LM, Koonin EV, Aravind L (2001) Adaptations of the helix-grip fold for ligand binding and catalysis in the START domain superfamily. Proteins **43:** 134-144

Jacob T, Ritchie S, Assmann SM, Gilroy S (1999) Abscisic acid signal transduction in guard cells is mediated by phospholipase D activity. Proc Natl Acad Sci U S A **96:** 12192-12197

Jadhav AS, Taylor DC, Giblin M, Ferrie AMR, Ambrose SJ, Ross ARS, Nelson KM, Irina Zaharia L, Sharma N, Anderson M, Fobert PR, Abrams SR (2008) Hormonal regulation of oil accumulation in Brassica seeds: Metabolism and biological activity of ABA, 7'-, 8'- and 9'-hydroxy ABA in microspore derived embryos of B. napus. Phytochemistry **69:** 2678-2688

Johnson RR, Wagner RL, Verhey SD, Walker-Simmons MK (2002) The abscisic acid-responsive kinase PKABA1 interacts with a seed-specific abscisic acid response element-binding factor, TaABF, and phosphorylates TaABF peptide sequences. Plant Physiol **130:** 837-846

Johnston CA, Temple BR, Chen JG, Gao Y, Moriyama EN, Jones AM, Siderovski DP, Willard FS (2007) Comment on "A G protein coupled receptor is a plasma membrane receptor for the plant hormone abscisic acid". Science **318:** 914; author reply 914

Kato-Noguchi H, Tanaka Y (2008) Effect of ABA-beta-D-glucopyranosyl ester and activity of ABA-beta-D-glucosidase in Arabidopsis thaliana. J Plant Physiol **165:** 788-790

Katsir L, Chung HS, Koo AJ, Howe GA (2008) Jasmonate signaling: a conserved mechanism of hormone sensing. Curr Opin Plant Biol **11:** 428-435

Kim K-N, Cheong YH, Grant JJ, Pandey GK, Luan S (2003) CIPK3, a Calcium Sensor-Associated Protein Kinase That Regulates Abscisic Acid and Cold Signal Transduction in Arabidopsis. Plant Cell **15:** 411-423

Kobayashi Y, Yamamoto S, Minami H, Kagaya Y, Hattori T (2004) Differential activation of the rice sucrose nonfermenting1-related protein kinase2 family by hyperosmotic stress and abscisic acid. Plant Cell **16:** 1163-1177

Koistinen K, Soininen P, Venalainen T, Hayrinen J, Laatikainen R, Perakyla M, Tervahauta A, Karenlampi S (2005) Birch PR-10c interacts with several biologically important ligands. Phytochemistry **66:** 2524 - 2533

Koncz C, Schell J (1986) The promoter of TL-DNA gene 5 controls the tissue-specific expression of chimaeric genes carried by a novel type of *Agrobacterium* binary vector. Molecular Genetics and Genomics **204:** 383-396

Koornneef M, Reuling G, Karssen CM (1984) The isolation and characterization of abscisic acid-insensitive mutants of *Arabidopsis thaliana*. Physiol Plant **61:** 377-383

Korte AS (2009) Identifizierung und Charakterisierung des Abscisinsäure-Responsregulators GCA2 in *Arabidopsis thaliana*. Technische Universität München

Kuhn JM, Boisson-Dernier A, Dizon MB, Maktabi MH, Schroeder JI (2006) The Protein Phosphatase AtPP2CA Negatively Regulates Abscisic Acid Signal Transduction in Arabidopsis, and Effects of abh1 on AtPP2CA mRNA. Plant Physiol **140:** 127-139

Kushiro T, Okamoto M, Nakabayashi K, Yamagishi K, Kitamura S, Asami T, Hirai N, Koshiba T, Kamiya Y, Nambara E (2004) The Arabidopsis cytochrome P450 CYP707A encodes ABA 8'-hydroxylases: key enzymes in ABA catabolism. Embo J **23:** 1647-1656

Kuzuyama T (2002) Mevalonate and nonmevalonate pathways for the biosynthesis of isoprene units. Biosci Biotechnol Biochem **66:** 1619-1627

Laemmli UK (1970) Cleavage of structural proteins during the assembly of the head of bacteriophage T4. Nature **227:** 680-685

Lebaudy A, Very AA, Sentenac H (2007) K+ channel activity in plants: genes, regulations and functions. FEBS Lett **581:** 2357-2366

Lee Y-H, Chun J-Y (1998) A new homeodomain-leucine zipper gene from *Arabidopsis thaliana* induced by water stress and abscisic acid treatment. Plant Molecular Biology **37:** 377-384

Lemtiri-Chlieh F, MacRobbie EA, Webb AA, Manison NF, Brownlee C, Skepper JN, Chen J, Prestwich GD, Brearley CA (2003) Inositol hexakisphosphate mobilizes an endomembrane store of calcium in guard cells. Proc Natl Acad Sci U S A **100:** 10091-10095

Leonhardt N, Kwak JM, Robert N, Waner D, Leonhardt G, Schroeder JI (2004) Microarray expression analyses of Arabidopsis guard cells and isolation of a recessive abscisic acid hypersensitive protein phosphatase 2C mutant. Plant Cell **16:** 596-615

Leube MP, Grill E, Amrhein N (1998) ABI1 of Arabidopsis is a protein serine/threonine phosphatase highly regulated by the proton and magnesium ion concentration. FEBS Lett **424:** 100-104

Leung J, Merlot S, Giraudat J (1997) The *Arabidopsis ABSCISIC ACID-INSENSITIVE2* (*ABI2*) and *ABI1* Genes Encode Homologous Protein Phosphatases 2C Involved in Abscisic Acid Signal Transduction. Plant Cell **9:** 759-771

Levchenko V, Konrad KR, Dietrich P, Roelfsema MR, Hedrich R (2005) Cytosolic abscisic acid activates guard cell anion channels without preceding Ca2+ signals. Proc Natl Acad Sci U S A **102:** 4203-4208

Li J, Wang XQ, Watson MB, Assmann SM (2000) Regulation of abscisic acid-induced stomatal closure and anion channels by guard cell AAPK kinase. Science **287:** 300-303

Li L, Masselon CD, Anderson GA, Pasa-Tolic L, Lee SW, Shen Y, Zhao R, Lipton MS, Conrads TP, Tolic N, Smith RD (2001) High-throughput peptide identification from protein digests using data-dependent multiplexed tandem FTICR mass spectrometry coupled with capillary liquid chromatography. Anal Chem **73:** 3312-3322

Lichtenthaler HK, Schwender J, Disch A, Rohmer M (1997) Biosynthesis of isoprenoids in higher plant chloroplasts proceeds via a mevalonate-independent pathway. FEBS Lett **400:** 271-274

Linsmaier EM, Skoog F (1965) Organic growth factor requirement of tobacco tissue cultures. Physiol Plant **18:** 100-127

Liu X, Yue Y, Li B, Nie Y, Li W, Wu WH, Ma L (2007) A G protein-coupled receptor is a plasma membrane receptor for the plant hormone abscisic acid. Science **315:** 1712-1716

Lorenzo O, Rodriguez D, Nicolas G, Rodriguez PL, Nicolas C (2001) A new protein phosphatase 2C (FsPP2C1) induced by abscisic acid is specifically expressed in dormant beechnut seeds. Plant Physiol **125:** 1949-1956

Lu C, Fedoroff N (2000) A mutation in the Arabidopsis HYL1 gene encoding a dsRNA binding protein affects responses to abscisic acid, auxin, and cytokinin. Plant Cell **12:** 2351-2366

Luan S, Kudla J, Rodriguez-Concepcion M, Yalovsky S, Gruissem W (2002) Calmodulins and calcineurin B-like proteins: calcium sensors for specific signal response coupling in plants. Plant Cell **14 Suppl:** S389-400

Luehrsen KR, De Wet JR, Walbot V (1992) Transient expression analysis in plants using firefly luciferase reporter gene. Methods Enzymol **216:** 397-414

Lytle BL, Song J, de la Cruz NB, Peterson FC, Johnson KA, Bingman CA, Phillips GN, Jr., Volkman BF (2009) Structures of two Arabidopsis thaliana major latex proteins represent novel helix-grip folds. Proteins **76:** 237-243

Ma Y (2010) Regulation of the abscisic acid response by protein phosphatase 2C-interacting proteins ABP7 and ABP9 in *Arabidopsis thaliana*. Technische Universität München

Ma Y, Szostkiewicz I, Korte A, Moes D, Yang Y, Christmann A, Grill E (2009) Regulators of PP2C phosphatase activity function as abscisic acid sensors. Science **324:** 1064-1068

Magnone M, Bruzzone S, Guida L, Damonte G, Millo E, Scarfi S, Usai C, Sturla L, Palombo D, De Flora A, Zocchi E (2009) Abscisic acid released by human monocytes activates monocytes and vascular smooth muscle cell responses involved in atherogenesis. J Biol Chem **284:** 17808-17818

Mano N, Goto J (2003) Biomedical and biological mass spectrometry. Anal Sci **19:** 3-14

Marcotte Jr WR, Russell SH, Quatrano RS (1989) Abscisic Acid-Responsive Sequences from the Em Gene of Wheat. Plant Cell **1:** 969-976

Marin E, Nussaume L, Quesada A, Gonneau M, Sotta B, Hugueney P, Frey A, Marion-Poll A (1996) Molecular identification of zeaxanthin epoxidase of Nicotiana plumbaginifolia, a gene involved in abscisic acid biosynthesis and corresponding to the ABA locus of Arabidopsis thaliana. Embo J **15:** 2331-2342

Markovic-Housley Z, Degano M, Lamba D, von Roepenack-Lahaye E, Clemens S, Susani M, Ferreira F, Scheiner O, Breiteneder H (2003) Crystal structure of a hypoallergenic isoform of the major birch pollen allergen Bet v 1 and its likely biological function as a plant steroid carrier. J Mol Biol **325:** 123-133

Marshall AG, Hendrickson CL, Jackson GS (1998) Fourier transform ion cyclotron resonance mass spectrometry: a primer. Mass Spectrom Rev **17:** 1-35

Mattila K, Renkonen R (2009) Modelling of Bet v 1 binding to lipids. Scand J Immunol **70:** 116-124

McCourt P, Creelman R (2008) The ABA receptors -- we report you decide. Curr Opin Plant Biol **11:** 474-478

Meinhard M, Grill E (2001) Hydrogen peroxide is a regulator of ABI1, a protein phosphatase 2C from Arabidopsis. FEBS Lett **508:** 443-446

Meinhard M, Rodriguez PL, Grill E (2002) The sensitivity of ABI2 to hydrogen peroxide links the abscisic acid-response regulator to redox signalling. Planta **214:** 775-782

Melcher K, Ng LM, Zhou XE, Soon FF, Xu Y, Suino-Powell KM, Park SY, Weiner JJ, Fujii H, Chinnusamy V, Kovach A, Li J, Wang Y, Peterson FC, Jensen DR, Yong EL, Volkman BF, Cutler SR, Zhu JK, Xu HE (2009) A gate-latch-lock mechanism for hormone signalling by abscisic acid receptors. Nature **462:** 602-608

Melotto M, Underwood W, Koczan J, Nomura K, He SY (2006) Plant Stomata Function in Innate Immunity against Bacterial Invasion. Cell **126:** 969-980

Merlot S, Gosti F, Guerrier D, Vavasseur A, Giraudat J (2001) The ABI1 and ABI2 protein phosphatases 2C act in a negative feedback regulatory loop of the abscisic acid signalling pathway. Plant J **25:** 295-303

Meyer K, Leube MP, Grill E (1994) A protein phosphatase 2C involved in ABA signal transduction in Arabidopsis thaliana. Science **264:** 1452-1455

Miao Y, Lv D, Wang P, Wang XC, Chen J, Miao C, Song CP (2006) An Arabidopsis glutathione peroxidase functions as both a redox transducer and a scavenger in abscisic acid and drought stress responses. Plant Cell **18:** 2749-2766

Michalska K, Fernandes H, Sikorski M, Jaskolski M (2010) Crystal structure of Hyp-1, a St. John's wort protein implicated in the biosynthesis of hypericin. J Struct Biol **169:** 161-171

Miyazono K, Miyakawa T, Sawano Y, Kubota K, Kang HJ, Asano A, Miyauchi Y, Takahashi M, Zhi Y, Fujita Y, Yoshida T, Kodaira KS, Yamaguchi-Shinozaki K, Tanokura M (2009) Structural basis of abscisic acid signalling. Nature **462:** 609-614

Moes D, Himmelbach A, Korte A, Haberer G, Grill E (2008) Nuclear localization of the mutant protein phosphatase abi1 is required for insensitivity towards ABA responses in Arabidopsis. Plant J **54:** 806-819

Mogensen JE, Wimmer R, Larsen JN, Spangfort MD, Otzen DE (2002) The major birch allergen, Bet v 1, shows affinity for a broad spectrum of physiological ligands. J Biol Chem **277:** 23684-23692

Mok DW, Mok MC (2001) Cytokinin Metabolism and Action. Annu Rev Plant Physiol Plant Mol Biol **52:** 89-118

Mori IC, Murata Y, Yang Y, Munemasa S, Wang YF, Andreoli S, Tiriac H, Alonso JM, Harper JF, Ecker JR, Kwak JM, Schroeder JI (2006) CDPKs CPK6 and CPK3 function in ABA regulation of guard cell S-type anion- and Ca(2+)-permeable channels and stomatal closure. PLoS Biol **4:** e327

Müller AH, Hansson M (2009) The barley magnesium chelatase 150-kD subunit is not an abscisic acid receptor. Plant Physiol **150:** 157-166

Mundy J, Yamaguchi-Shinozaki K, Chua NH (1990) Nuclear proteins bind conserved elements in the abscisic acid-responsive promoter of a rice rab gene. Proc Natl Acad Sci U S A **87:** 1406-1410

Murase K, Hirano Y, Sun TP, Hakoshima T (2008) Gibberellin-induced DELLA recognition by the gibberellin receptor GID1. Nature **456:** 459-463

Murashige T, Skoog F (1962) A revised medium for rapid growth and bioassay with tobacco tissue culture. Physiol Plant **15:** 473-497

Murray MG, Thompson WF (1980) Rapid isolation of high molecular weight plant DNA. Nucleic Acids Res **8:** 4321-4325

Mustilli AC, Merlot S, Vavasseur A, Fenzi F, Giraudat J (2002) Arabidopsis OST1 protein kinase mediates the regulation of stomatal aperture by abscisic acid and acts upstream of reactive oxygen species production. Plant Cell **14:** 3089-3099

Nakamura S, Lynch TJ, Finkelstein RR (2001) Physical interactions between ABA response loci of Arabidopsis. Plant J **26:** 627-635

Nakashima K, Fujita Y, Kanamori N, Katagiri T, Umezawa T, Kidokoro S, Maruyama K, Yoshida T, Ishiyama K, Kobayashi M, Shinozaki K, Yamaguchi-Shinozaki K (2009) Three Arabidopsis SnRK2 protein kinases, SRK2D/SnRK2.2, SRK2E/SnRK2.6/OST1 and SRK2I/SnRK2.3, involved in ABA signaling are essential for the control of seed development and dormancy. Plant Cell Physiol **50:** 1345-1363

Nambara E, Marion-Poll A (2005) Abscisic acid biosynthesis and catabolism. Annu Rev Plant Biol **56:** 165-185

Nambara E, Suzuki M, Abrams S, McCarty DR, Kamiya Y, McCourt P (2002) A screen for genes that function in abscisic acid signaling in Arabidopsis thaliana. Genetics **161:** 1247-1255

Narusaka Y, Nakashima K, Shinwari ZK, Sakuma Y, Furihata T, Abe H, Narusaka M, Shinozaki K, Yamaguchi-Shinozaki K (2003) Interaction between two cis-acting elements, ABRE and DRE, in ABA-dependent expression of Arabidopsis rd29A gene in response to dehydration and high-salinity stresses. Plant J **34:** 137-148

Neill SJ, Desikan R, Clarke A, Hancock JT (2002) Nitric oxide is a novel component of abscisic acid signaling in stomatal guard cells. Plant Physiol **128:** 13-16

Nemhauser JL, Hong F, Chory J (2006) Different plant hormones regulate similar processes through largely nonoverlapping transcriptional responses. Cell **126:** 467-475

Neudecker P, Schweimer K, Nerkamp J, Scheurer S, Vieths S, Sticht H, Rosch P (2001) Allergic cross-reactivity made visible: solution structure of the major cherry allergen Pru av 1. J Biol Chem **276:** 22756 - 22763

Nishimura N, Hitomi K, Arvai AS, Rambo RP, Hitomi C, Cutler SR, Schroeder JI, Getzoff ED (2009) Structural mechanism of abscisic acid binding and signaling by dimeric PYR1. Science **326:** 1373-1379

Nishimura N, Sarkeshik A, Nito K, Park SY, Wang A, Carvalho PC, Lee S, Caddell DF, Cutler SR, Chory J, Yates JR, Schroeder JI (2010) PYR/PYL/RCAR family members are major in-vivo ABI1 protein phosphatase 2C-interacting proteins in Arabidopsis. Plant J **61:** 290-299

Nishimura N, Yoshida T, Kitahata N, Asami T, Shinozaki K, Hirayama T (2007) ABA-Hypersensitive Germination1 encodes a protein phosphatase 2C, an essential component of abscisic acid signaling in Arabidopsis seed. Plant J **50:** 935-949

Nishimura N, Yoshida T, Murayama M, Asami T, Shinozaki K, Hirayama T (2004) Isolation and characterization of novel mutants affecting the abscisic acid sensitivity of Arabidopsis germination and seedling growth. Plant Cell Physiol **45:** 1485-1499

North HM, De Almeida A, Boutin JP, Frey A, To A, Botran L, Sotta B, Marion-Poll A (2007) The Arabidopsis ABA-deficient mutant aba4 demonstrates that the major route for stress-induced ABA accumulation is via neoxanthin isomers. Plant J **50:** 810-824

Nylander M, Svensson J, Palva ET, Welin BV (2001) Stress-induced accumulation and tissue-specific localization of dehydrins in Arabidopsis thaliana. Plant Mol Biol **45:** 263-279

Ohkuma K, Lyon JL, Addicott FT, Smith OE (1963) Abscisin II, an Abscission-Accelerating Substance from Young Cotton Fruit. Science **142:** 1592-1593

Ohta M, Guo Y, Halfter U, Zhu JK (2003) A novel domain in the protein kinase SOS2 mediates interaction with the protein phosphatase 2C ABI2. Proc Natl Acad Sci U S A **100:** 11771-11776

Outlaw WHJ (2003) Integration of cellular and physiological functions of guard cells. Crit Rev Plant Sci **22:** 503-529

Page JS, Masselon CD, Smith RD (2004) FTICR mass spectrometry for qualitative and quantitative bioanalyses. Curr Opin Biotechnol **15:** 3-11

Pandey GK, Cheong YH, Kim KN, Grant JJ, Li L, Hung W, D'Angelo C, Weinl S, Kudla J, Luan S (2004) The calcium sensor calcineurin B-like 9 modulates abscisic acid sensitivity and biosynthesis in Arabidopsis. Plant Cell **16:** 1912-1924

Pandey S, Nelson DC, Assmann SM (2009) Two novel GPCR-type G proteins are abscisic acid receptors in Arabidopsis. Cell **136:** 136-148

Pandey S, Zhang W, Assmann SM (2007) Roles of ion channels and transporters in guard cell signal transduction. FEBS Letters Plant Transporters and Channels **581:** 2325-2336

Parcy F, Valon C, Raynal M, Gaubier-Comella P, Delseny M, Giraudat J (1994) Regulation of gene expression programs during Arabidopsis seed development: roles of the ABI3 locus and of endogenous abscisic acid. Plant Cell **6:** 1567-1582

Park SY, Fung P, Nishimura N, Jensen DR, Fujii H, Zhao Y, Lumba S, Santiago J, Rodrigues A, Chow TF, Alfred SE, Bonetta D, Finkelstein R, Provart NJ, Desveaux D, Rodriguez PL, McCourt P, Zhu JK, Schroeder JI, Volkman BF, Cutler SR (2009) Abscisic acid inhibits type 2C protein phosphatases via the PYR/PYL family of START proteins. Science **324:** 1068-1071

Pasternak O, Biesiadka J, Dolot R, Handschuh L, Bujacz G, Sikorski MM, Jaskolski M (2005) Structure of a yellow lupin pathogenesis-related PR-10 protein belonging to a novel subclass. Acta Crystallogr D Biol Crystallogr **61:** 99-107

Pasternak O, Bujacz GD, Fujimoto Y, Hashimoto Y, Jelen F, Otlewski J, Sikorski MM, Jaskolski M (2006) Crystal structure of Vigna radiata cytokinin-specific binding protein in complex with zeatin. Plant Cell **18:** 2622-2634

Pei ZM, Ghassemian M, Kwak CM, McCourt P, Schroeder JI (1998) Role of farnesyltransferase in ABA regulation of guard cell anion channels and plant water loss. Science **282:** 287-290

Pei ZM, Kuchitsu K, Ward JM, Schwarz M, Schroeder JI (1997) Differential abscisic acid regulation of guard cell slow anion channels in *Arabidopsis* wild-type and *abi1* and *abi2* mutants. Plant Cell **9:** 409-423

Peng J, Carol P, Richards DE, King KE, Cowling RJ, Murphy GP, Harberd NP (1997) The Arabidopsis GAI gene defines a signaling pathway that negatively regulates gibberellin responses. Genes Dev **11:** 3194-3205

Perera IY, Hung CY, Moore CD, Stevenson-Paulik J, Boss WF (2008) Transgenic Arabidopsis plants expressing the type 1 inositol 5-phosphatase exhibit increased drought tolerance and altered abscisic acid signaling. Plant Cell **20:** 2876-2893

Pierce MM, Raman CS, Nall BT (1999) Isothermal titration calorimetry of protein-protein interactions. Methods **19:** 213-221

Priest DM, Ambrose SJ, Vaistij FE, Elias L, Higgins GS, Ross AR, Abrams SR, Bowles DJ (2006) Use of the glucosyltransferase UGT71B6 to disturb abscisic acid homeostasis in Arabidopsis thaliana. Plant J **46:** 492-502

Pysh LD, Wysocka-Diller JW, Camilleri C, Bouchez D, Benfey PN (1999) The GRAS gene family in Arabidopsis: sequence characterization and basic expression analysis of the SCARECROW-LIKE genes. Plant J **18:** 111-119

Qin X, Zeevaart JA (1999) The 9-cis-epoxycarotenoid cleavage reaction is the key regulatory step of abscisic acid biosynthesis in water-stressed bean. Proc Natl Acad Sci U S A **96:** 15354-15361

Radauer C, Lackner P, Breiteneder H (2008) The Bet v 1 fold: an ancient, versatile scaffold for binding of large, hydrophobic ligands. BMC Evolutionary Biology **8:** 286

Ramagli L, Rodriguez, L. V., (1985) Quantitation of microgram amounts of protein in two-dimensional polyacrylamide gel electrophoresis sample buffer. Electrophoresis **6:** 559-563

Risk JM, Day CL, Macknight RC (2009) Reevaluation of Abscisic Acid-Binding Assays Shows That G-Protein-Coupled Receptor2 Does Not Bind Abscisic Acid. Plant Physiol. **150:** 6-11

Risk JM, Macknight RC, Day CL (2008) FCA does not bind abscisic acid. Nature **456:** E5-E6

Ritchie S, Gilroy S (1998) Abscisic acid signal transduction in the barley aleurone is mediated by phospholipase D activity. Proc Natl Acad Sci U S A **95:** 2697-2702

Robert N, Merlot S, N'Guyen V, Boisson-Dernier A, Schroeder JI (2006) A hypermorphic mutation in the protein phosphatase 2C HAB1 strongly affects ABA signaling in Arabidopsis. FEBS Lett **580:** 4691-4696

Rubio S, Rodrigues A, Saez A, Dizon MB, Galle A, Kim TH, Santiago J, Flexas J, Schroeder JI, Rodriguez PL (2009) Triple loss of function of protein phosphatases type 2C leads to partial constitutive response to endogenous abscisic acid. Plant Physiol **150:** 1345-1355

Saavedra X, Modrego A, Rodriguez D, Gonzalez-Garcia MP, Sanz L, Nicolas G, Lorenzo O (2010) The nuclear interactor PYL8/RCAR3 of Fagus sylvatica

FsPP2C1 is a positive regulator of abscisic acid signaling in seeds and stress. Plant Physiol **152:** 133-150

Saez A, Apostolova N, Gonzalez-Guzman M, Gonzalez-Garcia MP, Nicolas C, Lorenzo O, Rodriguez PL (2004) Gain-of-function and loss-of-function phenotypes of the protein phosphatase 2C HAB1 reveal its role as a negative regulator of abscisic acid signalling. Plant J **37:** 354-369

Saez A, Robert N, Maktabi MH, Schroeder JI, Serrano R, Rodriguez PL (2006) Enhancement of Abscisic Acid Sensitivity and Reduction of Water Consumption in *Arabidopsis* by Combined Inactivation of the Protein Phosphatases Type 2C ABI1 and HAB1. Plant Physiol. **141:** 1389-1399

Saez A, Rodrigues A, Santiago J, Rubio S, Rodriguez PL (2008) HAB1-SWI3B interaction reveals a link between abscisic acid signaling and putative SWI/SNF chromatin-remodeling complexes in Arabidopsis. Plant Cell **20:** 2972-2988

Saito S, Hirai N, Matsumoto C, Ohigashi H, Ohta D, Sakata K, Mizutani M (2004) Arabidopsis CYP707As encode (+)-abscisic acid 8'-hydroxylase, a key enzyme in the oxidative catabolism of abscisic acid. Plant Physiol **134:** 1439-1449

Sanders D, Pelloux J, Brownlee C, Harper JF (2002) Calcium at the crossroads of signaling. Plant Cell **14 Suppl:** S401-417

Santiago J, Dupeux F, Round A, Antoni R, Park SY, Jamin M, Cutler SR, Rodriguez PL, Marquez JA (2009) The abscisic acid receptor PYR1 in complex with abscisic acid. Nature **462:** 665-668

Santiago J, Rodrigues A, Saez A, Rubio S, Antoni R, Dupeux F, Park SY, Marquez JA, Cutler SR, Rodriguez PL (2009) Modulation of drought resistance by the abscisic acid receptor PYL5 through inhibition of clade A PP2Cs. Plant J **60:** 575-588

Santner A, Estelle M (2009) Recent advances and emerging trends in plant hormone signalling. Nature **459:** 1071-1078

Sato A, Sato Y, Fukao Y, Fujiwara M, Umezawa T, Shinozaki K, Hibi T, Taniguchi M, Miyake H, Goto DB, Uozumi N (2009) Threonine at position 306 of the KAT1 potassium channel is essential for channel activity and is a target site for ABA-activated SnRK2/OST1/SnRK2.6 protein kinase. Biochem J **424:** 439-448

Scarfi S, Fresia C, Ferraris C, Bruzzone S, Fruscione F, Usai C, Benvenuto F, Magnone M, Podesta M, Sturla L, Guida L, Albanesi E, Damonte G, Salis A, De Flora A, Zocchi E (2009) The plant hormone abscisic acid stimulates the proliferation of human hemopoietic progenitors through the second messenger cyclic ADP-ribose. Stem Cells **27:** 2469-2477

Schroeder JI, Nambara E (2006) A quick release mechanism for abscisic acid. Cell **126:** 1023-1025

Schwartz SH, Leon-Kloosterziel KM, Koornneef M, Zeevaart JA (1997) Biochemical characterization of the aba2 and aba3 mutants in Arabidopsis thaliana. Plant Physiol **114:** 161-166

Schwartz SH, Qin X, Zeevaart JA (2001) Characterization of a novel carotenoid cleavage dioxygenase from plants. J Biol Chem **276:** 25208-25211

Schweighofer A, Hirt H, Meskiene I (2004) Plant PP2C phosphatases: emerging functions in stress signaling. Trends Plant Sci **9:** 236-243

Seo M, Peeters AJ, Koiwai H, Oritani T, Marion-Poll A, Zeevaart JA, Koornneef M, Kamiya Y, Koshiba T (2000) The Arabidopsis aldehyde oxidase 3 (AAO3) gene

product catalyzes the final step in abscisic acid biosynthesis in leaves. Proc Natl Acad Sci U S A **97:** 12908-12913

Sheard LB, Zheng N (2009) Plant biology: Signal advance for abscisic acid. Nature **462:** 575-576

Sheen J (1998) Mutational analysis of protein phosphatase 2C involved in abscisic acid signal transduction in higher plants. Proc Natl Acad Sci U S A **95:** 975-980

Shen Q, Zhang P, Ho T (1996) Modular Nature of Abscisic Acid (ABA) Response Complexes: Composite Promoter Units That Are Necessary and Sufficient for ABA Induction of Gene Expression in Barley. Plant Cell **8:** 1107-1119

Shen YY, Wang XF, Wu FQ, Du SY, Cao Z, Shang Y, Wang XL, Peng CC, Yu XC, Zhu SY, Fan RC, Xu YH, Zhang DP (2006) The Mg-chelatase H subunit is an abscisic acid receptor. Nature **443:** 823-826

Shi Y (2009) Serine/threonine phosphatases: mechanism through structure. Cell **139:** 468-484

Shimada A, Ueguchi-Tanaka M, Nakatsu T, Nakajima M, Naoe Y, Ohmiya H, Kato H, Matsuoka M (2008) Structural basis for gibberellin recognition by its receptor GID1. Nature **456:** 520-523

Siegel RS, Xue S, Murata Y, Yang Y, Nishimura N, Wang A, Schroeder JI (2009) Calcium elevation-dependent and attenuated resting calcium-dependent abscisic acid induction of stomatal closure and abscisic acid-induced enhancement of calcium sensitivities of S-type anion and inward-rectifying K channels in Arabidopsis guard cells. Plant J **59:** 207-220

Sirichandra C, Wasilewska A, Vlad F, Valon C, Leung J (2009) The guard cell as a single-cell model towards understanding drought tolerance and abscisic acid action. J. Exp. Bot. **60:** 1439-1463

Staxen II, Pical C, Montgomery LT, Gray JE, Hetherington AM, McAinsh MR (1999) Abscisic acid induces oscillations in guard-cell cytosolic free calcium that involve phosphoinositide-specific phospholipase C. Proc Natl Acad Sci U S A **96:** 1779-1784

Suzuki H, Park SH, Okubo K, Kitamura J, Ueguchi-Tanaka M, Iuchi S, Katoh E, Kobayashi M, Yamaguchi I, Matsuoka M, Asami T, Nakajima M (2009) Differential expression and affinities of Arabidopsis gibberellin receptors can explain variation in phenotypes of multiple knock-out mutants. Plant J **60:** 48-55

Szostkiewicz I, Richter K, Kepka M, Demmel S, Ma Y, Korte A, Assaad FF, Christmann A, Grill E (2010) Closely related receptor complexes differ in their ABA selectivity and sensitivity. Plant J **61:** 25-35

Tamura K, Dudley J, Nei M, Kumar S (2007) MEGA4: Molecular Evolutionary Genetics Analysis (MEGA) software version 4.0. Mol Biol Evol **24:** 1596-1599

Tan X, Calderon-Villalobos LI, Sharon M, Zheng C, Robinson CV, Estelle M, Zheng N (2007) Mechanism of auxin perception by the TIR1 ubiquitin ligase. Nature **446:** 640-645

Tang RH, Han S, Zheng H, Cook CW, Choi CS, Woerner TE, Jackson RB, Pei ZM (2007) Coupling diurnal cytosolic Ca2+ oscillations to the CAS-IP3 pathway in Arabidopsis. Science **315:** 1423-1426

Thompson AJ, Jackson AC, Symonds RC, Mulholland BJ, Dadswell AR, Blake PS, Burbidge A, Taylor IB (2000) Ectopic expression of a tomato 9-cis-epoxycarotenoid dioxygenase gene causes over-production of abscisic acid. Plant J **23:** 363-374

Tsujishita Y, Hurley JH (2000) Structure and lipid transport mechanism of a StAR-related domain. Nat Struct Biol **7:** 408-414

Tuteja N, Mahajan S (2007) Calcium signaling network in plants: an overview. Plant Signal Behav **2:** 79-85

Ueguchi-Tanaka M, Nakajima M, Katoh E, Ohmiya H, Asano K, Saji S, Hongyu X, Ashikari M, Kitano H, Yamaguchi I, Matsuoka M (2007) Molecular interactions of a soluble gibberellin receptor, GID1, with a rice DELLA protein, SLR1, and gibberellin. Plant Cell **19:** 2140-2155

Unneberg P, Merelo JJ, Chacón P, Morán F (2001) SOMCD: Method for evaluating protein secondary structure from UV circular dichroism spectra. Proteins: Structure, Function, and Genetics. **42:** 460-470

Uno Y, Furihata T, Abe H, Yoshida R, Shinozaki K, Yamaguchi-Shinozaki K (2000) Arabidopsis basic leucine zipper transcription factors involved in an abscisic acid-dependent signal transduction pathway under drought and high-salinity conditions. Proc Natl Acad Sci U S A **97:** 11632-11637

Vahisalu T, Kollist H, Wang YF, Nishimura N, Chan WY, Valerio G, Lamminmaki A, Brosche M, Moldau H, Desikan R, Schroeder JI, Kangasjarvi J (2008) SLAC1 is required for plant guard cell S-type anion channel function in stomatal signalling. Nature **452:** 487-491

van Loon L, Rep M, Pieterse C (2006) Significance of inducible defense-related proteins in infected plants. Annu Rev Phytopathol **44:** 135 - 162

Veenstra TD, Yates JR (2006) Proteomics for Biological Discovery.

Vlad F, Rubio S, Rodrigues A, Sirichandra C, Belin C, Robert N, Leung J, Rodriguez PL, Lauriere C, Merlot S (2009) Protein phosphatases 2C regulate the activation of the Snf1-related kinase OST1 by abscisic acid in Arabidopsis. Plant Cell **21:** 3170-3184

Vranova E, Tahtiharju S, Sriprang R, Willekens H, Heino P, Palva ET, Inze D, Van Camp W (2001) The AKT3 potassium channel protein interacts with the AtPP2CA protein phosphatase 2C. J Exp Bot **52:** 181-182

Walter M, Chaban C, Schutze K, Batistic O, Weckermann K, Nake C, Blazevic D, Grefen C, Schumacher K, Oecking C, Harter K, Kudla J (2004) Visualization of protein interactions in living plant cells using bimolecular fluorescence complementation. Plant J **40:** 428-438

Wang X, Kota U, He K, Blackburn K, Li J, Goshe MB, Huber SC, Clouse SD (2008) Sequential transphosphorylation of the BRI1/BAK1 receptor kinase complex impacts early events in brassinosteroid signaling. Dev Cell **15:** 220-235

Wasilewska A, Vlad F, Sirichandra C, Redko Y, Jammes F, Valon C, Frey NFd, Leung J (2008) An Update on Abscisic Acid Signaling in Plants and More. Mol Plant **1:** 198-217

Weinl S, Kudla J (2009) The CBL-CIPK Ca(2+)-decoding signaling network: function and perspectives. New Phytol **184:** 517-528

Wells JM, McLuckey SA (2005) Collision-induced dissociation (CID) of peptides and proteins. Methods Enzymol **402:** 148-185

Wong C, Sridhara S, Bardwell JCA, Jakob U (2000) Heating Greatly Speeds Coomassie Blue Staining and Destaining. BioTechniques **28:** 426-432

Xiong L, Gong Z, Rock CD, Subramanian S, Guo Y, Xu W, Galbraith D, Zhu JK (2001) Modulation of abscisic acid signal transduction and biosynthesis by an Sm-like protein in Arabidopsis. Dev Cell **1:** 771-781

Xiong L, Lee H, Ishitani M, Zhu JK (2002) Regulation of osmotic stress-responsive gene expression by the LOS6/ABA1 locus in Arabidopsis. J Biol Chem **277:** 8588-8596

Xue T, Wang D, Zhang S, Ehlting J, Ni F, Jakab S, Zheng C, Zhong Y (2008) Genome-wide and expression analysis of protein phosphatase 2C in rice and Arabidopsis. BMC Genomics **9:** 550

Yamaguchi-Shinozaki K, Shinozaki K (1994) A novel cis-acting element in an Arabidopsis gene is involved in responsiveness to drought, low-temperature, or high-salt stress. Plant Cell **6:** 251-264

Yamaguchi-Shinozaki K, Shinozaki K (2006) Transcriptional Regulatory Networks in Cellular Responses and Tolerance to Dehydration and Cold Stresses. Annu Rev Plant Biol **57:** 781-803

Yamamoto H, Inomata M, Tsuchiya S, Nakamura M, Uchiyama T, Oritani T (2000) Early Biosynthetic Pathway to Abscisic Acid in Cercospora cruenta. Bioscience, Biotechnology, and Biochemistry **64:** 2075-2082

Yang Y (2003) Signal transduction of abscisic acid in *Arabidopsis thaliana*: Identification and characterisation of protein interaction partners of ABI2. Technische Universität München

Yang Y, Sulpice R, Himmelbach A, Meinhard M, Christmann A, Grill E (2006) Fibrillin expression is regulated by abscisic acid response regulators and is involved in abscisic acid-mediated photoprotection. Proc Natl Acad Sci U S A **103:** 6061-6066

Yin P, Fan H, Hao Q, Yuan X, Wu D, Pang Y, Yan C, Li W, Wang J, Yan N (2009) Structural insights into the mechanism of abscisic acid signaling by PYL proteins. Nat Struct Mol Biol **16:** 1230-1236

Yoshida R, Hobo T, Ichimura K, Mizoguchi T, Takahashi F, Aronso J, Ecker JR, Shinozaki K (2002) ABA-activated SnRK2 protein kinase is required for dehydration stress signaling in Arabidopsis. Plant Cell Physiol **43:** 1473-1483

Yoshida R, Umezawa T, Mizoguchi T, Takahashi S, Takahashi F, Shinozaki K (2006) The regulatory domain of SRK2E/OST1/SnRK2.6 interacts with ABI1 and integrates abscisic acid (ABA) and osmotic stress signals controlling stomatal closure in Arabidopsis. J Biol Chem **281:** 5310-5318

Yoshida T, Fujita Y, Sayama H, Maruyama K, Mizoi J, Shinozaki K, Yamaguchi-Shinozaki K (2009) AREB1, AREB2, and ABF3 are master transcription factors that cooperatively regulate ABRE-dependent ABA signaling involved in drought stress tolerance and require ABA for full activation. Plant J (ahead of print)

Yoshida T, Nishimura N, Kitahata N, Kuromori T, Ito T, Asami T, Shinozaki K, Hirayama T (2006) ABA-Hypersensitive Germination3 Encodes a Protein Phosphatase 2C (AtPP2CA) That Strongly Regulates Abscisic Acid Signaling during Germination among Arabidopsis Protein Phosphatase 2Cs. Plant Physiol **140:** 115-126

Young JJ, Mehta S, Israelsson M, Godoski J, Grill E, Schroeder JI (2006) CO2 signaling in guard cells: Calcium sensitivity response modulation, a Ca2+-independent phase, and CO2 insensitivity of the *gca2* mutant. PNAS **103:** 7506-7511

Zalejski C, Zhang Z, Quettier AL, Maldiney R, Bonnet M, Brault M, Demandre C, Miginiac E, Rona JP, Sotta B, Jeannette E (2005) Diacylglycerol pyrophosphate is a second messenger of abscisic acid signaling in Arabidopsis thaliana suspension cells. Plant J **42:** 145-152

Zawadzki P, Slosarek G, Boryski J, Wojtaszek P (2010) A fluorescence correlation spectroscopy study of ligand interaction with cytokinin-specific binding protein from mung bean. Biol Chem **391:** 43-53

Zhang S, Cai Z, Wang X (2009) The primary signaling outputs of brassinosteroids are regulated by abscisic acid signaling. Proc Natl Acad Sci U S A **106:** 4543-4548

Zhang W, Qin C, Zhao J, Wang X (2004) Phospholipase D alpha 1-derived phosphatidic acid interacts with ABI1 phosphatase 2C and regulates abscisic acid signaling. Proc Natl Acad Sci U S A **101:** 9508-9513

Zhu SY, Yu XC, Wang XJ, Zhao R, Li Y, Fan RC, Shang Y, Du SY, Wang XF, Wu FQ, Xu YH, Zhang XY, Zhang DP (2007) Two calcium-dependent protein kinases, CPK4 and CPK11, regulate abscisic acid signal transduction in Arabidopsis. Plant Cell **19:** 3019-3036

Zimmermann P, Hennig L, Gruissem W (2005) Gene-expression analysis and network discovery using Genevestigator. Trends Plant Sci. **10:** 401-409

Appendix

Sequence alignment of six protein phosphatases 2C from clade A (top) and RCAR protein family (bottom).

Alignment was performed with MultAlin program. Red colour indicate high consensus, while blue low consensus.
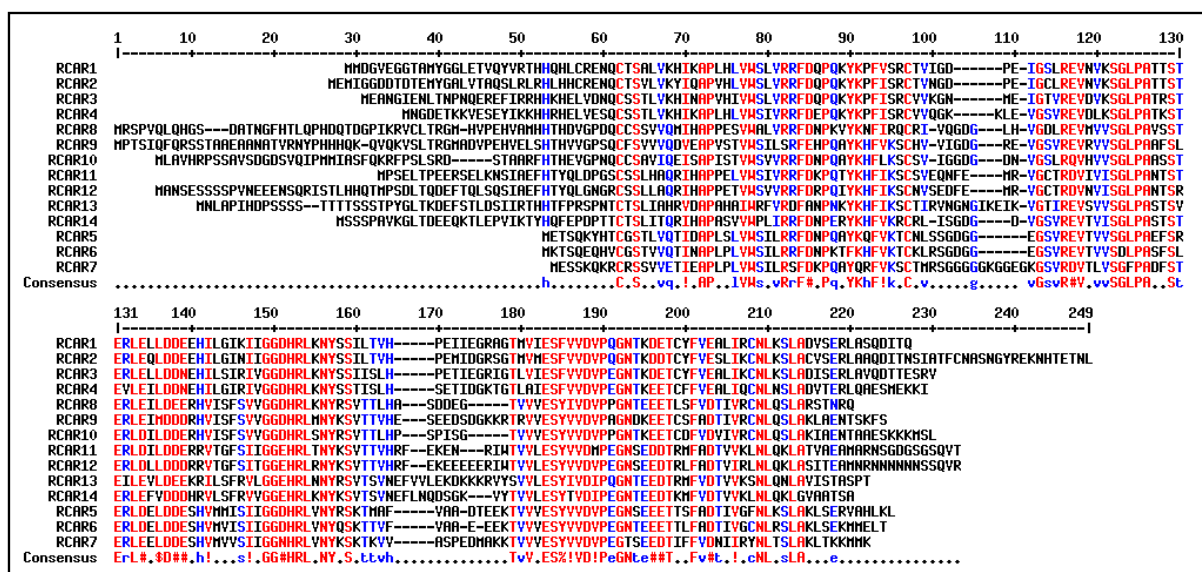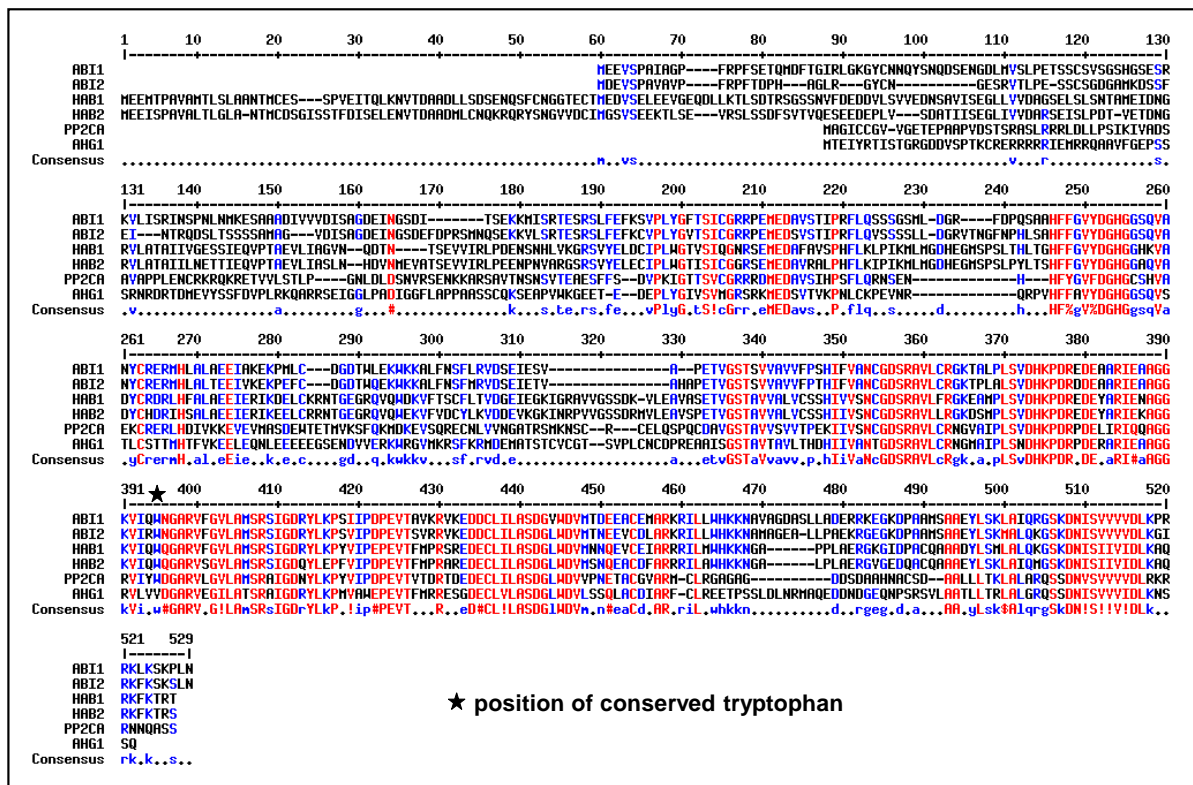
Sequence homology among RCAR family members

	R-1	R-2	R-3	R-4	R-5	R-6	R-7	R-8	R-9	R-10	R-11	R-12	R-13	R-14
R-1	100	84	70	69	52	50	44	50	49	53	46	47	42	46
R-2	84	100	72	65	70	47	43	49	46	51	47	48	45	43
R-3	70	72	100	76	49	47	41	50	46	53	46	48	44	44
R-4	69	65	76	100	47	46	45	50	49	49	43	44	38	43
R-5	52	70	49	47	100	81	63	53	58	57	51	53	43	50
R-6	50	47	47	46	81	100	65	54	59	55	51	51	44	52
R-7	44	43	41	45	63	65	100	46	52	49	46	46	40	43
R-8	50	49	50	50	53	54	46	100	63	66	51	50	50	51
R-9	49	46	46	49	58	59	52	63	100	69	49	48	42	49
R-10	53	51	53	49	57	55	49	66	69	100	53	53	47	51
R-11	46	47	46	43	51	51	46	51	49	53	100	80	52	54
R-12	47	48	48	44	53	51	46	50	48	53	80	100	49	51
R-13	42	45	44	38	43	44	40	50	42	47	52	49	100	60
R-14	46	43	44	43	50	52	43	51	49	51	54	51	60	100

List of strains used in this study

Construct	Organism	Resistance	Application	Strain list no.
	DH5alfa, EC		Preparation of competence cells	62, 2970
	XL1Blue, EC		Preparation of competence cells	120
	pREP4 (M15)		Preparation of competence cells	196
	Rosetta pLYS	Cam	Preparation of competence cells	2470
	DH5alfa, EC		Preparation of competence cells	62, 2970
	XL1Blue, EC		Preparation of competence cells	120
pMP90	C58 pGV3101, AT	Rif, Gen	Control plasmid for "floral dip"	845
pSKAscI*RAB18::LUC*	DH5alfa, EC	Amp	Reporter plasmid for transient expression	878 (879)
pSKAscI*RD29B::LUC*	DH5alfa, EC	Amp	Reporter plasmid for transient expression	880
pSK*35S::GUS*	DH5alfa, EC	Amp	Effector plasmid for transient expression	882 (883)
pBI221-*35S::ABI1*	DH5alfa, EC	Amp	Effector plasmid for transient expression	1102 (1103)
pBI221-*35S::abi1*	DH5alfa, EC	Amp	Effector plasmid for transient expression	1104 (1105)
pBI221-*35S::ABI2*	DH5alfa, EC	Amp	Effector plasmid for transient expression	1110 (1111)
pBI221-*35S::abi2*	DH5alfa, EC	Amp	Effector plasmid for transient expression	1112 (1113)
pBI221-*35S::RCAR1*	DH5alfa, EC	Amp	Effector plasmid for transient expression	1289 (1290)
pBI221-*35S::RCAR3*	DH5alfa, EC	Amp	Effector plasmid for transient expression	1287 (1288)
pHannibal::RCAR1	XL1Blue, EC	Amp	RNAi construct for transient expression	2192 (2193)
pHannibal::ACO2	DH5alfa, EC	Amp	RNAi construct for transient expression	2231 (2232)
pSPYCE-35S/pUC-SPYCE	DH5alfa, EC	Amp	Split-YFP-Interaction	1238 (1239)
pSPYNE-35S/pUC-SPYNE	DH5alfa, EC	Amp	Split-YFP-Interaction	1240 (1241)
pSPYCE-35S/pUC-*35S::YFPc-RCAR1*	DH5alfa, EC	Amp	Split-YFP-Interaction	1315 (1316)
pSPYNE-35S/pUC-*35S::YFPn-RCAR1*	DH5alfa, EC	Amp	Split-YFP-Interaction	1317
pSPYCE-35S/pUC-*35S::YFPc-RCAR3*	DH5alfa, EC	Amp	Split-YFP-Interaction	1318 (1319)
pSPYNE-35S/pUC-*35S::YFPn-RCAR3*	DH5alfa, EC	Amp	Split-YFP-Interaction	1320
pSPYCE-35S/pUC-*35S::YFPc-ABI1*	DH5alfa, EC	Amp	Split-YFP-Interaction	1257 (1258)
pSPYNE-35S/pUC-*35S::YFPn-ABI1*	DH5alfa, EC	Amp	Split-YFP-Interaction	1254 (1255)
pSPYCE-35S/pUC-*35S::YFPc-ABI2*	DH5alfa, EC	Amp	Split-YFP-Interaction	1381 (1382)

pSPYNE-35S/pUC-*35S::YFPn-ABI2*	DH5alfa, EC	Amp	Split-YFP-Interaction	1327
pQE30::RCAR1	XL1Blue, EC	Amp	Protein expression	1168 (1169)
p*RCAR1*::*RCAR1*::*GUS* in pBI121AscIBar	pGV3101, AT	Kan	Protein localization in plant	1251 (1252)
pQE30::delta N RCAR1	XL1Blue, EC	Amp	Protein expression	1299 (1300)
pQE30::delta C RCAR1	XL1Blue, EC	Amp	Protein expression	1301 (1302)
pQE30::RCAR3	XL1Blue, EC	Amp	Protein expression	1136 (1137)
pQE70::RCAR9	M15 pREP4, EC	Amp, Kan	Protein expression	2417 (2418)
pQE70::RCAR10	M15 pREP4, EC	Amp, Kan	Protein expression	2415 (2416)
pET-24a(+)::RCAR13	Rosetta pLYS, EC	Cam, Kan	Protein expression	2881
pET-24a(+)::RCAR14	Rosetta pLYS, EC	Cam, Kan	Protein expression	2882
pQE70::ABI1	M15 pREP4, EC	Amp, Kan	Protein expression	2158-2160
pQE70::ABI2	M15 pREP4, EC	Amp, Kan	Protein expression	2023
pQE70::abi2	M15 pREP4, EC	Amp, Kan	Protein expression	2024
pET-21a(+)::PP2CA	Rosetta pLYS, EC	Cam, Amp	Protein expression	2729 (2730)
pET-21a(+)::AIP1	Rosetta pLYS, EC	Cam, Amp	Protein expression	2731 (2732)
pGAD::RCAR1	HF7c, Y	Amp	Y2H	2104
pGAD::RCAR3	HF7c, Y	Amp	Y2H	2103
pGBT::ABI1	HF7c, Y	Amp	Y2H	2122
pGBT::ABI2	HF7c, Y	Amp	Y2H	2123

Acknowledgments

This study was performed in the laboratory of Prof. Dr. Erwin Grill in the Insitute of Botany, Technical University of Munich.

Hereby, my deepest gratitude goes to Professor Dr. Erwin Grill for providing me the chance to study in his laboratory and the excellent working conditions, and for his stimulating advice and constructive criticism during the years of research.

I extend my gratitude to Professor Dr. A. Gierl and Professor Dr. H. Schnyder for participation in my committee.

I would like to thank Dr. Alexander Christmann and Dr. Arthur Korte for their help, scientific and valuable discussions and suggestions from the beginning to the end of my PhD time in this laboratory. I gratefully acknowledge the scientific advices of Prof. Dr. Klaus Lendzian. My special thanks are devoted to Dr. Farhah Assaad for her constant help and critical reading of this manuscript.

I am deeply appreciative to many of my colleagues (Simone, Christian, Michal, Steve, Korny, Heidi, Claudia, Lisa, Karoline and Josef) in the Institute of Botany for their understanding and indispensable cooperation.

I would like to thank Beate Seeliger for her help in daily life and bureaucracy.

I am very grateful to Prof. Dr. Philippe Schmitt-Kopplin and Dr. Basem Kanawati from Helmholtz Zentrum München, for providing an opportunity and assistance for FT-ICR-MS analysis.

Finally, I want to express my sincere gratitude to my mother for her help, support, patience, and encouragement during all my life.

Lebenslauf

Persönliche Daten

Name	Izabela Szostkiewicz
Geboren am	27 August 1982 in Miedzyrzec Podlaski
Nationalität	Polnisch
Familienstand	ledig

Ausbildung

1998 – 2001   Abitur, Miedzyrzec Podlaski, Polen

2001 – 2006   Studium der Biotechnologie an der Maria Curie-Sklodowska
Universität, Lublin, Polen

2005 – 2006   Masterarbeit in der Polnische Akademie der Wissenschaften,
Warschau, Polen

2007 – 2010   Doktorarbeit am Lehrstuhl für Botanik der Technischen Universität
München (Arbeitsgruppe Prof. Dr. E. Grill) im Rahmen des EU
Projektes ADONIS (Marie Curie Fellowship)

Publikationen

The Plant Journal 2010
Szostkiewicz, I., Richter, K., Kepka, M., Demmel, S., Ma, Y., Korte, A., Assaad, FF.,
Christmann, A., Grill, E. (2010) Closely related receptor complexes differ in their ABA
selectivity and sensitivity. *Plant J.* 61, 25-35.

Science 2009
Ma, Y., **Szostkiewicz, I.**, Korte, A., Moes, D., Yang, Y., Christmann, A., Grill, E. (2009)
Regulators of PP2C phosphatase activity function as abscisic acid sensors. *Science* 324,
1064-1068.

The Journal of Biological Chemistry 2008
Skorupinska-Tudek, K., Poznanski, J., Wojcik, J., Bienkowski, T., **Szostkiewicz, I.**, Zelman-
Femiak, M., Bajda, A., Chojnacki, T., Olszowska, O., Grunler, J., Meyer, O., Rohmer, M.,
Danikiewicz, W., Swiezewska, E. (2008) Contribution of the mevalonate and
methylerythritol phosphate pathways to the biosynthesis of dolichols in plants. *J. Biol.
Chem.* 25, 21024-21035.